TESIS DOCTORAL
UNIVERSIDAD DE OVIEDO
Programa de Doctorado Ingeniería Energética

Captura de CO_2 en centrales termoeléctricas mediante cocombustión de carbón y biomasa en condiciones de oxicombustión

Juan Riaza Benito
Instituto Nacional del Carbón
INCAR-CSIC
2014

Universidad de Oviedo

Programa de Doctorado Ingeniería Energética

Captura de CO_2 en centrales termoeléctricas mediante cocombustión de carbón y biomasa en condiciones de oxicombustión

Tesis doctoral por

Juan Riaza Benito

Instituto Nacional del Carbón
INCAR-CSIC

2014

Agradecimientos

Quisiera dar las gracias en primer lugar a mis directores, los Doctores Covadonga Pevida García, Fernando Rubiera González y José Juan Pis Martínez. Su ayuda en todo momento y su gran confianza en mí me han impulsado para llegar a realizar esta tesis doctoral.

A mi compañera de viaje, la Doctora Lucía Álvarez, con quien he compartido tanto tiempo de laboratorio y trabajo por hacerlo siempre más agradable; y a la Doctora Victoria Gil, por su inestimable ayuda y colaboración durante estos años.

Al resto de mis compañeros del Grupo de Procesos Energéticos y Reducción de Emisiones del INCAR por su inestimable ayuda siempre que la he necesitado, y por hacer del trabajo un lugar agradable. También quisiera dar las gracias a los colegas de la Northeastern University, con los que fue un placer trabajar durante la estancia en Boston y cuya colaboración ha aportado un gran valor a esta tesis, en especial a Reza Khatami y al Profesor Yiannis Levendis.

Gracias al Consejo Superior de Investigaciones Científicas (CSIC), por autorizar la realización de este trabajo en el Instituto Nacional del Carbón, así como a los Directores de este centro, Dr. Carlos Gutiérrez Blanco y Dr. Juan Manuel Díez Tascón.

Al Gobierno de Asturias por concederme la ayuda predoctoral Severo Ochoa que me ha financiado durante 4 años para la realización de esta tesis doctoral así como la estancia temporal.

Al servicio de mantenimiento y taller del INCAR, con los que he trabajado con gran confianza, la destreza y valía de las personas que forman o han formado parte del taller ha sido fundamental. Especialmente a Nacho, Celes, Mejido y Andrés.

Quisiera hacer extensivo este agradecimiento a todo el personal del Instituto Nacional del Carbón, porque de una forma u otra han hecho posible la realización de la presente memoria.

Finalmente, a Fany por estar siempre a mi lado cargándome las pilas de ilusión, a mi familia animándome siempre, y especialmente a mis padres por su gran apoyo siempre incondicional.

Resumen

El carbón es y va a seguir siendo uno de los principales recursos energéticos para la generación de energía eléctrica. Sin embargo, en la combustión del carbón se libera CO_2, que es un gas de efecto invernadero y el principal causante del cambio climático. Una alternativa para la reducción parcial de emisiones de CO_2 consiste en sustituir parte del carbón utilizado en la combustión por biomasa, cuyas emisiones se consideran neutras. Sin embargo, para reducir de forma importante las emisiones de CO_2 han de considerarse medidas adicionales, entre las que se encuentran las tecnologías de captura y almacenamiento de CO_2, como la oxicombustión. Cuando el combustible se quema con O_2 puro y humos recirculados, es decir, en ausencia de N_2, se produce una corriente de alta concentración de CO_2 que tras un proceso de purificación, puede ser transportado a su lugar de inyección y almacenamiento. La oxicombustión es una tecnología en fase de demostración, sin embargo, su viabilidad económica dependerá de las políticas medioambientales, así como de los avances técnicos que se logren.

Se ha llevado a cabo el estudio del comportamiento en oxicombustión de un amplio rango de carbones y varias biomasas. La sustitución del N_2 por CO_2 y la mayor concentración de O_2 en la atmósfera de oxicombustión, implica cambios severos en la combustión del carbón y la biomasa que deben ser estudiados para mantener la estabilidad y eficacia de combustión. Se han usado varios dispositivos experimentales: termobalanza, reactor de caída libre y reactor de flujo en arrastre; en estos dispositivos se ha estudiado la ignición y combustión bajo diversas condiciones de oxicombustión, así como en atmósfera de aire que se ha tomado como referencia.

En el reactor de caída libre se estudió la combustión de partículas individuales de distintos carbones y biomasas. Los experimentos se realizaron en distintas atmósferas de oxicombustión así como aire. En este mismo dispositivo se llevaron a cabo mediciones con un pirómetro con el fin de obtener los perfiles de temperatura durante la combustión de las partículas de las distintas muestras de carbón y biomasa.

Con el objeto de conseguir unas condiciones experimentales cercanas a las existentes en una caldera de carbón pulverizado, se empleó un reactor de flujo en arrastre. Se llevó a cabo la desvolatilización de varios carbones y biomasas a 1000 °C, en atmósferas de N_2 y CO_2, con el fin de analizar el efecto de la atmósfera de desvolatilización, tanto sobre la estructura morfológica del *char* formado, como sobre su posterior reactividad. El análisis del comportamiento reactivo de los *chars* se realizó en un analizador termogravimétrico, en el que se realizaron experimentos de reactividad isotérmica y experimentos de reactividad no isotérmica en atmósfera de oxicombustión. Se aplicaron distintos modelos cinéticos para

predecir el comportamiento reactivo de dichos *chars*. Se analizó la reactividad de mezclas del char de carbón y biomasa con el fin de detectar posibles interacciones durante su combustión conjunta.

Se realizaron experimentos de ignición de mezclas de carbón y biomasa bajo diferentes atmósferas de oxicombustión en el reactor de flujo en arrastre, simulando condiciones de recirculación seca de gases (O_2/CO_2, 21-35% O_2) y recirculación húmeda de gases con concentraciones de vapor de 10 y 20%. A partir de los experimentos de ignición se determinó el efecto de distintas atmósferas de oxicombustión sobre la temperatura de ignición, así como el descenso en la temperatura de ignición con la adición de biomasa.

Se llevaron a cabo experimentos de cocombustión en condiciones de oxicombustión en termobalanza y en el reactor de flujo en arrastre. Los experimentos de combustión en el reactor de flujo en arrastre permitieron evaluar el efecto de la atmósfera de combustión sobre el grado de conversión alcanzado, así como sobre las emisiones de NO producidas durante la combustión de varios carbones y sus mezclas con biomasa, tanto en aire como en las atmosferas de oxicombustión. Los resultados arrojan una mejora en la eficacia de combustión con la adición de biomasa, así como un descenso de las emisiones de NO.

Abstract

Coal will continue to be one of the main energy resources for electricity generation in the future. However, coal combustion gives rise to CO_2 which is a greenhouse gas and the main source of climate change. One alternative for the reduction of CO_2 emissions is to replace part of the coal by biomass, whose emissions are considered neutral. However, to achieve any substantial reduction in CO_2 emissions, additional measures must be taken, such as CO_2 capture and storage technologies including oxy-fuel combustion. When fuel is burned in a mixture of pure O_2 and recycled exhaust gases (i.e., in absence of N_2) a highly concentrated stream of CO_2 is produced, which after the purification process, can be transported to a place of storage. Oxy-combustion technology is at present in the demonstration phase. However, its economic viability will depend not only on technological advances but also on environmental policies.

The performance of a wide range of coals and several biomasses under oxy-fuel combustion conditions has been studied. The replacement of N_2 by CO_2 and the higher O_2 concentrations in oxy-fuel combustion atmospheres entails several changes in coal and biomass combustion that must be addressed in order to maintain stability and combustion efficiency. Various experimental devices have been used including a thermogravimetric analyzer, a drop tube furnace and an entrained flow reactor. Ignition and combustion under different oxy-fuel combustion conditions, and under air as reference, have been studied using these devices.

Single coal and biomass particle combustion was studied in the drop tube furnace. Experiments were carried out under different oxy-fuel and air atmospheres. Measurements with a pyrometer were also carried out in the same furnace in order to obtain temperature profiles during the combustion of different single coal and biomass particles samples.

In order to reproduce some of the conditions that are present in a pulverised coal fired power station, an entrained flow reactor was employed. Coal devolatilization at 1000 ºC, under N_2 and CO_2 atmospheres, was conducted in the entrained flow reactor. In order to study the effect of the devolatilization atmosphere (CO_2, N_2), the morphological characteristics of the *chars* were compared and their reactivity was analyzed. The reactive behaviour of the *chars* was studied by means of isothermal and non-isothermal reactivity experiments in an oxy-fuel atmosphere using a thermogravimetric analyser. Different kinetic models were applied to predict the reactivity of these fuels. Coal char and biomass char blends were analyzed in order to detect possible interactions during the combustion of the blends.

Coal and biomass blend ignition tests were conducted in the entrained flow reactor under air and various oxy-fuel conditions at 1000 °C. Different oxy-fuel atmospheres were employed.

Both oxy-fuel combustion with dry recycling (O_2/CO_2, 21-35%O_2) and oxy-fuel combustion with wet recycling using up to 10 and 20% of H_2O were simulated. The effect of biomass addition and the combustion atmosphere on the ignition temperature was evaluated.

Co-firing experiments under oxy-fuel conditions were carried out in the thermogravimetric analyzer and in the entrained flow reactor. The coal and its blend with biomass were subjected to combustion experiments in the entrained flow reactor to evaluate the effect of the combustion atmospheres on coal burnout and NO emissions under oxy-fuel and air combustion.

Índice

Agradecimientos

Resumen

Abstract

Índice

Listado de Publicaciones

Lista de Figuras

1. Introducción

1.1 Energía y CO_2 1

1.1.1 Contribución de la humanidad al cambio climático 1

1.1.2 La necesidad de energía 4

1.2 Evolución del carbón como recurso energético 6

1.2.1 Reservas de carbón y cuota en el mix energético 6

1.2.2 Centrales térmicas de carbón pulverizado 8

1.3 Energía de la biomasa 11

1.4 Cocombustión de carbón y biomasa 16

1.5 Captura, Transporte y Almacenamiento de CO_2 21

1.5.1 Captura de CO_2 21

1.5.2 Transporte de CO_2 23

1.5.3 Almacenamiento de CO_2 24

1.6 Tecnología de Captura de CO_2 mediante oxicombustión 28

1.6.1 Esquema general 28

1.6.2 Unidad de producción de oxígeno 30

1.6.3 Plantas de demostración de tecnologías de oxicombustión 31

1.6.4 Combustión en condiciones de oxicombustión 33

1.6.5 Transmisión de calor en calderas de oxicombustión 34

1.6.6 Contaminantes en los humos de oxicombustión 37

1.6.7 Oxicombustión de carbón y biomasa 40

1.7 Objetivos 41

2. Dispositivos y metodologías experimentales 43
2.1 Muestras empleadas 43
2.2 Dispositivo para combustión de partículas 44
2.3 Reactor de flujo en arrastre 47
2.3.1 Descripción 47
2.3.2 Experimentos de combustión 50
2.3.3 Experimentos de desvolatilización 52
2.3.4 Experimentos de ignición 53
2.4 Analizadores termogravimétricos 55
2.4.1 Metodologías para los ensayos de reactividad en termobalanza 57
2.4.2 Modelos cinéticos 60
3. Combustión de partículas individuales de carbón y biomasa 65
3.1 Compendio de resultados 67
3.2 Publicaciones relacionadas 69
3.2.1 Publicación I 71
3.2.2 Publicación II 87
4. Reactividad y morfología de los chars 103
4.1 Desvolatilización y formación del char 103
4.2 Combustión del char 104
4.3 Compendio de resultados 104
4.4 Publicaciones relacionadas 105
4.4.1 Publicación III 107
4.4.2 Publicación IV 117
5. Ignición y combustión de carbón en atmósferas de oxicombustión 129
5.1 Ignición y oxicombustión 130
5.2 Emisiones de NOx 131
5.3 Compendio de resultados 132
5.4 Publicaciones relacionadas 133
5.4.1 Publicación V 135
5.4.2 Publicación VI 143
6. Efecto de la adición de biomasa en oxicombustión 157
6.1 Compendio de resultados 159
6.2 Publicaciones relacionadas 161
6.2.1 Publicación VII 163

6.2.2 Publicación VIII 173
6.2.3 Publicación IX 193
7. Conclusiones 203
8. Referencias bibliográficas 205
Anexo I Informe del factor de impacto de las publicaciones 215
Anexo II Producción científica no incluida 217

Listado de publicaciones

I **Single particle ignition and combustion of anthracite, semi-anthracite and bituminous coals in air and simulated oxy-fuel conditions**
J. Riaza, R. Khatami, Y.A. Levendis, L. Álvarez, M.V. Gil, C. Pevida, F. Rubiera, J.J. Pis. Combustion and Flame 2014, 161 pp 1096–1108. doi:0.1016/j.combustflame.2013.10.004

II **Combustion of single biomass particles in air and in oxy-fuel conditions**
J. Riaza, R. Khatami, Y. A. Levendis, L. Álvarez, M.V. Gil, C. Pevida, F. Rubiera, J.J. Pis. Biomass and Bioenergy, doi: 10 10.1016/j.biombioe.2014.03.018.1

III **Oxy-fuel combustion kinetics and morphology of coal chars obtained in N_2 and CO_2 atmospheres in an entrained flow reactor**
M.V. Gil, J. Riaza, L. Álvarez, C. Pevida, J.J. Pis, F. Rubiera. Applied Energy 2012, 91 (1) pp. 67 – 74. doi:10.1016/j.apenergy.2011.09.017

IV **Kinetic models for the oxy-fuel combustion of coal and coal/biomass blend chars obtained in N_2 and CO_2 atmospheres**
M.V. Gil, J. Riaza, L. Álvarez, C. Pevida, J.J. Pis, F. Rubiera. Energy 2012, 48 (1) pp. 510–518. doi:10.1016/j.energy.2012.10.033

V **Effect of oxy-fuel combustion with steam addition on coal ignition and burnout in an entrained flow reactor**
J. Riaza, L. Álvarez, M.V. Gil, C. Pevida, J.J. Pis, F. Rubiera. Energy 2011, 36 (8) pp. 5314 – 5319. doi:10.1016/j.energy.2011.06.039

VI **NO Emissions in oxy-coal combustion with addition of steam in an entrained flow reactor**
L. Álvarez, J. Riaza, M.V. Gil, C. Pevida, J.J. Pis, F. Rubiera**.** Greenhouse Gases: Science and Technology 2011, 1 (2) pp. 180-190. doi:10.1002/ghg.016

VII **A study of oxy-coal combustion with steam addition and biomass blending by thermogravimetric analysis.**
M.V. Gil, J. Riaza, L. Álvarez, C. Pevida, J.J. Pis, F. Rubiera. Journal of Thermal Analysis and Calorimetry 2012, 109 (1) pp. 49 – 55. doi:10.1007/s10973-011-1342-y

VIII **Ignition behaviour of coal and biomass blends under oxyfiring conditions with steam additions**
J. Riaza, , L. Álvarez, M.V. Gil, R. Khatami, Y.A. Levendis, J.J. Pis, C. Pevida, F. Rubiera. Greenhouse Gases: Science and Technology 2013, 3 (5), pp. 397-414. doi:10.1002/ghg.1368

IX **Oxy-fuel combustion of coal and biomass blends**
J. Riaza, M.V. Gil, L. Álvarez, C. Pevida, J.J. Pis, F. Rubiera. Energy 2012, 41 (1) pp. 429–435. doi: 10.1016/j.energy.2012.02.057

Lista de figuras

Figura 1.1	*Esquema de los principales flujos térmicos en la atmósfera [Kevin, 2008].*	2
Figura 1.2	*Cambios observados en: a) el promedio mundial de la temperatura en superficie; b) el promedio mundial del nivel del mar; y c) la cubierta de nieve del Hemisferio Norte [IPCC, 2007].*	3
Figura 1.3	*Evolución de la producción de energía eléctrica en España [REE, 2013].*	7
Figura 1.4	*Esquema de caldera típica de combustión de carbón pulverizado.*	9
Figura 1.5	*Central térmica de Sangüesa [IDAE, 2007].*	14
Figura 1.6	*Combustión en paralelo.*	17
Figura 1.7	*Esquema de combustión indirecta.*	18
Figura 1.8	*Cocombustión directa.*	19
Figura 1.9	*Ensuciamiento en tubos de caldera de carbón pulverizado tras ensayos de cocombustión con biomasa [Cieplik, 2011].*	20
Figura 1.10	*Esquema de diferentes procesos de separación de CO_2 [IPCC, 2005].*	22
Figura 1.11	*Recreación de un pozo de inyección de CO_2 [CIUDEN, 2014].*	24
Figura 1.12	*Diagrama de fases del CO_2.*	25
Figura 1.13	*Esquema de un proceso de inyección de CO_2 en un almacenamiento geológico [CIUDEN, 2014].*	26
Figura 1.14	*Estructuras favorables para el almacenamiento de CO_2 en España [Prado, 2008].*	27
Figura 1.15	*Esquema del proceso de oxicombustión.*	29
Figura 1.16	*Desarrollo histórico de los proyectos de oxicombustión [Wall, 2009b]*	31
Figura 1.17	*Fotografías de llamas de propano en (a) aire, (b) oxicombustión con 21% oxígeno, (c) oxicombustión con 27% oxígeno, y (d) oxicombustión con 45% oxígeno [Andersson, 2008a, 2008b].*	36
Figura 1.18	*Instalación de gasificación de biomasa entre calderas de lecho fluido (derecha) y carbón pulverizado (izquierda) en CIUDEN.*	40
Figura 2.1	*Fotografía del dispositivo experimental para el estudio de combustión de partículas en la Northeastern University (Boston, MA).*	45
Figura 2.2	*Esquema del dispositivo experimental para pirometría de combustión de partículas en la Northeastern University (Boston, MA).*	46

Figura 2.3 *Fotografía del reactor de flujo en arrastre utilizado en este trabajo.* 47

Figura 2.4 *Esquema del reactor de flujo en arrastre (EFR).* 48

Figura 2.5 *Perfil de temperaturas para una temperatura de operación de 1000ºC.* 49

Figura 2.6 *Calentamiento del reactor de flujo en arrastre a una velocidad de 10-15 ºC min^{-1}.* 54

Figura 2.7 *Ejemplo de determinación de la temperatura de ignición a partir de la concentración de CO_2.* 55

Figura 2.8 *Fotografía de la termobalanza Setaram TAG 24 modificada.* 56

Figura 2.9 *Detalle del generador de vapor de agua utilizado en la termobalanza.* 57

Figura 2.10 *Representación de los regímenes de control del proceso de combustión en función de la temperatura (E_a, energía de activación observada; E, energía de activación química).* 58

Figura 2.11 *Modelo de Reacción Volumétrico.* 62

Figura 2.12 *Modelo de Reacción de Núcleo Decreciente.* 63

Figura 3.1 *Imágenes de las biomasas: (a) SCB, (b) OR, (c) PI, (d) TOPI, durante la combustión de los volátiles en aire.* 68

1. Introducción

1.1 Energía y CO_2

1.1.1 Contribución de la humanidad al cambio climático

La energía es un factor esencial en la actividad económica de un país y, al mismo tiempo, la principal fuente de gases de efecto invernadero (GEI) que constituyen el origen de uno de los mayores problemas ambientales que sufre el planeta: el cambio climático.

Actualmente existe una gran preocupación por el incremento de las emisiones de GEI como el CO_2, ya que las consecuencias del cambio climático empiezan a ser perceptibles. El aumento de la concentración de GEI se debe en parte a la actividad del hombre y, dentro de las causas antropogénicas, la de mayor peso es la generación de energía.

Los combustibles fósiles provienen de materia orgánica transformada en los procesos geológicos de carbogénesis o petrogénesis y, por tanto, son en gran proporción materiales carbonosos. En su combustión siempre se libera CO_2, en mayor o menor medida, dependiendo de su composición.

Los GEI son necesarios, ya que mantienen la temperatura que hace posible la vida en la superficie terrestre. El CO_2 de la atmósfera produce un "efecto invernadero" debido a su comportamiento ante la radiación solar, manteniendo la temperatura de la Tierra. De no ser así, la Tierra se enfriaría paulatinamente. Los flujos térmicos entre la superficie terrestre y el espacio exterior son ciertamente complejos pero se pueden esquematizar tal como muestra la Figura 1.1.

El dióxido de carbono se encuentra de manera natural en la atmósfera, pero algunas actividades humanas, en especial la quema de combustibles fósiles incrementan significativamente su concentración. Esto se traduce en un aumento de este efecto invernadero y un progresivo calentamiento global.

Los principales GEI son vapor de agua, dióxido de carbono, metano y ozono. En las centrales termoeléctricas convencionales se producen varios de estos gases entre los que se encuentran el vapor de agua, dióxido de carbono y óxidos de nitrógeno. Las emisiones de dióxido de carbono y óxidos de nitrógeno son las que tienen mayor relevancia, en especial las de CO_2.

La radiación solar incide sobre la Tierra, parte de esta radiación es reflejada por la atmósfera, las nubes, y otra parte llega a la superficie terrestre. La superficie terrestre emite radiación debido a su temperatura, parte de esa emisión escapa al espacio exterior y otra parte es reflejada por los GEI. Las concentraciones de estos gases en la atmósfera definen la cantidad de energía reflejada hacia la superficie terrestre, manteniendo la temperatura media

de la Tierra en unos 15 ^{0}C. La temperatura media de la parte baja de la atmósfera depende principalmente de estos flujos de calor, y es un factor determinante para mantener el equilibrio que permite el funcionamiento de los ciclos naturales atmosféricos. La acción humana ha hecho que se emitan gases de efecto invernadero a la atmósfera, aumentando sus concentraciones. Esto provoca que aumente la cantidad de energía reflejada hacia la superficie terrestre y se eleve su temperatura.

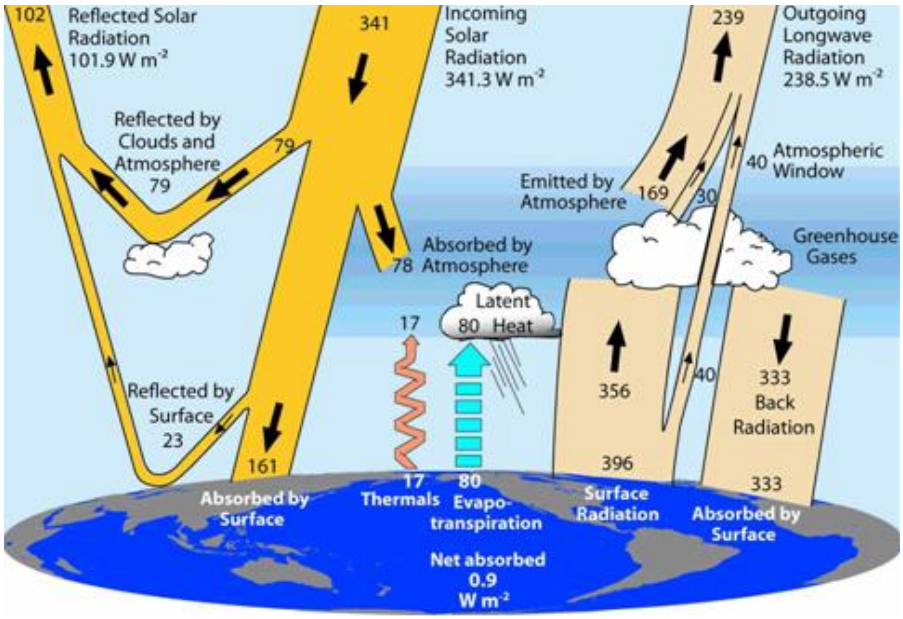

***Figura 1.1**. Esquema de los principales flujos térmicos en la atmósfera [Kevin. 2008].*

En el informe del año 2007 del Panel Intergubernamental sobre el Cambio Climático (IPCC) se presentó la evolución de la temperatura en el Hemisferio Norte en los últimos 1000 años, como se muestra en la Figura 1.2.

Las consecuencias de la rotura del equilibrio térmico son un probable calentamiento global y un consecuente cambio climático que definirá nuevos valores de las variables climáticas. Con ello se prevé un aumento de las sequías, inundaciones, desaparición o desplazamiento de especies animales y vegetales, proliferación de enfermedades infecciosas, además de otras consecuencias impredecibles.

La lucha contra el cambio climático es una necesidad para la conservación del Medio Ambiente, los recursos de la Tierra y las especies que viven en ella. Con la firma del Protocolo de Kioto (PK) se comienzan a impulsar en mayor medida las tecnologías de captura y almacenamiento de CO_2 dado que los países firmantes adquieren el compromiso de limitar sus emisiones.

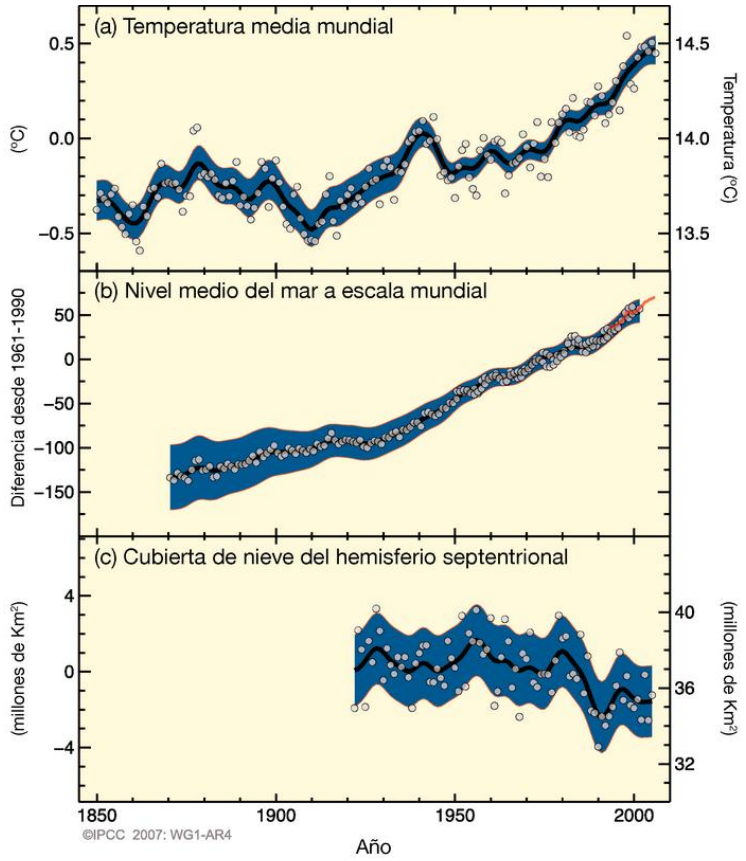

Figura 1.2. *Cambios observados en: a) el promedio mundial de la temperatura en superficie; b) el promedio mundial del nivel del mar; y c) la cubierta de nieve del Hemisferio Norte [IPCC, 2007].*

El PK ha supuesto un primer paso para la disminución de las emisiones de CO_2, pero no es suficiente y se hace cada vez más necesario un tratado internacional que no solo continúe lo acordado en el PK sino el compromiso firme de potencias como EEUU y China, responsables de la mayor parte de las emisiones de CO_2 a nivel mundial. Recientemente la Unión Europea ha adoptado un compromiso de reducción de las emisiones de GEI en un 40% en el año 2030 respecto a las emitidas en 1990 (UE, 2014). Sin embargo, hay que tener en cuenta que EEUU es el país con mayores reservas de carbón mientras que China es ya el mayor productor y exportador de carbón [BP, 2013]. Del compromiso de ambos países para la reducción de las emisiones de CO_2 dependerá su evolución a nivel mundial y la lucha contra el cambio climático. Las emisiones locales de cualquier lugar en la Tierra acaban en la atmósfera donde los vientos homogeneizan la concentración de CO_2 y por tanto el problema de la emisión de GEI y cambio climático es global. Los escenarios previstos por el IPCC contemplan una subida de la temperatura media de la Tierra entre los 0,3 y los 4,8 ^{0}C para el año 2100 [IPCC, 2013]. Para contrarrestar el incremento de la concentración de CO_2 en la atmósfera es necesario implementar una serie de medidas a nivel mundial como son: la mejora de la eficiencia

energética, el incremento en el uso de energías renovables, el incremento de la energía nuclear y la captura y almacenamiento de CO_2 (CAC).

1.1.2 La necesidad de energía

El nivel de desarrollo de un país y su capacidad de generación de energía están íntimamente ligados, de forma que la pobreza energética normalmente está ligada a un nivel bajo de desarrollo. El reto energético es hoy uno de los grandes desafíos que debe afrontar la humanidad. Deben tomarse decisiones cruciales para reducir drásticamente nuestras emisiones de CO_2 y luchar así contra el cambio climático. Al mismo tiempo se busca aumentar la capacidad de generación para hacer llegar la energía a más lugares y a un precio menor.

El reto para la generación de energía del futuro es que sea barata, accesible y sostenible. En 1987 el informe Brundtland [ONU, 1987] definió el *desarrollo sostenible* como aquel capaz de "*satisfacer las necesidades presentes de la humanidad sin comprometer la capacidad de las futuras generaciones para satisfacer las suyas*". Así, la transición a la sostenibilidad se ha convertido en una necesidad para el mantenimiento de la vida humana y la conservación de la biodiversidad, en un imperativo económico y ambiental, educativo y moral.

La energía procedente de recursos fósiles ha sido tradicionalmente la principal fuente de energía a nivel mundial. Hoy en día las diferentes tecnologías para la generación en base a energías renovables no son competitivas con los actuales precios de la energía. Por tanto, el carbón seguirá siendo una de las principales fuentes de energía a largo plazo debido a sus abundantes reservas y precios competitivos. La participación del carbón en el consumo mundial de energía fue del 30,3 % en 2011, frente al 33,1 % para el petróleo y el 23,7 % para el gas natural [BP, 2013].

Las necesidades en el campo energético se pueden resumir en la diversificación de las fuentes energéticas, la implementación de las tecnologías de captura y almacenamiento de carbono (CCS) y el aumento de la participación de las energías renovables en el mix energético, con el fin de reducir las emisiones de CO_2 a la atmósfera por debajo de los niveles de 1990. Aunque su uso está en continuo aumento, las fuentes de energía renovables son todavía minoritarias a nivel mundial. La captura y almacenamiento de CO_2 constituye una opción de tránsito desde la generación de energía actual en base a combustibles fósiles hasta que se desarrolle la tecnología suficiente para tener un modelo energético plenamente sostenible [UE, 2013].

En el caso de España se hace necesario definir políticas y medidas de reducción de emisiones que permitan cumplir con los compromisos internacionales asumidos, sin que se impongan cargas excesivas en la economía. Las nuevas leyes reguladoras están conduciendo a un desarrollo de nuevas tecnologías para reducir las emisiones, especialmente las de CO_2, ya que es el mayor contribuidor al aumento del efecto invernadero.

Las opciones para la mitigación del cambio climático comprenden:

- Mejora de la eficiencia energética.
- Ahorro energético.
- Preferencia de combustibles que dependan menos intensivamente del carbono.
- Aumento del empleo de energía nuclear.
- Aumento de las fuentes de energía renovable.
- Potenciación de los sumideros biológicos de CO_2.
- Reducción de las emisiones de gases de efecto invernadero diferentes del CO_2.

Como ya se ha mencionado anteriormente tras la firma del Protocolo de Kioto (PK) en 1997, se estableció un calendario de reducción de las emisiones de GEI. Se acordó para cada país un margen distinto en función de diversas variables económicas y medioambientales. En el periodo 2008-2012, la Unión Europea en su conjunto debía reducirlas en un 8% respecto a las de 1990 tomado como año base. España estaba obligada a no exceder las emisiones de GEI en un 15% respecto a las emisiones de 1990.

Las emisiones de GEI en España llegaron a alcanzar niveles superiores al 50 % respecto a los de 1990, principalmente debido al rápido crecimiento económico del país durante la última década. Sin embargo, las emisiones de CO_2 han caído drásticamente desde el año 2008, debido fundamentalmente a la crisis económica, y a finales de 2012 se encontraban tan solo un 18,7% por encima de las de 1990.

El PK no solo recoge la regulación de emisiones de gases de efecto invernadero sino que propone una serie de medidas, entre las que se encuentra el "desarrollo de las energías renovables y la captura y almacenamiento de CO_2" (Artículo 2). El PK tenía validez hasta el año 2012, pero ha sido prolongado hasta el año 2020 y debe ser sustituido por otro acuerdo con las mismas directrices generales, al que se sumen al menos los países más contaminantes y con objetivos ambiciosos.

Durante las distintas Cumbres del Clima (COP), organizadas por la Convención Marco de Naciones Unidas sobre Cambio Climático (UNFCCC, en sus siglas en inglés) y celebradas anualmente, se han mantenido negociaciones entre los líderes políticos para llegar a un acuerdo en materia de cambio climático. Los avances son escasos y no se alcanzó más que un acuerdo no vinculante legalmente. Los puntos clave de dicho acuerdo son los siguientes:

- Compromiso de no incrementar la temperatura global por encima de 2 ^{o}C.
- Compromiso de los países desarrollados a establecer un listado de objetivos de reducción de emisiones para el año 2020.

- La creación de un fondo a corto plazo de 30 mil millones de dólares para acciones desarrolladas hasta el año 2012, y un fondo de 100 mil millones de dólares anuales de financiación a largo plazo, para mecanismos que apoyen la transferencia de tecnologías y ciencias forestales.

El desafío se encuentra ahora en firmar un acuerdo legalmente vinculante en la cumbre que se celebrará en Paris en el año 2015, aunque hasta la fecha los avances son escasos y la crisis económica crea aún mayores reticencias.

La política energética común de la Unión Europea propone para el año 2020 combatir el cambio climático reduciendo las emisiones de GEI un 20% con respecto a los niveles de 1990, reduciendo el consumo energético, aumentando la eficacia energética en un 20% y aumentando el uso de las energías renovables hasta alcanzar un 20% del consumo total de energía, este objetivo es conocido como 20/20/20. Propone además que el 10% del consumo de combustibles en el transporte se realice con biocarburantes.

Las Directivas 2003/87/CE y 2004/101/CE recogen la regulación y reducción de emisiones de CO_2. Con esta última se crea el primer mercado de intercambio de Derechos de Emisión a nivel europeo. En España se transponen estas Directivas europeas y la regulación de emisiones en las instalaciones, desarrollándose planes y estrategias a seguir como se contempla en los sucesivos Planes de Energías Renovables (PER) que pretenden potenciar las fuentes de energía renovable, tanto en generación eléctrica como para la producción de calor y biocarburantes.

1.2 Evolución del carbón como recurso energético

1.2.1 Reservas de carbón y cuota en el mix energético

El carbón ha sido el motor principal de la revolución industrial, y no ha dejado de ser una de las principales fuentes de energía a nivel mundial. El carbón se utiliza principalmente para la producción de energía seguido por su empleo en la producción de acero. Las reservas probadas de carbón a nivel mundial se estiman en 860.938 millones de toneladas [WEC, 2010] y se estima que su duración será de más de 100 años. Su reparto geográfico es más variado y se encuentra en países más estables políticamente que el de otros recursos energéticos como el gas o petróleo, por lo que sus precios han sido más estables en el tiempo. En términos globales de explotación y consumo de carbón sobresale con diferencia China, ya que está constituyendo el motor de su industrialización. La producción de carbón en China aumentó un 135% en la última década. En 2012 China consumió por primera vez la mitad del carbón mundial [BP, 2013].

Los yacimientos de carbón de España se encuentran fundamentalmente en el tercio norte peninsular siendo los más importantes los de Castilla-León, Aragón y Asturias. La rentabilidad de la mayor parte de las explotaciones ha ido menguando hasta llegar al cierre de buena parte

de la minería del carbón en España. Más allá de que sean susceptibles de ser explotados económicamente, los recursos de carbón se deberían entender como una reserva estratégica.

El incremento de los precios de la energía y la dependencia de las importaciones de recursos energéticos debilitan la seguridad energética y la competitividad. Dado que España es un país deficitario energéticamente por no disponer de yacimientos de petróleo o gas, se intentan mantener activas las explotaciones de carbón de cara a posibles carencias en los mercados internacionales de recursos energéticos. Sin embargo, la política energética europea obligará a cerrar aquellas explotaciones que no sean rentables a partir del 2018 cuando se acabarán las ayudas para las explotaciones de carbón. Esta incertidumbre contrasta con la tendencia en el mercado internacional donde aumenta cada año la producción de carbón principalmente debido al desarrollo de China e India.

En España existen reservas y explotaciones de carbón que abastecen parte de la demanda de las centrales térmicas, si bien se importa parte del carbón consumido, el 53% en 2012 [UNESA, 2013]. Actualmente, el parque generador peninsular español se compone de 19 centrales térmicas de carbón con 11.113 MWe de potencia instalada [REE, 2013]. La mayor parte de las centrales térmicas de carbón están situadas en zonas donde hay explotaciones de carbón o cerca de instalaciones portuarias para minimizar el transporte. Aunque buena parte del carbón consumido es importado, este hecho es mucho más reciente que la edad de las centrales térmicas, que en un principio consumían en su mayoría sólo carbón nacional.

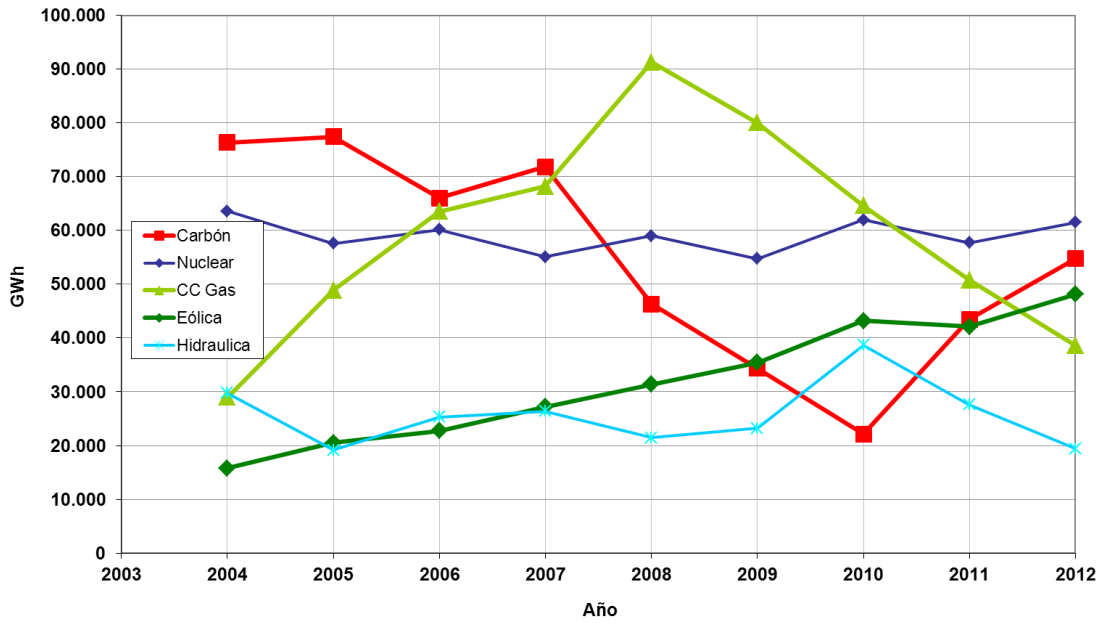

Figura 1.3. *Evolución de la producción de energía eléctrica en España [REE, 2013].*

La producción de energía eléctrica en los últimos años ha cambiado, variando las aportaciones de las diferentes fuentes como muestra la Figura 1.3. El carbón tiene una cuota fluctuante en el mix energético, que depende principalmente de la política energética, los precios de otras energías y la demanda eléctrica. Debido a la crisis económica se acusa un descenso de la demanda de energía eléctrica. Gracias a incentivos económicos se ha logrado un notable aumento de la generación con energías renovables, fundamentalmente la energía eólica. La demanda de energía a cubrir con otras fuentes es menor y por tanto las centrales térmicas de carbón y gas han reducido sus horas de funcionamiento.

Conforme a la entrada en vigor del Protocolo de Kioto las industrias más contaminantes como son las eléctricas o las cementeras tienen que pagar derechos por la emisión de CO_2. Las centrales de carbón son las de mayor intensidad de carbono y, por tanto, las más perjudicadas. Estas emisiones originan un sobrecoste por la compra de derechos de emisión de CO_2 que hace que la producción de energía eléctrica en base a carbón sea más cara. Sin embargo, el actual excedente de derechos de emisión en el mercado repercute en un precio del carbono que ha caído a mínimos, 4,30 € de media en 2013 (precio en 2011 y 2012 de 14,78 €/t CO_2 y 7,90 €/t CO_2, respectivamente).

1.2.2 Centrales térmicas de carbón pulverizado

Las centrales térmicas de carbón son instalaciones que han evolucionado mucho desde las primeras plantas de principios del siglo XX hasta las modernas centrales de hoy en día. El empleo continuado y global del carbón durante tanto tiempo ha logrado un gran avance en la tecnología, incrementando paulatinamente la eficiencia energética de las centrales. El calor generado mediante la combustión de carbón se utiliza para la producción de vapor y accionar una turbina de vapor (Figura 1.4). La eficacia teórica para convertir el calor en trabajo mecánico (rotación de la turbina) depende de la caída de temperatura del vapor en dicha turbina. Debido a las pérdidas de energía, la eficacia energética de las centrales en operación suele ser del orden de 30-38%, aunque puede llegar a alcanzar valores en el entorno del 40% con las modificaciones adecuadas. Sin embargo, el margen para la mejora del rendimiento es cada vez menor ya que está limitado por el propio ciclo de Rankine. Para una planta típica operando con una temperatura de vapor de 570 °C, la máxima eficacia teórica es de alrededor del 54%.

Las centrales térmicas de carbón pulverizado de diseños actuales son centrales con eficacias cercanas al 45% [Termuehlen, 2003], con mayor control en su operación para la optimización del proceso y el control de emisiones, con unidades de desulfuración, retención de partículas en suspensión y desnitrificación. Sin embargo, este control no puede evitar la emisión del CO_2 que se genera en la combustión.

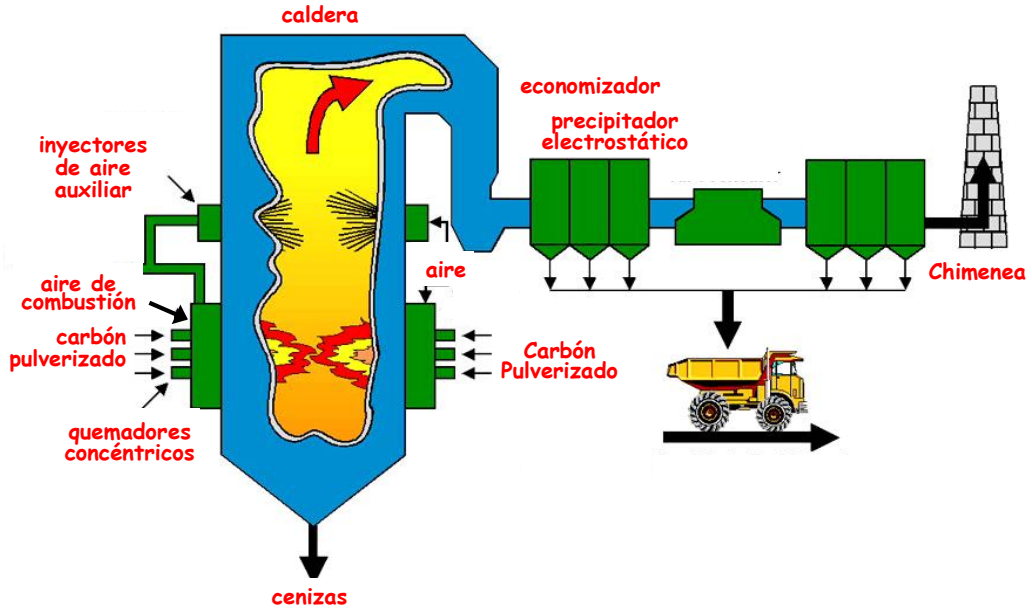

Figura 1.4. *Esquema de caldera típica de combustión de carbón pulverizado.*

El aprovechamiento de calores residuales de las corrientes de humos o vapor permite incrementar la eficacia, sin embargo, están ya muy optimizadas y no podrán ir mucho más allá. Se ha planteado en algunos estudios, emplear parte de la energía del agua de refrigeración en redes de calor para las zonas próximas a algunas centrales. Sin embargo, estos proyectos de cogeneración no han sido implantados en España en ninguna central térmica de carbón.

Se pretende continuar avanzando en los rendimientos aumentando la presión del vapor para llegar así a condiciones más allá del punto crítico en lo que se denomina estado supercrítico. Cuando se obtiene el vapor en condiciones *supercríticas* la tecnología se convierte, desde el punto de vista de eficacia energética, en la más eficaz de todas las existentes, con valores cercanos al 45%. Las dificultades más importantes que limitan el desarrollo de la tecnología de combustión de carbón en condiciones ultracríticas, se refieren sobre todo a problemas de materiales. Los intercambiadores de calor tanto en la región inmediatamente superior a los quemadores, como en los sobrecalentadores y en los recalentadores, se encuentran expuestos a corrosión interna por el vapor en condiciones supercríticas, y a corrosión externa tanto por los gases como por los depósitos corrosivos que se forman en su superficie. Actualmente se están desarrollando materiales resistentes a las condiciones particularmente arduas de este tipo de sistemas.

El control en la operación de estas centrales es fundamental para optimizar la eficacia energética, es por ello que las centrales actuales tienen sistemas complejos de monitorización. Asimismo cuentan con numerosos intercambiadores de calor para maximizar la energía disponible en los humos de combustión, aprovechando siempre los calores residuales de

procesos auxiliares. Las centrales térmicas cuentan con sistemas de limpieza de gases, así como de desulfuración y desnitrificación. Cuentan también con otras tecnologías en la propia caldera de combustión para la reducción de los óxidos de nitrógeno mediante quemadores de bajo NO_x. Esta evolución de los quemadores permite una combustión estable a menor temperatura que los convencionales. Se mantienen condiciones reductoras en una primera fase de la combustión para reducir la formación de NO_x. Para conseguirlo se alimenta el aire de forma estratificada a través de boquillas anulares ajustables.

Las centrales térmicas actuales utilizan en su mayoría la tecnología de carbón pulverizado. Sin embargo existen otras tecnologías como el lecho fluidizado o la gasificación integrada en ciclo combinado (GICC). Esta última presenta unas emisiones inferiores y un rendimiento superior ya que emplea una turbina de gas y una de vapor, sin embargo, el mayor coste y complejidad de la planta hacen que esta tecnología no haya prosperado como se esperaba. En España actualmente existe una planta de este tipo, ELCOGAS, en la localidad de Puertollano.

La tecnología de lecho fluidizado presenta varias ventajas respecto al carbón pulverizado. En estas centrales la combustión se realiza a una temperatura en torno a 850 ^{o}C que es inferior a la de formación de los óxidos de nitrógeno de origen térmico. Mediante la adición de caliza en el lecho se produce una reducción de las emisiones de SO_2 [Rubiera, 1991], debido a la reacción del CaO formado a partir de la calcinación de la caliza, para formar yeso según la reacción:

$$CaO + SO_2 + 1/2O_2 \longrightarrow CaSO_4$$

Esta reacción es también el principio en el que se basan las unidades de desulfuración de las centrales de carbón pulverizado en las que los humos se hacen pasar a través de una lechada de cal, generándose yeso que es posteriormente retirado.

El término "Tecnologías Limpias" ha llegado a constituir una expresión habitual en el entorno científico-técnico de la utilización del carbón. Se aplica generalmente en referencia a métodos de producción de energía en los que las emisiones de óxidos de azufre y de nitrógeno se encuentran reducidas a valores mínimos. Asimismo, procesos de elevada eficacia térmica, con bajas emisiones específicas de dióxido de carbono, se suelen considerar como "limpios", debido a su reducida incidencia en el efecto de calentamiento global de la atmósfera. Existen nuevos enfoques más allá del relacionado únicamente con la prevención y que, más que reducir, se preocupan de eliminar la propia generación de los contaminantes, situándose en el contexto de Tecnologías Limpias y Ecología Industrial. En suma, se pueden definir como Tecnologías Limpias de Utilización del Carbón aquéllas en las que se consiguen elevadas eficacias energéticas asociadas a un mínimo impacto ambiental [Pis, 2009]. Sin embargo, las emisiones que genera su combustión exige dar un paso más en esas tecnologías evitando estas emisiones mediante la captura y almacenamiento de CO_2.

1.3 Energía de la Biomasa

La creciente preocupación por las emisiones de CO_2 debidas al uso de combustibles fósiles y el aumento del precio del petróleo y derivados ha impulsado la búsqueda de combustibles alternativos que puedan ser competitivos en precio.

La energía de la biomasa se ha perfilado como una energía renovable con gran versatilidad de usos ya que puede usarse tanto en centrales estacionarias, como móviles gracias a los biocombustibles líquidos o gaseosos.

La biomasa es la materia orgánica derivada de los seres vivos. El aprovechamiento energético de la biomasa es tan antiguo como el descubrimiento y el empleo del fuego para calentarse y cocinar alimentos. La utilización térmica de la biomasa se aplica en el sector doméstico para calefacción, cocina, agua caliente sanitaria, con equipos individuales (estufas, cocinas, chimeneas, calderas), o bien con equipos centralizados o de distrito (calderas). También se realiza el aprovechamiento térmico de la biomasa en el sector industrial para obtener vapor, y agua o aire calientes, la biomasa es consumida como combustible para obtención de calor, electricidad o ambos a la vez en procesos de cogeneración.

Hasta la popularización de los pélets, los tipos de caldera que se utilizaban en biomasa eran de lecho fijo o de parrilla. Las calderas de llama invertida de unas decenas de kW reciben esta denominación por la posición de la cámara de combustión, situada debajo del hueco en el que se carga la leña. Otro tipo de calderas de mayor potencia, también de lecho fijo, son los denominados hornos o calderas de parrilla, y se pueden utilizar para cogeneración (producción de energía eléctrica y térmica). Pueden alcanzar hasta varios MWe de potencia, y se clasifican en función del movimiento de la parrilla. Algunos hornos de este tipo pueden quemar materiales con gran contenido en cenizas o humedad, como la biomasa forestal recién cortada.

Gracias a su forma cilíndrica, lisa y su pequeño tamaño, el pélet tiende a portarse como un fluido, lo que facilita el movimiento del combustible y la carga automática de las calderas. Eso ha permitido una gran expansión como biocombustible sólido. Con la popularización del pélet surgen calderas más específicas con quemadores de pélets tanto para calefacción doméstica, como para el sector industrial que abarcan potencias de hasta 1,5 MWt.

El interés por la biomasa radica en su contenido energético y este se establece a través de su poder calorífico. En el ámbito energético o en aplicaciones térmicas se utiliza el poder calorífico inferior (PCI). Los PCI de algunas biomasas, en kcal/kg, son las siguientes: cascarilla de arroz: 3.370; cáscara de almendra: 3.940; papel, cartón: 3.780; madera: (coníferas 3.650, frondosas 3.370); residuos de la industria aceitera como orujillo: 3.780, hueso de aceituna: 3.860. Estos valores están considerados con contenidos de humedad entre 10-20%, y son inferiores a los de carbones bituminosos que llegan a las 7.500 kcal/kg.

La biomasa de origen vegetal para uso energético tiene gran versatilidad de fuentes y se puede clasificar, del siguiente modo:

- Residuos forestales procedentes de podas, claras y cortas finales. Con las tareas de mantenimiento y cuidado de los árboles, tanto en monte como en los núcleos urbanos, se generan residuos de madera en forma de troncos, ramas y hojas.
- Residuos de industrias forestales procedentes de los procesos de primera y segunda transformación de la madera. Como recortes, serrín, viruta o restos de construcción o derribo.
- Restos de cultivos agrícolas: herbáceos (paja de cereales) o leñosos (podas de olivos, viñedos y frutales).
- Cultivos energéticos: herbáceos (cardo, sorgo, girasol, remolacha), leñosos (chopo, sauce, eucalipto).

La combustión de biomasa, al igual que cualquier producto orgánico, libera CO_2, sin embargo en el caso de la biomasa y bajo ciertos preceptos se debe considerar que esas emisiones son neutras ya que las plantas captan ese CO_2 de la atmósfera mediante el proceso de la fotosíntesis, liberando oxígeno y acumulando carbono en sus estructuras. De esta manera se cerraría el ciclo siempre que se mantenga suficiente masa forestal que permita la sustentabilidad del ciclo. En general, el uso de biomasa o de sus derivados puede considerarse neutro en términos de emisiones netas de CO_2, si sólo se emplea en cantidades a lo sumo iguales a la producción neta de biomasa del ecosistema que se explota. Tal es el caso de los usos tradicionales si no se supera la capacidad de carga del territorio.

Biomasa forestal residual es la producida durante cualquier tipo de tratamiento silvícola o aprovechamiento final de masas forestales. Por ejemplo, esto englobaría los restos de cortas finales, limpiezas de ribera, podas y saneamientos, preparación de terrenos para plantación, u otros procesos. En la actualidad gran parte de estos residuos son abandonados o quemados controladamente *in situ*. De un árbol se suele aprovechar el tronco como materia prima para la industria maderera. El resto del árbol suele ser inservible para la industria maderera. Esto incluye ramas, hojas y raíces.

La utilización de biomasa contribuye medioambientalmente en los siguientes aspectos:

- Mejora las condiciones de los montes.
- Protección de los montes ante incendios.
- Desarrollo del ámbito rural.
- Contribuye a los compromisos de España ante el Protocolo de Kioto.
- Reforestación.

Los bosques tienen un papel fundamental en la mitigación del cambio climático. Las plantas a través de la fotosíntesis absorben el CO_2 de la atmósfera y fijan el carbono en sus estructuras. La capacidad de fijación de los bosques y montes se puede aumentar con determinados tratamientos silvícolas, su conservación, la prevención de incendios y su correcta explotación. Por tanto, la potenciación de la biomasa puede ayudar a combatir el cambio climático mediante las repoblaciones y forestaciones, aumentando así la cantidad de CO_2 absorbida.

En lugares donde se ubican las zonas más pobladas forestalmente, así como donde se convive con un régimen de precipitaciones abundante durante todo el año, la biomasa vegetal crece rápidamente y se regenera a gran velocidad. La biomasa procedente de residuos forestales y agrícolas se presenta, por su disponibilidad, como una de las de mayor potencial para generación eléctrica. El uso energético de biomasa residual forestal es un método de prevención contra incendios y contribuye a la creación de empleo en el medio rural.

Cada año se desperdician miles de MWh de energía en incendios forestales provocados, nuestros bosques se queman, la fauna y la flora autóctona se destruyen y los propietarios pierden sus ahorros invertidos en plantaciones. La valorización de la biomasa forestal procedente de los distintos trabajos forestales públicos y privados, podría paliar los efectos de los incendios retirando parte del combustible mediante las limpiezas y desbroces y la creación de centros logísticos de biomasa, donde aglutinar combustible.

Dada la cantidad de superficie forestal en España se valora la energía de la biomasa como una gran potencialidad. Según el inventario nacional, se estima en 200 millones de toneladas, con una producción anual de 6,2 millones de toneladas [IFN3, 2007]. Buena parte de la superficie forestal o de montes de España pertenece a particulares, en muchos casos estos terrenos no tienen aprovechamiento ninguno ni, por tanto, rentabilidad, y en otros su uso maderero hace que sólo se tenga en cuenta estas posesiones en periodos de tiempo muy largos. El tamaño medio de las fincas también es un factor importante, cuanto más pequeñas son las parcelas más costosa se hace la recogida y movilización de la biomasa. Las parcelas además suelen estar subdivididas y tienen accesos muy difíciles para la maquinaria y en ocasiones imposibles para maquinaria de gran tamaño. La utilización de biomasa presenta ciertas dificultades e inconvenientes relacionados con el suministro, transporte, almacenamiento y su preparación como combustible. Lo más costoso es la retirada de esta biomasa de los montes y su traslado a una zona de almacenamiento. Es por tanto más barata aquella biomasa generada como residuo de las empresas madereras en la corta final de madera, es decir, el serrín, que la abandonada en su origen.

Es necesario avanzar en el desarrollo de las tecnologías que impulsen la creación de centrales termoeléctricas que se aproximen más a un balance neutro de emisiones de CO_2 a la atmósfera con el uso de biomasa residual forestal. Un hito destacable en la producción

eléctrica con biomasa lo constituyó la planta de generación eléctrica de Sangüesa en Navarra (Figura 1.5). Esta planta data del año 2002, se alimenta de pacas de paja de cereales (150.000 toneladas al año) y tiene una potencia de 25 MWe. La producción obtenida en esta planta es de 200.000 MWh /año [IDAE, 2007].

Figura 1.5. *Central térmica de Sangüesa [IDAE, 2007].*

Otro de los hitos en generación eléctrica con biomasa forestal fue la central de Corduente (Guadalajara). En esta central se emplean alrededor de 26.000 toneladas de residuos forestales al año, procedentes de la limpieza y la poda de los montes de la zona, lo que contribuye a evitar incendios y plagas en la zona del Parque Natural del Alto Tajo. La planta tiene una potencia de 2 MWe y fue la primera instalación del país en utilizar únicamente residuos forestales para generar energía eléctrica.

En los últimos años el aumento de la producción eléctrica en base a biomasa está ligado a la creación de numerosas unidades de cogeneración en las cuales se utiliza tanto la energía generada como el calor residual. Este es el caso del Grupo ENCE que emplea los residuos biomásicos para cogeneración en varias plantas papeleras.

Un problema para las empresas eléctricas ha sido la incertidumbre en la disponibilidad de biomasa ya que no solían tener garantizadas las grandes cantidades que se consumirían en una central. Gracias al fomento de la biomasa mediante incentivos económicos a su uso doméstico e industrial se ha conseguido instaurar una red de producción y distribución de biomasa. Sin duda la compactación de la biomasa en forma de pélets estandarizados ha sido una de las claves en el desarrollo del mercado de la biomasa para su uso doméstico.

El uso industrial de la biomasa como recurso energético ha crecido en los últimos años, sin embargo, no ha llegado a cumplir con las expectativas planteadas en los planes gubernamentales (PER 2005-2010, estando actualmente en vigor el PER 2011-2020). Las causas que frenan el aumento de la potencia térmica y sobre todo la potencia eléctrica

instalada en plantas industriales están relacionadas con los costes de la biomasa. Los precios de biomasa no densificada no son asumibles para la industria a partir de cierta distancia ya que su transporte resulta caro. La densificación encarece el producto a la par que disminuye los costes de transporte y permite una disponibilidad a mayor distancia.

La biomasa también puede alimentarse como parte del flujo de combustible en procesos industriales en el que el combustible principal sea el carbón. La mezcla de biomasa con el carbón es muy interesante, ya que aporta mejoras en la eficiencia de la combustión del carbón. La biomasa tiene un porcentaje de volátiles alto, muy superior al del carbón lo cual puede resultar beneficioso para el comportamiento de la mezcla en una caldera, especialmente en lo que respecta a la disminución de emisiones gaseosas.

Torrefacción

Una de las principales dificultades para el empleo de la biomasa es su manejabilidad, ya que por lo general su densidad es baja, tiene contenidos muy elevados en humedad y un carácter fibroso que dificulta su alimentación a cualquier sistema. La torrefacción es una técnica de pretratamiento de la biomasa que alivia estos problemas. Consiste en someter la biomasa a temperaturas entre 200 y 300 ^{o}C, generalmente en atmosfera inerte. De esta forma el material sufrirá cambios más allá de su secado, produciéndose las primeras etapas de pirólisis. Cuando los materiales lignocelulósicos sobrepasan temperaturas en torno a 150 ^{o}C, las moléculas de lignina comienzan a romper enlaces débiles, tiene lugar una liberación de CO_2, CO y algunos hidrocarburos de moléculas de pequeño tamaño. Por tanto hay una pequeña reducción en la cantidad de materia volátil de la biomasa torrefactada.

La torrefacción confiere a la biomasa propiedades muy interesantes como la hidrofobicidad, que permite su almacenamiento sin que aumente su contenido de humedad, problema muy común en las zonas de clima húmedo. También mejora su comportamiento en molienda, dado que la torrefacción fragiliza las fibras de la biomasa. En estudios de nuestro Grupo de Investigación (PrEM) se realizaron pruebas de molienda de biomasa torrefactada a distintas temperaturas y tiempos. Los resultados muestran cómo la torrefacción a pesar de requerir energía puede compensar este aporte energético con una menor demanda de energía para su molienda y la consiguiente mejora de su manejabilidad [Arias, 2008].

La gasificación de biomasa constituye otra de las opciones para su empleo como combustible, tanto en turbinas de gas, como para la obtención de otros combustibles derivados como el hidrógeno, o su empleo en cocombustión que se describirá en el apartado siguiente.

1.4 Cocombustión de carbón y biomasa

Las centrales térmicas de carbón pulverizado son grandes instalaciones con potencias instaladas normalmente en el entorno de los 150-300 MWe por grupo generador. Por tanto son también grandes consumidores de combustibles fósiles y emisores de CO_2. Se denominan además fuentes estacionarias y son susceptibles de actuar con mayor facilidad que las fuentes difusas en la reducción de emisiones y la captura de CO_2. La cocombustión consiste en el empleo de carbón y biomasa como combustibles para la generación conjunta de energía. La sustitución de parte del carbón por biomasa es ya un éxito en algunas centrales térmicas fuera de España. Sin embargo, no se ha realizado hasta la fecha de forma continuada más allá de periodos de pruebas en algunas centrales térmicas en España.

La cocombustión se refiere, fundamentalmente, a la que se lleva a cabo en centrales térmicas de carbón y consiste en sustituir un porcentaje del combustible convencional por biomasa. Es una tecnología que se usa ya en diversos países como Estados Unidos, Australia, Austria, Reino Unido, Alemania, Finlandia o Suecia. Por ejemplo, en Holanda la cocombustión se lleva a cabo en prácticamente todas sus centrales de carbón. La cocombustión es una alternativa para aumentar la contribución de la biomasa al mercado eléctrico español en un corto plazo de tiempo. Las ventajas de la cocombustión frente a una central térmica cuyo combustible sea sólo biomasa, son las siguientes:

- Menor inversión por unidad de potencia instalada. Se utiliza gran parte de la infraestructura existente de la central y sólo se requiere inversión para adaptarla al empleo de biomasa.
- Generación de energía eléctrica con un rendimiento superior. En una planta de biomasa se obtienen rendimientos en torno al 23% mientras que en las centrales de cocombustión los rendimientos superan el 30%.
- Mayor flexibilidad en la operación, ya que una central de cocombustión se adapta fácilmente a la disponibilidad de biomasa en cada momento gracias a que puede seguir operando con combustible convencional en mayor proporción o de forma exclusiva.

Existen diversas formas de aprovechar residuos de biomasa forestal conjuntamente con carbón, dependiendo de la forma que se introducen en la cámara de combustión: cocombustión en paralelo, directa o indirecta.

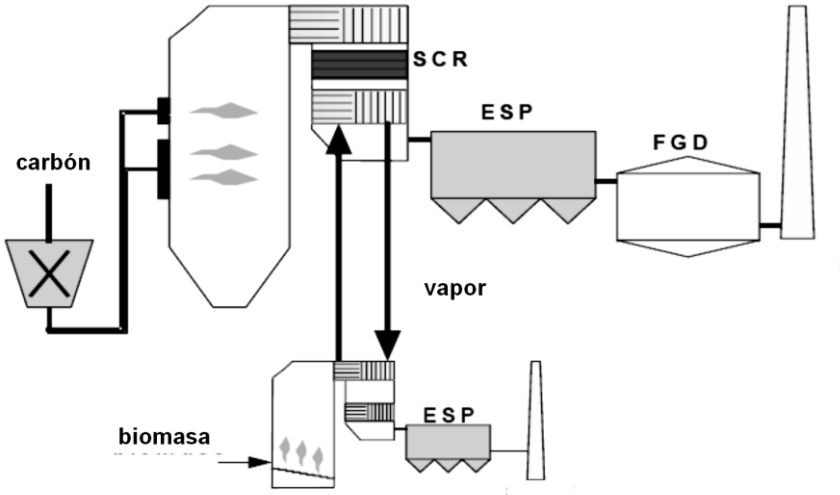

***Figura 1.6**. Combustión en paralelo.*

En la ***cocombustión en paralelo***, la biomasa y el carbón se queman en dos calderas independientemente (Figura 1.6). El vapor producido en la planta de biomasa se incorpora al circuito de vapor de la caldera de carbón. La biomasa tendrá en este caso otro proceso de combustión, de esta forma tendremos circuitos independientes para la biomasa y el carbón. No se trata en este caso de una cocombustión propiamente dicha sino más bien un aprovechamiento conjunto de la energía del carbón y la biomasa.

En la ***cocombustión indirecta*** se realiza todo el proceso de tratamiento de la biomasa, incluyendo su gasificación, en otra planta, de forma independiente al carbón, y los gases combustibles generados en el proceso se llevan a la caldera de carbón para su combustión (Figura 1.7). Esta metodología evita los problemas que se podrían originar en los molinos (atascos, incendios), ya que estos equipos han sido diseñados para tratar con carbón. De igual manera, también se reducen los posibles problemas que pudieran aparecer en la caldera por la utilización de un combustible distinto del de diseño, tales como la disminución del rendimiento, o el incremento de la corrosión y del ensuciamiento, por los componentes minerales que pueden contener algunos de los recursos biomásicos utilizados (K, Na). Asimismo, se puede dar una salida a las cenizas de carbón ya que si queman los dos combustibles en la misma caldera, suelen dar lugar a unas cenizas con una composición que no se ajusta a las especificaciones requeridas por la industria cementera. No obstante, la inversión necesaria para adaptar una central a esta tecnología es muy costosa y sólo se ejecuta en casos muy especiales.

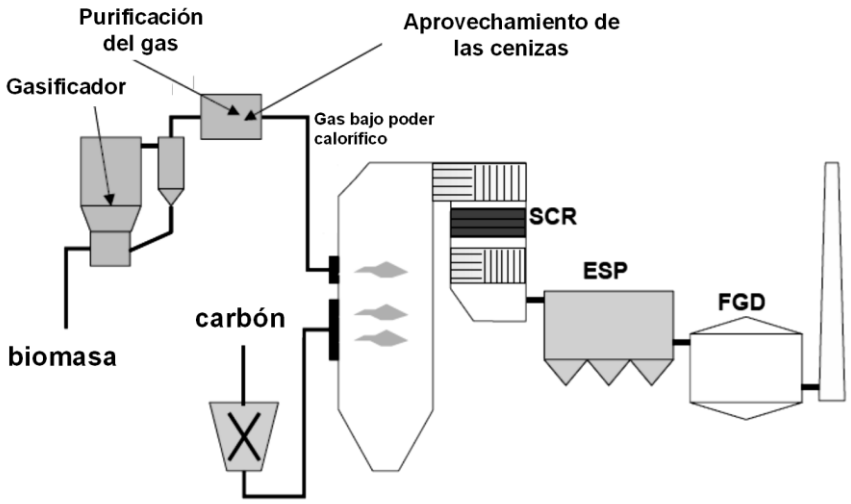

Figura 1.7. *Esquema de cocombustión indirecta.*

En la ***cocombustión directa*** la biomasa se alimenta directamente a la caldera junto con el carbón (Figura 1.8). Esta opción presenta a su vez, tres alternativas:

- Mezcla previa de biomasa y carbón e introducción conjunta en la caldera. En esta disposición la mezcla puede realizarse antes o después de los molinos y, en este último caso, se procede a la molienda de la biomasa de forma separada. La mezcla antes de molinos es la opción más sencilla y la que conlleva unos menores costes de capital. Sin embargo, es la que conlleva un riesgo más elevado de interferencia con la marcha de la caldera, que ha sido diseñada para carbón, originándose los problemas principalmente en los molinos donde la biomasa se puede acumular en ocasiones. Por este motivo se suelen realizar las mezclas para bajas relaciones de biomasa/carbón (menor del 10% en base energética). Esta opción es la que más se ha usado en las centrales de cocombustión del Reino Unido.
- Introducción de la biomasa en la caldera de forma independiente al carbón. En este caso se pueden utilizar los propios quemadores de carbón o se pueden instalar quemadores diseñados para la biomasa. En el primer caso la inversión requerida es mínima. Podemos introducir la biomasa a la misma altura de la caldera que el carbón o en una zona superior. Si los quemadores de biomasa están situados a la misma altura crearemos un combustible rico en volátiles que ayudará en la combustión del carbón y su ignición se producirá muy rápidamente al encontrarse con el oxígeno nada más entrar en la cámara de combustión. En cambio si los quemadores de biomasa se encuentran en una zona superior, por encima de la zona principal de combustión del carbón, se crea una zona rica en combustible y baja en oxígeno puesto que gran parte de este oxígeno ya ha sido consumido en la combustión del carbón. Este método es

empleado en cocombustión y permite una reducción de la concentración de NO_x al pasar los humos de combustión del carbón por una atmósfera reductora.

- Otro método de cocombustión directa consiste en quemar la biomasa en una parrilla situada en la parte inferior de la caldera de carbón. Esta es una opción más adecuada para calderas nuevas ya que se necesita espacio libre en la parte inferior de la caldera. La mayor ventaja de esta alternativa reside en los menores pretratamientos a que es necesario someter a la biomasa.

En este trabajo, se estudiará la combustión de la mezcla en una alimentación conjunta de la biomasa y del carbón; es decir, cocombustión directa en una caldera de carbón pulverizado.

La adaptación de una central térmica al empleo de biomasa en cocombustión implica modificaciones menores en varios sistemas de la central. Requieren inversiones modificaciones y paradas, pero su coste es menor que la construcción de una central exclusivamente de biomasa. Los problemas potenciales para una central térmica trabajando en cocombustión pueden surgir principalmente en la manejabilidad de la biomasa, o en la aglomeración de las cenizas.

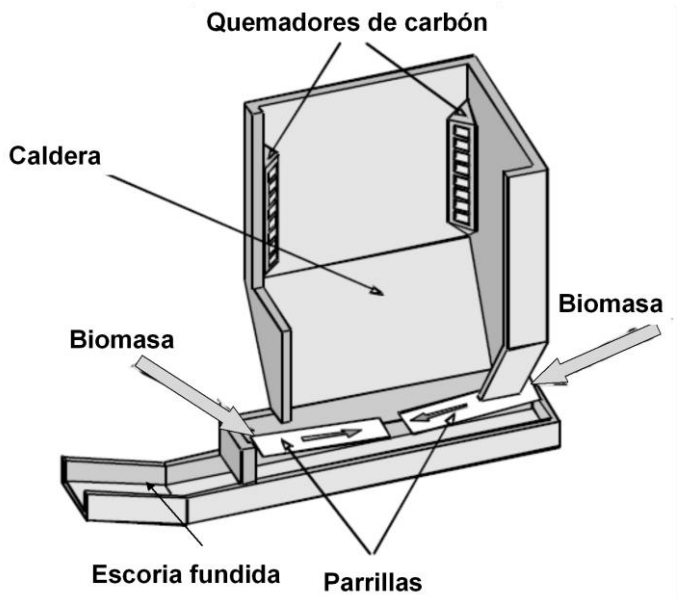

Figura 1.8. *Cocombustión directa*

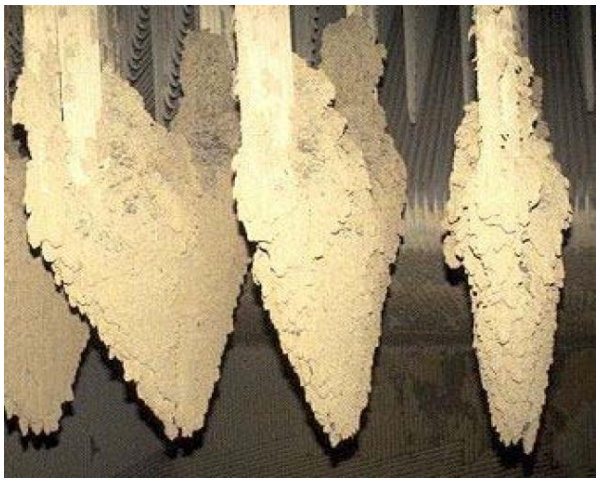

Figura 1.9. *Ensuciamiento en tubos de caldera de carbón pulverizado tras ensayos de cocombustión con biomasa [Cieplik, 2011].*

La variada composición de la biomasa puede originar problemas en el proceso de combustión, y estos además tendrán su efecto en la eficacia y las emisiones. Así, se pueden encontrar biomasas con humedades comprendidas entre 10 y 50% en peso. Esta humedad penaliza la eficacia del proceso dado que debe emplearse energía para la reducción normalmente a niveles por debajo del 10%. Los principales retos para obtener las mayores disminuciones posibles en emisiones de CO_2 en cocombustión se centran en la eficacia de la caldera y en el pretratamiento de biomasa. En algunos experimentos de cocombustión realizados en centrales de carbón pulverizado se ha notado una disminución de la eficacia de la caldera cercana al 1% por cada 10% (% en base energía) de biomasa añadida [Sebastián, 2011].

El contenido de cenizas es otro parámetro importante en la biomasa y puede variar desde el 1 al 20%, sin embargo debe tenerse en cuenta no sólo la cantidad de cenizas sino también su composición, ya que pueden presentar elevados contenidos en sílice, potasio o cloro con los problemas que ello puede originar [Arias, 2008].

Los problemas derivados de la presencia de estos compuestos se deben al punto eutéctico de determinadas composiciones de los óxidos de las cenizas con el consiguiente descenso de la temperatura de fusión de las cenizas, lo que provoca ensuciamientos indeseados en los tubos y paredes del hogar reduciendo la transmisión de calor.

Además, la biomasa presenta normalmente contenidos en otros elementos como nitrógeno desde 0,1 al 2% o azufre desde el 0 al 0,5% que provocan gases contaminantes en su combustión. Estos contenidos también suelen ser menores que los del carbón con lo que en cocombustión suele darse un notable descenso de las emisiones de SO_2 y NO_x.

1.5 Captura, Transporte y Almacenamiento de CO_2

La captura y almacenamiento de CO_2 (CAC), constituye una clara alternativa para reducir de forma drástica las emisiones debidas al sector energético; sin embargo los procesos de separación de CO_2 a gran escala tienden a ser costosos y a disminuir la eficacia energética. Por este motivo existe una intensa actividad de investigación en todo el mundo para desarrollar y mejorar estos procesos que permitan la CAC de una forma más competitiva y eficaz.

1.5.1 Captura de CO_2

Existen diferentes métodos para la separación del CO_2 que se pueden agrupar en tres diferentes grupos en el ámbito energético:

- **Postcombustión.** Consiste en separar el CO_2 del resto de gases después de la combustión.
- **Precombustión**. Mediante sistemas de gasificación se produce un gas de síntesis, compuesto principalmente por H_2 y CO. El CO se transforma en CO_2 mediante la reacción de desplazamiento con vapor de agua, y posteriormente se procede a la separación de este CO_2 de la corriente de gas rica en H_2.
- **Oxicombustión**. Es necesario un fraccionamiento del aire antes de la combustión para así realizar la combustión con O_2 puro mezclado con humos recirculados, obteniendo unos gases de chimenea con elevado contenido en CO_2.

La separación en procesos industriales no energéticos puede ser muy diversa y engloba otros procesos diferentes a los anteriores. En la Figura 1.10 se exponen esquemáticamente cada una de las formas de captura de CO_2.

Las *tecnologías de captura de CO_2 postcombustión* tienen la ventaja de ser aplicables a la corriente de humos de cualquier central térmica ya existente, sin incurrir en ninguna modificación de sus componentes. Es la opción, por tanto, de menor riesgo empresarial; sin embargo la inversión que supone limitará su implantación a aquellas centrales con perspectivas de larga duración, es decir, las que con las mejores tecnologías disponibles alcancen mayor rendimiento.

Una de las opciones de separación postcombustión se basa en el desarrollo de materiales adsorbentes regenerables. Esta línea está siendo investigada en nuestro Grupo de investigación (Procesos Energéticos y Reducción de Emisiones, PrEM), desarrollando adsorbentes sólidos de bajo coste con funcionalidades específicas para la adsorción preferencial de CO_2. La investigación se centra fundamentalmente en potenciar la química superficial del adsorbente, mediante distintas técnicas, para favorecer la captura de CO_2. Se

hace especial hincapié en la obtención de un sólido de bajo coste y fácil regeneración [González, 2013].

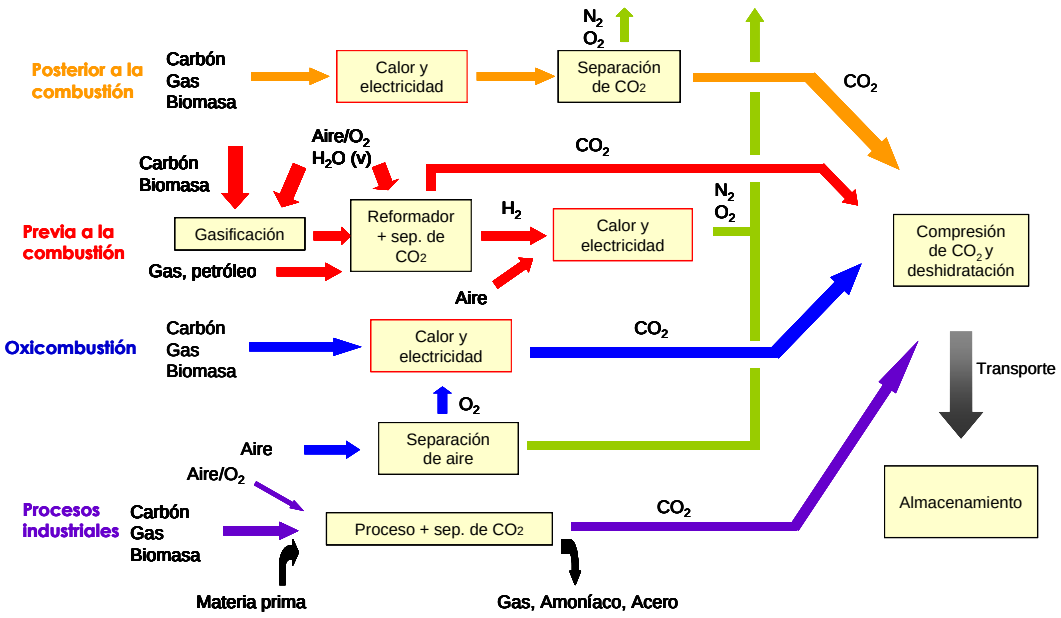

Figura 1.10. *Esquema de diferentes procesos de separación de CO_2 [IPCC, 2005].*

Otra de las rutas de mayor desarrollo es la carbonatación-calcinación, que se basa en la facilidad de la reacción del CO_2 con óxido de calcio (CaO) para producir polvo de caliza ($CaCO_3$). Son necesarios al menos dos reactores interconectados, un carbonatador y un calcinador, que operan a presión atmosférica y en un intervalo de temperaturas de 650 – 700ºC y 850 – 950ºC respectivamente. Esta tecnología ya cuenta con plantas piloto como la de 1,7 MWt instalada junto a la central termoeléctrica de lecho fluido de La Pereda en Asturias. Tiene una capacidad de captura de ocho toneladas de CO_2 al día con eficacias de captura del orden del 90 por ciento [ENDESA, 2014].

Los *tratamientos precombustión* son aquellos en los que el CO_2 es retirado de la corriente de gases antes de la combustión, para ello es necesaria una gasificación del combustible. Uno de los procesos de separación precombustión es el empleo de la reacción de desplazamiento de gas de agua (wáter gas shift, WGS), en la que tIene lugar la reacción del combustible gasificado (CO + H_2) con vapor de agua dando lugar a un gas compuesto por CO_2 y H_2 del cual se separaría el H_2 mediante el proceso de captura. El proceso es versátil y está aún por demostrar su viabilidad económica debido a que la complejidad del proceso conlleva una planta con gran inversión y alto riesgo.

En la central GICC de 330 MWe de ELCOGAS en Puertollano, se ha construido una planta piloto integrada en la planta GICC que trata 3.600 Nm^3/h de syngas. El proceso consiste en una

unidad shift para transformar el CO en CO_2, una unidad de separación de CO_2 mediante absorción con aminas y una unidad de purificación de H_2 (PSA). Los sistemas auxiliares y todo el control se integran en el GICC existente [ELCOGAS, 2014].

El *proceso de oxicombustión* consiste en realizar la combustión con oxígeno puro, es decir, en ausencia de nitrógeno. Debido a las altas temperaturas que se alcanzarían es necesaria la recirculación parcial de los humos para diluir el O_2 comburente. Los gases resultantes del proceso de combustión serán una mezcla mayoritaria de CO_2 y vapor de agua. La condensación del vapor de agua permite obtener una corriente de CO_2 casi listo para su compresión y almacenamiento. Tras el secado, desulfuración y purificación, el CO_2 se encuentra en las condiciones aptas para su almacenamiento. La implementación exitosa de la tecnología de oxicombustión depende de la plena comprensión de las dificultades que pueden surgir a partir de la sustitución de nitrógeno por CO_2 en la corriente de oxidante [Kazanc, 2011].

El vapor de H_2O se separa fácilmente del efluente por condensación, aunque persistirán todavía compuestos como los óxidos de nitrógeno, de azufre, mercurio o metales cuyas concentraciones deben ser controladas, por lo que es conveniente que las centrales de cualquier tipo de captura de CO_2 dispongan de unidades de purificación del CO_2 (CPU). Los contenidos en algunas sustancias minoritarias pueden producir problemas en las cadenas siguientes de compresión, transporte e inyección. Las concentraciones máximas de impurezas en la corriente gaseosa confrontan el funcionamiento de la CPU con la etapa posterior de transporte. El objetivo consiste en disminuir la concentración de las impurezas y minimizar las purgas y por tanto las emisiones debidas a la CPU. Se pueden llegar a alcanzar purezas del CO_2 cercanas al 100% pero el coste sería prohibitivo.

Las unidades CPU de las plantas piloto construidas hasta la fecha se caracterizan por su gran tamaño y elevada complejidad. Una vez obtenida la corriente de CO_2 es necesaria la compresión de los gases, que no resulta muy costosa y es fácilmente asimilable para una planta de generación eléctrica. Posteriormente, se debe transportar el CO_2 licuado hasta el punto de almacenamiento.

1.5.2 Transporte de CO_2

El CO_2 se transporta en la actualidad mediante tuberías (ceoductos) similares a los gaseoductos utilizados por la industria del gas natural. Si la fuente de CO_2 está muy alejada del área de almacenamiento, el transporte también puede hacerse en buques. El despliegue generalizado de la tecnología CAC requerirá una expansión equivalente de la red de ceoductos. Actualmente existen en el mundo más de 5.000 kilómetros de tuberías que transportan CO_2 [PTECO2, 2013a].

En la plataforma de CIUDEN en Cubillos del Sil (León) se está experimentando el transporte de CO_2. Esta instalación puede operar con CO_2 capturado desde la CPU (Unidad de Compresión y Purificación) u operar con CO_2 comercial. El equipo de transporte también dispone de 6 zonas experimentales para las pruebas de despresurización, fugas, fractura, corrosión, instrumentación y caída de presión.

Figura 1.11. *Recreación de un pozo de inyección de CO_2 [CIUDEN, 2014]*

1.5.3 Almacenamiento de CO_2

En la actualidad se está produciendo un auge considerable en los procesos que pretenden la valorización del CO_2 y su uso como producto en vez de su consideración de residuo. Sin embargo, su demanda en el mercado es muy inferior a las cantidades que supondrían la implementación de los procesos de captura de CO_2. Por ello están surgiendo investigaciones para el uso novedoso del CO_2 como la síntesis de biocombustibles a partir del crecimiento de algas [PTECO$_2$, 2013b]. No obstante, la mayoría de estos proyectos se encuentran en fase de laboratorio o de demostración a escala piloto. Por tanto, está actualmente aceptado que la mayor parte del CO_2 que se capture habrá de ser almacenado en yacimientos geológicos profundos. El CO_2 generado industrialmente en los procesos de combustión quedaría aislado de la atmósfera, minimizando así el efecto invernadero a escala global [PTECO$_2$, 2012]. Sin embargo, los riesgos que pueden derivarse de este método de almacenamiento inciden directamente en su aceptación pública [Solà, 2008]. La incertidumbre y, en otras ocasiones, el desconocimiento provocan desconfianza popular. Existe cierta resistencia al almacenamiento geológico llegando a estar prohibido por ley en algunos países como Alemania o Italia.

La identificación y selección de emplazamientos adecuados para almacenar volúmenes significativos de CO_2 constituye un aspecto clave. La identificación y selección de estos emplazamientos incluye la evaluación geológica de sistemas de almacenamiento como son las formaciones permeables profundas con agua salina, los yacimientos de hidrocarburos agotados y/o las capas de carbón profundas [Hurtado, 2008].

La profundidad de la formación geológica para almacenamiento ha de ser superior a 800 metros. Se almacena a tales profundidades, incluso cercanas a 3.000 metros o más, como en el caso de Lacq en Francia donde se hace a 4.500 metros. A presiones equivalentes a las que imperan a unos 800 metros de profundidad, el CO_2 sufre un brusco incremento en su densidad, lo que permite que la misma cantidad de CO_2 pueda almacenarse en volúmenes muchísimo menores en profundidad que los requeridos en superficie. En estos emplazamientos el CO_2 se encontraría en estado supercrítico, que como se puede ver en la Figura 1.12 corresponde a 31,1°C y 7,38 MPa.

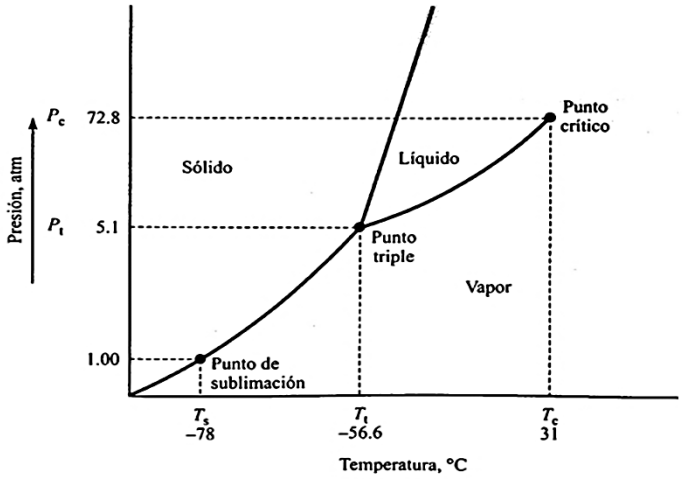

Figura 1.12. *Diagrama de fases del CO_2.*

Uno de los aspectos tecnológicos más importantes en el almacenamiento geológico de CO_2 es la inyección de éste en el seno de la roca almacén a grandes profundidades. En general, los emplazamientos para almacenar CO_2 deberán tener una formación almacén con adecuadas capacidades de almacenamiento e inyectividad, una roca muy porosa y permeable, denominada "roca almacén", a su vez recubierta por una "roca sello" que impide su desplazamiento hacia la superficie. Todo ello para garantizar su aislamiento, ya que la roca absorbe el CO_2 líquido a través de sus poros. Y un marco geológico suficientemente estable que evite comprometer la integridad del almacén [Ruiz, 2008].

En el Proyecto Singular Estratégico "Tecnologías Avanzadas de Generación, Captura y Almacenamiento de CO_2", promovido por el Ministerio de Ciencia e Innovación, se ha realizado un estudio acerca de los criterios de selección de almacenamientos y de las opciones para almacenar CO_2 en el territorio español. Este estudio ha requerido, en primera instancia, la identificación y selección de formaciones y/o estructuras geológicas que cumplan los criterios de idoneidad necesarios para garantizar la seguridad a largo plazo del CO_2 inyectado.

Las grandes cuencas sedimentarias ofrecen, en general, escenarios favorables para el almacenamiento definitivo de CO_2, bien como formaciones permeables profundas con aguas

salobres, o bien como estructuras que han contenido petróleo o gas. En la Península Ibérica se han estudiado las cuencas del Duero, Almazán y Ebro, utilizando la información generada en las campañas de exploración de petróleo, que está contenida en el Archivo Nacional de Hidrocarburos. Se han seleccionado una serie de formaciones que, por sus características relativas a disposición tectoestructural, extensión, profundidad, porosidad y permeabilidad, entre otros parámetros, podrían constituir futuros almacenamientos. Se ha prestado también una especial atención a las formaciones sello, que garantizarían la estanqueidad de los diferentes almacenes. Estas formaciones se han modelado mediante un SIG (Sistema de Información Geográfica) para la delimitación de áreas y volúmenes idóneos para inyectar CO_2 y se ha realizado una estimación preliminar de sus respectivas capacidades de almacenamiento, que si bien constituyen aún aproximaciones, permiten apostar por el potencial del territorio nacional para almacenar CO_2 a escala industrial.

A nivel mundial existen capacidades enormes en diferentes cuencas, en concreto algunas de ellas como la formación de Utsira en el Mar del Norte parece que podría almacenar el CO_2 generado en las centrales europeas durante 600 años [Statoil, 2010]. Actualmente se están realizando proyectos de almacenamiento de CO_2 en lugares tan dispares como el desierto (In Salah, Argelia) o el Mar del Norte (Sleipner, Noruega). En estos emplazamientos se separa el gas natural del CO_2 que contiene y se inyecta este CO_2 en yacimientos salinos cercanos. En la Figura 1.13 se muestra un esquema del proceso de almacenamiento de CO_2.

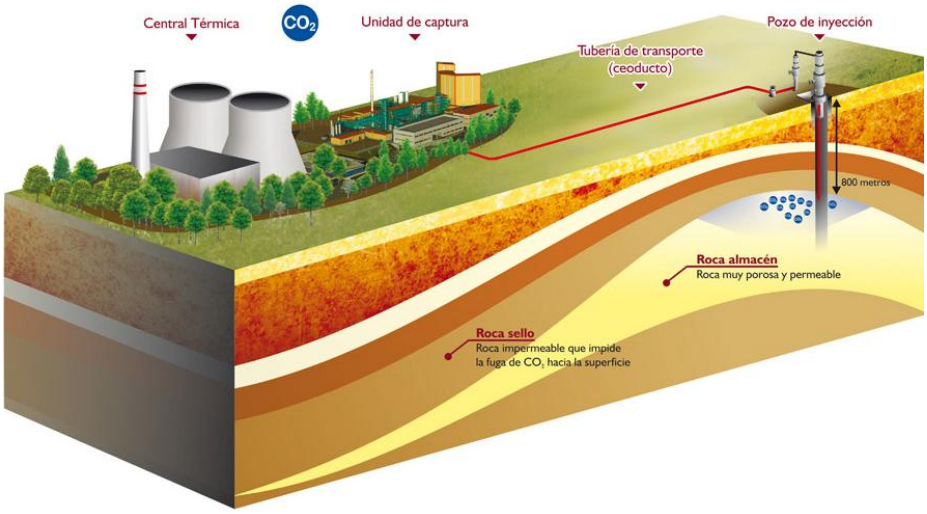

Figura 1.13. *Esquema de un proceso de inyección de CO_2 en un almacenamiento geológico [CIUDEN, 2014].*

También se realizan desde hace décadas, inyecciones de CO_2 para la recuperación mejorada de petróleo, como es el caso del yacimiento de Weyburn en Canadá, donde el CO_2 procedente de una planta de gasificación ubicada en Dakota del Norte (EEUU) es transportado una distancia de 330 km por tuberías hasta el yacimiento donde se han logrado recuperaciones

adicionales de petróleo gracias a la inyección de CO_2. El CO_2 inyectado aumenta la presión en el yacimiento, disuelve en parte los hidrocarburos de los poros de la roca y ayuda a su circulación a lo largo de las porosidades de la roca almacén, ya que su viscosidad mejora al mezclarse con el CO_2 licuado. Además del yacimiento de Weyburn, existen otros proyectos donde se ha inyectado CO_2, generalmente ligados a la recuperación mejorada de hidrocarburos o la purificación del gas natural.

En España (Figura 1.14) se vienen realizando estudios de viabilidad desde hace unos años y actualmente se centran en dos cuencas: la cuenca del Ebro y la cuenca del Duero. Asimismo, también se están estudiando otras cuencas en el litoral, que podrían permitir almacenamientos *offshore*, lejos de la costa en la plataforma marina.

El Programa de Almacenamiento Geológico de CO_2 de CIUDEN tiene por objetivo demostrar que es técnicamente factible y medioambientalmente seguro a largo plazo. Se desarrollarán metodologías y tecnologías de:

- Caracterización de la geología profunda.
- Modelización aplicada al almacenamiento geológico de CO_2.
- Ingeniería de almacenamiento e inyección del CO_2.

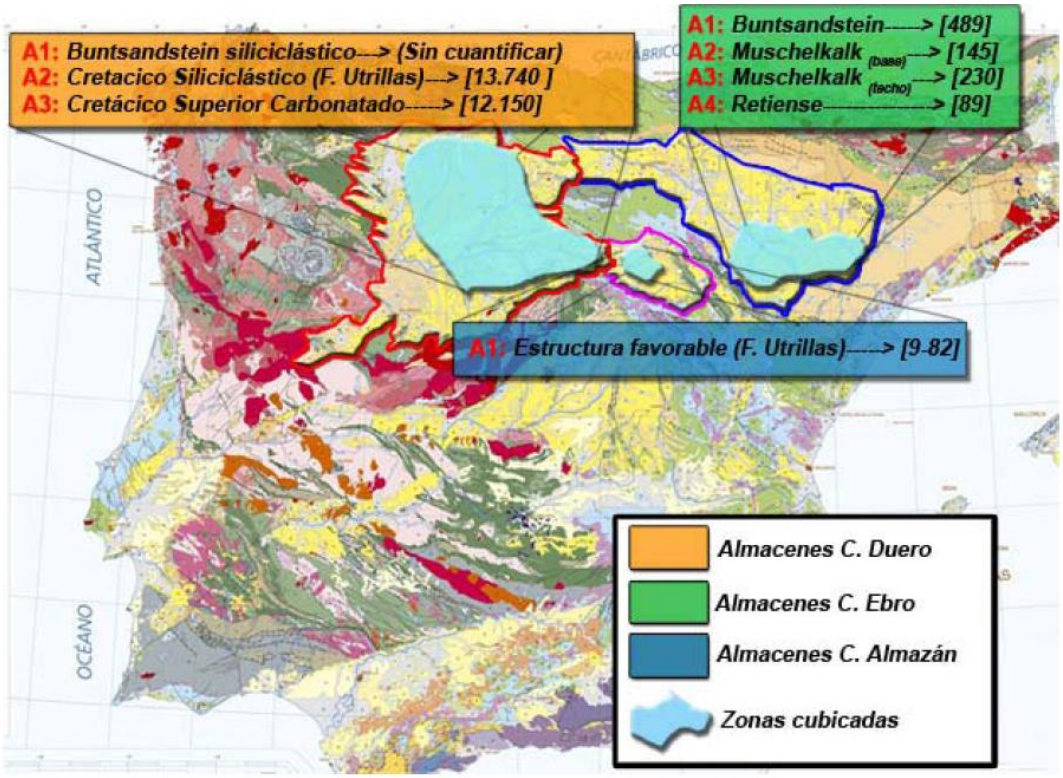

***Figura 1.14**. Estructuras favorables para el almacenamiento de CO_2 en España [Prado, 2008].*

Varios grupos de investigación de distintas universidades, empresas y organismos han colaborado durante años para buscar un emplazamiento para la Planta de Desarrollo Tecnológico de CIUDEN. Como resultado, se ha seleccionado una pequeña estructura geológica anticlinal, que se encuentra a 1.400 metros de profundidad en el subsuelo de la Merindad del Río Ubierna (Burgos), concretamente en la localidad de Hontomín. Esta estructura fue seleccionada porque:

- Está ubicada en un ámbito petrolífero, por lo que existe gran cantidad de información geológica del subsuelo profundo.
- Su forma de cuenco invertido permite que el CO_2 inyectado se quede confinado en un espacio definido.
- Tiene un tamaño adecuado que facilita la investigación; es pequeña y, por tanto, fácilmente controlable.
- Está a una profundidad adecuada (más de 800 metros).
- Las rocas sello y almacén tienen las características adecuadas.
- Las rocas que en esta zona se encuentran en profundidad afloran en superficie en su entorno regional, lo que facilita su muestreo y estudio.

Mediante la inyección de CO_2 en el yacimiento de Hontomín, el proyecto de investigación pretende determinar cómo reducir los costes de todas las etapas implicadas en esta tecnología. Se inyectarán cantidades de CO_2 suficientes para realizar investigaciones asociadas al almacenamiento geológico, desarrollar metodologías y tecnologías, evaluar el comportamiento del CO_2 en profundidad y reforzar los conocimientos sobre seguridad.

El seguimiento de la evolución del CO_2 inyectado es fundamental para demostrar la tecnología en otras estructuras geológicas de la cuenca del Duero. Dado el tamaño reducido de la estructura de almacenamiento es factible llegar a su colmatación en tiempos cortos. Acortando los plazos se puede tener la información de todo el proceso y la evolución del CO_2 en la estructura de almacenamiento geológico.

1.6 Tecnología de Captura de CO_2 mediante oxicombustión

1.6.1 Esquema general

La oxicombustión con recirculación de humos fue propuesta de forma prácticamente simultánea por Abraham et al. [Abraham, 1982] y Horn y Steinberg [Horn, 1982]. En la publicación de Abraham et al. se describe la oxicombustión como medio para obtener CO_2 de alta pureza de cara a la recuperación mejorada de petróleo. Horn y Steinberg [Horn, 1982] plantean la oxicombustión en respuesta al impacto de las emisiones de CO_2 en la generación de energía mediante combustibles fósiles. La concienciación en la problemática de las

emisiones de CO_2 a mediados de la década de los años 90 ha contribuido al impulso de la oxicombustión como una opción para la captura de CO_2.

Este proceso tiene como objetivo obtener un CO_2 muy puro a la salida de los humos de la cámara de combustión en ausencia casi total de N_2. Para ello, es necesario que la combustión se realice con oxígeno en lugar de con aire. De esta forma se evita la dilución del CO_2 en la corriente de humos, que en un proceso de combustión convencional estaría compuesta mayoritariamente de nitrógeno.

Con la oxicombustión se pueden obtener unos humos con gran concentración de CO_2, ya que los productos de la combustión del carbón son principalmente CO_2 y vapor de agua, y, en mucha menor medida (concentraciones de ppm) SO_2 y NO_x. El vapor de H_2O se puede separar fácilmente por condensación, obteniéndose una concentración de CO_2 del orden de 90-95 %. Esto permitirá la licuación directa del CO_2 y su posterior almacenamiento.

La temperatura de llama en la combustión de carbón y biomasa con oxígeno puro es muy elevada, lo que daría lugar a problemas de resistencia de materiales en el hogar. Para disminuir esa temperatura de llama se ha de mezclar el oxígeno con parte de los gases de salida de la cámara de combustión. Estos humos recirculados se mezclan con el O_2, que es el comburente, y entran en la caldera de nuevo. Los gases que estarán presentes como impurezas son SO_2, H_2O, CO y NO_x. En la Figura 1.15 se puede ver un esquema del proceso de oxicombustión y las unidades que lo componen.

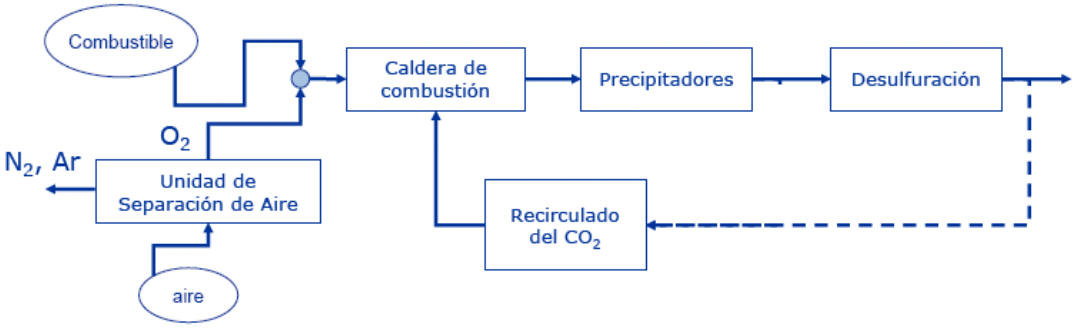

Figura 1.15. *Esquema del proceso de oxicombustión.*

El oxígeno necesario para la oxicombustión se obtiene del aire mediante procesos de fraccionamiento. Estas unidades de separación de aire (ASU del inglés Air Separation Unit) funcionan como componentes independientes de la central y suministran el caudal necesario de O_2. El fraccionamiento del aire antes de la combustión tiene el valor añadido de obtener N_2 como subproducto, que puede ser usado para otros fines como por ejemplo, inertización de atmósferas en la propia central. Por otro lado, las tecnologías de fraccionamiento de aire están bastante maduras en este momento, existiendo plantas muy desarrolladas en este campo. Sin

embargo, los requerimientos energéticos de estas unidades son altos y el coste del O_2 es el principal inconveniente a salvar para demostrar la viabilidad económica de esta tecnología.

El nitrógeno presente en el aire no entra en la cámara de combustión, ya que es retirado en la unidad de separación de aire con lo que se impide la formación de NO_x de origen térmico. Los óxidos de nitrógeno presentes en los humos serán únicamente aquellos provenientes de la composición del combustible, carbón o biomasa. También pueden provenir de aire que penetra en distintas partes del proceso como puede ser en los molinos.

Las partículas en suspensión de los humos son retenidas mediante precipitadores electrostáticos de forma análoga a las centrales termoeléctricas convencionales. Se han encontrado algunas diferencias en la composición química de las cenizas de la combustión normal y la combustión en atmósfera de oxicombustión debido a la alta presión parcial de CO_2 en la corriente de humos. También se ha de controlar el grado de quemado del carbón, dado que las partículas de inquemados podrían dar lugar a problemas de ensuciamiento en las superficies de los intercambiadores así como disminuir la eficacia del proceso de combustión [Fryda, 2010].

La ventaja principal de la oxicombustión frente a las otras tecnologías de captura es la pureza del CO_2 a la salida del proceso, con bajas concentraciones de N_2 y menores aún de NO_x. La calderas tendrán un tamaño menor que las de aire de igual potencia, dado que la concentración de O_2 es mayor y el flujo de reciclo será menor que el N_2 que se alimentaría con el aire.

Dada la necesidad de añadir equipos y procesos auxiliares respecto a las centrales térmicas convencionales, cobra mayor relevancia la eficiencia e integración energética de los equipos del proceso. Las nuevas necesidades respecto a una central convencional se deben a la necesidad de separar el oxígeno del aire y, por otro lado, de comprimir el CO_2 hasta el estado supercrítico. Ambos procesos requieren un aporte de energía extra que la propia planta debe asumir disminuyendo la eficiencia. Algunos autores tasan esta pérdida de eficacia en un 8 % sobre eficacia bruta [Seepana, 2010], ó 9 % sobre eficacia neta [Buhre, 2005].

1.6.2 Unidad de producción de oxígeno

La unidad de producción de oxígeno, es uno de los elementos más críticos en el diseño de una central de oxicombustión. Es una unidad con un consumo de energía muy relevante dentro de todos los sistemas auxiliares y su desarrollo para minimizar el consumo energético es clave en la viabilidad técnica de la tecnología de oxicombustión. Las tecnologías actuales para la producción de oxígeno han sido desarrolladas debido principalmente a las necesidades de la industria del acero. Actualmente destacan 3 tecnologías en la producción de oxígeno de alta pureza, separación por membranas, destilación criogénica y ciclos de adsorción con oscilación de presión (PSA). La destilación criogénica es la única tecnología actualmente capaz

de suministrar en cantidad y calidad O_2, según las necesidades de diseño de una planta de oxicombustión a gran escala. El oxígeno debe suministrase con una pureza del 95-97 %. Las impurezas presentes en esta corriente de O_2 al 95 % de pureza serán fundamentalmente Ar (3%) y N_2 (2%) [Santos, 2013; Perrin, 2013].

Para una central en torno a 500 MWe se requeriría una cantidad en torno a 10.000 toneladas al día de O_2. Estos requerimientos no son factibles por ninguna ASU actual, por tanto es necesaria la instalación de varios módulos de menor producción para cubrir la demanda de O_2. Los avances en la tecnología de destilación criogénica aumentan la disponibilidad de O_2 con plantas más eficientes, y un escalado progresivo. Con el escalado descienden los costes, y gracias también a la integración energética, se ha reducido la demanda energética. Se espera llegar a un 25-35 % menos de energía necesaria para producir O_2, con el objetivo de llegar a 140 KWh/t O_2, lo que supondría una disminución de la penalización energética del 10 %.

1.6.3 Plantas de demostración de tecnologías de oxicombustión

El objetivo global de la tecnología de oxicombustión es la demostración técnico-económica para el año 2020. Para lograr este objetivo se han construido ya plantas piloto en diversos lugares del mundo. Para llegar a la demostración de la tecnología es necesario construir plantas de mayores potencias progresivamente. Uno de los mayores hitos en el escalado ha sido la planta de Vattenfall en Schwarze-Pumpe (Alemania). La planta piloto de oxicombustión de lignito en una caldera de carbón pulverizado, que empezó las primeras pruebas en 2008, tiene un solo quemador de 30 MWt, y las instalaciones correspondientes para tratamiento de CO_2 y su posterior transporte.

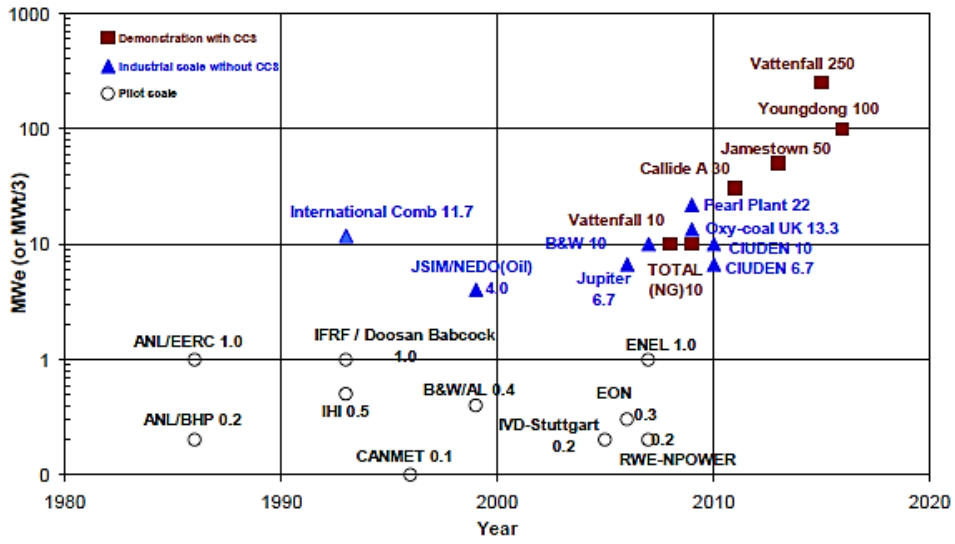

***Figura 1.16**. Desarrollo histórico de los proyectos de oxicombustión [Wall, 2009b]*

A nivel nacional se está desarrollando un proyecto financiado por el Ministerio de Ciencia e Innovación y la Unión Europea, liderado por CIUDEN. El proyecto de CIUDEN es de los más completos en tecnologías para la oxicombustión ya que cuenta con dos calderas, una de lecho fluido circulante (30 MWt) y otra de carbón pulverizado (20 MWt). En la Figura 1.16 se muestran los proyectos realizados hasta la fecha y proyectados para un futuro en la tecnología de oxicombustión.

La oxicombustión podría ser aplicada a cualquier combustible, como la biomasa o sus mezclas con carbón, sin embargo los mayores proyectos realizados hasta ahora están mayormente centrados en el carbón y el gas natural. En la actualidad existen varias plantas piloto en operación y algunas en construcción o diseño con vistas a operar en un futuro próximo, las más importantes son las siguientes:

- Vattenfall (2008): Localizada en Spremberg (Alemania) ha sido la primera planta de oxicombustión en demostrar toda la cadena completa de captura de CO_2. En ella se queman lignitos en un solo quemador de carbón pulverizado con una potencia de 30 MW térmicos.
- Total Lacq project (2009): Es el mayor hito en la oxicombustión de gas natural. Desarrolla tanto la captura como el almacenamiento y está localizada en Lacq (Francia).
- CIUDEN (2011): Localizada en Ponferrada (España) es una de las más completas dado que cuenta con una caldera de carbón pulverizado de 20 MW térmicos y otra de 30 MW térmicos de lecho fluido circulante. Es la primera planta de estas características en demostrar la oxicombustión en lecho fluido circulante.
- Callide Oxy-fuel Project (2011): Es la primera planta de oxicombustión conectada a la red eléctrica. Está localizada en Biloela (Australia), quema carbón pulverizado y tiene una potencia de 30 MW eléctricos.
- Future Gen 2.0 (2015-2016): Este ambicioso proyecto en Estados Unidos pretende reconvertir una central térmica a oxicombustión con una potencia de 200 MW eléctricos. Se encuentra en fase de diseño con previsión de comenzar a funcionar en 2015.
- Huazhong: En China con una potencia de 35 MW térmicos es el mayor que se desarrolla en Asia y se encuentra en fase de diseño.

Estos proyectos y la tendencia a mayores tamaños y potencias muestran el desarrollo alcanzado por la tecnología de oxicombustión. Sin embargo son proyectos más costosos a medida que aumenta la escala, por esta razón la Unión Europea planteó en 2008 un estudio de riesgo de las tecnologías de CAC como parte del programa de la plataforma tecnológica europea Zero Emission Fossil Fuel Power Plants [ZEP, 2008]. En 2010 se definieron las necesidades previstas en investigación y desarrollo de cada una de las tecnologías de captura

en el ámbito de la producción energética, industria del acero e industria del cemento [ZEP, 2011]. Más allá la intención del G8 es llegar a la puesta en marcha de 20 plantas de CAC en 2020, lo que requerirá la construcción de nuevas plantas de oxicombustión y la captura de más de 1 millón de toneladas de CO_2, aunque la previsión del número de plantas sea aún incierta. Existen otros proyectos que ante la coyuntura económica actual se han cancelado o pospuesto como el OXYCB300 en Compostilla (León). Del éxito de las plantas piloto y de demostración dependerá el desarrollo final y la implantación de estas tecnologías.

1.6.4 Combustión en condiciones de oxicombustión

El diseño de las calderas de oxicombustión difiere de las convencionales; el tamaño de la cámara de combustión podría ser mucho menor, ya que la corriente de gases disminuiría al no introducir N_2. Este gas inerte, presente en una concentración del 78% en el aire, hace que los caudales de aire en las calderas convencionales sean muy elevados, necesitando una caldera de gran tamaño. La necesidad de diluir el O_2 para controlar la temperatura en el interior de la cámara en condiciones de oxicombustión es un factor determinante para el cálculo de recirculaciones y del tamaño de la cámara de combustión. Sin embargo, el factor más importante en este diseño es sin duda la transmisión de calor. La gran variabilidad de posibilidades en los procesos de oxicombustión hace que los diseños de estas calderas sean mucho más complejos que las convencionales. Una de esas variables está constituida por las condiciones del reciclo, ya que puede realizarse antes o después de la condensación del vapor de agua de los humos o en una fase intermedia.

En cuanto a los quemadores diseñados y probados hasta ahora son similares a los empleados en aire. El empleo de O_2 puro y humos recirculados confiere mayor versatilidad en el diseño ya que se pueden introducir concentraciones de oxígeno optimizadas para cada corriente del quemador. En el diseño de estos quemadores se emplean prototipos de gran tamaño y por tanto están limitados a las plantas piloto o de demostración. La llama y los flujos de calor son distintos, debido a las diferentes propiedades del N_2 y el CO_2 que alteran los campos de temperatura, reacciones y flujos. La mezcla de O_2 y gases recirculados es un punto crítico en el diseño de nuevas centrales. La inyección de O_2 puro se plantea como una opción para garantizar la estabilidad de llama, sin embargo, existen riesgos de explosión en el manejo de corrientes de O_2 en concentraciones muy elevadas que han de ser tenidos en cuenta.

Debido a la mayor proporción de oxígeno en la atmósfera de oxicombustión que en aire y la ausencia de nitrógeno diluyente, se registran mayores concentraciones de vapor de agua que en la combustión convencional. El efecto que pudiera tener el vapor de agua en la cámara de combustión es uno de los aspectos menos estudiados hasta la fecha en oxicombustión. Esta concentración aún podría ser mayor de considerarse el reciclo húmedo, es decir, la recirculación de los humos previa a la condensación del vapor. La conveniencia de tomar el

reciclo húmedo o seco es otro aspecto importante a considerar en el diseño de centrales de oxicombustión.

Teniendo en cuenta que las presiones parciales de CO_2 y H_2O en la oxicombustión son mucho mayores que en la combustión convencional en aire, es esperable que las reacciones de gasificación tengan lugar en alguna etapa de la combustión. Ante la presencia de oxígeno, la contribución de las reacciones de gasificación tienen una importancia menor debido a la predominancia de la reacción de combustión. La gasificación es endotérmica, y el calor necesario es normalmente liberado por las reacciones de oxidación. Debido a esta endotermicidad, la partícula se enfriará reduciendo la velocidad de reacción [Hecht, 2011]. Várhegyi et al. [Várhegyi, 1996] midieron la pérdida de masa de char en atmósferas de Ar/O_2 y CO_2/O_2, resultando la velocidad de reacción proporcional a la concentración de oxígeno y, sin embargo, no se vio influenciada por la concentración de CO_2 a 950 ^oC.

La proporción de humos recirculados y, por tanto, la concentración de oxígeno en los gases introducidos en la caldera es el factor determinante en el diseño de la caldera. Los resultados obtenidos en plantas piloto como la de Swcharze-Pumpe indican que concentraciones de oxígeno en torno a 30-40 % arrojan las mejores eficacias en la caldera. Se han alcanzado buenos rendimientos y durabilidad de los quemadores en las pruebas realizadas. Por tanto la tendencia para las centrales de segunda generación parece ser la de introducir concentraciones superiores de O_2 [Tooper, 2013].

Una herramienta de gran utilidad en el diseño de los quemadores y de la caldera de combustión son los programas de fluidodinámica computacional mediante los cuales se pueden desarrollar modelos adaptados al caso de oxicombustión [Arias, 2004; Álvarez, 2012]. Las predicciones de estos modelos han de ser validadas posteriormente, pero resultan en un ahorro muy elevado de experimentación y coste respecto a los ensayos en planta piloto.

Existen tecnologías como el lecho fluido que son susceptibles de ser usadas también en la oxicombustión y presentan diferencias respecto a las calderas de carbón pulverizado. La combustión convencional en lecho fluido es una tecnología madura que presenta ventajas medioambientales por la reducción de los óxidos de nitrógeno debido a la menor temperatura y la retención de los óxidos de azufre mediante la adición de sorbentes en el propio lecho de combustión. Otra de las ventajas es la menor necesidad de molienda ya que en el lecho fluido no es necesario que el combustible alimentado esté pulverizado.

1.6.5 Transmisión de calor en calderas de oxicombustión

El diseño de una caldera de oxicombustión no difiere mucho estructuralmente de las tradicionales para combustión en aire. Su función principal ha de ser maximizar la transferencia de energía liberada en la combustión al circuito agua-vapor. Esta transferencia se

realiza mediante un sistema de tuberías por las que circula agua o vapor y por cuyo exterior fluyen los humos, y otros tubos que recubren las paredes de buena parte de la caldera. Cada conjunto de tubos de intercambio de calor recibe la denominación de vaporizador, sobrecalentador, recalentador, etc., en función de las condiciones de presión y temperatura del agua o vapor que circula por ellos. Los principales mecanismos de transmisión de calor en las calderas son la radiación en el hogar y la convección en los intercambiadores.

La transmisión de calor en una caldera industrial depende de las temperaturas alcanzadas en la llama, la del agua de refrigeración y de las paredes, así como de las propiedades del gas y las partículas, y del campo fluido aerodinámico. Las diferencias en las propiedades termo-físicas de N_2 y CO_2 conllevan diferencias en la transmisión de calor por radiación y convección.

Para la reconversión de plantas eléctricas de carbón existentes en centrales de oxicombustión, uno de los objetivos principales consiste en mantener la misma transmisión de calor en la caldera que en el caso de la combustión en aire con el objeto de mantener la estabilidad en la combustión, inquemados, escoriación y factor de ensuciamiento. Para nuevas centrales de oxicombustión, es importante evaluar el efecto de los parámetros de funcionamiento tales como la composición del oxidante, los niveles de exceso de oxígeno, la temperatura de llama y transmisión de calor en la caldera.

Wall et al. [Wall, 2009a] calcularon la fracción molar de oxígeno teórica requerida a la entrada del quemador para alcanzar temperaturas adiabáticas de llama similares (AFT) bajo aire y condiciones de oxicombustión. La AFT para la combustión en aire se estimó para un valor de oxígeno en exceso del 20 % y un concentración de O_2 en los humos de combustión de un 3,3 %. Los resultados computacionales mostraron que para lograr una AFT similar a la alcanzada durante la combustión en aire, la concentración de oxígeno en oxicombustión utilizando recirculación de los gases de combustión húmedos y secos tendría que ser de 28 y 35 %, respectivamente. Hjärtsman et al. [Hjärtstam, 2009] obtuvieron perfiles de temperatura durante la combustión de lignito en aire y en condiciones de oxicombustión en un combustor de 100 kW de potencia. Sus mediciones mostraron que bajo condiciones de oxicombustión la concentración de oxígeno en el oxidante debe encontrarse entre el 25-27% con el fin de conseguir temperaturas similares a las de aire.

Radiación

El principal contribuyente a la transmisión de calor de una llama producida por los combustibles convencionales es la radiación térmica a partir de vapor de agua, CO_2, CO, partículas de char y hollín. En la oxicombustión, debido al aumento de las concentraciones de CO_2 y vapor de agua en la atmósfera de combustión, la radiación térmica se incrementa significativamente. Por lo tanto, se puede esperar una mayor transmisión de calor radiante en la caldera que en la combustión convencional en aire.

La transmisión de calor por radiación en llamas de lignito y propano como combustible en oxicombustión fue estudiado por Andersson et al. [Andersson, 2008a, 2008b, 2011] en el laboratorio de la Universidad de Chalmers con un quemador de 100 kW. En los experimentos con lignito la tasa de reciclaje de gases de combustión se varió con el fin de garantizar la misma estequiometría en todos los casos, mientras que la concentración de oxígeno en la corriente de oxidante varió de 25 % a 29 %. La temperatura y la intensidad total de la radiación de las llamas de oxicombustión aumentaron a medida que se disminuyó la tasa de recirculación, debido al aumento de la concentración de oxígeno. Cuando se utilizó el reciclaje húmedo en la oxicombustión de lignito, la radiación debida al gas fue mayor y se acercó a la de las partículas.

Los estudios de Andensson et al. revelaron que la formación de hollín en las llamas de oxicombustión varía fuertemente en función de la proporción de reciclo. También afecta de manera significativa la intensidad de la radiación emitida por la llama (Figura 1.17). Se concluyó que la contribución del aumento de la intensidad de radiación debida al CO_2 tenía una importancia menor. Para las condiciones de oxicombustión con 27 % de oxígeno y reciclo seco, la temperatura era ligeramente inferior a la obtenida en aire, pero la intensidad de la radiación fue significativamente mayor. Esto se debió principalmente a un aumento significativo de la radiación del hollín. Imágenes de la llama bajo condiciones de oxicombustión con un 45 % de oxígeno indican claramente un aumento adicional en la intensidad de la radiación (Figura 1.17). Debido a su papel fundamental en la radiación de la llama, se necesita más investigación sobre la formación de hollín en oxicombustión.

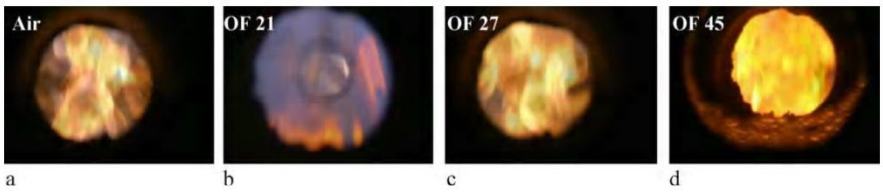

***Figura 1.17**. Fotografías de llamas de propano en (a) aire, (b) oxicombustión con 21% oxígeno, (c) oxicombustión con 27% oxígeno, y (d) oxicombustión con 45% oxígeno [Andersson, 2008a, 2008b]*

Convección

El flujo de convección de los gases de combustión, se puede evaluar de la siguiente manera:

$$q_{conv}^{n} = h\Delta T$$

Donde **h** es el coeficiente de transmisión de calor por convección (que está influenciada por la velocidad de flujo de gas y por propiedades tales como viscosidad, conductividad térmica, capacidad calorífica y densidad), y **ΔT** es la diferencia de temperatura entre el gas y el objeto

caliente. La relación entre el coeficiente de transmisión de calor en oxicombustión ($\mathbf{h_{oxy}}$) y en aire ($\mathbf{h_{air}}$) se puede expresar de la siguiente manera:

$$\frac{h_{oxy}}{h_{air}} = \left(\frac{\mathrm{Re}_{oxy}}{\mathrm{Re}_{air}}\right)^{m}\left(\frac{\mathrm{Pr}_{oxy}}{\mathrm{Pr}_{air}}\right)^{n}\left(\frac{k_{oxy}}{k_{air}}\right)$$

Donde ***Re*** y ***Pr*** son el número de Reynolds y el número de Prandtl, respectivamente; ***m*** y ***n*** son factores empíricos que varían para diferentes geometrías, y ***k*** es la conductividad térmica del fluido. La Tabla 1.1 resume las propiedades físicas de los principales gases presentes en condiciones de combustión en aire y en oxicombustión. El CO_2 tiene una conductividad térmica ligeramente superior a la del N_2, a pesar de que no cambia significativamente la transmisión de calor por conducción. Por otra parte, la menor viscosidad cinemática del CO_2 puede resultar en un número de Reynolds superior, y por lo tanto un coeficiente de transmisión de calor por convección superior en el caso del CO_2 respecto al N_2.

Tabla 1.1. Propiedades de los gases a 1400K y presión atmosférica

	$H_2O_{(v)}$	O_2	N_2	CO_2
Densidad (ρ) (kg/m^3)	0,157	0,278	0,244	0,383
Conductividad térmica (k) (W/mK)	0,136	0,087	0,082	0,097
Capacidad calorífica específica (c_p) (kJ/kmol K)	45,67	36,08	34,18	57,83
Viscosidad dinámica (μ) (kg/m s)	5,02 10^{-5}	5,81 10^{-5}	4,88 10^{-5}	5,02 10^{-5}
Viscosidad cinemática (v) (m^2/s)	3,20 10^{-4}	2,09 10^{-4}	2,0 10^{-4}	1,31 10^{-4}

Smart et al. [Smart, 2010, 2011] estudiaron el efecto de las condiciones de oxicombustión en la transmisión de calor radiante y convectivo. En estos estudios se obtuvieron mediciones de transmisión de calor radiantes y convectivas en un quemador de 0,5 MWt de RWE situado en Didcot, Reino Unido, para una semiantracita y dos carbones bituminosos. Las proporciones de reciclo variaron entre 65% y 75%, mientras que los valores de O_2 a la salida se mantuvieron en torno al 3%. Los resultados mostraron que los valores de flujo de calor radiante eran inversamente proporcionales a la relación de reciclo. Por el contrario, los valores de flujo de calor por convección tendieron a aumentar con el aumento de la proporción de reciclo. Para obtener valores de flujo de calor por radiación en oxicombustión similares a los que se obtuvieron en aire, la proporción de reciclo fue de 72-73 % para los carbones estudiados. En el caso del flujo de calor por convección se puede emplear un mayor relación de reciclo, en torno al 75%.

1.6.6 Contaminantes en los humos de oxicombustión

En la combustión de carbón se producen siempre emisiones de contaminantes como NO_x, SO_x, mercurio y partículas en suspensión formadas tanto por cenizas volantes como por hollines.

Óxidos de Nitrógeno

Norman et al. [Norman, 2009] realizaron una revisión de las emisiones de NO_x y su control en oxicombustión. Las emisiones de NO_x son menores en oxicombustión que en la combustión en aire. Cantidades mínimas de N_2 en la atmósfera de combustión inhiben la formación de NO térmico y súbito (*prompt*). Parte de los humos son recirculados lo que puede resultar en una reducción mayor de los óxidos de nitrógeno ya que las elevadas concentraciones de CO en la oxicombustión, debido a la disociación de las moléculas de CO_2 y la gasificación del *char*, actúan como agentes reductores que pueden contribuir a la reducción del NO para formar N_2.

Shaddix y Molina [Shaddix, 2011] midieron las concentraciones de NO durante la combustión de carbón pulverizado y *chars* de carbón a la temperatura de 1.050ºC en atmósferas de N_2/O_2 y O_2/CO_2 con concentraciones de O_2 entre 12 y 36 %. Encontraron que el nitrógeno del *char* alcanzaba conversiones ligeramente menores en atmósferas de CO_2. A medida que aumentaba la concentración de oxígeno también lo hacía la conversión del nitrógeno del combustible. Estos autores también introdujeron diferentes concentraciones de NO en el gas, para estudiar el efecto que tendría la recirculación de los gases de combustión. La recirculación resultó en una disminución importante de los NO_x, hasta un 20-40% menor. Nbide et al. [Nbide, 2013] obtuvieron resultados similares al quemar lignito y carbón bituminoso alto en volátiles en un reactor de flujo en arrastre a la temperatura de 1.100ºC en aire y en oxicombustión, con concentraciones de O_2 entre 21 y 40 %. Las emisiones de NO resultaron significativamente menores en oxicombustión que en aire, y aumentaron a medida que aumentó la proporción de oxígeno en el comburente.

Se han propuesto varios mecanismos para explicar la reducción de los óxidos de nitrógeno, Okazaki y Ando [Okazaki, 1997] evaluaron la importancia de cada uno de los tres mecanismos principales bajo condiciones de oxicombustión en un reactor a escala de laboratorio. El mecanismo más importante, entre un 50 y 80% del total, resultó ser la reducción de los compuestos intermedios formados de cianuro y amonio por hidrocarburos. El segundo mecanismo más importante fue la reducción de NO a N_2 a través de reacciones con otras especies de nitrógeno, mayormente NH_3 y HCN, de acuerdo con el esquema de De Soete [De Soete, 1975] al que atribuyen entre un 10 y un 50 %. Por último, las reacciones heterogéneas de reducción de NO con el char resultaron las de menor relevancia en las atmósferas de oxicombustión.

Óxidos de azufre

Stanger et al. [Stanger, 2011] estudiaron la conversión del azufre en oxicombustión pero no encontraron diferencias significativas en la oxidación del azufre en condiciones de oxicombustión respecto a la combustión en aire. Sin embargo, debido al menor volumen de

gases y la recirculación de parte de los gases, las concentraciones de NO_x y SO_x en la corriente de humos serán significativamente mayores.

Debido a la mayor concentración de SO_x y H_2O (v), la temperatura del punto de rocío resultará mayor [Fleig, 2011] y la condensación se producirá entre 130 y 160ºC [Toftegaard, 2010]. Esto podría causar problemas de corrosión en la caldera y a lo largo de la conducción de los humos si la temperatura desciende por debajo del punto de rocío. El efecto del SO_2 en la oxidación del fuel ha sido estudiado por Giménez-López et al. [Giménez-López; 2011], quienes encontraron que el SO_2 puede inhibir la oxidación del CO; sin embargo este efecto se observó más en aire que en condiciones de oxicombustión.

Stam et al. [Stam, 2011] investigaron el equilibrio termodinámico de la composición de las cenizas y las escorias en oxicombustión, y no encontraron diferencias significativas en la composición de las cenizas obtenidas en aire y en oxicombustión. Sin embargo, debido a las temperaturas menores de las partículas en oxicombustión, la vaporización de los elementos metálicos y sus óxidos fue significativamente menor. Por tanto, no se forman partículas submicrométricas de cenizas volantes [Sheng, 2007]. Suriyawong et al. [Suriyawong, 2006] compararon la formación de cenizas en aire y en 20%O_2-80%CO_2 encontrando un número de partículas finas menor en oxicombustión que en aire.

Con los estudios realizados hasta la fecha en lo que respecta a los fenómenos de deposición y ensuciamiento se puede concluir que no habría cambios fundamentales durante la oxicombustión que afecten a la operación de la planta. Esto ha sido corroborado por los estudios realizados en una planta piloto del Argonne National Laboratory de 3 MW térmicos [Payne, 1989] y en una planta de 1,2 MW térmicos [Wall, 2011]. En otros estudios se ha encontrado una mayor acumulación de carbonatos en los depósitos formados sobre los cambiadores debido a la mayor proporción de CO_2 en la atmósfera de combustión. Sin embargo, los índices de corrosión están en el mismo rango que en la combustión convencional [Stein-Brzozowska, 2013].

Existen pocos datos acerca de la oxidación del mercurio y su retención en las cenizas volantes en oxicombustión. En experimentos realizados por Babcock-Wilcox en una planta piloto de 30 MW térmicos, la concentración de mercurio en los humos resultó mayor en oxicombustión que en aire. Suriyawong et al. [Suriyawong, 2006] midieron las emisiones de mercurio en aire y en oxicombustión de un carbón sub-bituminoso en un reactor de flujo laminar, determinando la relación entre las formas elemental y oxidada del mercurio. Se encontró que estas proporciones eran similares tanto en aire como en varias atmósferas de oxicombustión. También se han desarrollado modelos predictivos basados en la fluidodinámica computacional, CFD, como el desarrolado por Gharebaghi et al. [Gharebaghi, 2011] para predecir la especiación del mercurio en los humos de oxicombustión.

1.6.7 Oxicombustión de mezclas de carbón y biomasa

Del mismo modo que en la cocombustión convencional, las opciones para la oxicocombustión de carbón y biomasa son: paralela, de forma directa, o indirecta. La oxicocombustión no se ha llevado a cabo en instalaciones de gran tamaño, aunque en la actualidad se prevé realizar experimentos en las instalaciones de CIUDEN. La Fundación Ciudad de la Energía promueve, junto al CIEMAT e INERCO, el proyecto DOTGe cuyo objetivo es la demostración a escala industrial de la tecnología de generación de energía eléctrica a partir de gasificación de biomasa en lecho fluido burbujeante.

Figura 1.18. *Instalación de gasificación de biomasa entre calderas de lecho fluido (derecha) y carbón pulverizado (izquierda) en CIUDEN.*

El proyecto "Demostración y Optimización de la Tecnología de biomasa en lecho fluido burbujeante para Generación de Energía Eléctrica (DOTGe)", abre nuevas líneas de investigación para estudiar la tecnología de gasificación de biomasa aplicada a otros aprovechamientos, como la integración con plantas de oxicombustión de carbón y la producción de biocombustibles. Dentro del alcance del proyecto, la actuación principal es el diseño, construcción, puesta en marcha y operación de una planta de producción de energía eléctrica a partir de gasificación de biomasa, aunque se incluye la realización de estudios para evaluar la oxigasificación (gasificación con mezclas de oxígeno y CO_2), la cocombustión indirecta y la gasificación con aire enriquecido y vapor.

1.7 Objetivos

El objetivo General del presente trabajo ha sido estudiar el **comportamiento en cocombustión de mezclas de carbones de diferente rango con distintos tipos y porcentajes de biomasa, para su oxicocombustión directa en calderas de carbón pulverizado.**

El trabajo se ha llevado a cabo desde un punto de vista experimental, **utilizando equipos a escala de laboratorio y semi-piloto**.

Los objetivos específicos se resumen a continuación:

1. Estudiar la combustión de partículas individuales de carbón y biomasa en un reactor de caída libre en atmósferas de aire y en distintas concentraciones de O_2/CO_2.
2. Evaluar la desvolatilización de carbón en un reactor de flujo en arrastre en atmósferas de N_2 y CO_2, y su efecto sobre la reactividad de los *chars* formados.
3. Determinar la variación en las temperaturas y mecanismos de ignición de mezclas de carbón y biomasa, en atmósferas de oxicombustión.
4. Estudiar la combustibilidad de carbones y sus mezclas con biomasa, en un reactor de flujo en arrastre; con especial énfasis en el grado de conversión que alcanzan y las emisiones gaseosas producidas durante su cocombustión directa en atmósferas de O_2/CO_2.

2. Dispositivos y metodologías experimentales

2.1 Muestras empleadas

Los carbones empleados en este trabajo han cubierto un amplio espectro, abarcando un rango desde bituminoso alto en volátiles hasta antracita. El carbón de mayor rango es la antracita (an) AC, procedente de una explotación minera de Cangas de Narcea, Asturias. HV es una semiantracita (sa) de la cuenca leonesa, procedente de la empresa minera Hullera Vasco-Leonesa. BA es un carbón procedente del lavadero Batán, en Asturias, propiedad de Hunosa, y CAB es un carbón bituminoso alto en volátiles (hvb), típico de la cuenca Asturiana. Los carbones restantes son importados desde Sudáfrica (SAA, SAB), China (DAB), Nueva Zelanda (NZ), México (UM, M6N), y han sido suministrados por centrales térmicas de carbón pulverizado; todos ellos son bituminosos altos (hvb) o medios (mvb) en volátiles.

Las muestras se prepararon siguiendo procedimientos estandarizados de desmuestre, molienda y tamizado, obteniéndose finalmente las muestras con una granulometría de 75-150 micras. Para los análisis inmediato y elemental se usaron los equipos LECO TGA-601 y LECO CHNS-932, respectivamente. El poder calorífico superior se determinó empleando una bomba calorimétrica adiabática IKA C4000. Los resultados de los análisis se muestran en la Tabla 2.1.

Tabla 2.1. *Análisis inmediato, elemental y poder calorífico superior (PCS) de los carbones.*

		Análisis inmediato (%)				Análisis Elemental (% cp)					PCS
Carbón	**Rango**	**Humedad**	**Cenizas (bs)**	**M. V. (bs)**	**C. F.* (bs)**	**C**	**H**	**N**	**S**	**O***	**(MJ/Kg)**
DAB	hvb	2,9	10,9	29,0	60,1	81,9	5,0	1,1	1,2	10,8	28,83
SAA	mvb	2,6	14,9	25,7	59,4	78,6	4,9	2,0	0,7	13,8	27,95
NZ	hvb	11,5	2,9	47,9	49,2	67,5	5,3	1,0	0,2	26,0	27,94
HVN	sa	1,1	10,6	9,2	80,2	91,7	3,5	1,9	1,6	1,3	31,78
UM	mvb	0,5	21,1	23,8	55,1	86,2	5,5	1,6	0,8	5,9	27,83
M6N	hvb	1,8	30,2	30,6	39,2	76,7	6,2	1,6	1,2	14,3	23,06
SAB	hvb	2,4	15,0	29,9	55,1	81,5	5,0	2,1	0,9	10,5	27,78
CAB	hvb	4,4	4,5	39,6	55,9	83,0	5,6	1,7	0,5	9,2	30,97
BA	hvb	1,2	6,9	33,9	59,2	88,4	5,5	1,9	1,1	3,1	33,08
AC	an	2,3	14,2	3,6	82,2	94,7	1,6	1,0	0,7	2,0	29,16

bs: base seca; cp: combustible puro; * calculado por diferencia

Todas las biomasas son de origen regional o nacional, salvo la muestra de bagazo de caña de azúcar (SCB) proveniente de Brasil. Todas las biomasas han de ser secadas según se reciben

para evitar su degradación y posteriormente se han sometido a un proceso de molienda y ulterior tamizado (75-150 micras).

El serrín de pino (PI) procede de residuos de aserradero. Parte de esta muestra se destinó a un proceso de torrefacción, dando lugar al serrín de pino torrefactado (TOPI). El proceso de torrefacción mejora la manejabilidad de las biomasas y sus propiedades de molienda, lo cual es muy beneficioso ya que dado el carácter fibroso de la biomasa, contenido de humedad y baja densidad, tiende a formar atascos y complicar el correcto funcionamiento de los equipos. Este proceso de torrefacción se comienza a emplear en la industria y es por ello que se consideró oportuno utilizar serrín de pino torrefactado.

El proceso de torrefacción se realizó en un reactor vertical, de acuerdo con un procedimiento descrito en una publicación del Grupo de Investigación [Arias, 2008]. La muestra de pino se sometió a una temperatura de 280 ºC durante 1 h en atmósfera inerte de N_2.

La caracterización de la biomasa se hizo en base al análisis inmediato, análisis elemental y poder calorífico, y los resultados se muestran en la Tabla 2.2.

Tabla 2.2. *Análisis inmediato, elemental y poder calorífico superior (PCS) de las biomasas.*

Biomasa	Origen	Análisis inmediato (% bs)			Análisis elemental (%, cp)					PCS (MJ/kg)
		Cenizas	M.V.	C.F.*	C	H	N	S	O*	
OR	Orujillo aceituna	7,6	71,9	20,5	54,3	6,6	1,9	0,2	37,0	19,91
SCB	Bagazo caña azúcar	4,2	87,8	8,0	46,3	5,9	0,2	0,1	47,5	16,30
PI	Serrín de pino	3,8	79,8	16,4	45,9	6,1	0,7	0	47,3	18,89
TOPI	Serrín de pino torrefactado	4,2	75,5	20,3	51,2	5,7	0,9	0	42,2	19,27

bs: base seca; cp: combustible puro; * calculado por diferencia

El poder calorífico de los carbones es superior al de las biomasas, lo que indica una menor energía liberada en la combustión de la biomasa. En el análisis inmediato destaca una alta proporción de materia volátil en todas las biomasas que mejora la combustibilidad y un menor contenido en cenizas que la mayoría de los carbones, lo que es interesante para el funcionamiento de la central termoeléctrica.

2.2 Dispositivo para combustión de partículas

Estos experimentos se llevaron a cabo en el marco de una estancia en el laboratorio de la Northeastern University en Boston, MA, EE.UU. En este laboratorio se dispone de un reactor de caída libre de flujo laminar calentado eléctricamente. El reactor está constituido por un

tubo de alúmina transparente con un diámetro interno de 7 cm. El horno envolvente dispone de varias aperturas longitudinales desde las que se puede visualizar el interior. En una de las aberturas se acopla una cámara de alta velocidad y alta resolución (modelo NAC HotShot 512SC, con objetivo Olympus-Infinity Model K2). En la abertura opuesta se dispone un foco para obtener un contraste mayor en las imágenes de video. El software de captura de imágenes permite ajustar la velocidad de toma que se fijó en 1000 imágenes por minuto. Por la parte inferior del horno se introduce un tubo cerámico con un hilo de espesor calibrado para hacer el enfoque de la cámara con mayor precisión.

Concéntrico al reactor y por su parte superior se encuentra el inyector. Este se encuentra refrigerado con agua y posee un diámetro interior de 1 cm. Tiene una conexión para introducir la corriente de gases que son controlados mediante rotámetros y una pequeña oquedad para introducir la jeringuilla con la que se introducen las muestras. La jeringuilla presenta una modificación en la punta para portar una pequeña cantidad de muestra, inferior a 1 mg, que al introducirla en el inyector y hacerla vibrar suavemente hace caer las partículas por el inyector.

Figura 2.1. *Fotografía del dispositivo experimental para el estudio de combustión de partículas en la Northeastern University (Boston, MA).*

El pirómetro está situado en la parte superior del inyector, en este punto se reciben las señales irradiadas desde el reactor a lo largo de la trayectoria ideal de la partícula y que son transmitidas mediante fibra óptica. Las señales son filtradas para separar y registrar las intensidades medidas en 3 longitudes de onda distintas: 0,640, 0,810 y 0,998 µm. Los detectores transmiten la señal amplificada en forma de voltaje y éste es registrado en el

ordenador mediante el software *Labview*. Este aparato fue calibrado mediante una lámpara de tungsteno según un procedimiento detallado previamente por Khatami et al. [Khatami, 2011] y Bejarano et al [Bejarano, 2008]. Para tratamiento de los resultados y el cálculo de las temperaturas se empleó el software *Matlab.*

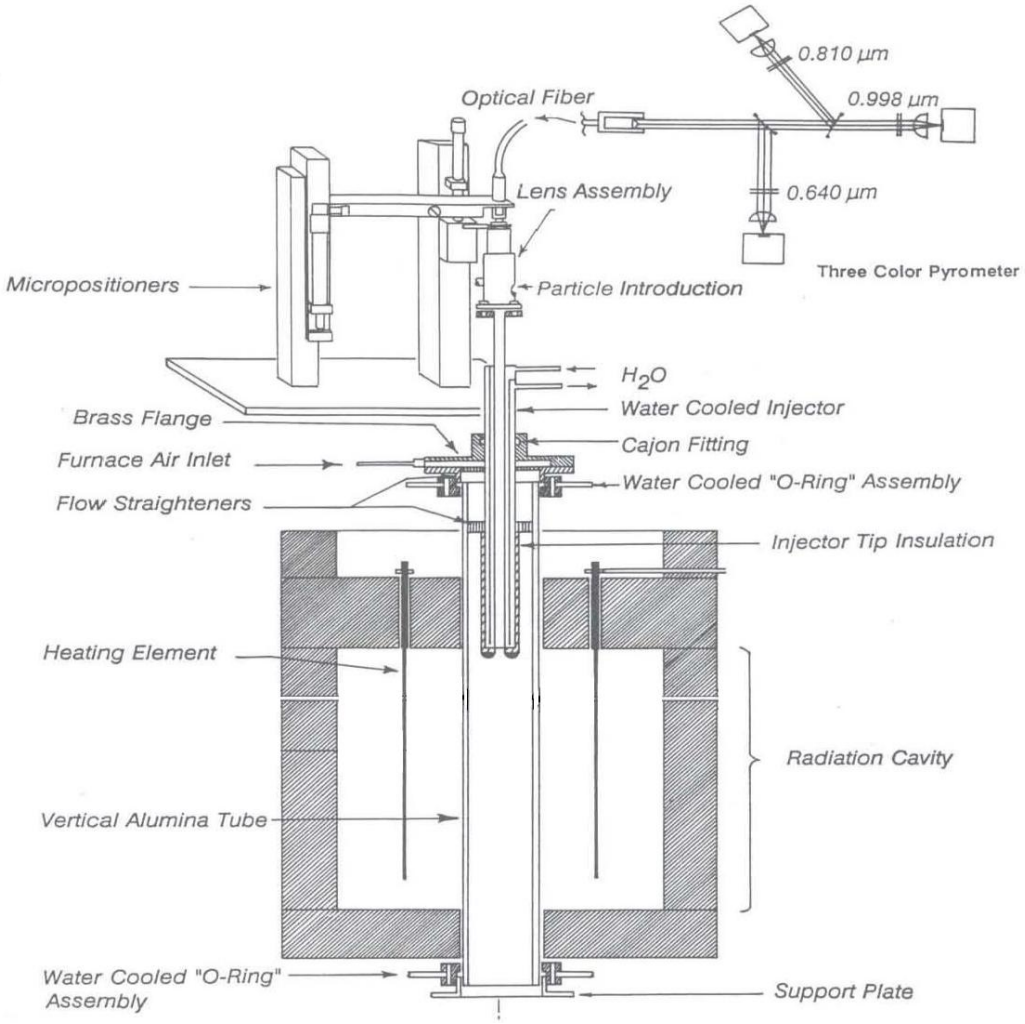

Figura 2.2. *Esquema del dispositivo experimental para pirometría de combustión de partículas en la Northeastern University (Boston, MA).*

Se realizaron los experimentos en atmósferas de aire y oxicombustión bajo diferentes porcentajes de oxígeno y dióxido de carbono. La combinación de 4 carbones (AC, HVN, SAB, UM) y 4 biomasas (PI, TOPI, OR, SCB), en 5 atmósferas (21%O_2/79%N_2, 21%O_2/79%CO_2, 30%O_2/70%CO_2, 35%O_2/65%CO_2, 50%O_2/50%CO_2) y dos tipos de experimentos (cámara y pirómetro) dieron lugar a 80 experimentos distintos. Cada experimento ha de ser repetido varias veces hasta obtener suficientes partículas aisladas para su procesamiento posterior, bien de la imagen o de los datos de temperatura y tiempo obtenidos con el pirómetro. La

dificultad de alimentar partículas individuales de forma manual hizo necesario realizar una media de 8 repeticiones, variando en función de las condiciones en las que se desarrollaba el experimento. Del total de las grabaciones se realiza una limpieza manual para recortar y obtener sólo aquellos períodos en los que se obtiene la señal de una partícula individual aislada; este laborioso proceso es especialmente crítico en los experimentos de pirometría para un cálculo correcto de la temperatura y para la medición del tiempo de quemado.

2.3 Reactor de flujo en arrastre

2.3.1 Descripción

En la Figura 2.3 se muestra una fotografía del reactor de flujo en arrastre (Entrained Flow Reactor, EFR, en inglés) que ha sido diseñado y puesto a punto por el Grupo de Procesos Energéticos y Reducción de Emisiones del INCAR (PrEM); en la Figura 2.4 aparece representado un esquema del reactor y los sistemas auxiliares.

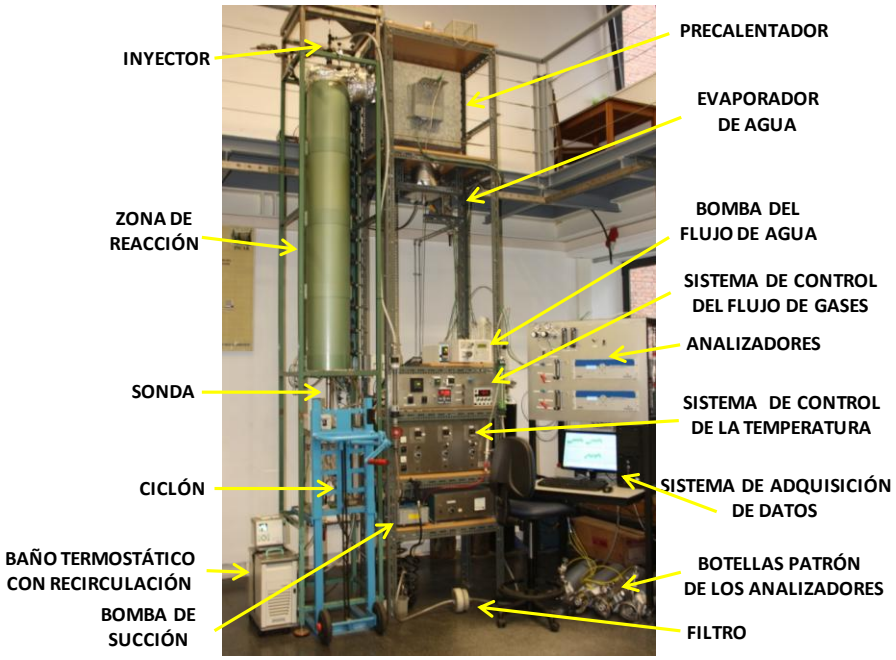

Figura 2.3. *Fotografía del reactor de flujo en arrastre utilizado en este trabajo.*

La zona de reacción del reactor de flujo descendente en arrastre que se utilizó para llevar a cabo los experimentos, tiene una forma tubular con un diámetro interno de 4 cm y una longitud de 180 cm. La zona de reacción está constituida por doce resistencias en serie, arrolladas dentro de soportes cerámicos. Las características de los materiales de construcción del horno permiten que su temperatura máxima de trabajo sea de 1.100 ^{o}C.

Las doce resistencias están agrupadas en cuatro módulos cuya distribución permite un ajuste adecuado del perfil de temperatura a lo largo del reactor. La longitud máxima de reacción es de 180 cm. Se dispone de una sonda inferior móvil, que se encuentra refrigerada por agua y que se puede introducir en el horno hasta conseguir una longitud mínima de 118 cm en la zona de reacción. Las tres zonas operativas del reactor se controlan mediante termopares tipo S y controladores P.I.D. Los termopares están situados en el punto intermedio de cada zona y se encuentran alineados con la pared interna del horno. Mediante este sistema se puede controlar cada zona de manera independiente y conseguir una temperatura uniforme dentro del reactor. Se comprueba periódicamente la temperatura en el interior del reactor con un termopar de longitud adecuada que se introduce por la parte inferior del reactor. Las mediciones se realizan a diferentes alturas, obteniendo un perfil de temperaturas uniforme en el entorno de 1.000 ºC a lo largo de todo el reactor, como se muestra en la Figura 2.5.

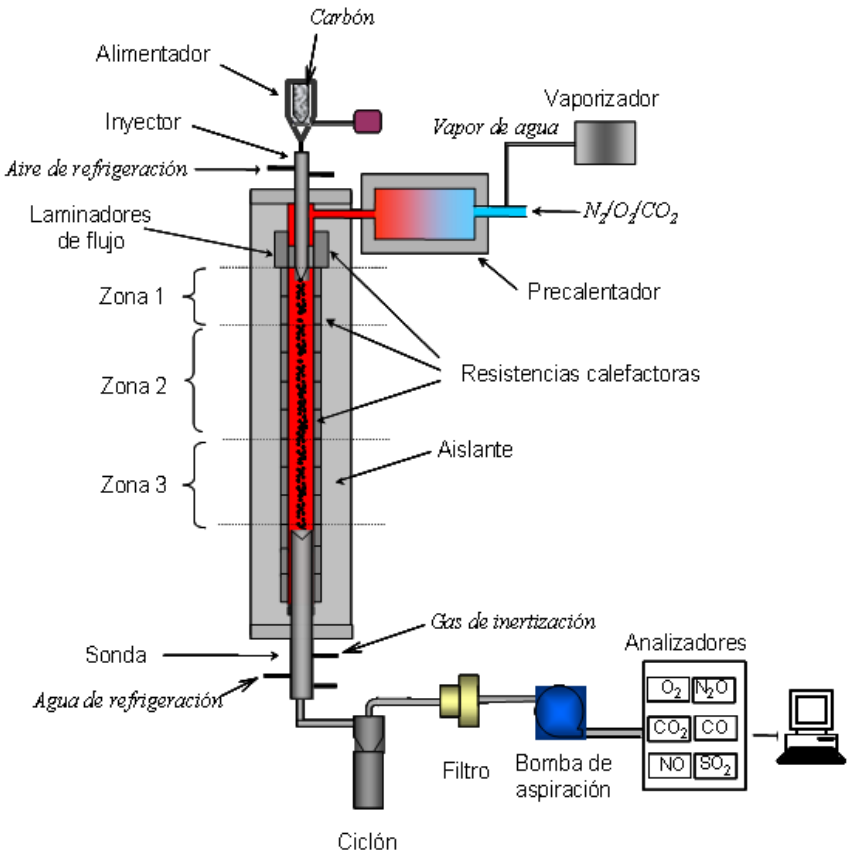

***Figura 2.4**. Esquema del reactor de flujo en arrastre (EFR).*

El carbón se alimenta al reactor desde un silo que está apoyado sobre un husillo conectado a un motor, que le comunica un movimiento de giro. El silo y el husillo se encuentran en un soporte cerrado con una entrada para el gas primario y una salida en la parte inferior para el

flujo de carbón. El husillo presenta una serie de oquedades, con objeto de facilitar la alimentación de carbón. El flujo de carbón se regula mediante la velocidad de giro del husillo y en función del volumen de huecos que éste tenga. Para flujos elevados se utilizan husillos con huecos grandes y profundos, y para flujos bajos aquellos que tienen huecos pequeños.

La homogeneización de las mezclas con distintas proporciones de biomasa y carbón se hace manualmente antes de introducirlas en el silo del EFR. El sistema de alimentación se diseñó para carbón y presenta dificultades para alimentar biomasa leñosa, debido a su naturaleza fibrosa. Por ello, se realizaron mezclas de carbón con biomasa y se observó que hasta concentraciones másicas del 30% de biomasa no existían problemas de alimentación.

El inyector se encuentra refrigerado mediante aire. Con este sistema se consigue que el flujo de carbón entre al reactor a una temperatura inferior a 60 ^{o}C. De esta forma se asegura que el carbón no sufre ninguna transformación antes de entrar a la zona de reacción.

Los gases introducidos a la zona de reacción se calientan a la temperatura del reactor en un horno de precalentamiento. Seguidamente, llegan al reactor a través de una conducción calefactada y se introducen al mismo a través de la cabecera del reactor. Esta cabecera se encuentra calentada con una resistencia que permite ajustar la temperatura del gas secundario, ya que en la conducción existen ciertas pérdidas de calor.

Una vez que el gas atraviesa la cabecera del reactor, se introduce en la zona de reacción a través de dos laminadores de flujo. El laminador de flujo consiste en un anillo cilíndrico en el que se han practicado una serie de orificios. Esta pieza es necesaria para evitar las perturbaciones que provoca la cabecera del reactor sobre el flujo de gas, de forma que se minimizan las turbulencias en la zona de inyección del carbón.

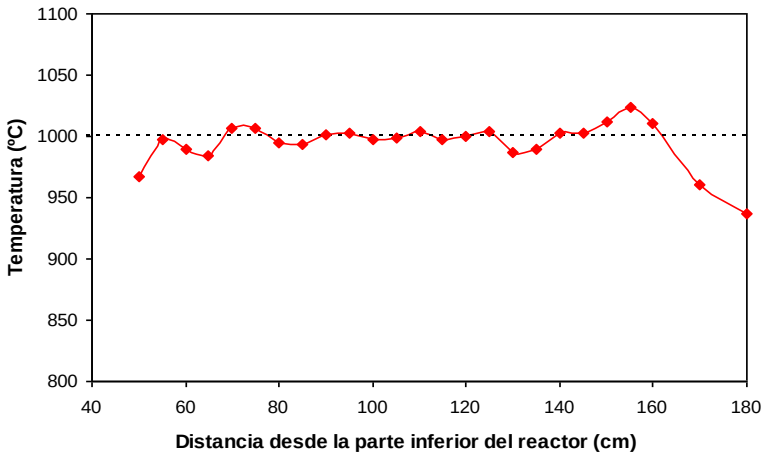

Figura 2.5. *Perfil de temperaturas a lo largo del reactor para una temperatura de operación de 1.000 ^{o}C.*

La sonda de recogida está situada sobre un soporte móvil que permite cambiar su posición dentro de la zona de reacción. La sonda está constituida por cuatro tubos concéntricos. El más interno es por el que se recoge el *char* y los gases. El espacio más externo se utiliza para el gas de inertización y los dos intermedios para la refrigeración. La sonda se encuentra refrigerada con un baño criostático que mantiene la temperatura del agua de refrigeración en 50 ^{o}C. En la zona superior de la sonda de recogida se inyecta nitrógeno a temperatura ambiente que se mezcle con la corriente de gases y partículas que salen del reactor. Se consigue así aumentar la velocidad de enfriamiento de los gases y partículas y, en el caso de la combustión, se reduce la concentración de oxígeno, asegurando un apagado de las partículas. El flujo de nitrógeno de apagado se ajusta en función del caudal de gases que circula por el reactor, siendo siempre superior o igual al caudal de gases salientes.

En la parte inferior de la zona de reacción hay un cierre que permite el sellado del reactor cuando se realiza un experimento. Este cierre consiste en un prensaestopas que cierra el espacio que hay entre la sonda y el tubo de reacción. La corriente de gases que sale del reactor es aspirada mediante una bomba. El caudal de succión se ajusta de tal forma que sea igual al de los gases de salida del reactor más el flujo de nitrógeno de apagado. De este modo se trabaja de forma isocinética, evitando una segregación de la muestra, y asegurando así la representatividad de la misma.

Antes de llegar a la bomba de aspiración, los gases y las partículas pasan a través de un ciclón y un filtro, sucesivamente. En el ciclón se recogen las partículas de mayor tamaño y en el filtro los finos. En el caso de la combustión, en el ciclón se recoge casi la totalidad de la muestra. En los experimentos de pirólisis en el ciclón se recogen, fundamentalmente, las partículas de *char*, y en el filtro los hollines producidos.

Una vez que los gases están limpios de partículas se secan mediante un lecho de anhidrona y una membrana semipermeable "*Permapure*". Seguidamente son conducidos a una batería de analizadores donde se mide la concentración de diferentes especies gaseosas. Dicha batería consta de dos analizadores Emerson X-Stream X2GP de 2 y 4 canales en los que se miden las especies: O_2, CO_2, CO, SO_2, N_2O y NO. Se utilizan gases patrón de concentración conocida para el calibrado de cada canal. Los analizadores están conectados a un ordenador, de forma que se puede registrar en continuo la concentración de las especies gaseosas, en función del tiempo.

2.3.2 Experimentos de combustión

Metodología para los ensayos de combustión en el reactor de lecho en arrastre

El reactor de flujo en arrastre se ha empleado para llevar a cabo experimentos de combustión, desvolatilización e ignición. Las variables de operación que se fijan en el caso de la combustión son: la temperatura del reactor, el tiempo de residencia del combustible en la

zona de reacción, y el flujo de combustible con el que se va a llevar a cabo la combustión. En primer lugar se ajusta la temperatura en la zona de reacción, a continuación el flujo de gases, que establece el tiempo de residencia y, por último, el flujo de combustible, que determina el exceso de oxígeno para la combustión. La temperatura en la zona de reacción se ajusta a 1000 ^{o}C y el tiempo de residencia a 2,5 segundos. Para realizar el ajuste del flujo de combustible hay que tener en cuenta la composición elemental del mismo, y considerar la estequiometría de las reacciones que van a tener lugar.

A partir del flujo de gas que circula por el reactor y el exceso con el que se quiere llevar a cabo la combustión, se calcula el flujo de combustible que hay que alimentar. Para ello se considera la estequiometría de las reacciones principales que ocurren durante la combustión del combustible (en este caso carbón o mezclas de carbón y biomasa):

$$C + O_2 \rightarrow CO_2$$

$$H + ¼\ O_2 \rightarrow 1/2\ H_2O$$

$$S + O_2 \rightarrow SO_2$$

A partir de estas ecuaciones se puede calcular la masa de combustible que se debe alimentar por cada gramo de oxígeno necesario para realizar la combustión completa.

$$\text{Oxígeno estequiométrico} \quad \frac{\text{g } O_2}{\text{g combustible}} = \frac{2{,}67\ \text{C} + 8\ \text{H} + \text{S} - \text{O}}{100} \qquad [2.1]$$

Dado que el flujo de oxígeno es un parámetro determinado por el caudal de la corriente de gases y la proporción de oxígeno en los mismos, se puede calcular el flujo de combustible estequiométrico según:

$$\text{Combustible estequiométrico} \quad \frac{\text{g}}{\text{h}} = \frac{\text{flujo másico } O_2 \times 60}{O_2 \text{ estequiométrico}} \qquad [2.2]$$

Sin embargo el flujo que interesa conocer y al que se ajusta el alimentador es el flujo de combustible para un exceso dado, que se calcula en función del estequiométrico y el exceso de oxígeno deseado:

$$\text{Flujo de combustible} \left(\frac{\text{g}}{\text{h}}\right) = \frac{\text{combustible estequiométrico}}{1 + \frac{\text{exceso de } O_2}{100}} \qquad [2.3]$$

Se define la *Fuel ratio* como la proporción entre el combustible alimentado y el estequiométrico, es decir:

$$\text{Fuel ratio} = \frac{\text{Flujo de combustible}}{\text{Flujo de combustible estequiométrico}} \qquad [2.4]$$

La relación entre la *fuel ratio* y el exceso de oxígeno es:

$$\text{Exceso de Oxígeno } \% = \frac{1}{Fuel\ Ratio} - 1 \times 100 \quad [2.5]$$

Para cada muestra, se realizan series de experimentos con distintos excesos de oxígeno, con la medición de las correspondientes concentraciones medias en los humos durante cada experimento, y la obtención de cenizas e inquemados en el ciclón, con las que se calcula el grado de quemado obtenido.

Determinación del grado de conversión o grado de combustión

El grado de conversión (B) es la pérdida de masa que experimenta un carbón o combustible carbonoso en un proceso de combustión. Se define como:

$$B = \frac{M_{CO} - M_{CF}}{M_{CO}} x100 \quad [2.6]$$

Donde:

M_{CO} es la masa combustible de la alimentación de carbón.

M_{CF} es la masa de residuo obtenido a la salida.

El grado de conversión (B) que se obtiene en la combustión del carbón y de las mezclas se determinó a partir de un balance de materia. El cálculo se ha realizado utilizando las cenizas como trazador. Este método se basa en que la cantidad de cenizas del carbón original y del residuo obtenido es la misma. Para ello es necesario conocer el contenido en cenizas en el carbón o la mezcla, antes de la combustión, y el contenido en cenizas del residuo carbonoso que obtenemos después de la combustión. Expresando la definición en función de la fracción másica de materia combustible (X_c) y de materia mineral (A_c) se obtiene:

$$B = \frac{M_O X_{CO} - M_F X_{CF}}{M_O X_{CO}} x100 = \frac{M_O\ 1 - A_{CO}\ - M_F(1 - A_{CF})}{M_O(1 - A_{CO})} x100 \quad [2.7]$$

Donde:

M_O es el flujo de carbón alimentado.

M_F el flujo de material sólido a la salida.

Haciendo un balance de materia a las cenizas:

$$M_O A_{CO} = M_F A_{CF} \quad [2.8]$$

Despejando **M_F** de la Ecuación [2.8], sustituyendo en la Ecuación [2.7] y simplificando la expresión se obtiene:

$$B = \frac{A_{CF} - A_{CO}}{A_{CF}(1 - A_{CO})} x100 \quad [2.9]$$

Con esta expresión se puede calcular el grado de conversión a partir del contenido en cenizas del carbón original, $\mathbf{A_{CO}}$, y del *char* recogido, $\mathbf{A_{CF}}$. De igual manera, se puede determinar el rendimiento en volátiles de un carbón a partir del contenido en cenizas.

Los experimentos se han llevado a cabo en distintas mezclas O_2/CO_2 (21-35% O_2) y en aire (21%O_2/79%N_2).

2.3.3 Experimentos de desvolatilización

Se han llevado a cabo en el reactor de flujo en arrastre con una sistemática similar a los experimentos de combustión. La diferencia es que los gases introducidos son sólo CO_2 o N_2, es decir, no se introduce aire ni O_2, por tanto no se produce combustión. La temperatura a la que se realizaron estos experimentos es de 1.000ºC con un tiempo de residencia de 2,5 segundos. El flujo de muestra se mantiene en valores similares a los de combustión. El muestreo isocinético recoge el flujo de gases y las partículas de combustible desvolatizado (*char*). Los gases propios de la desvolatilización no pueden ser medidos con los analizadores de combustión instalados ya que algunos componentes los dañarían y, por tanto, se dispone de un sistema de condensación y los gases no condensables son venteados. El experimento se prolonga hasta obtener suficiente cantidad de muestra. Esto depende principalmente de la cantidad de materia volátil de la muestra, variando los tiempos entre 5 minutos para los carbones de alto rango, y hasta 30 minutos para algunas biomasas.

Los desvolatilizados obtenidos en atmósfera de N_2 o CO_2 se someten posteriormente a experimentos en termobalanza con objeto de determinar su reactividad. Estos experimentos se han llevado a cabo debido a que las reacciones heterogéneas entre el agente oxidante y el *char*, son las controlantes de la velocidad de reacción global y de la conversión final. La determinación de la velocidad de reacción, su variación con el transcurso de la reacción, y los mecanismos de estas reacciones heterogéneas, son fundamentales para el diseño y mejora de los reactores de combustión. Se han desarrollado numerosos modelos teóricos con el fin de poder describir y predecir el comportamiento reactivo de los sólidos combustibles; resulta de gran interés su inclusión en la modelización de la combustión de carbón a gran escala, por ejemplo en una caldera de carbón pulverizado, mediante técnicas de fluidodinámica computacional.

2.3.4 Experimentos de ignición

Determinación de la temperatura de ignición

Se ha usado una sistemática experimental puesta a punto con anterioridad en nuestro Grupo de Investigación [Faúndez, 2005, 2007] para determinar la temperatura de ignición de carbones y sus mezclas con biomasa en el reactor de flujo en arrastre, tanto en aire como en

condiciones de oxicombustión. Estos experimentos se han utilizado para estudiar el efecto de la coutilización de biomasa en las propiedades de ignición del carbón.

La identificación del fenómeno de ignición en un reactor de flujo en arrastre se puede hacer de manera directa, con algún tipo de dispositivo que permita la observación visual del fenómeno, o bien de manera indirecta. No existe una norma establecida para determinar de forma indirecta la temperatura de ignición.

La metodología utilizada en este trabajo determina la temperatura de ignición a partir de la medición de los gases de salida del reactor de flujo en arrastre [Arias, 2008]. Para ello se alimenta la muestra de manera continua mientras que se aumenta la temperatura de la zona de reacción desde una temperatura inferior a la de desvolatilización del carbón, hasta elevadas temperaturas, del orden de 800-900 ^{o}C, que aseguren la ignición de la muestra, tal como se muestra en la figura 2.6.

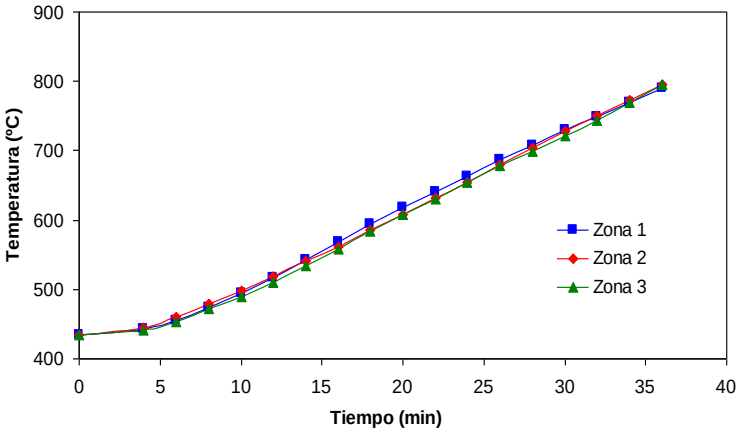

Figura 2.6. *Calentamiento del reactor de flujo en arrastre a una velocidad de 10-15 ^{o}C min^{-1}.*

A temperaturas relativamente bajas, cuando la ignición de la muestra no ha tenido lugar, se produce fundamentalmente un aumento de la concentración de CO, debido a la combustión parcial de la materia volátil liberada durante la desvolatilización del carbón. Al aumentar la temperatura, se alcanza un punto en el que se produce la ignición de la muestra, y se registra un aumento brusco de la concentración de CO_2 y NO, así como una disminución de O_2 y CO.

Durante los experimentos de ignición se mide la concentración de los gases a la salida del reactor (O_2, CO_2, CO, NO). Para determinar la temperatura de ignición se calculan las derivadas normalizadas de las curvas de evolución de las distintas especies gaseosas. El criterio que se ha establecido para determinar la temperatura de ignición es tomar el valor de temperatura a la que las derivadas de las concentraciones alcanzan un valor del 10%. La temperatura de ignición determinada para cada experimento se calcula a partir de la media de las temperaturas calculadas con cada uno de los gases. En la Figura 2.7 se muestra un ejemplo de cómo se determina la temperatura de ignición a partir de la concentración de CO_2.

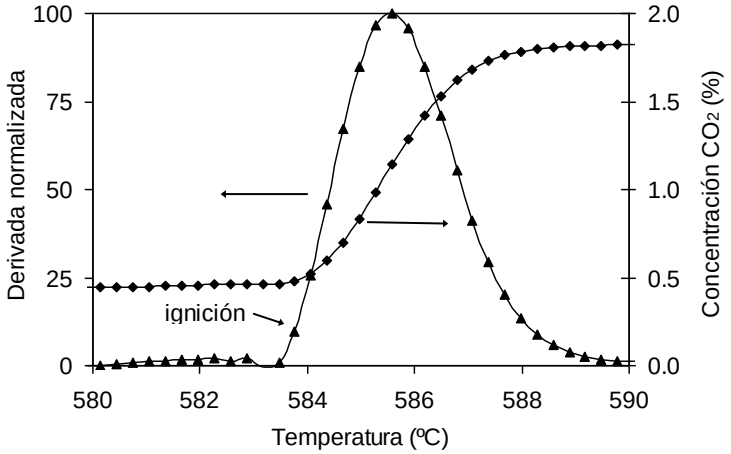

***Figura 2.7**. Ejemplo de determinación de la temperatura de ignición a partir de la concentración de CO_2.*

2.4 Analizadores termogravimétricos

La termogravimetría es una técnica que somete una muestra a un programa controlado de calentamiento o enfriamiento, en una atmósfera específica, mientras se registra la variación de la temperatura o el tiempo. El instrumento que se utiliza para realizar la medida se llama analizador termogravimétrico (ATG) o termobalanza. Consiste en una combinación de horno y microbalanza, con un dispositivo de control y medida de temperatura y de masa de muestra en cada instante del experimento.

El registro de variación de masa se realiza habitualmente según el principio del punto nulo: a medida que la masa varía y el brazo de la balanza comienza a desviarse de su posición normal, un sensor corrige esta desviación manteniendo el brazo constantemente en posición de cero o punto nulo. La fuerza aplicada en esta corrección es directamente proporcional al cambio de masa, por lo que el aparato convierte los distintos impulsos del sensor en variaciones de masa.

La representación de la pérdida de masa frente a la temperatura o el tiempo, es lo que se denomina curva termogravimétrica o curva TG. Una curva muy utilizada es la curva de velocidad de pérdida de masa o curva DTG.

En la aplicación de estas técnicas hay que considerar una serie de factores que pueden influir en los resultados del análisis termogravimétrico, así como en su interpretación [Carpenter, 1993]. La cantidad de muestra que se utiliza para hacer el análisis es un factor importante, que debe ser optimizado. Una pequeña cantidad favorece la resolución de los picos, la eliminación de volátiles y la minimización de los gradientes térmicos. Los inconvenientes de utilizar poca cantidad de muestra son la pérdida de precisión y los problemas de homogeneidad y representatividad de la misma. El tamaño de partícula, su

forma y su empaquetamiento, son otras variables que deben tenerse en cuenta, ya que afectan a la difusión de gases y a la transmisión de calor dentro del lecho. La velocidad de calentamiento que se utiliza durante el experimento influye sobre la posición y la separación de los picos del termograma. Al aumentar la velocidad de calentamiento los picos presentan un desplazamiento hacia temperaturas más elevadas. El flujo de gases debe ser tal que no perturbe la medida de la microbalanza. Por último, hay que considerar el diseño del equipo ATG (tamaño, posición del horno respecto a la muestra, dirección del gas, tipo de microbalanza y sensibilidad), ya que ejerce una gran influencia sobre los resultados obtenidos.

Pese a que se trabaje en las mejores condiciones de operación, existen factores que introducen desviaciones en los valores medidos, como es el efecto de empuje. Este efecto se genera por fenómenos de convección debidos a la presencia de un flujo de gas y la variación de la densidad de éste con la temperatura. La corrección de este efecto se tiene en cuenta mediante la realización de un experimento sin muestra.

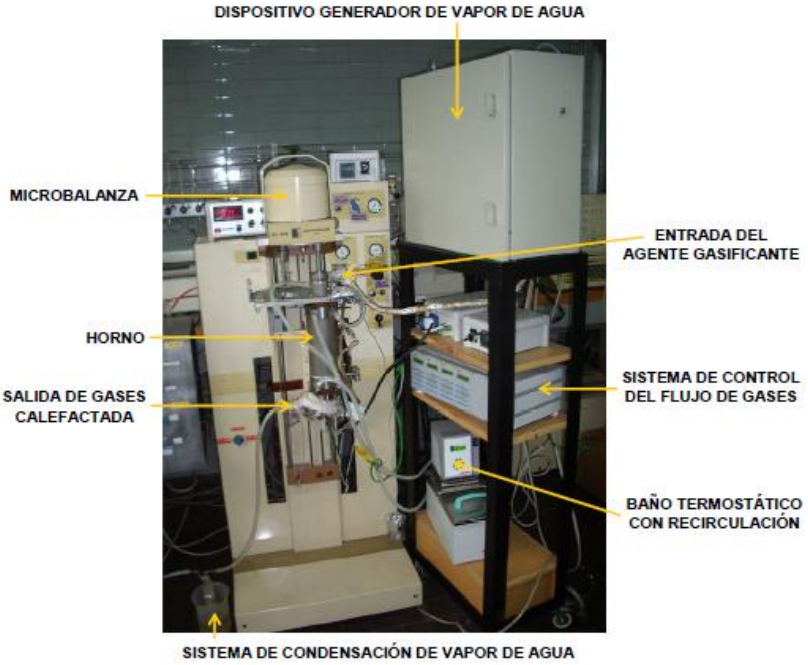

Figura 2.8. *Fotografía de la termobalanza Setaram TAG 24 modificada.*

Para realizar este trabajo se han utilizado unas termobalanzas de la casa Setaram modelos TAG24 y TG92, que permiten registrar datos de la variación de masa (TG) durante el experimento. Las termobalanzas utilizadas tienen dos entradas de gas: una superior, que se utiliza para ensayos con gases inertes, y otra lateral para experimentos con gases reactivos. El flujo dentro del horno tiene una dirección descendente. El horno de la termobalanza se encuentra dividido en tres zonas; un cabezal superior, donde se encuentra la entrada de gases inertes, una zona central donde está situada la resistencia de grafito que calienta el horno y la

entrada lateral para los gases reactivos y, por último, la zona inferior, a través de la que salen los gases del sistema. Los gases empleados han sido aire, mezclas O_2/N_2, y mezclas ternarias $O_2/CO_2/H_2O$.

Con objeto de llevar a cabo los perfiles de combustión en atmósfera $O_2/CO_2/H_2O(v)$ se llevaron a cabo una serie de modificaciones en la termobalanza para poder introducir vapor de agua. Se añadió un sistema de generación de vapor de agua, y se instaló un circuito de agua que se mantuvo a una temperatura de unos 85 ^oC, utilizando un baño termostático con recirculación, para calefactar los cabezales superior e inferior de la termobalanza, y evitar así la condensación del vapor introducido. Asimismo, se empleó un circuito de agua fría en la zona central del horno, para evitar el sobrecalentamiento de la resistencia de grafito. En la Figura 2.8 se puede ver una fotografía de la termobalanza modificada.

El dispositivo de generación de vapor de agua consta de un depósito de acero de 1,5 L de capacidad en el que se introduce agua destilada. Se utilizan dos controladores de flujo másico (Bronkhorst®, modelo F-201C, 0-200 mL min^{-1}) para introducir O_2 y N_2/CO_2. Este último controlador se utiliza para presurizar el depósito de agua a 2 atm de presión, y facilitar así el flujo de agua hacia el controlador de flujo másico de líquidos (Bronkhorst®, Liqui-Flow®, 0-30 g h^{-1}). A continuación, el flujo de O_2 y el de agua líquida se mezclan en un evaporador-mezclador (Bronkhorst®, CEM®), del cual sale la mezcla de gases a una temperatura de 150 ^oC. La línea de gases desde la salida del sistema de generación de vapor hasta la entrada al precalentador, se encuentra calefactada a 150 ^oC, para evitar la condensación del vapor de agua, y perfectamente aislada para evitar pérdidas de calor. En la Figura 2.9 se puede ver en detalle la configuración del sistema de generación de vapor.

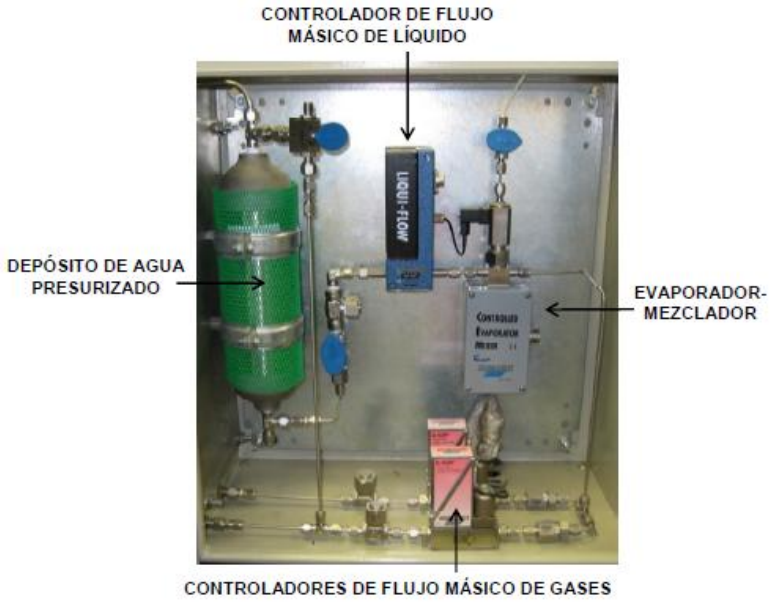

***Figura 2.9**. Detalle del generador de vapor de agua utilizado en la termobalanza.*

2.4.1 Metodología para los ensayos de reactividad en termobalanza

La temperatura es un factor determinante sobre las etapas que controlan la combustión, Walker *et al.* [Walker, 1959] propusieron tres regímenes cinéticos en función de la temperatura de combustión, tal y como se presenta en la Figura 2.10.

La zona I o zona de régimen químico se encuentra para temperaturas relativamente bajas, de manera que la velocidad de reacción química es mucho más lenta que la difusión de las moléculas de oxígeno, tanto a través de la superficie externa de la partícula como de su estructura porosa. En estas condiciones la velocidad de reacción global está controlada por la velocidad de reacción química.

La zona II o de régimen de difusión interna corresponde a temperaturas moderadas. A medida que la temperatura se incrementa, se produce un aumento de la velocidad de reacción química, de forma que, bajo estas condiciones, tanto la reacción química como la difusión del oxígeno en los poros de la partícula influyen en la velocidad de la reacción global.

Por último, *la zona III o de régimen de difusión externa* corresponde a temperaturas elevadas, a las que la velocidad de reacción entre el oxígeno y el carbono es tan rápida que la concentración de oxígeno sobre la superficie de la partícula es prácticamente despreciable. Bajo estas condiciones, la velocidad de reacción global estará controlada por fenómenos de difusión.

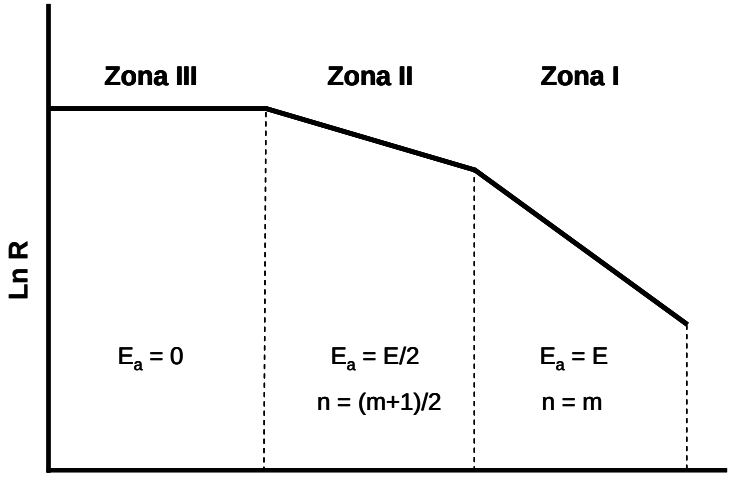

Figura 2.10. *Representación de los regímenes de control del proceso de combustión en función de la temperatura (E_a, energía de activación observada; E, energía de activación química).*

La reacción principal de combustión de un sólido carbonoso puede expresarse de la siguiente forma:

$$C_{(s)} + O_{2\,(g)} \rightarrow CO_{2\,(g)} \qquad [2.10]$$

El avance de la reacción o grado de conversión del sólido carbonoso se define como:

$$X = \frac{m_o - m}{m_o - m_f} \qquad [2.11]$$

donde m_0 es la masa inicial de carbono o materia carbonosa libre de volátiles, m es la masa carbonosa a un tiempo dado, y m_f es la masa final.

Se denomina reactividad a la velocidad de reacción del sólido con el gas reactivo (oxígeno, dióxido de carbono, vapor de agua, etc.). La reactividad se suele expresar como la velocidad de desaparición de masa de sólido en base a una propiedad característica del mismo, como la superficie externa de las partículas [Hamor, 1973] o la superficie interna específica de las partículas, en cuyo caso se denomina reactividad intrínseca [Smith, 1982]. Sin embargo, la determinación de estas superficies presenta dificultades, ya que no permanecen constantes durante la combustión del *char* [Feng, 2003]. Debido a estas dificultades, la propiedad utilizada más habitualmente es la masa inicial de carbono, con lo cual la reactividad se puede expresar como:

$$R = \frac{dX}{dt} = -\frac{1}{m_o}\frac{dm}{dt} \qquad [2.12]$$

Se pueden emplear varios parámetros para comparar la reactividad de diferentes materiales carbonosos, como la reactividad media [Tsai, 1987], o bien la reactividad para la cual la pérdida de masa es máxima [Jenkins, 1973]. Esta reactividad máxima se define como:

$$R_{max} = -\frac{1}{m_o}\left.\frac{dm}{dt}\right|_{max} \qquad [2.13]$$

También se puede emplear la reactividad para una conversión dada, que es interesante para la determinación del tiempo para alcanzar una conversión del 50% ($t_{0,5}$), ya que a partir de este parámetro no sólo se determina la reactividad para una conversión del 50%, sino también el denominado índice de reactividad, R. Este índice se define mediante la siguiente expresión [Miura, 1989]:

$$R = \frac{0{,}5}{t_{0,5}} \qquad [2.14]$$

Perfiles de combustión o reactividad no isotérmica

En los experimentos llevados a cabo en este apartado se ha partido de una masa de muestra en torno a 5 mg y se calienta de forma constante en un flujo de 50 mL/min del agente oxidante, siguiendo una rampa de calentamiento de 15 ^{o}C/min. Alrededor de 100°C la muestra pierde la humedad, posteriormente al aumentar la temperatura comienza la desvolatilización y combustión de los volátiles y posteriormente tiene lugar la combustión del residuo carbonoso. Cuando la masa ya no varía a temperaturas relativamente elevadas, la combustión se da por concluida y la masa final nos indica el contenido de cenizas. La curva de variación de la masa con respecto al tiempo o temperatura así como su derivada, es decir la velocidad de pérdida de masa es característica de cada material, y es lo que se conoce como perfil de combustión. A partir de estos experimentos se obtienen unos parámetros y temperaturas características, que permiten comparar la combustibilidad de distintos materiales. En este trabajo se han llevado a cabo experimentos de combustión a temperatura programada para obtener los perfiles de combustión de las muestras originales, así como de sus *chars*. Estos experimentos se han llevado a cabo en atmósfera de aire así como en atmósferas propias de oxicombustión: $O_2/CO_2/H_2O$.

Reactividad isotérmica en termobalanza

Los experimentos de reactividad isotérmica se realizaron como su nombre indica manteniendo constante la temperatura seleccionada. Este tipo de experimentos se realizan sobre el *char* únicamente, por tanto conllevan una desvolatilización previa que puede realizarse en la propia termobalanza o en otros dispositivos. En todos los trabajos expuestos en esta tesis los *chars* se han obtenido a partir de experimentos de desvolatilización en atmósferas de N_2 o CO_2, en el reactor de flujo en arrastre.

Para la realización de los experimentos en termobalanza, se calientan los chars en un flujo de 50 mL/min en atmósfera inerte de N_2 a 15 ^{o}C/min hasta 850 ^{o}C. Se mantiene esta temperatura durante 15 minutos y se enfría posteriormente hasta la temperatura del experimento. Cuando la masa y temperatura están estables se cambia la corriente de gas inerte, a la corriente oxidante que en los experimentos realizados han sido mezclas ternarias propias de las atmósferas de oxicombustión $O_2/CO_2/H_2O$, así como aire; en todos los casos el flujo de gas oxidante utilizado fue de 50 mL/min y la masa de muestra en torno a 5 mg.

2.4.2 Modelos cinéticos

Los parámetros cinéticos relativos a la combustión del char se pueden determinar, bien mediante métodos de reactividad isotérmica, o bien mediante métodos de reactividad no isotérmica. En el análisis no isotérmico la muestra se calienta con una rampa de calentamiento constante, y se obtiene una curva de pérdida de masa frente a la temperatura. En el análisis isotérmico esta curva de pérdida de masa se representa frente al tiempo, mientras que la

temperatura se mantiene constante. Aunque para determinar los parámetros cinéticos mediante un análisis no isotérmico, se necesitan menos experimentos y de menor duración, estos parámetros no son independientes de la velocidad de calentamiento empleada [Sima-Ella, 2005]. El análisis no isotérmico ha sido empleado tradicionalmente para la determinación de parámetros cinéticos referentes a la desvolatilización, mientras que el isotérmico se ha aplicado para la obtención de parámetros cinéticos referentes a la combustión del *char*.

En el intervalo de temperaturas en el que no existen limitaciones difusionales, es decir, en la zona de régimen químico, la velocidad de reacción depende de las condiciones de reacción y de la reactividad del *char*. La reactividad del *char* varía durante la combustión como consecuencia del cambio en la estructura porosa de las partículas y el consumo de centros activos. En ausencia de efectos catalíticos, la reactividad está determinada por el número de centros activos por unidad de masa de *char*. Por tanto, la velocidad de reacción de las reacciones heterogéneas gas-sólido no catalíticas, como la combustión de *char*, se puede expresar como:

$$\frac{dX}{dt} = k\ P_i, T\ f\ X \qquad [2.15]$$

donde $k(P_i, T)$ es el factor de velocidad química o constante de reacción aparente, la cual describe la relación entre la velocidad de reacción y las condiciones de reacción, y $f(X)$ es el factor de estructura. Este factor expresa el número total de centros activos por unidad de volumen de *char*, como una función de la conversión de carbono. Generalmente, al inicio de la reacción los *chars* presentan una estructura porosa incipiente produciéndose un aumento de la superficie interna del sólido con la conversión, de ahí que se incremente la velocidad de reacción. Sin embargo, a medida que aumenta el volumen de poros, los microporos empiezan a coalescer en poros mayores (macroporos y mesoporos), lo cual hace que disminuya la superficie interna del sólido, y con ello la velocidad de reacción.

La constante de velocidad aparente, $k(P_i, T)$, depende tanto de la temperatura (T) a la que se lleve a cabo la reacción, como de la presión parcial del gas reactivo utilizado (P_i). La dependencia de la temperatura puede expresarse en términos de la ecuación de Arrhenius:

$$k = k_o e^{-E_a\ RT} \qquad [2.16]$$

donde k_0 es el factor pre-exponencial, E_a es la energía de activación, T es la temperatura absoluta en K, y R es la constante universal de los gases. En el caso de que se cumpla que la presión parcial del gas reactivo sea constante, su efecto se incluye en el factor pre-exponencial. En cambio, si esta presión parcial no es constante, la dependencia de la constante de velocidad con la presión parcial del gas reactivo se puede expresar como:

$$k = k' P_i^n \qquad [2.17]$$

donde P_i es la presión parcial del gas reactivo, y *n* es el orden de reacción con respecto al gas reactivo utilizado. En el caso de que la temperatura de reacción sea constante, su efecto se incluye en la constante *k*'.

En este trabajo se han aplicado tres modelos cinéticos para tratar de describir el comportamiento reactivo de *chars* de carbones, durante su combustión en una atmósfera típica de oxicombustión (30%O_2/70%CO_2), y así obtener una expresión cinética capaz de predecir la reactividad de dichos carbones. Los modelos estudiados han sido: el modelo de reacción volumétrico (VM), el modelo de reacción de núcleo decreciente (GM), y el modelo de distribución aleatoria de poros (RPM).

Modelo de Reacción Volumétrico (VM)

El Modelo de Reacción Volumétrico o Modelo de Conversión Progresiva asume que la reacción tiene lugar en los centros activos uniformemente distribuidos por todo el sólido, disminuyendo linealmente la superficie de reacción del *char* con la conversión a medida que transcurre la reacción. Este modelo considera que el gas reaccionante penetra y reacciona simultáneamente en toda la partícula sólida; por consiguiente, el reactante sólido se está convirtiendo continua y progresivamente en toda la partícula, como se muestra en la Figura 2.11 La velocidad de reacción se expresa mediante la ecuación:

$$\frac{dX}{dt} = k(P_i, T)(1-X) = k_{VM}(1-X) \qquad [2.18]$$

donde k_{VM} es la constante de velocidad de reacción aparente.

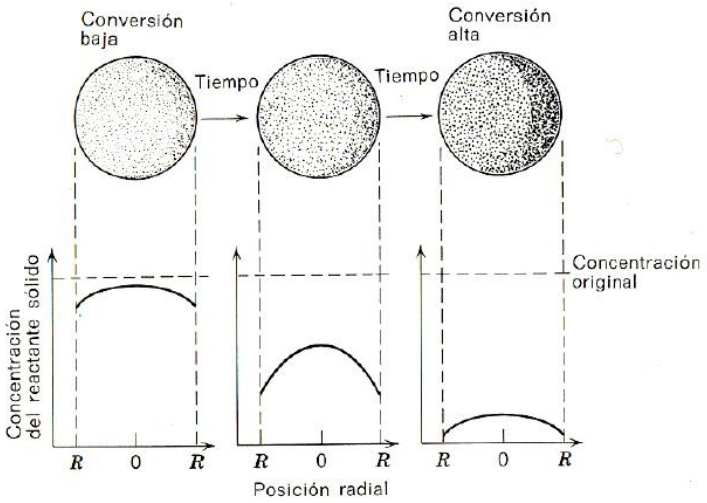

***Figura 2.11**. Modelo de Reacción Volumétrico.*

Modelo de Reacción de Grano (GM)

Según el Modelo de Reacción de Grano o Modelo de Núcleo Decreciente, un sólido poroso consiste en una unión uniforme de granos no porosos, constituyendo el espacio entre los granos la red de poros del sólido. Este modelo supone que la reacción tiene lugar en la superficie exterior de la partícula, la zona de reacción se va desplazando hacia el interior del sólido, dejando atrás el material completamente convertido ("cenizas"). De este modo, el gas reactivo difunde a través de la capa de cenizas formada y reacciona con el núcleo, disminuyendo su tamaño a medida que transcurre la reacción, a la vez que va aumentando la capa de cenizas, como se muestra en la Figura 2.12.

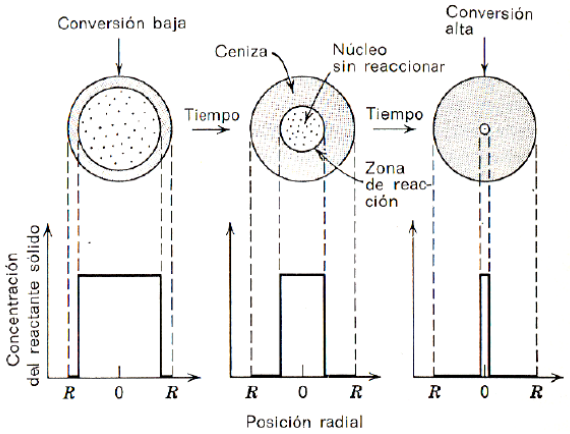

***Figura 2.12**. Modelo de Reacción de Núcleo Decreciente.*

Este comportamiento de núcleo decreciente se aplica a cada uno de los granos que constituyen el sólido. En el presente trabajo se ha considerado que las partículas de *char* están constituidas por granos esféricos de idéntico tamaño. Según este modelo, en el régimen controlado por la reacción química, la velocidad de reacción se puede expresar de la forma:

$$\frac{dX}{dt} = k(P_i, T)\frac{S_0}{1-\varepsilon_0}(1-X)^h = k_{GM}(1-X)^h \qquad [2.19]$$

donde k_{GM} es la constante de velocidad de reacción aparente, y h está definido como un factor de forma que depende de la geometría de los granos que constituyen el sólido. Para esferas h=2/3, en el caso de cilindros h=1/2, y para geometrías en forma de láminas h=0. En este trabajo se ha asumido que los granos tienen forma esférica. Este modelo incorpora parámetros estructurales del sólido, en términos de porosidad inicial, ε_0, y área superficial inicial, S_0.

Aunque el modelo de núcleo sin reaccionar constituye la mejor representación sencilla, para la mayor parte de los sistemas reaccionantes gas-sólido [Levenspiel, 1979], no tiene en cuenta el crecimiento y coalescencia de los poros y capilares de las partículas sólidas.

Modelo de Distribución Aleatoria de Poros (RPM)

El modelo RPM, desarrollado por Bhatia y Perlmutter [Bhatia, 1980], considera que las partículas sólidas presentan una considerable superficie interna en forma de poros y capilares, que pueden crecer y coalescer a medida que transcurre la reacción. Las reacciones gas-sólido con crecimiento de volumen de poros, siempre muestran un máximo en el área superficial y, como consecuencia de ello, un máximo en la velocidad de reacción. Por esta razón, este modelo puede predecir un máximo en la velocidad de reacción frente a la conversión, ya que considera los efectos competitivos de aumento de la superficie interna del sólido, debido al crecimiento de los poros durante las primeras etapas de combustión, y de disminución de dicha superficie al comenzar a coalescer los poros al aumentar su volumen. La expresión de la velocidad de reacción para este modelo viene dada por la ecuación:

$$\frac{dX}{dt} = k(P_i,T)\frac{S_0}{1-\varepsilon_0}(1-X)\sqrt{\left[1-\psi\ln(1-X)\right]} = \\ = k_{RPM}(1-X)\sqrt{\left[1-\psi\ln(1-X)\right]} \qquad [2.20]$$

donde k_{RPM} es la constante de velocidad de reacción aparente, y ψ es un parámetro que está relacionado con la estructura porosa de la muestra de *char* sin reaccionar (X=0). Este parámetro se puede calcular mediante la expresión:

$$\psi = \frac{4\pi L_0(1-\varepsilon_0)}{S_0^2} \qquad [2.21]$$

donde S_0 representa el área superficial inicial por unidad de volumen de poro, L_0 la longitud total de los poros por unidad de volumen, y ε_0 es la porosidad inicial del sólido. Algunos autores han calculado el parámetro ψ como un parámetro de ajuste para minimizar los errores medios referentes a la conversión y pérdida de masa [Fermoso, 2009a]. Otra forma de estimar ψ es a partir del dato de conversión para el cual la velocidad de reacción es máxima [Zolin, 1998; Ochoa, 2001]. Otros autores han incluido modificaciones en el parámetro ψ para tener en cuenta su variación durante el transcurso de la reacción, especialmente para altos grados de conversión [Fei, 2011].

3. Combustión de partículas individuales de carbón y biomasa

El estudio de la combustión de partículas es de gran utilidad para comprender los fenómenos que tienen lugar en la combustión industrial en un quemador. Constituye un estudio elemental de la combustión y de cómo se diferencian las partículas de distintos tipos de muestras al introducirlas en una cámara de combustión bajo diferentes condiciones. En las calderas de carbón pulverizado, la combustión tiene lugar a temperaturas elevadas, la reacción es rápida y tiene lugar bajo un régimen de control difusional (Zona III). En el caso de la oxicombustión, si se realiza con baja concentración de oxígeno, la reacción podría tener lugar bajo régimen químico difusional (Zona II) dada la peor difusividad del oxígeno en CO_2 que en N_2. Ello afectaría el flujo de oxígeno hacia la partícula, disminuyendo la velocidad de combustión y reduciendo la liberación de calor de las partículas de carbón [Li, 2010].

A pesar que la combustión de los volátiles tiene una cinética muy rápida respecto a la combustión del char, se han encontrado diferencias entre su combustión en aire y en oxicombustión. Así, se ha observado una disminución de la cinética de combustión de los volátiles debido a la menor difusión de los hidrocarburos de menor tamaño liberados durante la desvolatilización en CO_2, respecto a la que tiene lugar en atmósfera de N_2 [Zhang, 2010; Molina, 2007].

Glarborg y Bentzen [Glarborg, 2008] estudiaron el efecto de la concentración de CO_2 en la oxidación de metano y encontraron que al aumentar la concentración de CO_2 éste competía con el O_2 en las reacciones con hidrogeno atómico, contribuyendo a la formación de monóxido de carbono a través de la reacción:

$$CO_2 + H \leftrightarrow CO + OH$$

Además, las reacciones de CO_2 con los hidrocarburos de los volátiles contribuyen a un aumento de la formación de CO. Glarborg y Mendiara [Glarborg, 2008; Mendiara, 2009] observaron además que al aumentar la concentración de CO_2 aumenta la relación OH/H.

En este sentido, Andersen et al. [Andersen, 2009] confirmaron las predicciones de varios modelos desarrollados en investigaciones previas. Estos autores observaron que las reacciones iniciales permanecían inalteradas mientras que las reacciones que involucraban a H_2-CO-CO_2 tuvieron que ser implementadas con mayor detalle en los modelos, para predecir correctamente la formación de CO en estado estacionario.

El empleo de la pirometría para la determinación de la temperatura durante la combustión fue publicado por primera vez por Timothy et al. [Timothy, 1982] y constituye una herramienta muy útil para el estudio de los procesos de combustión. Asimismo, el empleo de cámaras de video de alta velocidad y alta resolución permite observar la evolución de la combustión, así como obtener imágenes durante la combustión de partículas de carbón o biomasa.

El trabajo expuesto en este Capítulo se desarrolló en el marco de una estancia en la Northeastern University de Boston, Massachusetts (EEUU), en el grupo del Profesor Yiannis Levendis, autor de numerosas publicaciones en la temática del trabajo desarrollado y con amplia experiencia en las técnicas empleadas. Durante esta estancia se realizó el trabajo experimental empleando los equipos de dicha universidad. Posteriormente se realizó el tratamiento y discusión de los resultados que dieron lugar a las dos publicaciones que se muestran en el Apartado 3.3.

En trabajos previos en los laboratorios de la Northeastern University, Bejarano y Levendis [Bejarano, 2008] y Khatami et al. [Khatami, 2012a, 2012b], estudiaron el comportamiento de partículas individuales de carbones bituminosos altos en volátiles, sub-bituminosos y lignitos, así como una biomasa (bagazo de caña de azúcar), en atmósferas de aire y de oxicombustión. Estos autores indicaron que el aumento de la concentración de oxígeno en la corriente oxidante en oxicombustión, debe compensar el mayor calor específico molar del CO_2 respecto al N_2 y la menor difusividad tanto de los volátiles como del oxígeno en CO_2. Bejarano y Levendis [Bejarano, 2008] obtuvieron unas temperaturas menores y unos tiempos de combustión mayores durante la combustión de partículas de *char* en atmósferas de CO_2 que en N_2.

La combustión y los fenómenos de ignición de partículas de carbones bituminosos se encuentra documentada ampliamente en la bibliografía [Atal, 1995; Bejarano, 2008; Faúndez, 2007; Levendis, 1992, 2012; Liu, 2011; Khatami, 2012a, 2012b; Zhang, 2010]. Sin embargo, los estudios sobre la ignición y combustión de partículas de carbones de alto rango como antracita y semiantracita son muy escasos. El trabajo que se presenta en la Publicación I, a continuación, tiene como objetivo analizar el comportamiento durante las distintas etapas de la combustión, de partículas individuales de carbones bituminosos de contenido medio y alto en materia volátil, así como de antracitas y semiantracitas.

Por otra parte, los estudios relacionados con la combustión de partículas de biomasa son muy escasos. Wornat et al. [Wornat, 1996] estudiaron la combustión de partículas de *char* de dos tipos de biomasa, mijo (*Panicum virgatum*) y serrin de pino, con concentraciones de O_2 entre 6 y 12 % (balance N_2) a la temperatura de 1.327 ^{o}C. Según estos autores, las partículas de biomasa tienen una reactividad menor que las partículas de carbones de bajo rango y mayor que las antracitas, siendo comparable con las de carbones bituminosos. En otro estudio sobre la combustión de partículas de mazorca de maíz en aire [Austin, 1996], se determinó la

relación entre los tiempos de quemado de los volátiles y el retraso en la ignición, así como su relación con la densidad y diámetro de la partícula.

El objetivo de los trabajos que se presentan en este Capítulo ha consistido en la evaluación del efecto de la concentración de oxígeno sobre las características de ignición y combustión de dos carbones bituminosos, una semiantracita y una antracita (Publicación I). Asimismo, se emplearon varios tipos de biomasa; orujillo de aceituna como biomasa de origen agroalimentario, serrín de pino como biomasa de origen forestal y pino torrefactado (Publicación II). Las muestras se molieron y tamizaron, para obtener la fracción entre 75-150 micras, y se sometieron a ensayos de oxicombustión en atmósferas de O_2/CO_2, variando la concentración de O_2 entre 21-50 %; los resultados se compararon con los determinados en atmósfera de aire (21 % O_2/79 % N_2). Los experimentos se llevaron a cabo en el reactor de caída libre de flujo laminar de la Northeastern University. El comportamiento durante la ignición y combustión de las partículas individuales se observó por medio de pirometría óptica de tres colores y cinematografía de alta resolución y de alta velocidad.

Se realizaron dos tipos de experimentos en el mismo reactor: experimentos con pirómetro y experimentos de filmación con cámara de video de alta velocidad y de alta resolución. La combinación de ambas técnicas permite conocer con claridad los fenómenos que tienen lugar durante el transcurso de la combustión de las partículas individuales, así como verificar hipótesis que no podrían ser contrastadas mediante el empleo de una sola técnica.

3.1 Compendio de resultados

La utilización de las técnicas de pirometría y de filmación con cámara de video de alta velocidad y de alta resolución, han permitido visualizar las grandes diferencias que presentan las biomasas y carbones durante su combustión. Las diferencias entre las biomasas son relativamente menores, mientras que en los carbones estas diferencias están relacionadas principalmente con el rango del carbón. En el caso de las biomasas, que liberan una gran cantidad de volátiles, la desvolatilización y posterior ignición de los volátiles forma una aureola en el entorno de la partícula. Esta aureola es esférica, independientemente del carácter fibroso y alargado o redondeado de las partículas. En esta aureola se distinguen varias intensidades, que se atribuyen a una zona interna con defecto de oxígeno y una envolvente o aro exterior donde se completa la combustión de los volátiles.

A diferencia de los carbones, la desvolatilización y combustión de los volátiles en las biomasas llega a tardar más que la combustión del *char* y comprende la mayor parte del tiempo total de combustión de la partícula. En las muestras SCB, TOPI y PI se registraron en la atmósfera 30%O_2-70%CO_2, tiempos de 105, 64 y 82 ms de media en la desvolatilización y combustión de los volátiles mientras que la combustión de los respectivos chars duró 15, 24 y 19 ms.

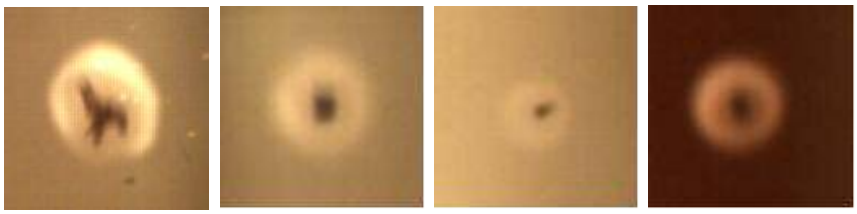

Figura 3.1 *Imágenes de las biomasas: (a) SCB, (b) OR, (c) PI, (d) TOPI, durante la combustión de los volátiles en aire.*

En los carbones bituminosos los volátiles crean llamas con mayor irradiación y mayor temperatura que en el caso de las biomasas. La liberación de gran cantidad de calor en tiempos muy cortos hace que en el pirómetro se lleguen a registrar temperaturas en la combustión de los volátiles en torno a la partícula cercanas a los 1.700 ^{o}C en la atmósfera 30%O_2-70%CO_2.

En las partículas de los carbones de alto rango, antracita y semiantracita, la desvolatilización es imperceptible y la ignición transcurre de forma heterogénea.

En los carbones bituminosos y biomasas tras la combustión de los volátiles se produce la ignición del *char*. En los carbones bituminosos el intervalo de tiempo entre la extinción de los volátiles y la ignición del *char* es muy corto y la atmósfera de combustión ejerce un gran efecto, siendo mayor ese intervalo en atmósfera de oxicombustión que en aire e inversamente proporcional a la concentración de O_2. Para concentraciones de O_2 elevadas, 50%O_2-50%CO_2, la diferencia entre la extinción de los volátiles y la ignición del *char* es prácticamente indistinguible.

La combustión del *char* en los carbones se produce a una temperatura prácticamente constante. Esta temperatura media de combustión del *char* es proporcional a la concentración de oxígeno en la atmósfera de oxicombustión. En las biomasas, los tiempos de combustión son tan cortos que no permiten la estabilización de la temperatura.

Sin embargo, la mayor concentración de oxígeno no produce un descenso proporcional en los tiempos de quemado siendo notable en el cambio de 21%O_2-79%CO_2 a 30%O_2-70%CO_2 y mucho menor de 35%O_2-65%CO_2 a 50%O_2-50%CO_2, debido a la limitación de la propia cinética de las reacciones de combustión. Las temperaturas registradas durante la combustión fueron menores en la atmósfera de CO_2 que en la de N_2 con la misma concentración de O_2 (21%). Sin embargo, los tiempos de combustión son mayores en la atmósfera de CO_2 que en la de N_2, con la misma concentración de O_2 (21%), para todas las muestras de carbón y biomasa estudiadas.

3.2 Publicaciones relacionadas

I **Single particle ignition and combustion of anthracite, semi-anthracite and bituminous coals in air and simulated oxy-fuel conditions.**
J. Riaza, R. Khatami, Y.A. Levendis, L. Álvarez, M.V. Gil, C. Pevida, F. Rubiera, J.J. Pis. Combustion and Flame 2014. 161 pp 1096–1108.
doi:0.1016/j.combustflame.2013.10.004

II **Combustion of single biomass particles in air and in oxy-fuel conditions.**
J. Riaza, R. Khatami, Y. A. Levendis, L. Álvarez, M.V. Gil, C. Pevida, F. Rubiera, J.J. Pis Biomass and Bioenergy. doi: 10 10.1016/j.biombioe.2014.03.018.1

3.2.1 *Publicación I*

Single particle ignition and combustion of anthracite, semi-anthracite and bituminous coals in air and simulated oxy-fuel conditions.

J. Riaza, R. Khatami, Y.A. Levendis, L. Álvarez, M.V. Gil, C. Pevida, F. Rubiera, J.J. Pis.
Combustion and Flame
2014. 161 pp 1096–1108.
doi:0.1016/j.combustflame.2013.10.004

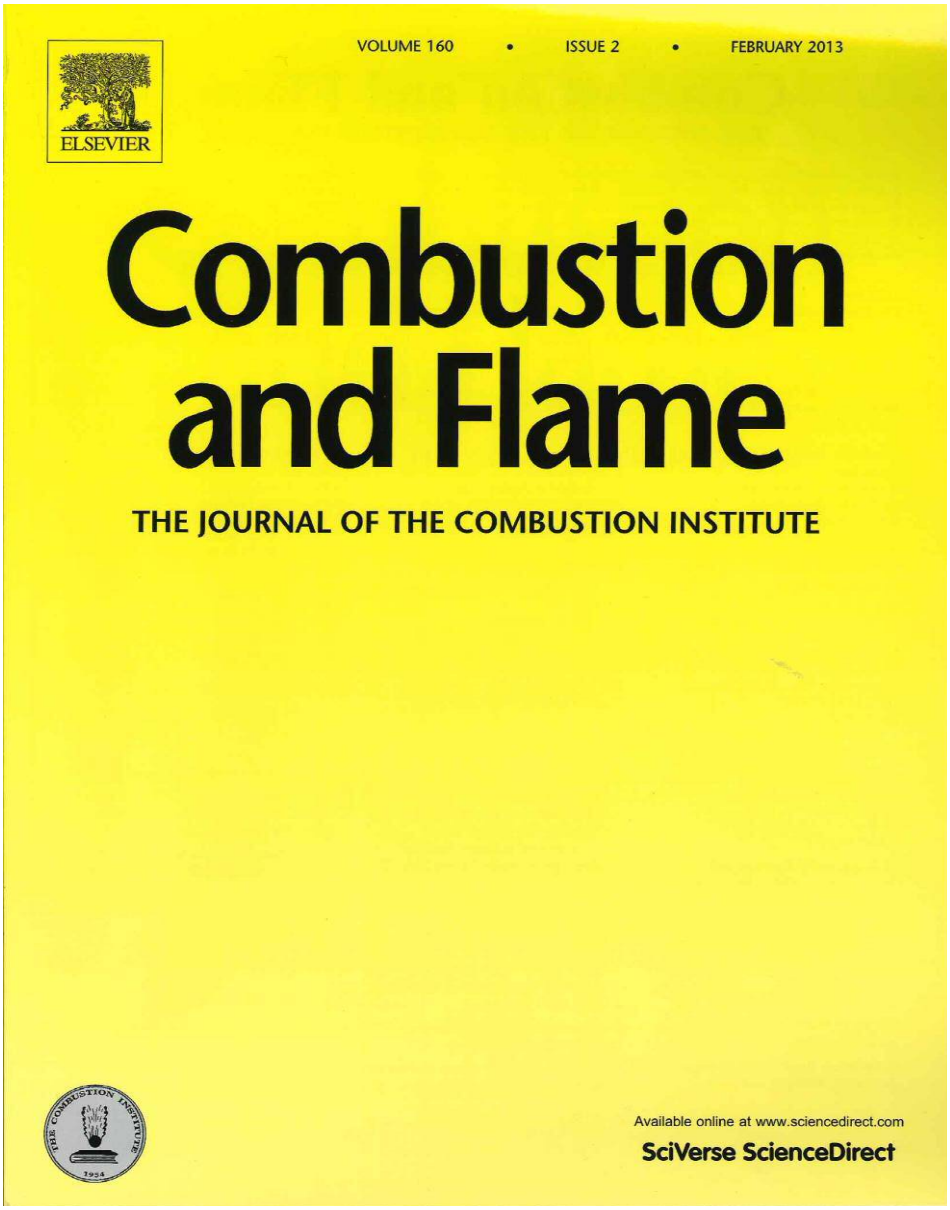

Combustion and Flame 161 (2014) 1096–1108

Contents lists available at ScienceDirect

Combustion and Flame

journal homepage: www.elsevier.com/locate/combustflame

Single particle ignition and combustion of anthracite, semi-anthracite and bituminous coals in air and simulated oxy-fuel conditions

Juan Riaza [a], Reza Khatami [b], Yiannis A. Levendis [b,*], Lucía Álvarez [a], María V. Gil [a], Covadonga Pevida [a], Fernando Rubiera [a], José J. Pis [a]

[a] Instituto Nacional del Carbón, INCAR-CSIC, Apartado 73, 33080 Oviedo, Spain
[b] Mechanical and Industrial Engineering Department, Northeastern University, Boston, MA 02115, USA

ARTICLE INFO

Article history:
Received 18 June 2013
Received in revised form 22 August 2013
Accepted 3 October 2013
Available online 23 October 2013

Keywords:
Oxy-fuel combustion
Ignition
Single particle
Pyrometry

ABSTRACT

A fundamental investigation has been conducted on the combustion behavior of single particles (75–150 μm) of four coals of different ranks: anthracite, semi-anthracite, medium-volatile bituminous and high-volatile bituminous. A laboratory-scale transparent laminar-flow drop-tube furnace, electrically-heated to 1400 K, was used to burn the coals. The experiments were performed in different combustion atmospheres: air (21%O_2/79%N_2) and four simulated dry oxy-fuel conditions: 21%O_2/79%CO_2, 30%O_2/70%CO_2, 35%O_2/65%CO_2 and 50%O_2/50%CO_2. The ignition and combustion of single particles was observed by means of three-color pyrometry and high-speed high-resolution cinematography to obtain temperature–time histories and record combustion behaviors. On the basis of the observations made with these techniques, a comprehensive examination of the ignition and combustion behaviors of these fuels was achieved. Higher rank coals (anthracite and semi-anthracite) ignited heterogeneously on the particle surface, whereas the bituminous coal particles ignited homogeneously in the gas phase. Moreover, deduced ignition temperatures increased with increasing coal rank and decreased with increasing oxygen concentrations. Strikingly disparate combustion behaviors were observed depending on the coal rank. The combustion of bituminous coal particles took place in two phases. First, volatiles evolved, ignited and burned in luminous enveloping flames. Upon extinction of these flames, the char residues ignited and burned. In contrast, the higher rank coal particles ignited and burned heterogeneously. The replacement of the background N_2 gas of air with CO_2 (i.e., changing from air to an oxy-fuel atmosphere) at the same oxygen mole fraction impaired the intensity of combustion. It reduced the combustion temperatures and lengthened the burnout times of the particles. Increasing the oxygen mole fraction in CO_2 to 30–35% restored the intensity of combustion to that of air for all the coals studied. Volatile flame burnout times increased linearly with the volatile matter content in the coal in both air and all oxygen mole fractions in CO_2. On the other hand, char burnout times increased linearly or quadratically versus carbon content in the coal, depending on the oxygen mole fraction in the background gas.

© 2013 The Combustion Institute. Published by Elsevier Inc. All rights reserved.

1. Introduction

Coal has been, and will continue to be, one of the major energy resources in the long term because of its abundant reserves and competitively low price, especially for use in power generation. The share of coal in world energy consumption was 30.3% in 2011, as opposed to 33.1% for oil and 23.7% for natural gas [1]. A diverse power generation portfolio including Carbon Capture and Storage (CCS) technologies and renewable energies is needed to reduce atmospheric CO_2 to below 1990 levels [2]. The deployment of oxy-fuel combustion in coal-fired utility boilers is seen as one of the major options for CO_2 capture. In this technology instead of using air as oxidizer, a mixture of oxygen and recycled flue gas (mainly CO_2 if dried) is employed to yield an effluent stream, rich in CO_2. However, the successful implementation of oxy-fuel combustion technology depends on fully understanding the difficulties that can arise from replacing nitrogen (inert) by CO_2 (reactive) in the oxidizer stream. Several factors such as char and volatile combustion or flame ignition and stability may be affected [3].

Previous work in this laboratory contrasted the combustion behaviors of single solid fuel particles of a bituminous high-volatile type-A coal, three low rank coals (low carbon content and low heating value coals): a sub-bituminous and two different lignites, as well as biomass (sugarcane bagasse) under air and under simulated dry oxy-firing conditions [4,5]. This work aims at examining the combustion behavior of additional bituminous coals (high- and medium-volatile types-B) as well as high rank coals (high carbon

* Corresponding author. Fax: +1 (617) 373 2921.
E-mail address: y.levendis@neu.edu (Y.A. Levendis).

0010-2180/$ - see front matter © 2013 The Combustion Institute. Published by Elsevier Inc. All rights reserved.
http://dx.doi.org/10.1016/j.combustflame.2013.10.004

content and high heating value coals), i.e., anthracite and semi-anthracite. The combustion and emission studies of bituminous coals has been well-documented in the aforementioned studies of Khatami et al. and Kazanc et al. in this laboratory [4–6] as well as in other studies including those of [7–10]. However, studies on anthracite and semi-anthracite coal particle ignition and combustion are scarce.

There are several possible oxy-fuel combustion zones which are a function of the preheat temperature and oxygen mole fraction of the oxidant stream [11]. Air-like oxy-fuel combustion systems have been viewed not only as an appropriate technology for new units but also as a retrofit strategy for existing coal-fired power plants. Oxygen concentrations that are similar to, or higher than, those of air combustion systems are used in these oxy-fuel regimes (with a flue gas recycle rate of 60–80 vol%, the oxygen mole fraction is about 30% in the oxidizer stream). However, oxygen-enriched combustion (where the oxygen mole fraction is significantly higher than 21%) and full oxy-fuel combustion with neat oxygen are of industrial interest for several reasons (e.g., improved coal ignition, higher flame temperature, greater flame stability, reduction in boiler size and consequently lower plant costs).

The aim of the present work is to evaluate the effect of oxygen mole fraction on the ignition and combustion characteristics of bituminous and higher rank coals. The coals selected were burned in different O_2/CO_2 environments (21–50% O_2) in a laboratory-scale, electrically-heated, laminar-flow drop-tube furnace fitted with a transparent quartz tube. An air combustion atmosphere (i.e., $21\%O_2/79\%N_2$) was used as a baseline for comparison with O_2/CO_2 background gases. The ignition and combustion behavior of single particles was observed by means of three-color optical pyrometry and simultaneous high-speed high-resolution cinematography. The data obtained contributes to the understanding of coal combustion phenomena, in both air and in oxy-firing conditions.

Table 1
Proximate and ultimate analyses of the coals.

Coal	AC	HVN	UM	SAB
Origin	Spain	Spain	Mexico	S. Africa
Rank	an	sa	mvb	hvb
Proximate analysis (wt.%, db)				
Ash	14.2	10.7	21.1	15.0
V.M.	3.6	9.2	23.7	29.9
F.C.[a]	82.2	80.1	55.2	55.1
Ultimate analysis (wt.%, daf)				
C	94.7	91.7	86.2	81.5
H	1.6	3.5	5.5	5.0
N	1.0	1.9	1.6	2.1
S	0.7	1.6	0.8	0.9
O[a]	2.0	1.3	5.9	10.5
High heating value (MJ kg^{-1}, db)	29.2	31.8	27.8	27.8

an: Anthracite; sa: semi-anthracite; mvb: medium-volatile bituminous coal; hvb: high-volatile bituminous coal.
db: Dry basis; daf: dry and ash free bases.
[a] Calculated by difference.

2. Materials and methods

2.1. Coal samples

Four coals of different ranks were burned: an anthracite from Asturias, Spain (AC), a semi-anthracite from the Hullera Vasco Leonesa in León, Spain (HVN), a South African high-volatile bituminous coal supplied by the Aboño power plant in Asturias (SAB), and a medium-volatile bituminous coal from Mexico (UM). The semi-anthracite coal (HVN) is a physical blend of approximately 90% anthracitic and 10% low volatile bituminous coal from the same mine. The coals were ground and sieved to a particle size cut of 75–150 μm. The fuels were dried prior to the experiments. Proximate analyses were obtained using a LECO TGA-601 in accordance with ASTM D7582-10 [12]. Ultimate analyses was determined using a LECO CHNS-932 instrument in accordance with

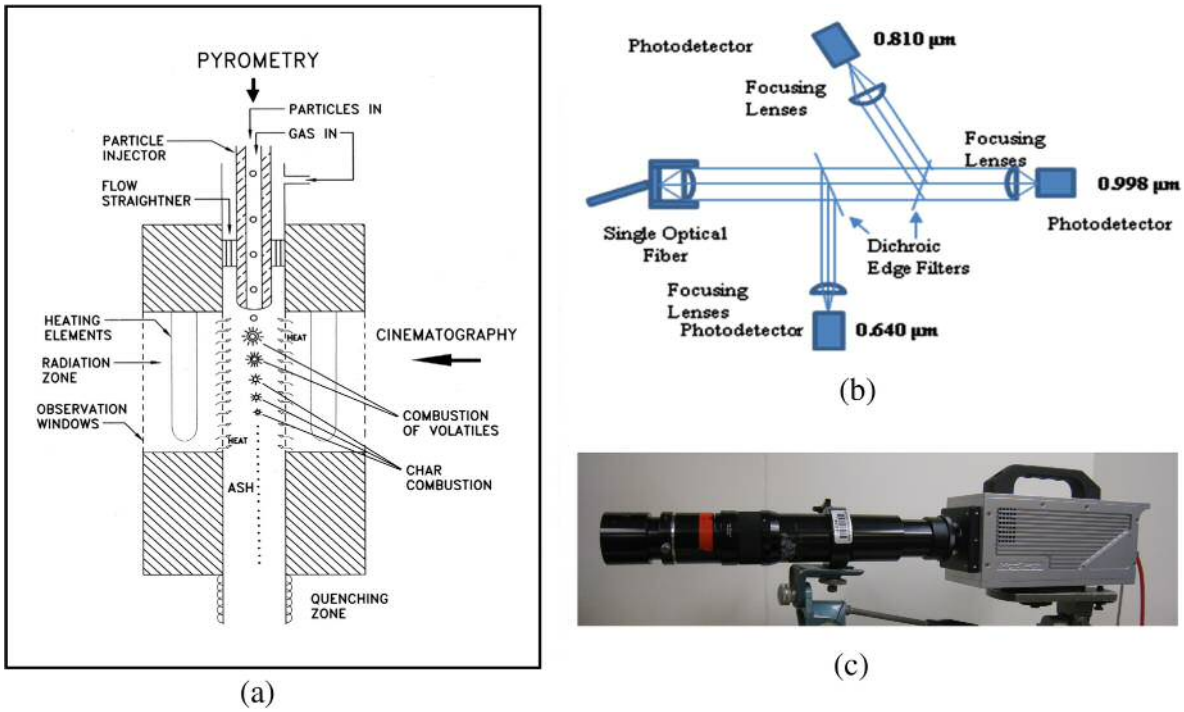

Fig. 1. Schematic of the experimental setup and diagnostic facilities. (a) Drop tube furnace (DTF), (b) three-color optical pyrometer and (c) high speed camera.

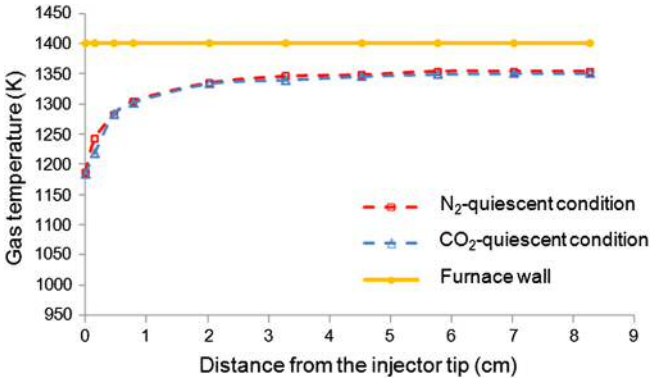

Fig. 2. Centerline gas temperature inside the drop-tube furnace filled with either neat N_2 or neat CO_2. The furnace wall temperature was set at 1400 K.

ASTM D3176-89 [13]. Results of the analyses of the coals are presented in Table 1.

2.2. Experimental apparatus and procedure

The combustion studies of free-falling coal particles were performed in an electrically-heated laminar-flow drop-tube furnace, a detailed description of which has been provided elsewhere [14]. Here only a brief description of the reactor is given. The radiation cavity of the furnace (an *ATS* unit) is 25 cm long and is heated with molybdenum disilicide heating elements. A sealed transparent quartz tube with a 7-cm inner diameter was fitted in this furnace. A water-cooled injector was used to introduce single fuel particles at the top of the furnace (Fig. 1a). The furnace wall temperatures (T_f) were continuously monitored by means of type-S thermocouples embedded in the wall. The particle heating rates were high, calculated to be of the order of 10^4 K/s. Optical access to the radiation zone of the furnace was achieved through three observation ports: one at the top (used for pyrometry) and two orthogonally situated at the sides of the furnace (used for cinematography).

Pyrometric observations of the burning single particles were conducted from the top of the furnace injector, viewing downwards along the central axis of the furnace, as this ideally would be the particle's trajectory. In this way, complete luminous burnout histories of the single coal particles – from ignition to extinction – were recorded. Details of the pyrometer optics, electronics, calibration hardware and performance have been reported elsewhere [15], so here only a brief description is provided. An optical fiber made up of a high-transmittance (>99.5%) fused silica core and doped fused silica cladding with an *f*-number of 2.2, transmitted light from the furnace to the pyrometer assembly. The pyrometer used two dichroic edge filters as spectrum splitters to direct the light to the three interference filters (see Fig. 1b) having effective wavelengths of 0.640, 0.810 and 0.998 μm and bandwidths (FWHM) of 70 nm. In conjunction with the interference filters, silicon diode detectors were employed, the voltage outputs of which represented spectral radiation intensities of burning particles. These signals were used to deduce particle temperatures [16].

High-speed cinematography was conducted through the slotted side quartz windows of the drop-tube furnace against backlight (Fig. 1a). A *NAC HotShot 512SC* self-contained digital high-speed video camera was used, set to speeds of 1000 or 2000 frames/s. The camera was fitted with an *Olympus-Infinity* Model K2 long-distance microscope lens to provide high-magnification images of the combustion events (see Fig. 1c).

The morphology of the coal chars was examined by means of scanning electron microscopy (SEM). Secondary electron images of the samples were obtained with a field emission scanning electron microscope (Quanta FEG-650-FEI) operated at 30 kV.

2.3. Furnace gas temperature and composition

Coal particle combustion experiments were conducted under quiescent gas conditions (i.e., no gas flow in the drop-tube furnace)

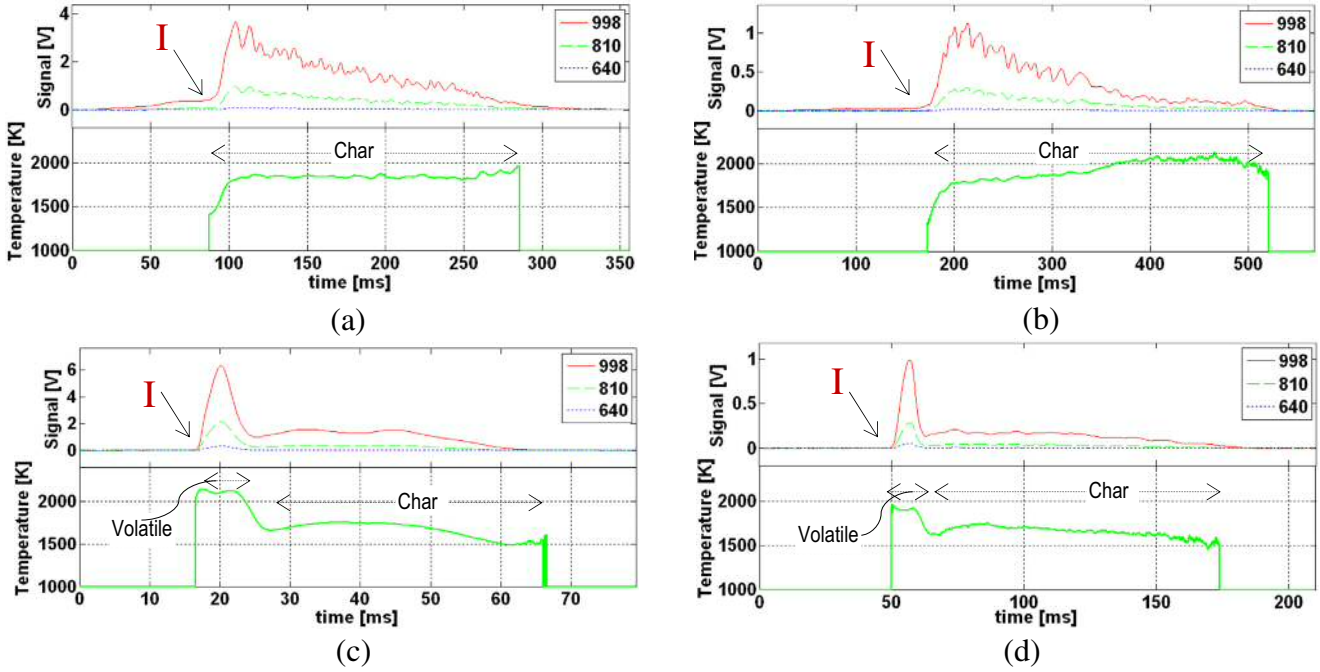

Fig. 3. Examples of pyrometric profiles of (a) anthracite (AC), (b) semi-anthracite (HVN), (c) hvb bituminous (SAB), (d) mvb bituminous (UM) particles (75–150 μm) during their combustion in air, at a wall temperature of 1400 K and their deduced particle temperatures. Volatile flame and char combustion phases are denoted. The three pyrometric signals were centered at 998, 810 and 640 nm. I stands for the onset of ignition.

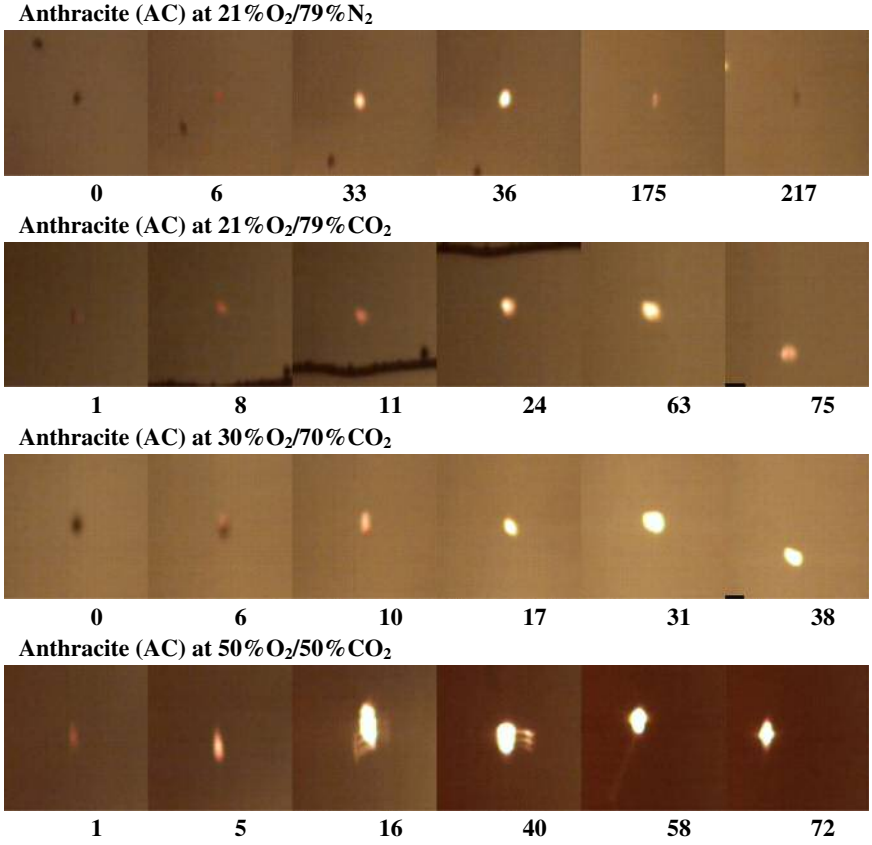

Fig. 4. High-speed, high magnification cinematography images of single particles (75–150 μm) of anthracite coal (AC) in air and different O_2/CO_2 atmospheres. The displayed numbers in each frame denote milliseconds. A thermocouple wire (100 μm) is shown in the 21%O_2/79%CO_2 case to facilitate assessment of the particle/flame size.

in order to equalize the axial temperature profiles of N_2- and CO_2-containing furnace gases, as documented by Khatami et al. [5]. As shown in Fig. 2, under quiescent gas conditions (no flow), the axial gas temperature profiles in the furnace increased along its centerline and in a short distance from the particle injector tip they reached asymptotically 1340 K. The gas compositions inside the furnace included air as well as the following four binary mixtures of O_2/CO_2 (21%O_2/79%CO_2, 30%O_2/70%CO_2, 35%O_2/65%CO_2 and 50%O_2/50%CO_2).

3. Results

3.1. Temperature–time history of coal particles

Typical examples of radiation intensity–time and temperature–time profiles of single coal particles during their entire burnout history in air-firing conditions are displayed in Fig. 3. The radiation intensity traces were represented by the output voltage signals S_n of all three wavelength channels of the pyrometer. The temperature deduction method has been described in Ref. [16].

In the case of the bituminous coals two separate combustion phases were distinguished by three-color pyrometry (see Fig. 3c and d). In contrast, the anthracitic and most of the semi-anthracite coal particles experienced only one combustion phase (see Fig. 3a and b).

3.2. High-speed cinematography stills

Selected images from high-speed, high-resolution cinematography of particles of the four coals burning in air (21%O_2/79%N_2) and in three of the simulated oxy-fuel atmospheres studied (21%O_2/79%CO_2, 30%O_2/70%CO_2 and 50%O_2/50%CO_2), are shown in Figs. 4–7.

Most of the AC coal particles in air burned with no evidence of volatile matter flames (see Fig. 4). These coal particles ignited and burned heterogeneously by direct attack of oxygen on their surfaces. Due to the known low reactivity of the anthracite AC particles [17], their ignition was delayed. The color of the particles changed from dark (black) to bright (nearly-white) as their surfaces became incandescent; this change occurred gradually over a few milliseconds.

As the HVN coal is a physical blend of approx. 90% anthracitic and 10% low volatile bituminous coal from the same mine, most HVN coal particles burned in the same way as the AC anthracite coal particles. A few particles, however, experienced small enveloping flames attributed to combustion of volatiles (see Fig. 5, second frames in first and fourth cases). Once the flames were extinguished, the resulting chars proceeded to burn heterogeneously.

The two bituminous coals of this study, UM and SAB, experienced similar combustion trends, as exemplified in Figs. 6 and 7, including homogeneous ignition and combustion of volatiles in envelope flames, followed by heterogeneous ignition, combustion and extinction of the resulting chars. The volatiles produced large sooty flames that ignited in the gas phase and completely surrounded individual particles. The different relative velocities between the free-falling particles and the surrounding furnace gas led to the formation of con-trails that burned in the wake of the particles; sometimes the gas flames expanded backwards from the particles. Since the volatiles contain tars, in some cases drops of burning tars can be distinguished inside the flame as sources

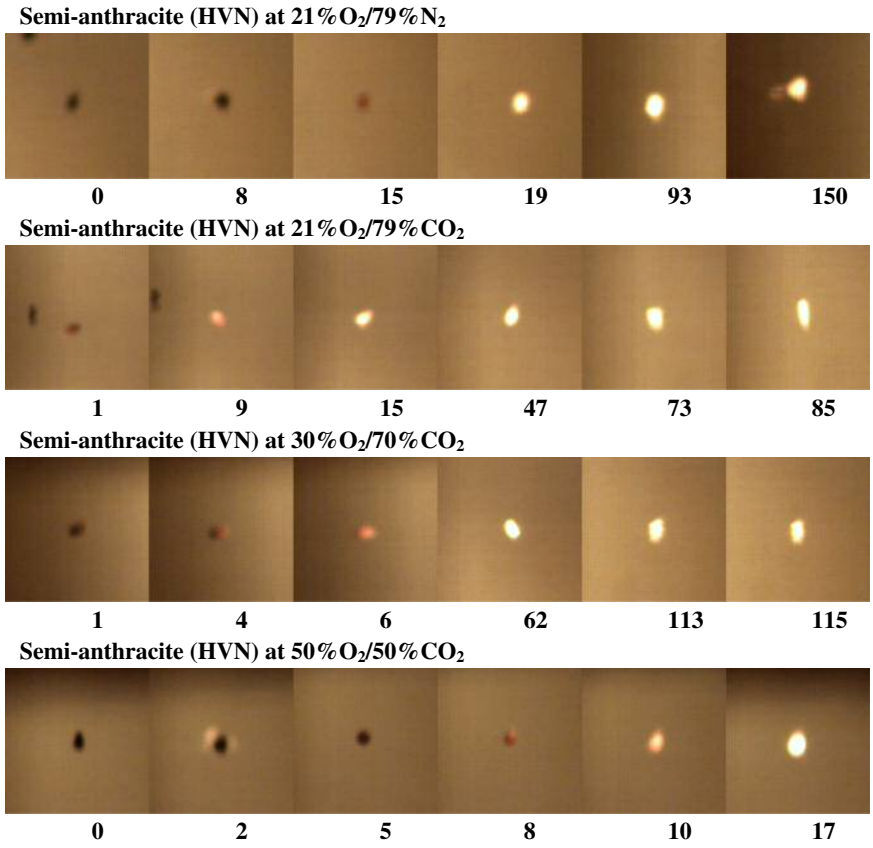

Fig. 5. High-speed, high magnification cinematography images of single particles (75–150 μm) of semi-anthracite coal (HVN) in air and different O_2/CO_2 atmospheres. The displayed numbers in each frame denote milliseconds.

of high luminosity. Tars need more time to burn up, hence occasionally some of these drops continued to burn while the flame burned out. In atmospheres containing 21% O_2 the drops were sometimes quenched before completely burning out resulting in the formation of soot ligaments. This phenomenon was especially noticeable in the 21%O_2/79%CO_2 atmosphere. Upon extinction of a volatile flame, the luminous combustion of the char commenced. The recorded cinematographic images suggest the final diameters of the chars approached those of the estimated size of ash residues, as discussed in the Appendix A.

For the four coals studied, when N_2 was replaced with CO_2, keeping the oxygen mole fraction constant, the burning particles appeared dimmer. This is indicative of slower oxidation, which causes lower flame/particle temperatures. Dim combustion was also observed by Zhang et al. [18], who reported that the average intensity of coal particles burning in O_2/CO_2 with oxygen concentrations below 30%, was much lower than that in air. Moreover, in our study the brightness and intensity of combustion increased drastically with O_2 in the O_2/CO_2 environments, which is indicative of rapid oxidation. In fact, particle combustion images of the 30%O_2/70%CO_2 atmosphere resembled those in air.

3.3. Morphology of coal chars

The chars obtained from coal devolatilization under N_2 and CO_2 background gases in an entrained reactor were examined by SEM; sample images are shown in Fig. 8. These photographs were obtained in prior experiments, described in Ref. [19], at an average reactor gas temperature of 1273 K. This temperature is in the range of gas temperatures encountered in the experiments herein in the region of the furnace herein where particle devolatilization has been observed to take place prior to ignition, i.e., in the first centimeter of the furnace, see temperature profile shown in Fig. 2. As shown in Fig. 8, the anthracite (AC) and the semi-anthracite (HVN) coal chars consist of angular solid particles with sharp edges. The AC chars have sharper edges (see Fig. 8a, b, e, and f) than the HVN chars. The medium volatile bituminous UM chars have striking bubble-like network-type structures (Fig. 8c and g). The particles must have exhibited intense swelling and bubbling during devolatilization to form cenospheric char particles with almost transparent walls. Large blow-holes often appear on the surfaces, particularly in CO_2 (Fig. 8g). Cenospheric char formation with associated swelling was also observed in the case of the high-volatile bituminous SAB particles (Fig. 8d and h). However, the walls of the SAB cenospheres appear to be much thicker and much more opaque than those of the UM cenospheres.

4. Discussion

The ignition and combustion behavior of anthracite, semianthracite and bituminous coal particles were determined based on the combined diagnostic techniques of pyrometry and back-light cinematography, in conjunction of scanning electron microscopy.

4.1. Ignition phenomena and ignition temperatures

4.1.1. Ignition mode

Ignition-related events of anthracite, semi anthracite and bituminous coal particles, are illustrated in the initial stills of the photographic sequences depicted in Figs. 4–7. The determination of ignition mode in this work relied on luminous emissions. Anthracite and semi-anthracite coal particles ignited heterogeneously

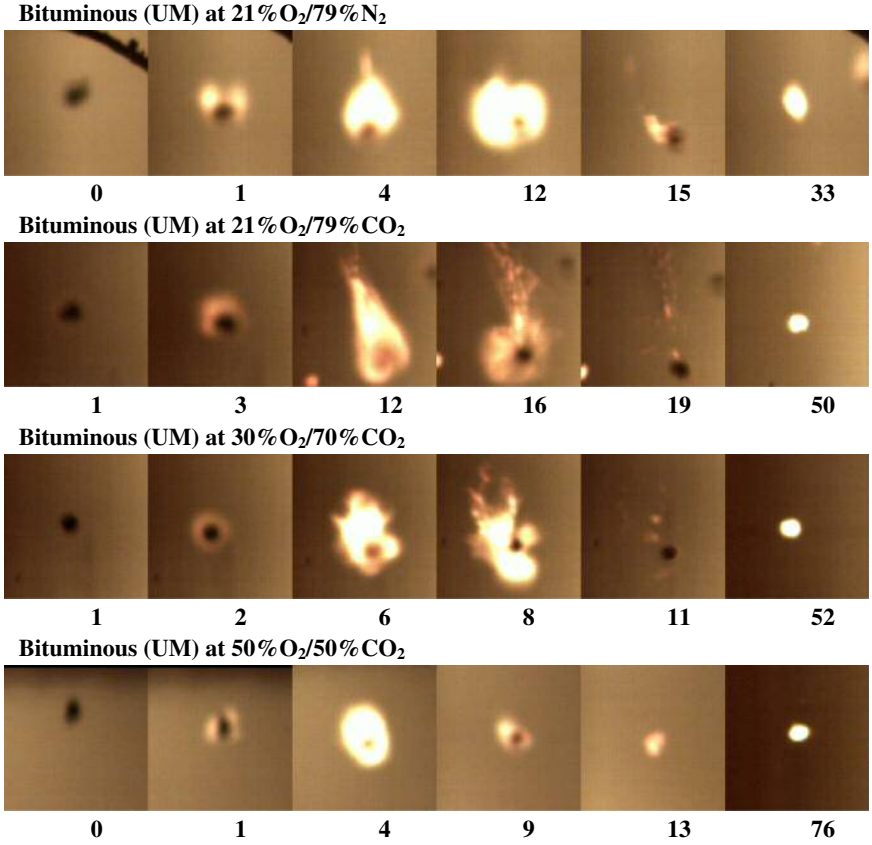

Fig. 6. High-speed, high magnification cinematography images of single particles (75–150 μm) of medium volatile bituminous coal (UM) in air and different O_2/CO_2 atmospheres. The displayed numbers in each frame denote milliseconds. A thermocouple wire (100 μm) is shown in the 21%O_2/79%N_2 case to facilitate assessment of the particle/flame size.

on the particle surfaces. Such ignition mode is attributed to the low volatile matter content and high fixed carbon content of these coals. In the case of a few semi-anthracite particles, gas-phase (homogeneous) ignition took place due to their higher volatile matter content as discussed earlier. The nature of the heterogeneous ignition of anthracite and semi-anthracite particles is however different to that of lignite coals, previously studied in this laboratory [5]. Although the lignite coal particles contained sufficient amounts of volatile matters for gas-phase ignition, their extensive fragmentation and the small fragment sizes were the main reasons for their heterogeneous ignition [5]. The much higher volatile content bituminous coal particles of this study ignited in the gas phase (homogeneously). The homogeneous ignition mode of bituminous coal in the current study is in line with previous observations in this laboratory for the Pittsburgh #8 high-volatile bituminous coal [5].

4.1.2. Ignition temperatures

In this study, ignition temperature was defined as the first point where the maximum particle temperature gradient (dT_p/dt) was recorded, see Fig. 9a. Figure 9b shows the ignition temperatures in air as well as in different O_2/CO_2 atmospheres for various fuels, under the conditions of this study. Each data point in this figure represents average ignition temperatures from at least 8 randomly-selected particles. Ignition temperature data for lignite coal particles from a previous study in this laboratory [4] are also displayed in this figure for comparison.

Figure 9 illustrates that higher rank coals ignited at higher temperatures. Moreover, replacing N_2 with CO_2 increased the ignition temperature, but only negligibly. Increasing oxygen mole fraction in CO_2 consistently decreased the ignition temperature for all coal ranks.

4.2. Combustion mode

Single particle combustion modes were discussed comprehensively in previous studies [4,5,20]. In summary, Howard and Essenhigh [20] studied the combustion phenomena of coal particles and proposed a model to assess whether the burning of the volatiles and char takes place sequentially or simultaneously. Khatami et al. [4,5] employed that model to a number of coals from different ranks in a variety of oxygen–nitrogen and oxygen-carbon dioxide environments. The terms *two-mode* and *one-mode* combustion were used to respectively signify events where gas-phase combustion of the volatiles takes place in an enveloping flame, prior to heterogeneous char particle combustion, and where volatile and solid char combustion take place simultaneously.

(a) *Anthracitic* and the majority *of semi-anthracite coal* particles exhibited only one wide peak in each pyrometric profile, which is attributed to heterogeneous combustion of the char (see Fig. 3a and b) with possible simultaneous burning of volatiles. This observation is consistent with the cinematographic behavior, where there is no evidence of an enveloping flame corresponding to volatiles combustion, but only that of the incandescent burning char. Such anthracitic coals produced no incandescent trails of volatiles (see Figs. 4 and 5). Moreover, most of the anthracite particles and some semi-anthracite particles exhibited striking undulation patterns (wave patterns) in their radiation intensity pyrometric

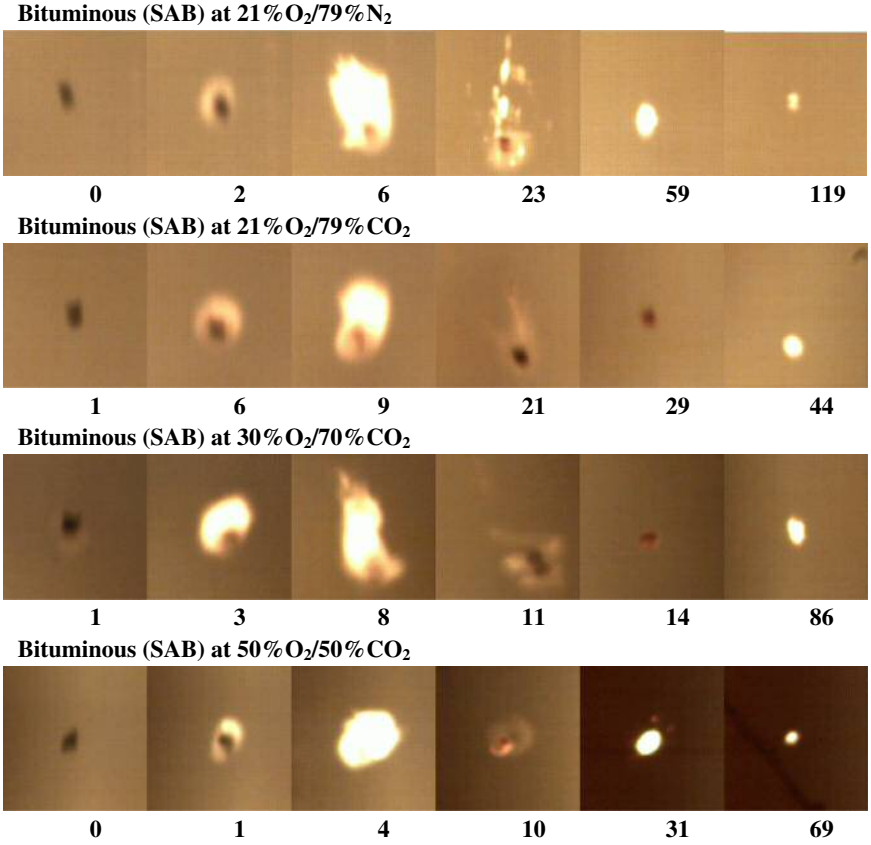

Fig. 7. High-speed, high magnification cinematography images of single particles (75–150 μm) of high volatile bituminous coal (SAB) in air and different O_2/CO_2 atmospheres. The displayed numbers in each frame denote milliseconds.

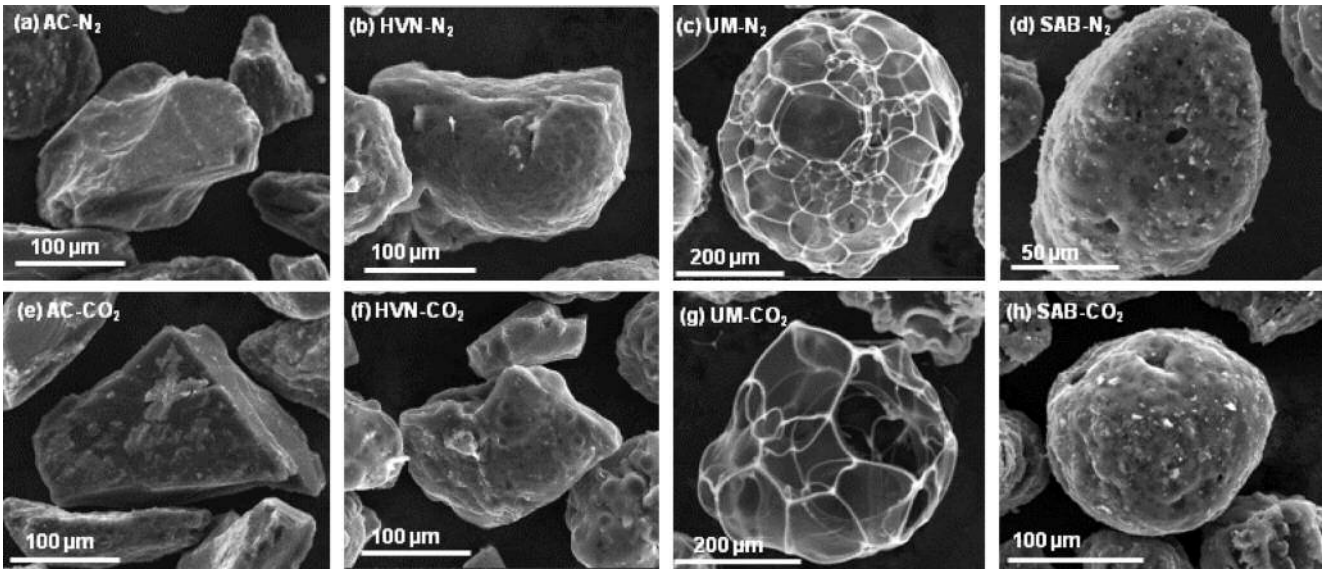

Fig. 8. SEM images of the anthracite (AC), semi-anthracite (HVN) and medium- and high-volatile bituminous (UM, SAB) coal char particles obtained under N_2 (a–d) and CO_2 (e–h) in an entrained flow reactor (EFR) at 1273 K and a particle residence time of 2.5 s [19].

signals. As the deduced temperature profiles do not show such undulations, but deduced luminous cross sectional areas do (with a method outlined in Ref. [16]), such conspicuous undulation patterns were attributed to particle rotations during combustion. Such patterns can indeed be detected in cinematographic sequences as the one shown in Fig. 10. Somehow the anthracite char particles, which as documented earlier (see Section 3.3) retain their planar and angular shapes upon devolatilization and supposedly throughout char combustion, experienced rotation

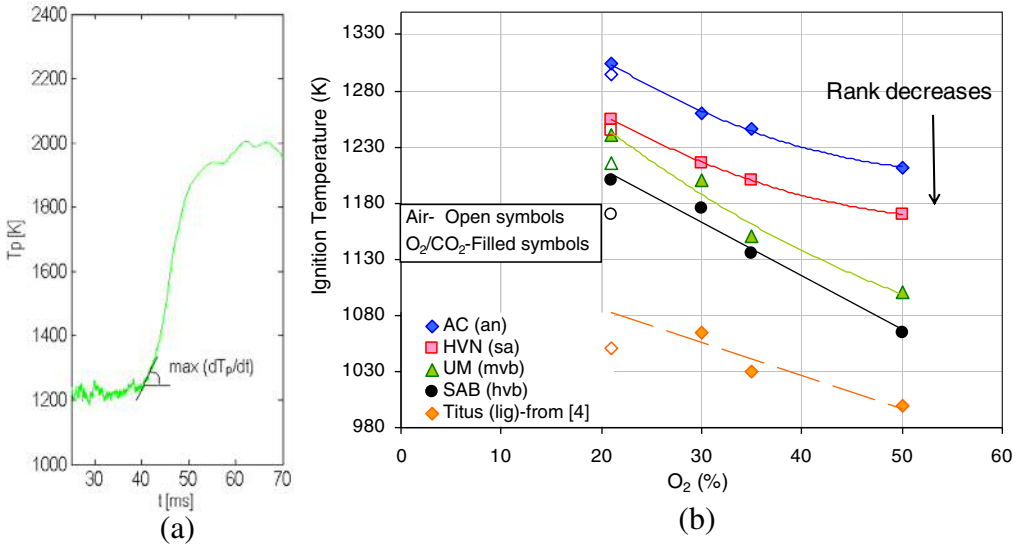

Fig. 9. (a) Typical ignition temperature criterion for a pyrometric profile which is defined as the point where the maximum particle temperature gradient was recorded (b) Average deduced ignition temperatures for the four coals of the current study in air and different oxy-fuel environments. Ignition temperatures of lignite, a low rank coal, were also inserted herein from a previous study in this laboratory [4].

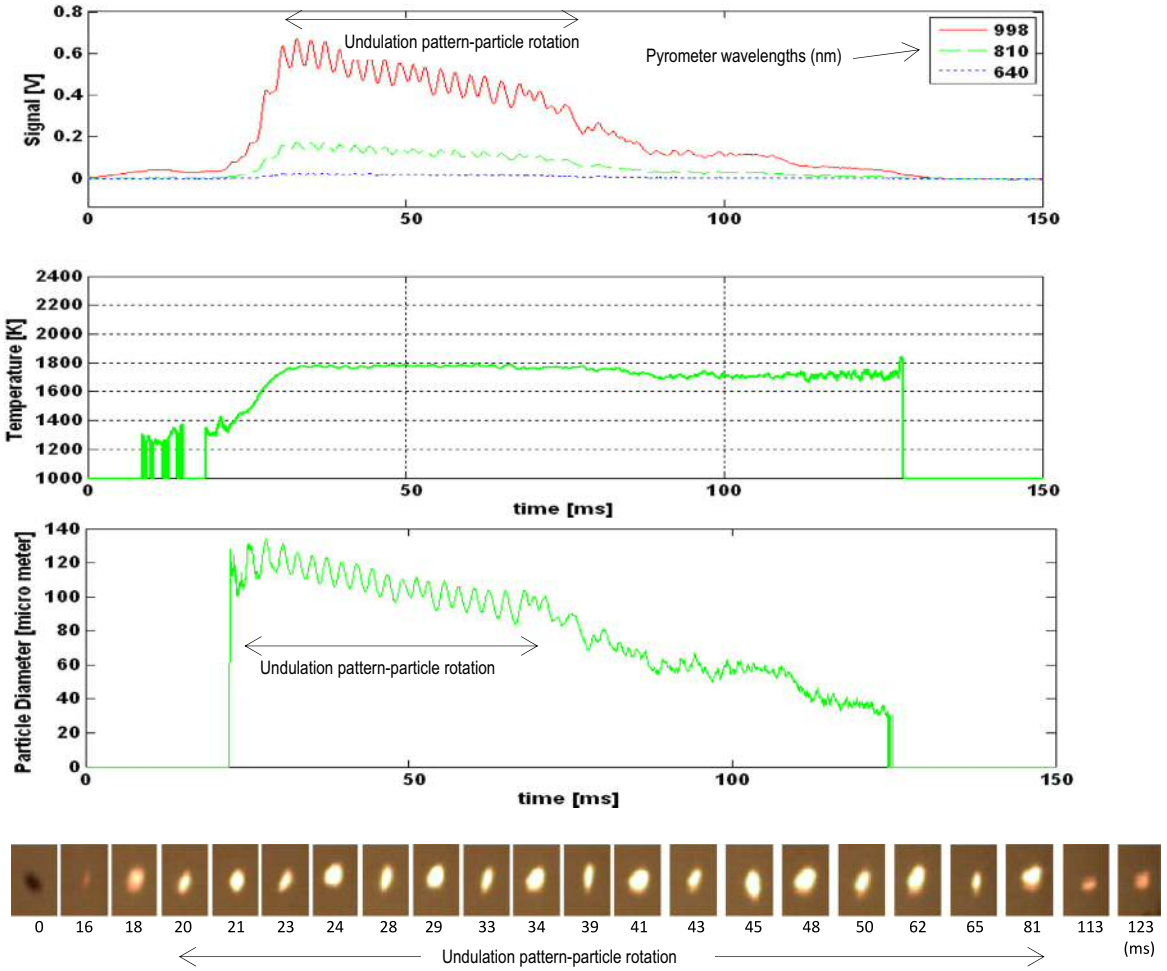

Fig. 10. An example of a pyrometric profile of an anthracite coal particle (75–150 μm) burning in air, at a wall temperature of 1400 K and its deduced particle temperature profile.

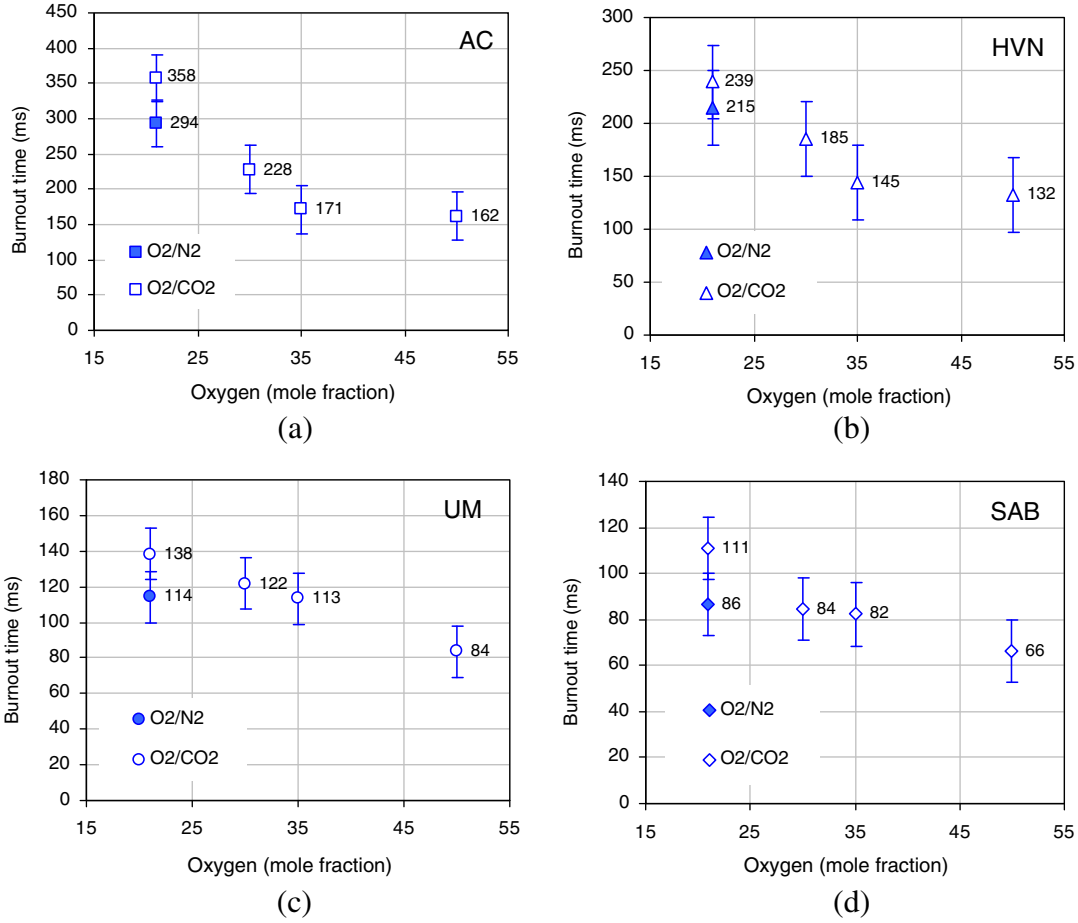

Fig. 11. Average burnout times for the four coals (a–d) studied in air and different oxy-fuel environments. The error bars represent standard deviations of the data (2σ).

(tumbling) as they fell in the drop tube furnace. These coals are non-swelling and they release much fewer volatiles than the bituminous coals, as also reported by Seeker et al. [21].

(b) The *bituminous coal* particles exhibited two peaks in each profile, an exceedingly strong first peak followed by a less pronounced second peak (see Fig. 3c and d). The first peak is attributed to volatiles burning homogeneously in luminous enveloping flames, whereas the second peak is attributed to the heterogeneous combustion of char. The combustion of the chars was lengthy and bright. The bituminous coals are rich in volatile hydrocarbons and tars, some of which are soot precursors [22]. Bituminous coals typically swell up and form cenospheric spheroid chars, as illustrated in Section 3.3. In doing so, they expel volatiles in jets or trails (e.g. Fig. 6, 30%O_2/70%CO_2, 8 ms, Fig. 7, 21%O_2/79%N_2, 23 ms), forming condensed matter around a particle. In the regions where there are no jets of volatiles, there is a possibility of heterogeneous surface reaction with oxygen. The temperatures of most bituminous chars experienced small variations with time, whereas the spectral radiation intensity and particle diameter plateaued for a time and then, slowly decreased. This behavior of the bituminous particles is clearly illustrated in the cinematographic images (see Figs. 6 and 7), and has been well documented in the literature [4,14,21,23,24].

4.3. Effect of fuel type on temperature and burnout time

The burnout time data and temperatures are shown in Figs. 11 and 12, respectively. The pyrometric burnout times are based on the duration of the pyrometer signal from its onset (particle ignition) to its termination (particle extinction), both defined herein when the highest-intensity signal ($\lambda = 998$ nm) of a particular event exceeds the baseline by a factor of at least 10, i.e., $S_{signal}/S_{baseline} > 10$. The temperatures displayed were the maximum temperatures deduced from the single particle combustion histories (as exemplified in Fig. 3). Each data point represents the mean values from at least 15–20 individual particle combustion events.

In this sub-section only the examples in the air atmosphere are described for a clearer comparison between the coals. The burnout times of the bituminous particles were much shorter than the burnout times of the anthracitic particles. This may be due to the higher volatile matter content of the bituminous coals (which enhances subsequent char combustion), and to their higher reactivity. As high rank coals release few volatiles, there were very small differences between the chars and the original coal particles. On the other hand, in the case of the bituminous coals, their chars showed significant signs of swelling after devolatilization [19]. This created more specific surface area, and therefore enhanced particle reactivity. As can be seen from Fig. 11, the burnout times in air for the anthracitic coals were the longest, 294 ms and 215 ms for AC and HVN, respectively; whereas for bituminous coals UM and SAB the burnout times were 114 ms and 86 ms, respectively.

As can be seen in the cinematographic records, bituminous coals displayed a tendency to burn in *two-mode* combustion. Volatiles often contain a large amount of stored energy (heating value) and, as can be seen in Fig. 12, the combustion of volatiles was the hottest and the fastest (typically lasting 10–15 ms in air). Lower temperatures were reached during char combustion. The

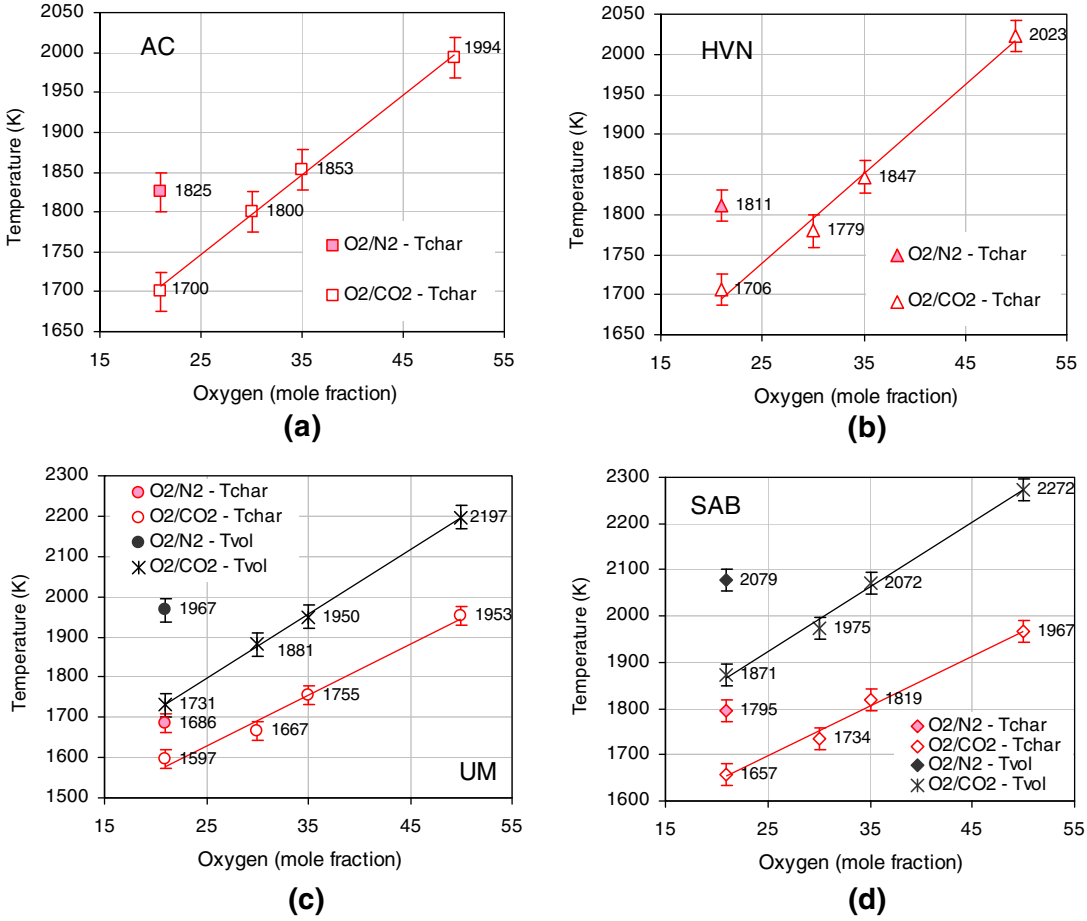

Fig. 12. Average char and volatile matter combustion temperatures for the four coals studied (a–d) in air and different oxy-fuel environments. The error bars represent standard deviations of the data (2σ).

Table 2
Oxygen content (%) in the O_2/CO_2 required to achieve the same char and volatile temperature as in air-firing conditions.

	AC	HVN	UM	SAB
Equivalent $T_{volatile}$	–	–	35.7	36.2
Equivalent T_{char}	32.8	31.5	29.4	34.1

high-volatile bituminous SAB coal contained the highest amount of volatile matter. The average temperatures reached during its combustion in air were also the highest, 2079 K and 1795 K for volatiles and char, respectively, whereas in the combustion of the medium volatile bituminous UM coal in air, which has a lower volatile matter content, average temperatures of 1967 K and 1686 K were reached for volatiles and char, respectively. On the other hand, anthracitic coals burned in *one-mode* combustion by direct attack of oxygen on the char surface. During the combustion of AC and HVN in air, the average char temperatures reached were 1825 K and 1811 K, respectively.

4.4. Effect of the diluent background gases (N_2 and CO_2) and oxygen mole fraction on temperatures and burnout times

As can be seen in Fig. 12 the particle temperatures (in the case of bituminous coals for both volatiles and chars) were higher during their combustion in 21%O_2/79%N_2 than in 21%O_2/79%CO_2, whereas their corresponding burnout times were shorter (see Fig. 11). A factor controlling the particle temperatures is the volumetric heat capacity of the surrounding gas mixture, which is higher in O_2/CO_2 than in O_2/N_2, atmospheres causing both the volatile matter flame temperatures and the char temperatures to drop [4,8,25]. Other important factors which influence char combustion temperature are the lower binary diffusion of O_2 in CO_2 and the endothermicity of the char-CO_2 reactions [25–27]. Larger CO concentrations, formed partly due to incomplete combustion of the volatiles, and partly driven from char CO_2 gasification reactions, would also contribute to the worsening of the burning properties of the coal, by forming a persistent cloud around the particle, thereby preventing the access of oxygen to the surface of the particle [17].

The particle temperature (in the case of the bituminous coals for both the char and the volatiles) increased and the burnout times decreased with the enhancement of the oxygen content in the CO_2 mixture. However, the shortening in the burnout times and the enhancement of temperatures was not the same for all the coals studied. It was more marked in the case of the anthracitic coals since the bituminous coals reached a high burnout value in atmospheres with lower oxygen content (i.e., 21%O_2/79%N_2 and 21%O_2/79%CO_2) [28] . Increasing the O_2 percentage in the CO_2 mixture up to 50% was still insufficient to match the heat capacity of air (Heat capacity of pure gases (at 1400 K) are N_2 34.18 kJ/kmol K; O_2 36.08 kJ/kmol K and CO_2 57.83 kJ/kmol K. Therefore, heat capacity of the air and some of the O_2/CO_2 environments in this study are: Air = 34.6 kJ/kmol K, 21%O_2/79%CO_2 = 53.3 kJ/kmol K, 50%O_2/50%CO_2 = 47 kJ/kmol K.). However, the rise in the mass flux rate increased the reactivity characteristic of the local mixture [27]. Bejarano and Levendis [8] found that the higher the oxygen mole fraction, the higher the char surface temperature and the shorter

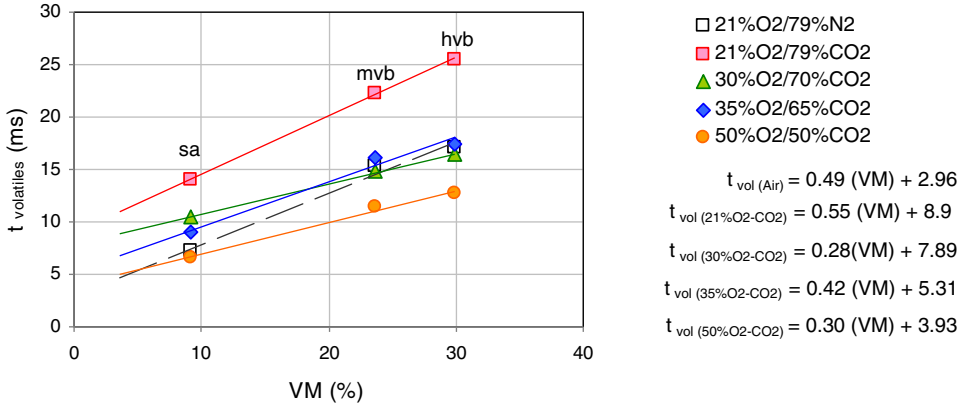

Fig. 13. Average observed volatile burnout times versus volatile matter content (VM) of the coals. Experiments were performed at 1400 K furnace temperature with particle diameters in the range 75–150 μm.

the burnout time. In addition, if there is sufficient oxygen, the homogeneous combustion of the gasification-derived CO to CO_2 could provide extra heat. Joutsenoja and Saastamoinen [29] measured temperature snapshots of burning single particles in an entrained flow reactor using a pyrometric method, when the oxygen mole fraction ranged between 3% and 30% and they also reported that the particle temperature increased with oxygen mole fraction.

In summary, coals burned hotter and faster in N_2 than in CO_2 background gases at comparable oxygen mole fractions. To attain the same volatiles flame and char temperatures as in air (21%O_2), the oxygen content in CO_2 mixtures had to be increased to ~35% for these bituminous coals, and to ~30% for these anthracitic coals. The values of oxygen needed to achieve the same particle char and volatiles temperatures in oxy-fuel conditions as in air-firing, are shown in Table 2. Increasing the oxygen concentration to such values also led to shortened burnout times and temperature hikes, although they are less remarkable. These results are in agreement with previous studies carried out for other fuels with different experimental devices [10,30,31]. These observations have practical ramifications in the operation of future furnaces under oxy-coal combustion conditions. The successful implementation of O_2/CO_2 technology in conventional pulverized coal boilers requires a full understanding of the changes that occur when N_2 is replaced by CO_2 in a combustion atmosphere; this is essential for designing and modeling oxy-fuel combustion at an industrial scale. One should keep in mind however, that had combustion occurred in active flow conditions in the furnace and not under the quiescent conditions of this study (which resulted in the gas temperature profiles depicted in Fig. 2) the O_2/CO_2 gas temperatures would have been lower than the O_2/N_2 gas temperatures, since CO_2 heats up slower [5]. This would have resulted in lower coal particle temperatures in CO_2 background gases than those reported herein. Hence, somewhat higher oxygen mole fractions in CO_2 would have been needed than those shown in Table 2 to match the particle temperatures in conventional air combustion. Alternatively, preheating of the O_2/CO_2 gases could have been implemented to compensate for their slower heating rate in the furnace. In this case the mole fractions listed in Table 2 may still be valid, depending on the degree of preheating.

4.5. Effect of volatile matter (VM) content on the volatile flame burnout times

Figure 13 shows the volatile flame burnout times of the different coals in this study versus volatile matter content of the fuels burning in air and in various O_2/CO_2 atmospheres. The volatile burnout times increased linearly with increasing volatile matter content (VM) of the coals in all gas environments. The linear dependency equations of volatile burnout times ($T_{volatiles}$) and volatile matter content in the coal (VM) are shown in Fig. 13. It should be mentioned that the linear equations in Fig. 13 were derived for the experimental conditions of this study (i.e., T_f = 1400 K and

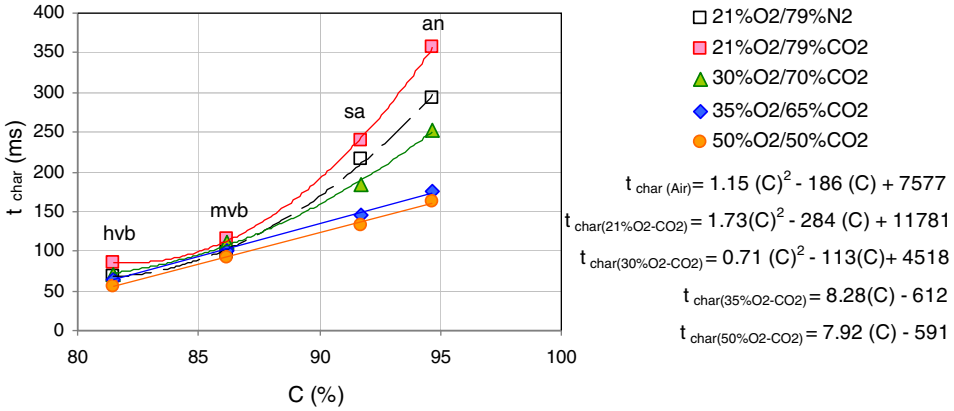

Fig. 14. Average char burnout times versus carbon content (C) of the coals. Experiments were performed at 1400 K furnace temperature with particle diameters in the range 75–150 μm.

particle sizes 75–150 μm) and may not be necessarily valid for different experimental/operating conditions.

4.6. Effect of carbon content (C) on the char burnout times

Figure 14 shows the char burnout times of different coals versus carbon content of the fuels burning in air and in various O_2/CO_2 atmospheres. The char burnout times increased with increasing carbon content (C) of the coals in all gas environments. However, the dependency of char burnout times versus carbon content (C) was quadratic for air and lower oxygen mole fractions in CO_2 (21%O_2), whereas this dependency became linear at higher O_2 mole fractions (35%O_2, 50%O_2). The quadratic and linear equations of char burnout times (T_{char}) versus carbon content of the coal (C) are also displayed in Fig. 14. It should be again mentioned that the equations shown in Fig. 14 were derived for the experimental conditions of this study (T_f = 1400 K and particle sizes 75–150 μm) and, again, may not be necessarily valid for different experimental/operating conditions.

5. Conclusions

Pulverized fuel particles (75–150 μm) from four high and medium rank coals were burned in a drop-tube furnace, set at 1400 K, under air and simulated dry oxy-firing conditions. The goal was to assess the ignition and combustion behaviors of single coal particles in different combustion atmospheres with combined cinematographic and pyrometric diagnostic tools. The most important conclusions are as follows:

(a) High rank coals (anthracite and semi-anthracite) ignited heterogeneously at the particle surface, whereas bituminous coals ignited in the gas phase (homogeneously).
(b) Ignition temperatures increased with the enhancement of coal rank in either air or oxy-fuel combustion conditions. Increasing oxygen mole fraction from 21% to 50% in CO_2 decreased the ignition temperature for all coals.
(c) Replacing the N_2 in air by CO_2 slightly increased the ignition temperature (30–40 K).
(d) Particles of the two bituminous coals burned with distinct volatile matter and char combustion phases (i.e., two-mode combustion), whereas the anthracitic and most semi-anthracite coal particles burned in a single combustion phase, which was mostly attributed to char. The temperatures of the bituminous coal char particles were lower than those of the anthracitic coals, and their combustion durations were much shorter.
(e) For the four coals studied, particle luminosity and the deduced temperatures were higher in the 21%O_2/79%N_2 atmosphere than in 21%O_2/79%CO_2. The replacement of N_2 by CO_2 reduced the bituminous volatiles flame temperatures by as much as 210 K, and coal char surface temperatures by as much as 140 K, at comparable oxygen mole fractions. The corresponding drop for anthracitic coals was around 125 K. The combustion times increased by as much as 60 ms in the case of the anthracitic coals, and 30 ms in the case of bituminous coals.
(f) As the oxygen concentration in the CO_2 mixtures increased from 21% to 50%, the temperature of the char particles increased up to 320 K for the anthracitic coals and 310 K for the bituminous coals. The temperature of the volatile flames increased by as much as 400 K for the bituminous coals. Also an important reduction in burnout time was observed, especially in the case of anthracitic coals.
(g) Equivalent temperatures and burnout times of bituminous coal volatiles and chars to those measured in air were attained when the oxygen content in the CO_2 mixtures was ~30–35%. This observation has practical ramifications in the operation of practical systems.
(h) The volatile burnout times increased linearly with increasing volatile matter content (VM) of the coals in all gas environments.
(i) The dependency of char burnout times versus carbon content (C) was quadratic for air and comparable oxygen mole fractions in CO_2 (21%O_2) while this dependency was linear at higher O_2 mole fractions (35%O_2, 50%O_2).

Acknowledgments

The authors acknowledge financial assistance from the US-NSF award CBET-0755431. J. Riaza acknowledges funding from the Government of the Principado de Asturias (Severo Ochoa program). M.V. Gil and L. Álvarez acknowledge funding from the CSIC JAE program, co-financed by the European Social Fund. Support from the CSIC (PIE 201080E09) is also gratefully acknowledged.

Appendix A. Calculation of diffusion-limited burnout times

The average oxygen mole fraction on the char particle surface can be estimated by the following formula [32]:

$$y_{O_2 s} = (4/3 + y_{O_2 \infty}) e^{-\left(\frac{a_0^2 RT_m \rho_c}{56 P_{tot} D t_{B,obs}}\right)} - 4/3 \quad (A.1)$$

In this relation the surface oxygen mole fraction, $y_{O_2 s}$ is assumed to be an average value. a_i, ρ_c, T_m, D, t_B, R and P_{tot} are initial burning particle radius, initial particle density, film temperature between the char particle and flow, bulk diffusion coefficient of O_2 in the diluent gas, observed particle burnout time, gas universal constant and total pressure of the system, respectively.

If $y_{O_2 s}$ is zero or close to zero, the combustion takes place under diffusion limited conditions (Regime III), whereas if $y_{O_2 s}$ is close to $y_{O_2 \infty}$, the combustion occurs under kinetically limited conditions (Regime I). Any $y_{O_2 s}$ in-between the above values results under a combination of kinetic-diffusion limited conditions (Regime II).

The time t_B required for combustion under diffusion control (Regime III) becomes [32]:

$$t_B = \frac{\rho_c (a_i^2 - a_f^2)}{56} \frac{RT_m}{D} \frac{1}{\ln\left(1 + \frac{3}{4} y_{O_2 \infty}\right)} \quad (A.2)$$

In Eq. (A.2), a_f is the final particle radius after extinction, which herein is calculated based on the ash content in the parent coal composition and assuming shrinking core combustion and comparable char and ash residue densities [14].

For instance, for anthracite (AC) burning in air with the observed parameters of this study a_{0i} = 56.25 μm, a_f = 19 μm, ρ_c = 1 g/cm^3 [33], T_m = 1612 K, P_{tot} = 1 atm, D_{O2-N2} = 3.37 cm^2/s, $t_{B\text{-}obs}$ = 294 ms, R = 82 atm cm^3/mol K, oxygen mole fraction on the particle surface from (A.1), $y_{O_2 s}$, was calculated to be 0.09 and the diffusion limited burnout time from (A.2), t_B, was calculated to be 134 ms. On the other hand, for anthracite (AC) burning in 21%O_2–79%CO_2, T_m = 1550 K, D_{O2-CO2} = 2.63 cm^2/s, $t_{B\text{-}obs}$ = 358 ms and the rest of parameters are similar to those of combustion in air. In this case, oxygen mole fraction on the particle surface from (A.1), $y_{O_2 s}$, was 0.09 and the diffusion limited burnout time from (A.2), t_B, was 165 ms. Therefore, under the experimental conditions of this study, combustion of anthracite in either air or oxy-fuel condition (21%O_2/79%CO_2) took place in Regime II which is a combination of kinetic and diffusion limited cases.

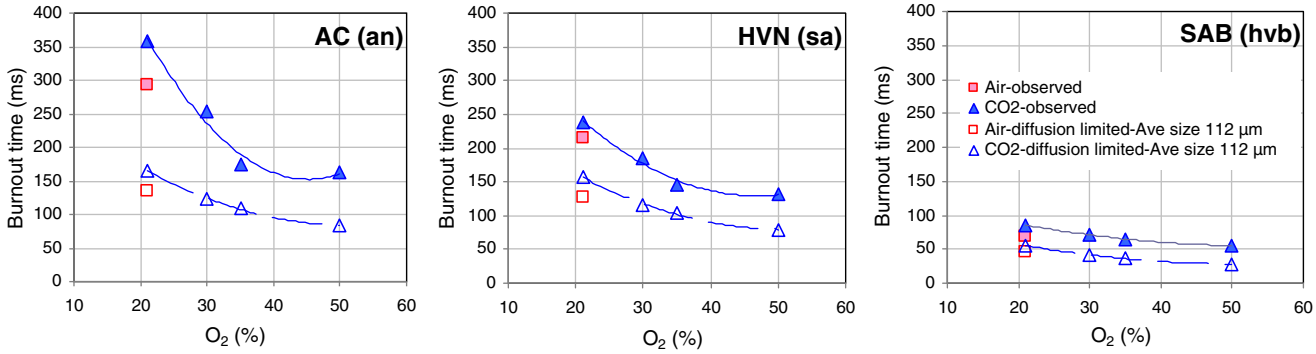

Fig. A.1. Comparison of experimentally-observed and calculated diffusion-limited burnout times of anthracite, semi-anthracite and bituminous char particles, plotted against bulk oxygen mole fraction.

The resulted observed burnout times and calculated diffusion limited burnout times versus oxygen concentration for anthracite (AC), semi-anthracite (HV) and one of the bituminous coals (SAB) in different oxy-fuel condition are shown in Fig. A.1.

References

[1] BP, Statistical Review of World Energy, 2012.
[2] IEA, World Energy Outlook, 2011.
[3] M.B. Toftegaard, J. Brix, P.A. Jensen, P. Glarborg, A.D. Jensen, Prog. Energy Combust. Sci. 36 (2010) 581–625.
[4] R. Khatami, C. Stivers, K. Joshi, Y.A. Levendis, A.F. Sarofim, Combust. Flame 159 (2012) 1253–1271.
[5] R. Khatami, C. Stivers, Y.A. Levendis, Combust. Flame 159 (2012) 3554–3568.
[6] F. Kazanc, R. Khatami, P.M. Crnkovic, Y.A. Levendis, Energy Fuels 25 (2011) 2850–2861.
[7] J. Faúndez, B. Arias, F. Rubiera, A. Arenillas, X. García, A.L. Gordon, J.J. Pis, Fuel 86 (2007) 2076–2080.
[8] P.A. Bejarano, Y.A. Levendis, Combust. Flame 153 (2008) 270–287.
[9] L. Zhang, E. Binner, Y. Qiao, C.-Z. Li, Fuel 89 (2010) 2703–2712.
[10] Y. Liu, M. Geier, A. Molina, C.R. Shaddix, Int. J. Greenhouse Gas Control S5 (2011) S36–S46.
[11] L. Chen, S.Z. Yong, A.F. Ghoniem, Prog. Energy Combust. Sci. 38 (2012) 156–214.
[12] ASTM, ASTM D7582: Standard Test Methods for Proximate Analysis of Coal and Coke by Macro Thermogravimetric Analysis. Annual Book of ASTM Standards, American Society for Testing and Materials, West Conshohocken, PA, 2010.
[13] ASTM, ASTM D3176-89: Standard Practice for Ultimate Analysis of Coal and Coke, Annual Book of ASTM Standards. American Society for Testing and Materials, West Conshohocken, PA, 2002.
[14] Y.A. Levendis, K. Joshi, R. Khatami, A.F. Sarofim, Combust. Flame 158 (2011) 452–465.
[15] Y.A. Levendis, K.R. Estrada, H.C. Hottel, Rev. Sci. Instrum. 63 (1992) 3608–3622.
[16] R. Khatami, Y.A. Levendis, Combust. Flame 158 (2011) 1822–1836.
[17] M.V. Gil, J. Riaza, L. Álvarez, C. Pevida, J.J. Pis, F. Rubiera, Energy 48 (2012) 510–518.
[18] L. Zhang, E. Binner, L. Chen, Y. Qiao, C.-Z. Li, S. Bhattacharya, Y. Ninomiya, Energy Fuels 24 (2010) 4803–4811.
[19] M.V. Gil, J. Riaza, L. Álvarez, C. Pevida, J.J. Pis, F. Rubiera, Appl. Energy 91 (2012) 67–74.
[20] J.B. Howard, R.H. Essenhigh, Proc. Combust. Inst. 11 (1967) 399–408.
[21] W.R. Seeker, G.S. Samuelsen, M.P. Heat, J.D. Trolinger, Proc. Combust. Inst. 18 (1981) 1213–1226.
[22] A. Ergut, S. Granata, J. Jordan, J. Carlson, J.B. Howard, H. Ritcher, Y.A. Levendis, Combust. Flame 144 (2006) 757–772.
[23] L.D. Timothy, A.F. Sarofim, J.M. Beer, Proc. Combust. Inst. 19 (1982) 1123–1130.
[24] W.J. McLean, D.R. Hardesty, J.H. Pohl, Proc. Combust. Inst. 18 (1981) 1239–1248.
[25] T. Maffei, R. Khatami, S. Pierucci, T. Fravelli, E. Ranzi, Y.A. Levendis, Combust. Flame 160 (2013) 2559–2572.
[26] C.R. Shaddix, A. Molina, Proc. Combust. Inst. 32 (2009) 2091–2098.
[27] A. Molina, C.R. Shaddix, Proc. Combust. Inst. 31 (2007) 1905–1912.
[28] J. Riaza, L. Álvarez, M.V. Gil, C. Pevida, J.J. Pis, F. Rubiera, Energy 36 (2011) 5314–5319.
[29] T. Joutsenoja, J. Saastamoinen, Energy Fuels 13 (1999) 130–145.
[30] J. Riaza, M.V. Gil, L. Álvarez, C. Pevida, J.J. Pis, F. Rubiera, Energy 41 (2012) 429–435.
[31] Q. Li, C. Zhao, X. Chen, W. Wu, B. Lin, Chem. Eng. Process. Intensif. 49 (2010) 160–164.
[32] Y.A. Levendis, R.C. Flagan, G.R. Gavalas, Combust. Flame 76 (1989) 221–241.
[33] J.E. Metcalfe, M. Kawahata, P.L. Walker, Molecular Sieve Properties of Activated Anthracite, Fuel Technology Department report, Penn state University, pp. 41–46.

3.2.2 *Publicación II*

Combustion of Single Biomass Particles in Air and in Oxy-Fuel Conditions.

J. Riaza, R. Khatami, Y. A. Levendis, L. Álvarez, M.V. Gil, C. Pevida, F. Rubiera, J.J. Pis
Biomass and Bioenergy**.**
doi: 10 10.1016/j.biombioe.2014.03.018.1

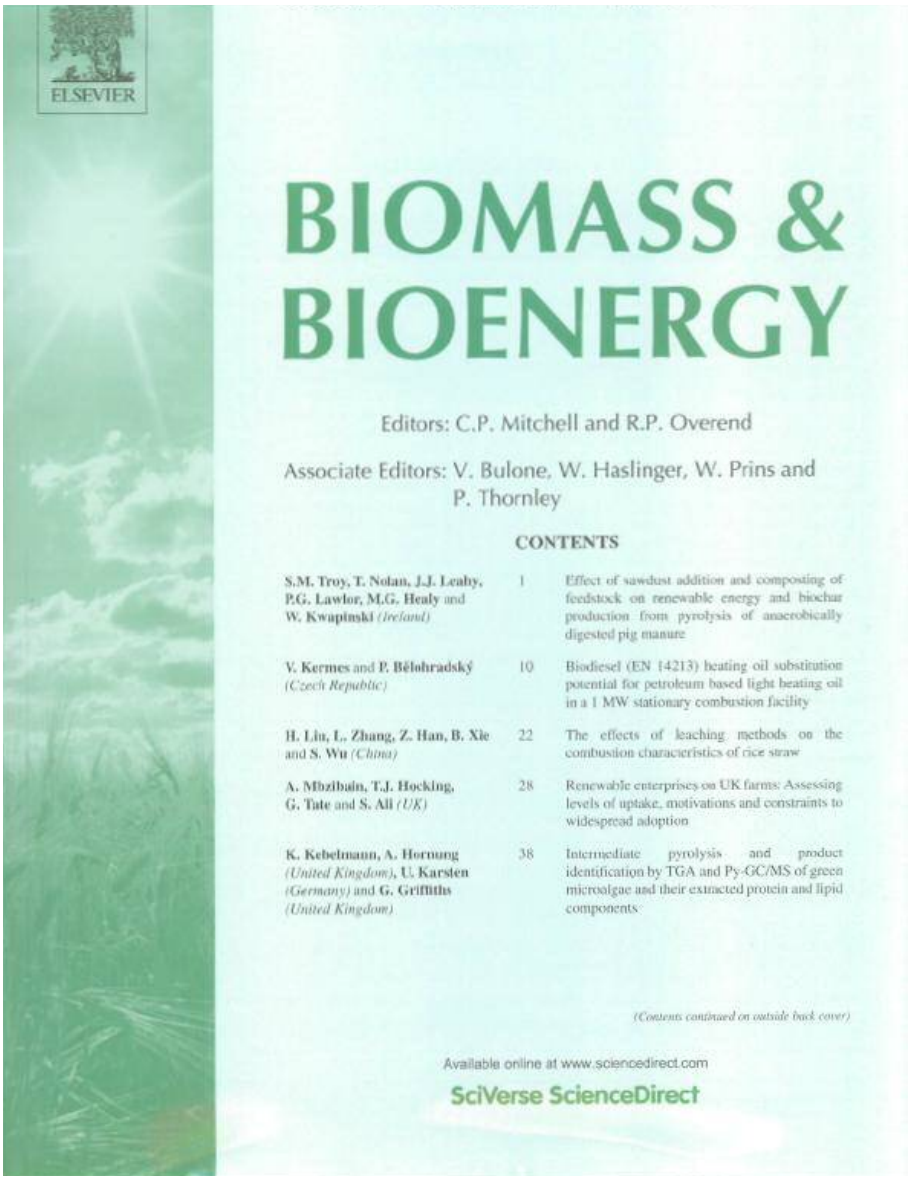

BIOMASS AND BIOENERGY XXX (2014) 1–13

Available online at www.sciencedirect.com

ScienceDirect

http://www.elsevier.com/locate/biombioe

Combustion of single biomass particles in air and in oxy-fuel conditions

Juan Riaza [a], *Reza Khatami* [b], *Yiannis A. Levendis* [b,*], *Lucía Álvarez* [a], *María V. Gil* [a], *Covadonga Pevida* [a], *Fernando Rubiera* [a], *José J. Pis* [a]

[a] *Instituto Nacional del Carbón, INCAR-CSIC, Apartado 73, 33080 Oviedo, Spain*
[b] *Mechanical and Industrial Engineering Department, Northeastern University, Boston, MA 02115, USA*

ARTICLE INFO

Article history:
Received 18 September 2012
Received in revised form
4 March 2014
Accepted 11 March 2014
Available online xxx

Keywords:
Biomass process residues
Torrefied biomass
Combustion
Ignition
Single particle
Pyrometry

ABSTRACT

The combustion behaviors of four different pulverized biomasses were evaluated in the laboratory. Single particles of sugarcane bagasse, pine sawdust, torrefied pine sawdust and olive residue were burned in a drop-tube furnace, set at 1400 K, in both air and O_2/CO_2 atmospheres containing 21, 30, 35, and 50% oxygen mole fractions. High-speed and high-resolution images of single particles were recorded cinematographically and temperature–time histories were obtained pyrometrically. Combustion of these particles took place in two phases. Initially, volatiles evolved and burned in spherical envelope flames of low-luminosity; then, upon extinction of these flames, char residues ignited and burned in brief periods of time. This behavior was shared by all four biomasses of this study, and only small differences among them were evident based on their origin, type and pre-treatment. Volatile flames of biomass particles were much less sooty than those of previously burned coal particles of analogous size and char combustion durations were briefer. Replacing the background N_2 gas with CO_2, i.e., changing from air to an oxy-fuel atmosphere, at 21% O_2 impaired the intensity of combustion; reduced the combustion temperatures and lengthened the burnout times of the biomass particles. Increasing the oxygen mole fraction in CO_2 to 28–35% restored the combustion intensity of the single biomass particles to that in air.

© 2014 Elsevier Ltd. All rights reserved.

1. Introduction

Biomass has higher volatile matter content than coal, but it has less carbon, more oxygen and a lower energy content (heating value). The use of biomass in existing pulverized coal power plants requires only minor modifications as compared to the construction of new biomass-specific fired power plants, making the co-firing of biomass with coal an easier and less costly way for generating power. Co-firing is becoming more common in coal power plants because replacing part of the coal with biomass results in lower pollutant and greenhouse gas emissions, as compared to firing neat coal [1,2]. Co-firing biomass and coal reduces the emissions of SO_2, NO_x and CO_2. Altogether elimination of such emissions may be achieved in future power plants (termed zero emission power plants) by implementing carbon dioxide capture and storage (CCS) techniques. However, co-firing coal with biomass reduces the power output of a power-plant in proportion to the amount of the latter fuel [3–5].

* *Corresponding author*. Tel.: +1 617 373 3806; fax: +1 617 373 2921.
E-mail addresses: y.levendis@neu.edu, yal@coe.neu.edu (Y.A. Levendis).
http://dx.doi.org/10.1016/j.biombioe.2014.03.018
0961-9534/© 2014 Elsevier Ltd. All rights reserved.

Oxy-fuel combustion is a promising technology for facilitating CCS. It burns fuel in a mixture of oxygen and recycled flue gases (mainly CO_2) instead of air in conventional combustion. The exhaust flue gases consist mainly of CO_2, approx. 95% on a dry volume basis, and small amounts of excess oxygen, nitrogen and, to a lesser extent, pollutants, such as nitrogen oxides (NO_x) and sulfur oxides (SO_x) (approx. 0.1–0.2% dry volume basis) [6]. The combination of oxy-fuel combustion, as a CCS technology, with biomass [2] could effectively provide a method which would not only avoid further CO_2 emissions but, perhaps even help reduce the atmospheric CO_2. Simpson et al. [7] compared the efficiency of oxy-fuel combustion and post-combustion carbon dioxide separation cycles by thermodynamic analysis. They concluded that the air separation efficiency in oxy-fuel technology must increase sufficiently to offset the additional cost and inefficiency of requiring a CO_2 purification unit on the back end. They proposed that oxy-fuel combustion may be more attractive for systems operating with oxygenated fuels such as biomass. For such systems, the development of near-stoichiometric combustors would not need expensive CO_2 purification units. Moreover, a recent investigation [8] suggested that biomass/coal blend combustion may be a method for controlling the excess heat generated from oxy-combustion of coal in neat oxygen, a proposed "clean" coal technology. They utilized a TGA-DSC technique at 1173 K to burn blends of a lignite coal and two biomasses, at high oxygen partial pressures. They reported that the heat flux from the combustion of lignite increased dramatically when the oxidizing medium was altered from dry air to neat oxygen. However, in the case of co-firing lignite with biomass under neat oxygen, the excess heat flux arising from the combustion of lignite was reduced and the temperature of the combustion chamber was thus controlled. Based on their results, they suggested that co-combustion of coal/biomass blends in enriched oxygen environments may be an alternative method to CO_2 recycling in future oxy-fuel combustion systems.

All biomasses are composed of three main components: cellulose, hemicellulose and lignin. For instance, the sugarcane bagasse sample burned herein contained 41.3% cellulose, 34.3% hemicelluloses and 13.8% lignin. Whereas cellulose and hemicellulose are macromolecules constructed from different sugars, lignin is an aromatic polymer synthesized from phenylpropanoid precursors [9]. Hemicellulose is easily degraded, and its pyrolysis takes place at temperatures in the range of 493–588 K. The pyrolysis of cellulose occurs in the 588–673 K range, whereas that of lignin covers a wider temperature range (423–1176 K) [10].

Torrefaction is a useful pre-treatment for the biomass materials as they are sometimes difficult to fluidize and introduce into furnaces because of their fibrous shapes [11]. The management and milling of torrefied biomass is easier than that of the parent biomass. That is why the torrefaction process is being introduced to industrial practices [12,13]. This process consists of heating the biomass in nitrogen, or in a low oxygen-containing atmosphere, to temperatures up to 573 K. In this process, the biomass dries, and as the temperature increases, certain changes take place in the molecular structure. Light hydrocarbon molecules are released through the decomposition of the reactive hemicellulose fraction [14]. Torrefied fuels are easier to manage, and they contain more fragile particles as well as a higher energy density than the parent biomass particles [15,16]. During the torrefaction process, the biomass loses typically 30% of its mass, but only 10% of its energy content [17]. The resulting higher energy density of the torrefied fuel reduces the transportation costs.

Biomass pyrolysis has been investigated in numerous studies. Results are highlighted in several reviews, including those in Refs. [3,18–22]. The pyrolytic products are H_2, H_2O, CO, CO_2, CH_4, other light hydrocarbons, tar, ash and char. At temperatures below 773 K, biomass fuels decompose into primary volatiles. At these temperatures, tars are produced by depolymerisation reactions while pyrolytic water is produced by dehydration reactions. The main gaseous products of pyrolysis are CO_2 and CO. At temperatures above 773 K, the primary volatiles are subject to a secondary pyrolysis, during which tars are converted into a variety of gaseous species, especially CO, light hydrocarbons, hydrogen and CO_2. At high heating rates, biomass decomposes expediently generating mostly gas, vapors and char [23]. The char that remains upon termination of the pyrolysis reactions is enriched in carbon [24].

Implementation of optical pyrometry and high-speed cinematography for the study of ignition and combustion of single coal particles and streams of coal particles has been well documented [25–33]. However, there is a scarcity of analogous studies on biomass particle ignition and combustion characteristics. On the other hand, Wornat et al. [34] studied the combustion rates of single particles of two biomass chars (southern pine and switch grass), with nominal sizes in the range of 75–106 μm, in a laminar-flow reactor with 6% and 12% O_2 mole fraction (balance N_2) at 1600 K. *In situ* measurements using a two-color optical pyrometer and a video camera revealed that biomass char particles burned over a wider temperature range (1500–1950 K, $\Delta T \approx 450$ K) than high volatile bituminous and lignite coal particles (1800–1950 K, i.e., $\Delta T \approx 150$ K versus 1900–2000 K, i.e., $\Delta T \approx 100$ K, respectively). Austin et al. [35] conducted an experimental study in a drop-tube furnace, burning 300–1500 μm corncob particles in air using a video camera (50–100 frames per second) and an infrared phototransistor. They determined that the burning times of the volatiles and the ignition delay times increased with the increase of the initial particle density and diameter. Meesri and Moghtaderi [36] burned pine sawdust particles at drop-tube furnace temperatures of 1473 K in air and reported particle temperatures circa 1700 K. They also reported that the char oxidation reactions occurred in Regime II, where chemical reactions and pore diffusion happen concurrently. Arias et al. [37] studied the ignition and combustion characteristics of coal/biomass blends under oxy-fuel conditions. They burned a bituminous coal and bituminous coal/eucalyptus biomass blends (90%–10% or 80%–20%, by weight). Their experiments were performed in an electrically-heated entrained flow reactor (EFR) set to 1273 K. Oxy-fuel combustion of pulverized fuels (75–150 μm) occurred with 21%, 30% and 35% O_2 mole fraction in CO_2, and was compared with results obtained in air. When coal was blended with the biomass, its ignition temperature in air was reduced. However, this effect was less pronounced in the case of oxy-fuel combustion, regardless of O_2 concentration. The effect of blending biomass and coal on burnout effectiveness was negligible. Riaza et al. [2] observed similar results. Borrego et al. [38] obtained chars from different biomasses by

pyrolysis in air and in oxy-fuel environments, and reported no significant differences between the char characteristics, i.e., pore volume, morphology, surface area and reactivity.

In addition to the above studies, some other notable investigations reported on experiments and numerical modeling of single-particle biomass combustion [39–42]; however, the number of experimental works on this topic is very limited [43]. Additional studies are warranted to document the entire combustion behavior of biomass fuels, especially the phase of the volatile matter combustion. Such studies may be instrumental in assessing the radiating behavior of biomass particles in furnaces. In particular, little (if anything) has been reported on the experimental combustion behavior of individual biomass particles in oxy-combustion conditions, and this is of special interest to co-firing coal and biomass in future oxy-fuel power plants. The present work reports on a systematic *in situ* combustion study of different biomasses (residual or torrefied) in a laboratory-scale drop-tube furnace, under both conventional (air) and oxy-fuel conditions by means of optical pyrometry and high-speed back-light cinematography. Comparisons with the combustion characteristics of coal particles studied in previous work in this laboratory are made.

2. Bio-fuel characteristics and experimental methods

2.1. *Biomass samples*

Four different residue biomasses were studied, olive residue (OR), which are residues from the olive oil production industry, pine sawdust (PI), torrefied pine sawdust (TOPI), and sugarcane bagasse (SCB), which is a residue of bio-ethanol and sugar production. Olive residue is the part of the olive that remains after the olive oil has been extracted. Nowadays olive residue biomass is used as a low cost renewable fuel for domestic and industrial heating. The olive residue sample used in this work was supplied by ELCOGAS, S.A., which is an IGCC power station located in Puertollano (Ciudad Real, Spain), that processes a 50:50 blend (based on weight) of coal and petcoke, and occasionally also includes biomass in the fuel blend. The pine sawdust sample was obtained from a pellets industry, Pellets Asturias, S.L., situated in Tineo (Asturias, Spain), which has a yearly production of 30,000 tons of pellets. The torrefaction of pine sawdust was carried out at INCAR-CSIC. The torrefaction treatment conditions were selected according to the results obtained in previous studies [15]. Briefly, the torrefaction of pine sawdust was performed using a horizontal quartz reactor, where 10–15 g of biomass was heated at a rate of 10 K min^{-1} under a nitrogen flow rate of 50 mL min^{-1} up to 513 K. The samples were kept at the final temperature for 1 h. The mass loss from the sample was measured and then the sample was sieved to 75–150 μm. Sugarcane bagasse was collected directly from a mill located in Brazil – São Paulo State. The bagasse was washed, dried at 363 K for 24 h, chopped in a household blender and sieved. All biomass samples were less than a year old and were kept in closed glass bottles in the laboratory under standard temperature and pressure conditions.

Photographs and scanning electronic microscope images of the different biomasses samples are presented in Fig. 1. All of the samples were ground and sieved to 75–150 μm. The proximate and ultimate analyses and gross calorific values of the biomasses are given in Table 1.

Fig. 1 – Physical appearance of the biomasses residue; (a) original biomasses, as received, (b) ground and sieved, (c) SEM micrographs detailing individual particles.

Table 1 – Biomass type, origin and chemical composition.

Sample	Origin	Proximate analysis (wt%, db)			Ultimate analysis (wt%, daf)					HHV (MJ/kg)
		Ash	V.M.	F.C.[a]	C	H	N	S	O[a]	
OR	Olive residue	7.6	71.9	20.5	54.3	6.6	1.9	0.2	37.0	19.9
SCB	Sugarcane bagasse	4.2	87.8	8.0	46.3	5.9	0.2	0.1	47.5	16.3
PI	Pine sawdust	3.8	79.8	16.4	45.9	6.1	0.7	0	47.3	18.9
TOPI	Torrefied pine sawdust	4.2	75.5	20.3	51.2	5.7	0.9	0	42.2	20.2

[a] Determined by difference.

2.2. *Experimental approach*

2.2.1. *Drop-tube furnace (DTF)*

An electrically-heated laminar-flow drop-tube furnace was used for the combustion experiments. The furnace (an *ATS* unit) was fitted with an alumina tube (*Coors*) with an inner diameter of 7 cm. It was heated with molybdenum disilicide heating elements, defining a radiation zone of 25 cm in length. The furnace was fitted at the top with a water-cooled injector (Fig. 2(a)). Details of the design of the furnace injector are provided elsewhere [30,44]. To introduce single biomass particles into the furnace injector, the following technique was used. A few particles were placed inside the tip of a beveled syringe needle. The needle was inserted into a port at the top of the injector, which was rotated half a revolution back and forth and then gently tapped. Single particles could thus be dropped into the furnace injector. Upon exiting the injector, the particles reacted with the preheated furnace gases. The furnace wall temperatures (T_f) were continuously monitored by type-S thermocouples embedded in the wall. Particle heating rates were very high, calculated to be in the order of 10^4 K s^{-1}. Optical access to the radiation zone of the furnace was achieved through three observation ports: one at the top (Pyrometer) and two orthogonally situated at the sides of the furnace. The pyrometer and the high-speed cinematography camera were used as experimental devices to study the burning of single biomass particles.

2.2.2. *Optical pyrometer*

Pyrometric observations of burning single particles were conducted from the top of the furnace injector, viewing downward along the central axis of the furnace which is typically a particle's path-line. Thus, complete luminous burnout histories of single biomass particle – from ignition to extinction – were monitored. An optical fiber made up of a high-transmittance (>99.5%) fused silica core and doped fused silica cladding with an *f*-number of 2.2, transmitted light from the furnace to the pyrometer assembly. The pyrometer used two dichroic edge filters as spectrum splitters to direct the light to the three interference filters (Fig. 2(b)). These filters had effective wavelengths of 0.640, 0.810 and 0.998 μm with bandwidths (FWHM) of 70 nm. In conjunction with these

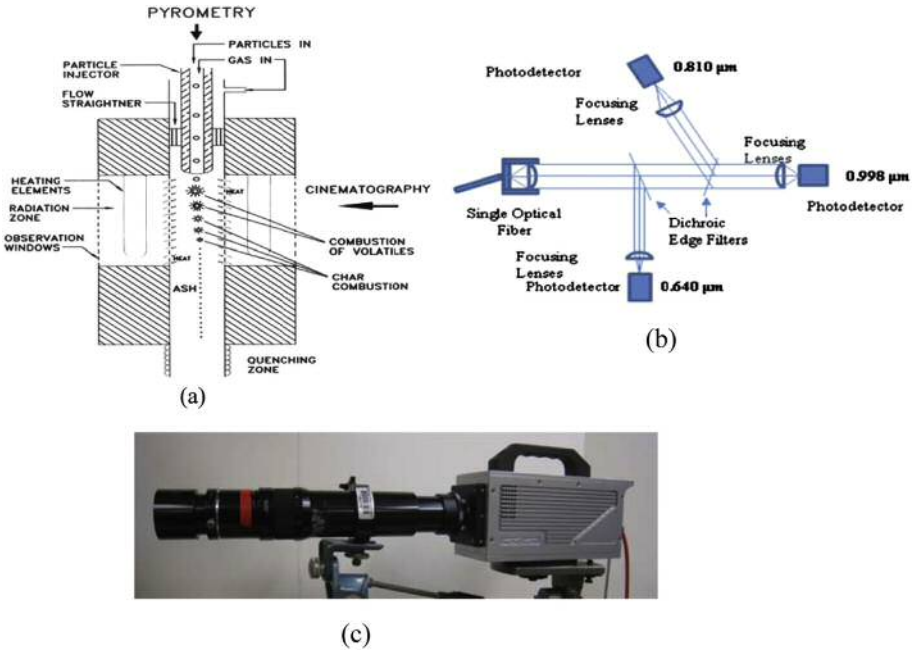

Fig. 2 – Schematic of the experimental setup and diagnostic facilities. (a) Laminar-flow, electrically-heated drop-tube furnace (DTF), (b) Three-color optical pyrometer, (c) High-speed camera (NAC) fitted with a long-range microscope lens (*Infinity* K2).

interference filters, silicon diode detectors were employed to maximize the signal sensitivity. They also possessed good stability and linearity. Details of the pyrometer optics and electronics were supplied by Levendis et al. [28,30]. The voltage signals generated by the three detectors were amplified and then processed by a microcomputer using *LabView* software. The temperature was deduced from the three output voltage signals of the pyrometer using a non-linear least square method, based on Planck's radiation law. Details of this method were supplied by Khatami and Levendis [44].

2.2.3. *High-speed camera*

High-speed cinematography was conducted through the slotted side quartz windows of the drop-tube furnace against backlight (Fig. 2(a)). A *NAC HotShot 512SC* self-contained digital high-speed video camera was used, at speeds of 1000 or 2000 frames/s. The camera was fitted with an *Infinity* model K2 long-distance microscope lens to provide high-magnification images of the combustion events (Fig. 2(c)).

2.3. *Gas temperatures and furnace gas compositions*

Combustion experiments of biomass particles were conducted under a quiescent gas condition (i.e., no gas flow). Quiescent gas condition was created by turning off the gas flows 10 s prior to the particle injection. The design of this experiment has been documented by Khatami et al. [33]. A slender bare thermocouple (*Omega* type K) was used to measure the axial profile of the centerline gas temperature. The measured temperatures with this method were corrected for radiation effects as outlined by Khatami et al. [33]; results are illustrated in Fig. 3. Under the quiescent gas condition (no flow), the gas temperature profiles were similar in either N_2 or CO_2 environments. Both temperatures increased along the centerline of the furnace and stabilized at an estimated 1340 K. The furnace wall set-point temperature (T_w) was 1400 K, as monitored by type-S thermocouples embedded in the wall. The gas compositions in the furnace included air as well as mixtures of oxygen (mole fractions of 21% O_2, 30% O_2, 35% O_2 and 50% O_2) in carbon dioxide to simulate oxy-combustion conditions. In this manuscript all gas compositions are given on a mole fraction basis, which is equivalent to a volume fraction basis, as percentages (%).

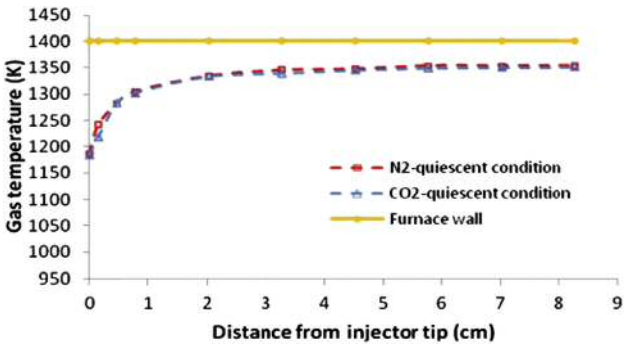

Fig. 3 – The centerline furnace gas temperature under quiescent conditions (no gas flow) [47].

3. Results and discussion

3.1. *Cinematographic observations*

Six snapshot photographic sequences for each biomass sample at different gas atmospheres during burnout history of the particle are shown in Fig. 4. The particles ignited very close to the injector tip at the top of the DTF, immediately upon entering the radiation zone. Upon ignition, the flames surrounding individual particles grew bigger and increasingly luminous. For all biomass fuels at all gas compositions, the envelope flames had strikingly spherical shapes with fairly uniform luminosity. Some other similar burning characteristics were also observed for all the biomasses. The similarities included the sequential particle devolatilization with ignition and burning of the volatiles around the particle, followed by the ignition, combustion and extinction of the char residues.

The ignition of particles was determined visually as the onset of luminous combustion. However, the determination of the precise initial instant of ignition of the volatile matter proved to be difficult for several reasons. Firstly, as Grotkjaer et al. [45] have already pointed out, the ignition temperatures of biomass are fairly low and lie in the range of 500–600 K in air. In this study, the volatiles ignition took place at temperatures much lower than the furnace wall temperature (1400 K) and could not be categorically discerned by optical techniques. Secondly, the volatiles envelope flames had low luminosities and typically exhibited low contrast with the background furnace surfaces.

3.2. *Pyrometric signals*

Fig. 5 shows sample radiation intensity signals, corresponding to the 0.640, 0.810 and 0.998 μm pyrometric wavelengths, obtained from single particles of each type of biomass burning in air. As can be seen in this figure, the signals of the PI, TOPI and SCB particles exhibit two different zones: the first peak corresponds to volatiles combustion in envelope flames and the second peak corresponds to subsequent char combustion. The first peak (corresponding to volatiles combustion) of OR signals is much weaker than that of other biomass samples.

3.3. *Combustion temperatures and burnout times*

To facilitate a quantitative comparison between the different biomass fuels burning in the diverse atmospheres of this study, burnout times of the volatiles and burnout times of chars were directly obtained from both pyrometric and cinematographic observations, whereas char combustion temperatures were deduced from pyrometric data. The particle burnout times, displayed in Figs. 6 and 7, were deduced from pyrometric signals for volatile matter and char combustion phases, based on the duration of the recorded highest-intensity signal ($\lambda = 0.998$ μm) of a particular event from its onset (particle ignition) to its termination (particle extinction), both defined when the signal exceeded its baseline by a factor of at least one thousand, i.e., $S_{signal}/S_{baseline} > 1000$. Each data point represents mean values from a minimum of 15 individual particle combustion events. Standard deviation bars

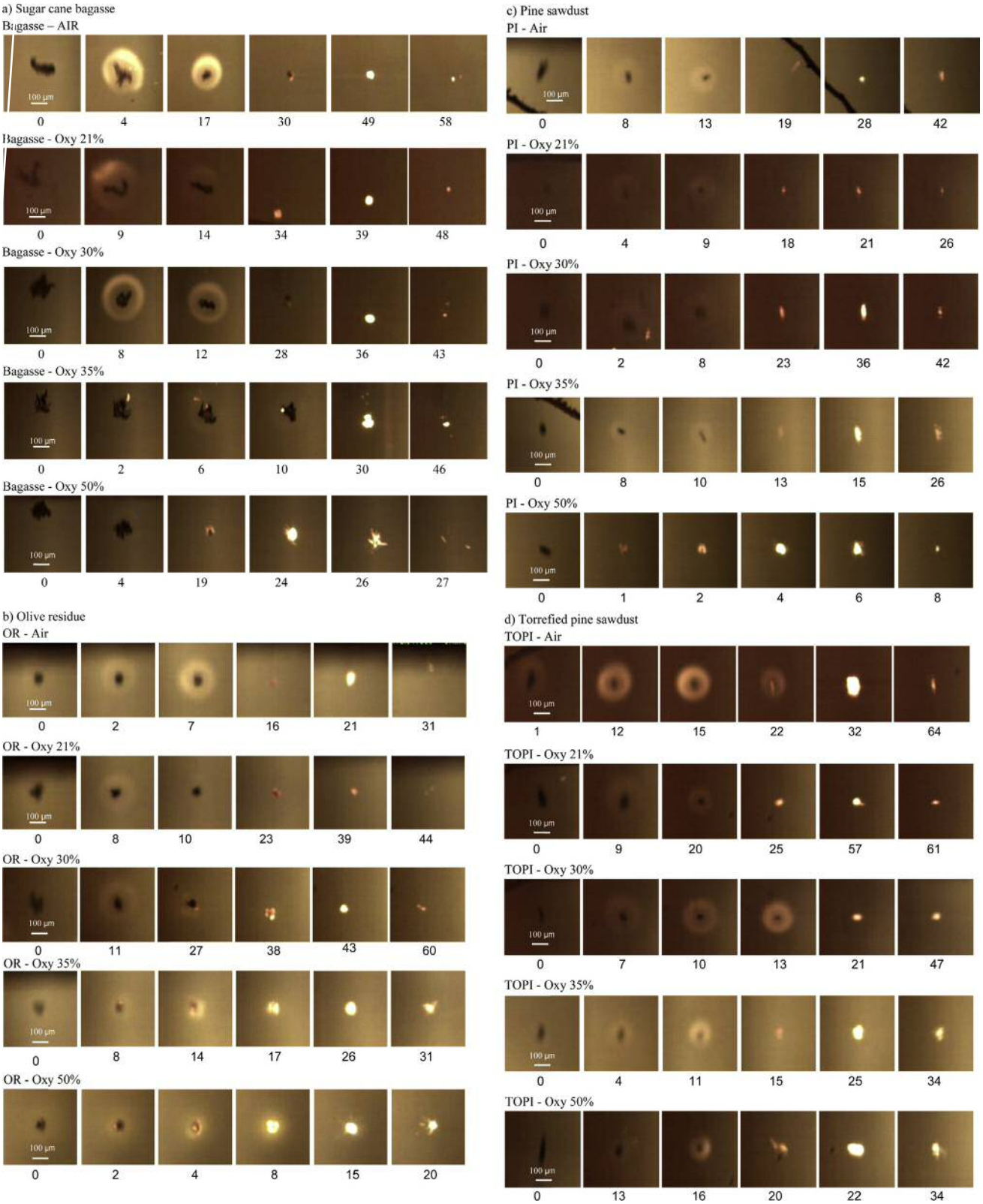

Fig. 4 – High-speed, high-magnification cinematography images of single particles of biomass residues in different atmospheres. Displayed numbers under each image represent frame times of combustion in milliseconds. Biomass samples are: (a) sugarcane bagasse (SCB), (b) olive residue (OR), (c) pine sawdust (PI), and (d) torrefied pine sawdust (TOPI).

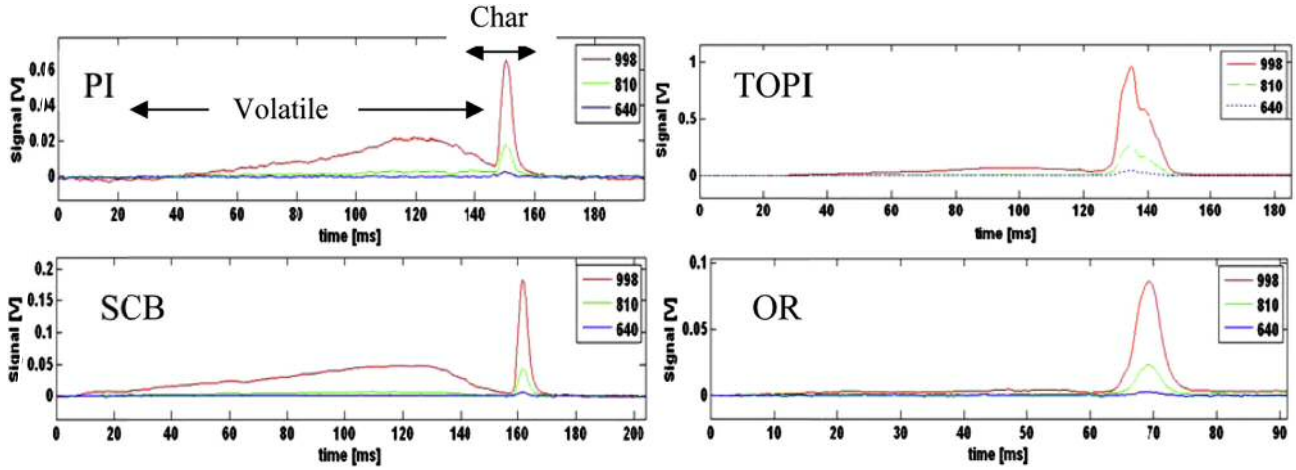

Fig. 5 – Three-color pyrometry – generated signals from single particles of biomass residues burning in air. Biomass samples are: pine sawdust (PI), torrefied pine sawdust (TOPI), sugarcane bagasse (SCB), and olive residue (OR).

(2σ) are shown on each datum point. Volatile burnout times recorded by cinematography (e.g., see Fig. 4) were typically shorter (by 10%) than the pyrometric volatile burnout times (Fig. 6). The discrepancy between pyrometric and cinematographic volatile burnout times was attributed to the fact that low-luminosity, nearly-transparent flames are hard to identify visually in photographic records (visible bandwidth is 0.4–0.7 μm), whereas the pyrometer is able to record radiation emanating from lowly-sooty or non-sooty flames at the near-infrared wavelengths of 0.81 μm and 0.998 μm. In the case of the olive residue biomass (OR) which has lower volatile matter content than the other biomasses, the duration of the volatile matter combustion phase could not be reliably assessed because even the pyrometric signals were too weak. However, the volatiles combustion peaks were clearly distinguishable in the cases of SCB, PI and TOPI biomasses (see Fig. 5).

The volatile matter flame temperature deduction method is currently under development in this laboratory for such lowly-sooty flames, for which the gray-body emissivity assumption [44] may not be valid. Thus, the temperatures of the volatile matter flames are not reported herein. The presented char temperatures in Fig. 8 are peak temperatures recorded in individual particle burnout histories, averaged over at least 15 single particle cases. Char temperatures were deduced by the method of Khatami and Levendis [44].

3.4. *Effect of atmospheric composition (replacement of N_2 by CO_2) and O_2 mole fraction*

3.4.1. *Combustion behavior*

The weakest particle combustion intensities were obtained in the 21% O_2–79% CO_2 atmosphere for all biomass samples. The weaker particle combustion intensities in 21% O_2–79% CO_2 atmosphere than in air are due to the lower particle temperatures, which resulted from the lower diffusivity of oxygen in CO_2 than in N_2 [46,47]. It has also been determined that the higher volumetric heat capacity of CO_2 (than N_2) contributes to the lower particle temperatures [47].

At 21% O_2, both in the N_2 and CO_2 environments, the ignition and combustion of the volatiles and the ignition of the char residues occurred sequentially in a particle's time-history profile (Fig. 4). When the combustion of the volatiles was completed, the flame extinguished and, subsequently, char ignition took place. Some differences were observed in the time periods between volatile extinction and char ignition in air and in the 21% O_2/79% CO_2 atmosphere; the former was in the neighborhood of 2 ms, whereas the latter was much lengthier, at 5–8 ms.

At higher oxygen mole fractions (>30%) in CO_2, the following behaviors were observed: (i) ignition of the volatiles started earlier, i.e., the ignition delay period was briefer; (ii) the volatile flames were less bright (e.g., see Fig. 4: bagasse at 35% and 50% O_2 mole fractions), most likely because under such conditions soot oxidation reactions were more prominent than soot formation reactions in the envelope flames; and finally, (iii) the incandescent residual char particles of all fuels emitted stronger radiation and they appeared brighter. In the 50% O_2–50% CO_2 atmosphere, chars ignited while the volatiles were still burning. At such an elevated oxygen mole fraction, the phases of the homogeneous volatiles combustion and heterogeneous residual char combustion became nearly indistinguishable. Moreover, char combustion was very fast.

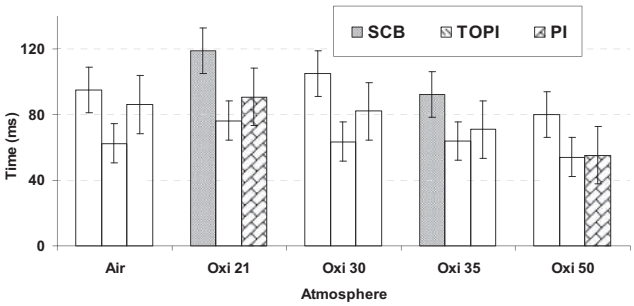

Fig. 6 – Average burnout times for the volatiles of three of the biomass fuels of this work (sugarcane bagasse (SCB), pine sawdust (PI) and torrefied pine sawdust (TOPI)) burning in air and in different oxy-fuel atmospheres.

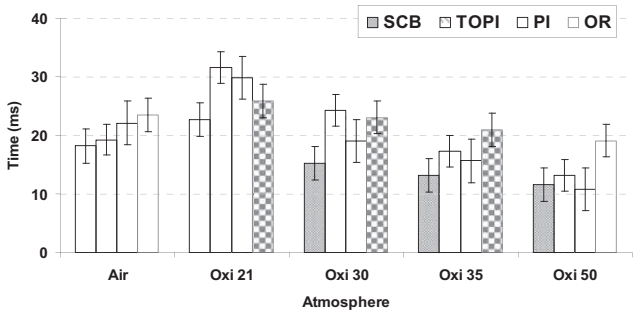

Fig. 7 – Average burnout times for the chars of all the biomass fuels of this work (sugarcane bagasse (SCB), pine sawdust (PI), torrefied pine sawdust (TOPI and olive residue (OR))) burning in air and in different oxy-fuel atmospheres.

3.4.2. *Temperatures and burnout times*

Devolatilization of particles occurs both pre- and post-ignition in the furnace. Pre-ignition devolatilization times are affected by the ignition delay period, which is in turn influenced by the volumetric heat capacity (heat sink) of the surrounding gas. Post-ignition devolatilization times are affected by the flame temperature, which is influenced by the composition, and thus, the properties of the surrounding gas. Hence, both times are affected by the substitution of N_2 with CO_2 gas in oxy-combustion. In this work, only the post-ignition devolatilization and simultaneous volatiles combustion phenomena could be monitored. In general, longer volatile and char burnout times were observed when N_2 was replaced by CO_2, at the same oxygen mole fraction (i.e., longer burnout times in 21% O_2/79% CO_2 than in 21% O_2/79% N_2), see Figs. 6 and 7. Moreover, the burnout time decreased as the oxygen mole fraction increased from 21% to 35%. These results are in agreement with previous studies which were carried out for coal particles of all ranks [2,32,48]. In the cases of both coal and biomass char particles it is likely that combustion occurred in Regime II, i.e., under both kinetic and diffusion control [44]. For biomass chars this was illustrated with calculations outlined in the Appendix, whereas for coal chars, burning under identical conditions, similar calculations have been performed in Refs. [32,48]. Fig. 7 shows that increasing the O_2 mole fraction further, from 35% to 50%, had a less pronounced effect on the char burnout time. Peak char temperatures, averaged over many (15) particles, during combustion of biomass in both air and simulated oxy-fuel conditions, shown in Fig. 8, are heavily dependent on the oxygen mole fraction. The temperatures of all biomass particles burning in air were higher than those burning in 21% O_2 diluted with CO_2. At higher oxygen mole fractions (>21%) in CO_2, the char combustion temperatures increased while the durations of char combustion decreased. Increasing the oxygen mole fraction in CO_2 to 30–35% restored the combustion intensity of single fuel particles to the level found in conventional combustion in air, for all biomass fuels tested herein. This is in agreement with observations on coal particle combustion reported in Ref. [33].

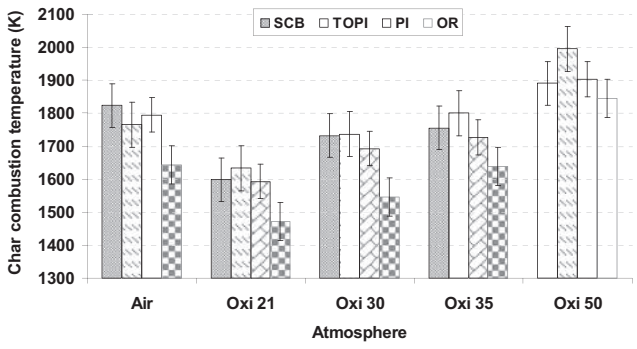

Fig. 8 – Average deduced temperatures for the burning chars of all the biomass fuels of this work (pine sawdust (PI), torrefied pine sawdust (TOPI), sugarcane bagasse (SCB), and olive residue (OR)) burning in air and in different oxy-fuel atmospheres.

3.5. *Effect of biomass type*

Biomass particles burned expediently under the conditions of this work. Biomass devolatilization commences at low temperatures (at around 473 K [19,45]). As the particles heated up, devolatilization accelerated until most of the volatiles were released. The heating rate of the particles in the drop-tube furnace was high (in the order of 10^4 K s^{-1} [32]). Biomass structures, and heavy hydrocarbons and tars, produced by the devolatilization step have been reported to expediently convert into smaller molecules by cracking reactions in the proximity of the devolatilizing particles [49]. In fact, previous work in this laboratory [50–53] pyrolyzed various biomasses under relevant high heating-rate conditions and elevated furnace temperatures and found that the pyrolytic products were mainly light hydrocarbon gases (such as methane, ethylene, ethane, acetylene, propylene, benzene, ethyl-benzene, etc.), as well as hydrogen, carbon monoxide and carbon dioxide.

The proximate and ultimate analyses of the different biomasses were similar, see Table 1, and so was their combustion behavior. The sugarcane bagasse, SCB, has the highest volatile matter content, therefore extra time was likely needed for devolatilization, and the combustion duration of the volatiles of this fuel was indeed observed to be lengthier (see Fig. 6). On the other hand, SCB has the least fixed carbon content and, thus, it exhibited the shortest char burnout duration (Fig. 7).

The envelope flames of olive residues, OR, were slightly less distinguishable cinematographically than those of the other biomass fuels. The corresponding pyrometric signals were also weaker than those of the rest of the samples. It is notable that OR had the lowest volatile matter content than the rest of the biomasses examined herein. Moreover, it was found that the OR char temperatures were the lowest among those of the other fuels, in all gas atmospheres in the DTF and the burnout times of the OR chars were less influenced by the oxygen mole fraction in the gas, as shown in Fig. 7. Regarding the combustion behavior of the chars, it is notable that OR had the highest ash, which may have increased the catalytic effect on the char burnout and have thus decreased the influence of oxygen content of the surrounding gas. High ash content and possible, yet unexplored, physical structure-related reasons (pore sizes, porosity, tortuosity) may have been responsible for the lower char temperatures of this biomass.

The torrefied pine sawdust (TOPI) chars burned hotter than the other biomass chars under all oxy-fuel conditions. Differences in the combustion behavior of the pine sawdust (PI) and the torrefied pine sawdust (TOPI) were very small. However, a more luminous flame was observed in the case of TOPI (Fig. 4). This is perhaps because a lower amount of CO_2 was supposedly released with the TOPI volatiles as a consequence of the torrefaction pre-treatment while the hydrogen content of the torrefied sample and, therefore, the release of hydrocarbon gases (e.g. CH_4 and C_2H_6) remained unchanged [15]. The CO_2 dilutes the rest of the combustible gases and produces lower luminosity flames. The TOPI biomass released a greater amount of energy per unit mass during combustion due to the fact that its calorific value was higher than that of raw biomass (PI). This effect was confirmed by the typically hotter char temperatures of TOPI. Average volatile burnout times of the original PI were longer; however, the char combustion times were generally similar, perhaps a little shorter for the original PI in comparison with the torrefied TOPI under oxy-fuel atmospheres.

3.6. *On the differences of single biomass and single coal particle combustion*

Several recent studies in this laboratory have focused on the combustion behavior of coal particles of all ranks in conventional (air) and oxy-fuel conditions [30–32,48]. In comparison to coal, biomass particles exhibit certain physical and chemical differences, the most prominent of which have as follows: (1) Raw biomasses have a highly fibrous nature. (2) The biomass particles are less dense than coal particles, therefore the total mass burnt for the same nominal particle size is lower. (3) Biomass has much lower heating value than coals [20], see also Table 1 and Table A2 in Appendix 2. (4) Biomass has a different elemental composition with a high proportion of oxygen, see Table 1 and Table A2 in Appendix 2. (5) The proximate composition of the biomass is different, i.e., biomass contains a higher proportion of volatile matter and a smaller proportion of fixed carbon than coal. Biomasses contain 70–80% volatile matter while the volatile matter contents of coals studied in this laboratory did not exceed 45%, see Table 1 and Table A2 in Appendix 2. The aforementioned structural and chemical composition disparities resulted in the following combustion behavior differences between biomass studied herein and coal reported in Refs. [32,33,48]:

(i) Pyrometric combustion intensities

The radiation intensity signals captured by the pyrometer during the combustion of biomass particles were weaker than those captured during combustion of coal particles under identical experimental conditions [48], especially during the phase of volatiles combustion. Moreover, the variability of the pyrometric signals of biomass particles was higher than those of coal, as there were more particle-to-particle size variations and shape irregularities in the biomass samples.

(ii) Volatile particle envelope flame combustion

The compounds released from biomass in the form of volatiles are different than those from coal. The cellulose and hemicellulose components of biomass decompose to small molecules in the form of volatile gases, tars and pyrolytic water [54]. These volatiles are generally lighter than those formed from coal [23]. The volatile flames of biomasses were observed to be typically transparent, and nearly non-sooty, similar to those of low rank coals [32], whereas those of the bituminous coals were sooty. The percentage of bonded oxygen in biomasses is much higher than that of coals (Table 1 and Table A2). Therefore, the volatiles contain high quantities of CO and CO_2 as well as hydrogen and light hydrocarbons [24,50,51]. They also contain smaller amounts of tars and other condensables than the volatiles of coal particles. To the contrary, bituminous coal volatiles contain mostly heavy hydrocarbons, tars, condensables and light hydrocarbons [53]. In previous studies [31–33,48], bituminous coal particles released a high amount of volatiles, with long soot-containing contrails forming in the wake of each settling particle (see also Ref. [55]), whereas lignite coal particles released light hydrocarbons and CO, resulting in occasional, faint and brief volatile flames with a large extent of char fragmentation. Anthracite coals released very small amount of volatiles and did not establish envelope flames. Biomass particles burned with distinctive volatiles flames without contrails. Unlike the combustion behavior of coals, which differs widely with rank, type and seam, the combustion behavior of biomasses from the four different sources of this study appears to be more unified. The ignition of biomass volatiles started earlier (shorter ignition delays) and their ensuing combustion occurred in envelope flames that were spherical and peripherally-uniform, even in the cases of elongated or otherwise irregularly-shaped particles. Furthermore, as biomass has a lower apparent density than coal, representative values for which have been reported as 1.32 g cm^{-3} for bituminous, 1.30 g cm^{-3} for sub-bituminous and 1.29 g cm^{-3} for lignite [56], whereas for biomasses is typically in the range of 0.4–0.5 g cm^{-3} [57], the burning biomass particles were very buoyant and settled very slowly in the furnace. The observed volatile flame burnout times (Fig. 8) of the biomasses were generally much lengthier than those of the coal flames; for instance, they were lengthier than those of bituminous coal particles of comparable nominal size by a factor of eight [31,32], which is much higher than the ratio of their volatile contents. This is likely due to the fact that because of their elongated shapes and, thus, their higher aspect ratios, biomass particles tend to be overall bigger than coal of the same size cut.

(iii) Char combustion

Whereas coal chars typically exhibited a rather uniform temperature profile during their combustion before experiencing a slow decrease towards burnout [30–32,48], the temperature profile of biomass chars increased throughout their combustion history. Examples of biomass (bagasse) char and coal (bituminous) particle temperature–time profiles are illustrated in Fig. 9 (the temperature of the volatile envelope flames of the biomass particles is not included in this plot, as it is currently under investigation). In general, biomass chars burned at a somewhat higher average temperature than bituminous char particles (by 50–100 K), as can be attested by

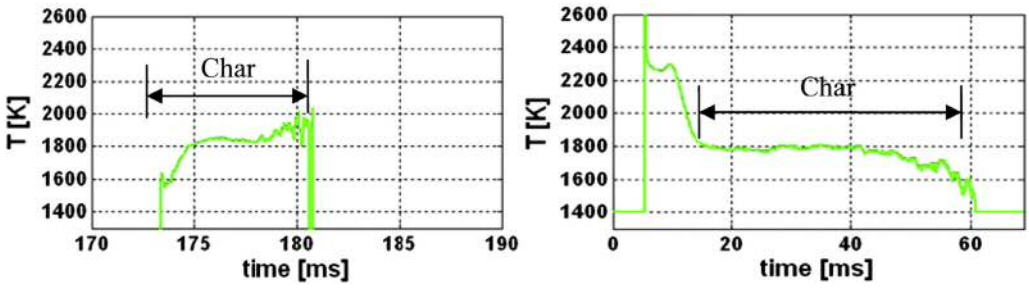

Fig. 9 – Deduced temperature–time profiles of single particles of biomass (sugarcane bagasse) and coal (bituminous) burning in air. The original particle sizes are 75–90 μm for both fuels. The biomass char size is 25–30 μm. The temperature of biomass char increases during the combustion history of the particle whereas that of the coal char remains mostly constant.

comparing the results shown in Fig. 8 and those in Refs. [30–32,48]. Biomass char particles burned with lower average temperatures (by 100–200 K) than lignite char particles in similar gas environments. Moreover, the biomass char burnout times were much briefer than the coal particle chars burnout times due to lower fixed carbon content of the biomass. Biomass chars have higher reactivity than coal chars, as reported by Matsumoto et al. [58] and Ollero et al. [59]. Matsumoto et al. [58] showed that a woody biomass char had five times higher reactivity than a sub-bituminous coal char at high heating rates encountered in an entrained flow reactor and gas temperatures in the range of 1200–1450 K. The higher reactivity of biomass char was partly attributed to faster char gasification reactions, such as $C(s) + CO_2 => 2CO$. This was also related to the higher concentration of alkali metals, which act as a catalyst and to the higher oxygen to carbon ratio in biomass char [58,59].

4. Conclusions

Biomass particles were burned in a laboratory-scale drop-tube furnace at 1400 K in air and in different oxy-fuel atmospheres, simulated by dry O_2/CO_2 gases. Experiments were performed under quiescent gas conditions. Striking differences were observed between the combustion behavior of the biomass particles burned herein and those of coal particles of all ranks investigated in previous studies in this laboratory. The biomass particles released large amounts of volatiles that burned in the form of spherical envelope flames. Ensuing biomass char combustion produced stronger pyrometric signals than the combustion of the volatile matter. Increasing the oxygen mole fraction in CO_2 reduced the luminosity of the flames. The combustion intensity of the biomass was stronger in air (21% O_2–79% N_2) than in an oxy-fuel atmosphere with the same oxygen mole fraction (21% O_2–79% CO_2). Increasing the oxygen mole fraction in the CO_2 background gas enhanced the combustion intensity of biomass. It decreased the burnout times of volatiles and of the char residues, whereas it increased the temperature of the burning char particles. Similar trends were observed for all tested biomass samples from disparate sources, including the raw and torrefied pine sawdust. Thus, unlike the combustion behavior of coals, which differs widely with rank, type and seam, the combustion behavior of biomasses from the four different sources of this study appears more unified. Olive residue chars (OR) burned at lower temperatures than the other biomass fuels, whereas bagasse chars (SCB) burned at higher temperatures than the other biomass fuels. The volatile flames of biomass particles are less sooty than those of bituminous coal particles.

Acknowledgments

The authors acknowledge financial assistance from the US National Science Foundation (NSF) award CBET-0755431. J. Riaza acknowledges funding from the Government of the Principado de Asturias (Severo Ochoa program). M.V. Gil and L. Álvarez acknowledge funding from the CSIC JAE programme co-financed by the European Social Fund.

Appendix 1

Calculation of the oxygen mole fraction at the biomass char particle surface and of the diffusion limited burnout time.

Based on a derivation by Levendis et al. [26], the average oxygen mole fraction on the char particle surface can be estimated by the following formula:

$$y_{O_2 s} = \left(4/3 + y_{O_2 \infty}\right) e^{-\left(\frac{a_0^2 RT m \rho_c}{56 P_{tot} D_{B,obs}}\right)} - 4/3 \qquad (A.1)$$

In this relation, y_{O_2} is assumed to be an average value. a_i, ρ_c, T_m, D, t_B, R and P_{tot} are initial burning particle radius, initial particle density, film temperature between the char particle and flow, bulk diffusion coefficient of O_2 in the diluents gas, observed particle burnout time, gas universal constant and total pressure of the system, respectively.

If $y_{O_2 s}$ is zero or close to zero, the combustion takes place at diffusion limited conditions (Regime III), whereas if $y_{O_2 s}$ is close to $y_{O_2 \infty}$, the combustion happens at kinetically limited condition (Regime I). Any $y_{O_2 s}$ in-between the above values results in kinetic-diffusion limited condition (Regime II).

The time t_B required for combustion under diffusion control (Regime III) becomes [26]:

$$t_B = \frac{\rho_c\left(a_i^2 - a_f^2\right)}{56}\frac{RT_m}{D}\frac{1}{\ln\left(1+\frac{3}{4}y_{O_2\infty}\right)} \quad (A.2)$$

In Eq. (A.2), a_f is the final particle radius after extinction, which herein is estimated based on the ash content in the parent biomass composition.

For instance, for sugarcane bagasse burning in air with the observed parameters of this study $a_{0i} = 15$ (μm), $a_f = 2.5$ (μm), $\rho_c = 0.2$ (g cm^{-3}), $T_m = 1600$ K, $P_{tot} = 1$ (atm), $D_{O_2-N_2} = 3.49(cm^2/s)$, $t_{B\text{-obs}} = 18$ (ms), $R = 82$ (atm cm^3/mol K), oxygen mole fraction on the particle surface from (A.1), y_{O_2s}, was calculated to be 0.08 and the diffusion limited burnout time from (A.2), t_B, was calculated to be 10 (ms). On the other hand, for sugarcane bagasse burning in 21% O_2–79% CO_2, $T_m = 1500$ K, $D_{O_2-CO_2} = 2.73(cm^2/s)$, $t_{B\text{-obs}} = 23$ (ms) and the rest of parameters are similar to those of combustion in air. In this case, the oxygen mole fraction on the particle surface from (A.1), y_{O_2s}, was 0.09 and the diffusion limited burnout time from (A.2), t_B, was 12 (ms). Therefore, under the experimental conditions of this study, combustion of bagasse in either air or oxy-fuel condition (21% O_2–79% CO_2) took place in Regime II which is a combination of kinetic and diffusion limited cases. From Eq. (A.2) for diffusion limited case, the burnout time is inversely proportional to the mass diffusivity of oxygen in the diluents gas and this seems to be the case in the current work, because:

$$\frac{t_{B\text{-obs-Air}}}{t_{B\text{-obs-21\%O}_2/79\%CO_2}} = \frac{18}{23} = 0.78 \approx \frac{D_{O_2-CO_2}}{D_{O_2-N_2}} = \frac{2.73}{3.49} = 0.77$$

The resulted observed burnout times and calculated diffusion limited burnout times versus oxygen concentration for sugarcane bagasse in different oxy-fuel condition is shown in Fig. A1.

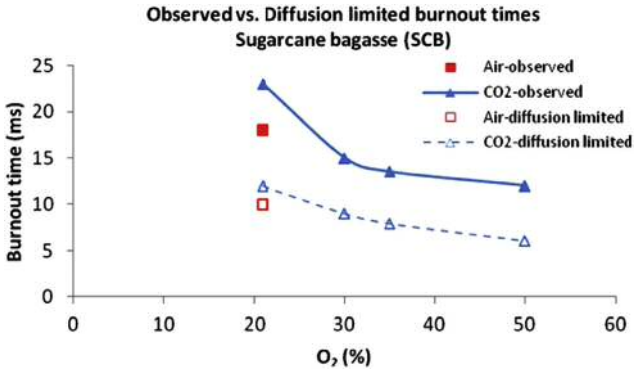

Fig. A.1 – Comparison of experimentally-observed and calculated diffusion limited burnout times of sugarcane bagasse char particles, plotted against bulk oxygen mole fraction.

Appendix 2

Characterization of coals used for comparison with the biomasses [32,48].

Table A2 – Coals used for purposes of comparison with biomasses as received: rank/type and chemical composition [32,48].

Sample	Rank/Type	Proximate analysis (wt%, db)			Ultimate analysis (wt%, daf)					HHV (MJ/kg)
		Ash	V.M.	F.C.[a]	C	H	N	S	O[a]	
AC [48]	Anthracite	14.2	3.6	82.2	94.7	1.6	1.0	0.7	2.0	29.2
PSOC-1451 [32]	Bituminous	13.6	34.4	52	83.3	5.4	1.7	1.6	8.0	31.5
DECS-26 [32]	Sub-bituminous	7.6	44.9	47.5	75.5	6.1	1.0	0.4	17.0	28.2
PSOC-1443 [32]	Lignite	21.4	61.8	16.8	72.2	5.2	1.4	0.9	20.3	23.0

[a] Determined by difference.

REFERENCES

[1] Kazanc F, Khatami R, Crnkovic PM, Levendis YA. Emissions of NO_x and SO_2 from coals of various ranks, bagasse, and coal-bagasse blends burning in O_2/N_2 and O_2/CO_2 environments. Energy Fuels 2011;25(7):2850–61.
[2] Riaza J, Gil MV, Álvarez L, Pevida C, Pis JJ, Rubiera F. Oxy-fuel combustion of coal and biomass blends. Energy 2012;41(1):429–35.
[3] Tillman DA. Biomass cofiring: the technology, the experience, the combustion consequences. Biomass Bioenergy 2000;19(6):365–84.
[4] Baxter L. Biomass-coal co-combustion: opportunity for affordable renewable energy. Fuel 2005;84(10):1295–302.
[5] Smart JP, Patel R, Riley GS. Oxy-fuel combustion of coal and biomass, the effect on radiative and convective heat transfer and burnout. Combust Flame 2010;157(12):2230–40.
[6] Álvarez L, Riaza J, Gil MV, Pevida C, Pis JJ, Rubiera F. NO emissions in oxy-coal combustion with the addition of steam in an entrained flow reactor. Greenh Gases Sci Technol 2011;1(2):180–90.
[7] Simpson AP, Simon AJ. Second law comparison of oxy-fuel combustion and post-combustion carbon dioxide separation. Energy Convers Manage 2007;48(11):3034–45.
[8] Haykiri-Acma H, Turan AZ, Yaman S, Kucukbayrak S. Controlling the excess heat from oxy-combustion of coal by blending with biomass. Fuel Process Technol 2010;91(11):1569–75.
[9] Saidur R, Abdelaziz EA, Demirbas A, Hossain MS, Mekhilef S. A review on biomass as a fuel for boilers. Renew Sustain Energy Rev 2011;15(5):2262–89.
[10] Yang H, Yan R, Chen H, Lee DH, Zheng C. Characteristics of hemicellulose, cellulose and lignin pyrolysis. Fuel 2007;86(12–13):1781–8.
[11] Cui H, Grace JR. Spouting of biomass particles: a review. Bioresour Technol 2008;99(10):4008–20.
[12] Ratte J, Fardet E, Mateos D, Héry JS. Mathematical modelling of a continuous biomass torrefaction reactor: TORSPYD column. Biomass Bioenergy 2011;35(8):3481–95.
[13] Rousset P, Aguiar C, Labbé N, Commandré J-M. Enhancing the combustible properties of bamboo by torrefaction. Bioresour Technol 2011;102(17):8225–31.
[14] Fisher EM, Dupont C, Darvell LI, Commandré JM, Saddawi A, Jones JM. Combustion and gasification characteristics of chars from raw and torrefied biomass. Bioresour Technol 2012;119:157–65.
[15] Arias B, Pevida C, Fermoso J, Plaza MG, Rubiera F, Pis JJ. Influence of torrefaction on the grindability and reactivity of woody biomass. Fuel Process Technol 2008;89(2):169–75.
[16] van der Stelt MJC, Gerhauser H, Kiel JHA, Ptasinski KJ. Biomass upgrading by torrefaction for the production of biofuels: a review. Biomass Bioenergy 2011;35(9):3748–62.
[17] Verhoeff F, Adell A, Boersma AR, Pels JR, Lensselink J, Kiel JHA. TorTech: torrefaction as key technology for the production of (solid) fuels from biomass and residue; 2011. p. 22. ECN report, ECN-E–11–039.
[18] Demirbas A. Combustion characteristics of different biomass fuels. Prog Energy Combust Sci 2004;30(2):219–30.
[19] Williams A, Pourkashanian M, Jones JM. Combustion of pulverised coal and biomass. Prog Energy Combust Sci 2001;27(6):587–610.
[20] van Loo S, Koppenjan J. The handbook of biomass combustion and co-firing. London: Earthscan; 2008.
[21] Bridgwater AV. Review of fast pyrolysis of biomass and product upgrading. Biomass Bioenergy 2012;38:68–94.
[22] White J, Catallo W, Legendre B. Biomass pyrolysis kinetics: a comparative critical review with relevant agricultural residue case studies. J Anal Appl Pyrolysis 2011;91(1):1.
[23] Babu BV, Chaurasia AS. Heat transfer and kinetics in the pyrolysis of shrinking biomass particle. Chem Eng Sci 2004;59(10):1999–2012.
[24] Neves D, Thunman H, Matos A, Tarelho L, Gómez-Barea A. Characterization and prediction of biomass pyrolysis products. Prog Energy Combust Sci 2011;37(5):611–30.
[25] Timothy LD, Sarofim AF, Beer JM. Characteristics of single particle coal combustion. Proc Combust Inst 1982;19(1):1123–30.
[26] Levendis YA, Flagan RC, Gavalas GR. Oxidation kinetics of monodisperse spherical carbonaceous particles of variable properties. Combust Flame 1989;76(3–4):221–41.
[27] Loewenberg M, Levendis YA. Combustion behavior and kinetics of synthetic and coal-derived chars: comparison of theory and experiment. Combust Flame 1991;84(1–2):47–65.
[28] Levendis YA, Estrada KR, Hottel HC. Development of multicolor pyrometers to monitor the transient response of burning carbonaceous particles. Rev Sci Instrum 1992;63(7):3608–22.
[29] Atal A, Levendis YA. Comparison of the combustion behaviour of pulverized residue tyres and coal. Fuel 1995;74(11):1570–81.
[30] Bejarano PA, Levendis YA. Single-coal-particle combustion in O_2/N_2 and O_2/CO_2 environments. Combust Flame 2008;153(1–2):270–87.
[31] Levendis YA, Joshi K, Khatami R, Sarofim AF. Combustion behavior in air of single particles from three different coal ranks and from sugarcane bagasse. Combust Flame 2011;158(3):452–65.
[32] Khatami R, Stivers C, Joshi K, Levendis YA, Sarofim AF. Combustion behavior of single particles from three different coal ranks and from sugar cane bagasse in O_2/N_2 and O_2/CO_2 atmospheres. Combust Flame 2012;159(3):1253–71.
[33] Khatami R, Stivers C, Levendis YA. Ignition characteristics of single coal particles from three different ranks in O_2/N_2 and O_2/CO_2 atmospheres. Combust Flame 2012;159(12):3554–68.
[34] Wornat MJ, Hurt RH, Davis KA, Yang NYC. Single-particle combustion of two biomass chars. Symp Int Combust 1996;26(2):3075–83.
[35] Austin PJ, Kauffman CW, Sichel M. Ignition and volatile combustion of cellulosic dust particles. Combust Sci Technol 1996;112(1):187–98.
[36] Meesri C, Moghtaderi B. Experimental and numerical analysis of sawdust-char combustion reactivity in a drop tube reactor. Combust Sci Technol 2003;175(4):793–823.
[37] Arias B, Pevida C, Rubiera F, Pis JJ. Effect of biomass blending on coal ignition and burnout during oxy-fuel combustion. Fuel 2008;87(12):2753–9.
[38] Borrego AG, Garavaglia L, Kalkreuth WD. Characteristics of high heating rate biomass chars prepared under N_2 and CO_2 atmospheres. Int J Coal Geol 2009;77(3–4):409–15.
[39] Yang YB, Sharifi VN, Swithenbank J, Ma L, Darvell LI, Jones JM, et al. Combustion of a single particle of biomass. Energy Fuels 2008;22(1):306–16.
[40] Lu H, Robert W, Peirce G, Ripa B, Baxter LL. Comprehensive study of biomass particle combustion. Energy Fuels 2008;22(4):2826–39.
[41] Thunman H, Leckner B, Niklasson F, Johnsson F. Combustion of wood particles – a particle model for Eulerian calculations. Combust Flame 2002;129:30–46.
[42] Karlström O, Brink A, Hupa M. Time dependent production of NO from combustion of large biomass char particles. Fuel 2013;103:524–32.

[43] Toftegaard MB, Brix J, Jensen PA, Glarborg P, Jensen AD. Oxy-fuel combustion of solid fuels. Prog Energy Combust Sci 2010;36(5):581–625.
[44] Khatami R, Levendis YA. On the deduction of single coal particle combustion temperature from three-color optical pyrometry. Combust Flame 2011;158(9):1822–36.
[45] Grotkjaer T, Dam-Johansen K, Jensen AD, Glarborg P. An experimental study of biomass ignition. Fuel 2003;82(7):825–33.
[46] Shaddix C, Hecht E, Geier M, Molina A, Haynes B. Effect of gasification reactions on oxy-fuel combustion of pulverized coal char. In: Proceedings of the 35th conference of coal combustion and fuel systems, Clearwater, Florida; July 1–5, 2010.
[47] Maffei T, Khatami R, Pierucci S, Faravelli T, Ranzi E, Levendis YA. Experimental and modeling study of single coal particle combustion in O_2/N_2 and oxy-fuel (O_2/CO_2) atmospheres. Combust Flame 2013;160:2559–72.
[48] Riaza J, Khatami R, Levendis YA, Álvarez L, Gil MV, Pevida C, et al. Single particle ignition and combustion of anthracite, semi-anthracite and bituminous coals in air and simulated oxy-fuel conditions. Combust Flame 2014;161:1096–108.
[49] Sun S, Tian H, Zhao Y, Sun R, Zhou H. Experimental and numerical study of biomass flash pyrolysis in an entrained flow reactor. Bioresour Technol 2010;101(10):3678–84.
[50] Alves J, Zhuo C, Levendis YA, Tenorio J. Catalytic conversion of wastes from the bio-ethanol production into carbon nanomaterials. Appl Catal B – Environ 2011;106:433–44.
[51] Davies A, Soheilian R, Zhuo C, Levendis YA. Pyrolytic conversion of biomass residues to gaseous fuels for electricity generation. J Energy Resour Technol Trans ASME 2013;136(2):021101–7.
[52] Bragato M, Joshi K, Carlson JB, Tenório JAS, Levendis YA. Combustion of coal, bagasse and blends thereof: part I: emissions from batch combustion of fixed beds of fuels. Fuel 2012;96:43–50.
[53] Bragato M, Joshi K, Carlson JB, Tenório JAS, Levendis YA. Combustion of coal, bagasse and blends thereof: part II: speciation of PAH emissions. Fuel 2012;96:51–8.
[54] Zhang H, Xiao R, Wang D, He G, Shao S, Zhang J, et al. Biomass fast pyrolysis in a fluidized bed reactor under N_2, CO_2, CO, CH_4 and H_2 atmospheres. Bioresour Technol 2010;102(5):4258–64.
[55] McLean W, Hardesty D, Pohl J. Direct observations of devolatilizing pulverized coal particles in a combustion environment. Proc Combust Inst 1981;18(1):1239–48.
[56] Wood G, Kehn T, Carter M, Culbertson W. Coal resource classification system of the U.S. Geological Survey. U.S. Geological Survey Circular; 1983. p. 891.
[57] Basu P. Biomass gasification, pyrolysis and torrefaction: practical design and theory. 4th ed. London: Elsevier Inc.; 2013.
[58] Matsumoto K, Takeno K, Ichinose T, Ogi T, Nakanishi M. Gasification reaction kinetics on biomass char obtained as a by-product of gasification in an entrained-flow gasifier with steam and oxygen at 900–1000°°C. Fuel 2009;88(3):519–27.
[59] Ollero P, Serrera A, Arjona R, Alcantarilla S. The CO_2 gasification kinetics of olive residue. Biomass Bioenergy 2003;24(2):151–61.

4. Estudio de la morfología y reactividad de los chars

La combustión del carbón puede dividirse en tres etapas: desvolatilización, combustión de los volátiles y combustión del char. La desvolatilización es la primera de esas etapas y una de las más importantes, ya que condiciona las siguientes. La desvolatilización de un sólido combustible permite estudiar algunos de los factores que determinan el grado de conversión final, como es el rendimiento en volátiles y la reactividad del desvolatilizado generado. Asimismo, la desvolatilización controla el reblandecimiento, el hinchamiento, la aglomeración de partículas y la estructura física del residuo carbonoso o char.

El rango del carbón ejerce una gran influencia sobre su reactividad. Como norma general, la reactividad intrínseca de los *chars* procedentes de carbones de mayor rango es inferior que la de los procedentes de carbones de menor rango. Esto es debido a diferencias estructurales, ya que los carbones de alto rango presentan una estructura carbonosa más ordenada y, por tanto, menos reactiva frente al oxígeno. Además, existen otros factores relacionados con la naturaleza del carbón que afectan a su reactividad, como pueden ser su composición maceral, el contenido, composición y propiedades catalíticas de la materia mineral, o la concentración y accesibilidad a los centros activos.

4.1 Desvolatilización y formación del char

La desvolatilización es la etapa inicial del proceso global de combustión y adquiere una relevancia mayor cuanto mayor es el contenido de materia volátil del combustible. La desvolatilización es un proceso endotérmico y su desarrollo depende primordialmente de las condiciones de temperatura, velocidad de calentamiento y tipo de combustible. La cinética de este proceso ha sido muy estudiada, típicamente en atmósfera de N_2 y, por tanto, las características de la desvolatilización en atmósfera de CO_2 son particularmente interesantes en los procesos de oxicombustión. Las condiciones de desvolatilización de las partículas de carbón (temperatura, tiempo de residencia y velocidad de calentamiento) también son factores determinantes en la reactividad del *char* formado, ya que condicionan la morfología y estructura del *char*. No obstante, las condiciones de desvolatilización no afectan a la reactividad de todos los carbones por igual, ya que ejercen un efecto mayor sobre la reactividad de los *chars* de carbones de bajo rango respecto a los de carbones de alto rango [Miura, 1989].

Ratham et al. [Ratham, 2009] llevaron a cabo experimentos de desvolatilización de un carbón bituminoso en N_2 y CO_2 en un sistema termogravimétrico, TGA. Los resultados fueron muy similares hasta una temperatura de 777 ^{o}C; a temperaturas superiores la pérdida de masa

en la atmósfera de CO_2 era mucho mayor, lo que se atribuyó a la reacción de gasificación del *char* con CO_2. Naredi et al. [Naredi, 2011] realizaron experimentos de desvolatilización en un reactor de flujo en arrastre a temperaturas desde 900 a 1.400 ^{0}C en atmósferas de N_2 y CO_2, y encontraron mayores rendimientos en la liberación de volátiles en la atmosfera de CO_2 que en la de N_2. Sin embargo, otros autores como Brix et al. [Brix, 2010] realizaron experimentos similares en un reactor de flujo en arrastre sin encontrar diferencias en la morfología de los *chars* ni en el rendimiento en volátiles en ambas atmosferas. Las áreas BET obtenidas a partir de isotermas de adsorción de N_2, de los *chars* de los carbones desvolatilizados en CO_2 y N_2 no presentaban diferencias significativas. En los trabajos presentados en este Capítulo (Publicaciones III y IV) se llevaron a cabo experimentos de desvolatilización de 4 carbones de distinto rango y una biomasa, serrín de pino torrefactado, en el reactor de flujo en arrastre en atmósferas de N_2 y CO_2 (cf. Apartado 2.3.3). Posteriormente se determinó la reactividad de los *chars* obtenidos mediante experimentos en termobalanza, según se ha descrito en el Apartado 2.4.1.

4.2 Combustión del char

Para que tenga lugar la combustión del *char*, el oxígeno debe difundir hasta la superficie externa de la partícula, y reaccionar con los centros activos de la misma, o bien difundir dentro de la partícula a través de los poros y reaccionar en el interior. En este proceso influyen en gran medida las condiciones de combustión del *char*, siendo la de mayor importancia la temperatura.

Tras los experimentos de desvolatilización se recogieron los distintos *chars* en el ciclón del reactor de flujo en arrastre, y se plantearon dos metodologías para determinar la reactividad de las muestras: experimentos de reactividad isotérmica y reactividad no isotérmica en atmósfera de oxicombustión.

La reactividad no isotérmica es experimentalmente menos laboriosa que la isotérmica ya que requiere menos experimentos, son más sencillos de llevar a cabo y transcurren durante un tiempo menor. La comparación entre los resultados obtenidos mediante ambas metodologías se incluye en la discusión de la Publicación IV.

4.3 Compendio de resultados

Se han llevado a cabo desvolatilizaciones de carbones de distinto rango, así como de biomasas a 1.000 ^{o}C, en atmósfera propia de combustión en aire (N_2), y de condiciones de oxicombustión (CO_2). La desvolatilización de carbones y biomasas en CO_2 produce mayor pérdida de masa que en N_2 y, por tanto, un mayor rendimiento en desvolatilización.

A partir de las imágenes de SEM, se ha observado que la morfología de los *chars* obtenidos en CO_2 y en N_2 de los carbones de alto rango es muy similar y no difiere en demasía de la del

carbón original, principalmente debido a que liberan pocos volátiles. Sin embargo, los carbones bituminosos presentan morfologías muy distintas a las de las partículas iniciales debido a la liberación de los volátiles y la deformación que experimentan al pasar por un estado pseudoplástico. Además se observan ligeras diferencias entre los chars obtenidos en N_2 y en CO_2, ya que en los chars obtenidos en CO_2 se observa cierta porosidad en su superficie, debido a la reacción de gasificación del *char* con CO_2. Esta reacción de gasificación explica la mayor pérdida de masa observada tras la desvolatilización en CO_2, en comparación con N_2.

Se han aplicado tres modelos cinéticos (VM, GM y RPM) para tratar de predecir el comportamiento reactivo de los *chars*. Se ha puesto de manifiesto que el modelo de reacción RPM es el que mejor predice la reactividad de los *chars* procedentes de carbones de alto rango, mientras que los modelos VM y RPM ofrecen ajustes similares para *chars* procedentes de carbones de bajo rango. Los parámetros cinéticos y los índices de reactividad obtenidos, indican que los *chars* obtenidos en atmósfera de N_2 son ligeramente más reactivos que los obtenidos en atmósfera de CO_2.

En los experimentos de reactividad no isotérmica en atmósferas de oxicombustión, los modelos cinéticos que proporcionan un mejor ajuste a los resultados experimentales son los modelos RPM y VM. La adición de *char* de biomasa no afecta la reactividad del *char* de carbón, ambos queman de forma individual sin detectarse ningún tipo de interacción durante su combustión conjunta en condiciones de oxicombustión.

Los resultados expuestos en este Capítulo ponen de manifiesto la necesidad de estudiar la desvolatilización en CO_2 a temperaturas más elevadas, ya que a dichas temperaturas las reacciones de gasificación con CO_2 tendrían más influencia sobre la morfología de los *chars* formados, y por extensión sobre su posterior reactividad.

4.4 Publicaciones relacionadas:

III **Oxy-fuel combustion kinetics and morphology of coal chars obtained in N_2 and CO_2 atmospheres in an entrained flow reactor.**
M.V. Gil, J. Riaza, L. Álvarez, C. Pevida, J.J. Pis, F. Rubiera. Applied Energy 2012. 91 (1) pp. 67 – 74. doi:10.1016/j.apenergy.2011.09.017

IV **Kinetic models for the oxy-fuel combustion of coal and coal/biomass blend chars obtained in N_2 and CO_2 atmospheres.**
M.V. Gil, J. Riaza, L. Álvarez, C. Pevida, J.J. Pis, F. Rubiera. Energy 2012. 48 (1) pp. 510–518. doi:10.1016/j.energy.2012.10.033

4.4.1 Publicación III

Oxy-fuel combustion kinetics and morphology of coal chars obtained in N_2 and CO_2 atmospheres in an entrained flow reactor.

M.V. Gil, J. Riaza, L. Álvarez, C. Pevida, J.J. Pis, F. Rubiera.
Applied Energy
2012. 91 (1) pp. 67 – 74.
doi:10.1016/j.apenergy.2011.09.017

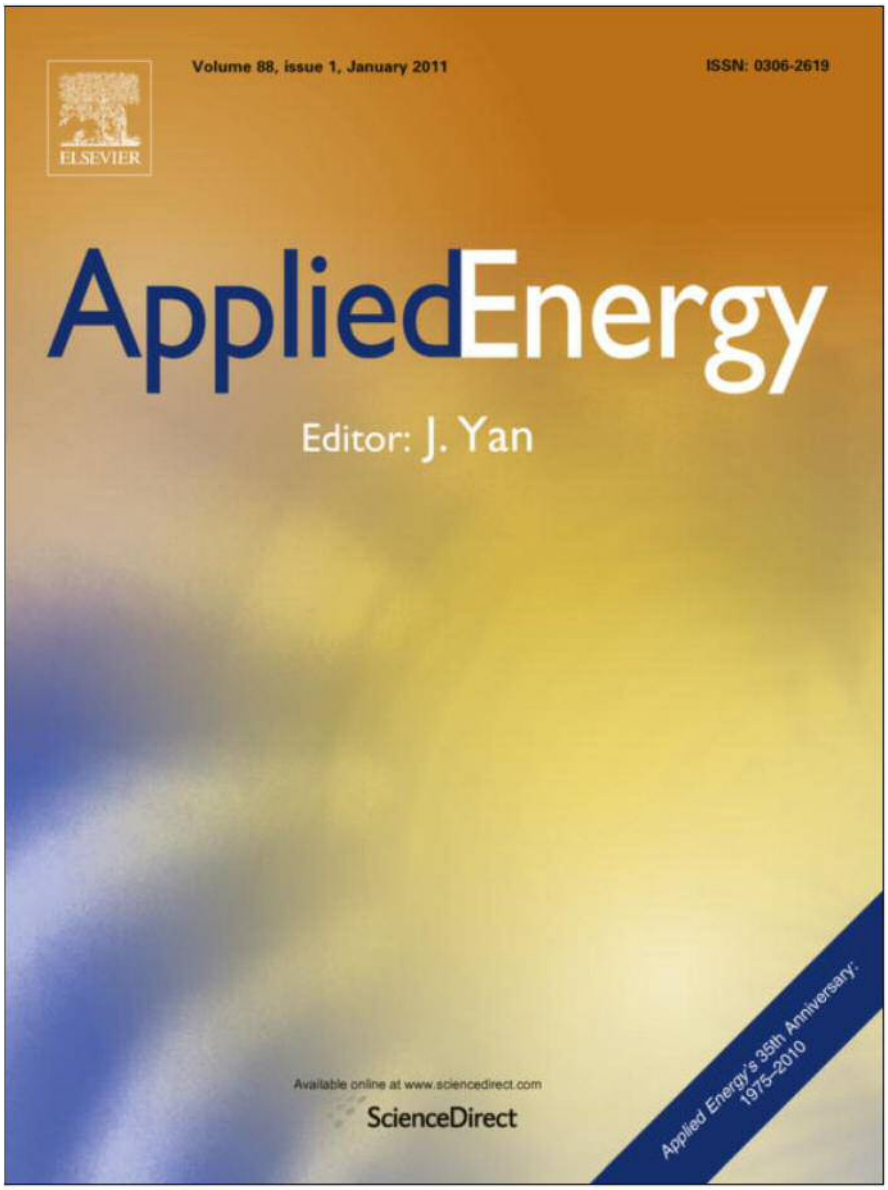

Applied Energy 91 (2012) 67–74

Contents lists available at SciVerse ScienceDirect

Applied Energy

journal homepage: www.elsevier.com/locate/apenergy

Oxy-fuel combustion kinetics and morphology of coal chars obtained in N_2 and CO_2 atmospheres in an entrained flow reactor

M.V. Gil, J. Riaza, L. Álvarez, C. Pevida, J.J. Pis, F. Rubiera *

Instituto Nacional del Carbón, INCAR-CSIC, Apartado 73, 33080 Oviedo, Spain

ARTICLE INFO

Article history:
Received 21 July 2011
Received in revised form 5 September 2011
Accepted 8 September 2011
Available online 5 October 2011

Keywords:
Coal
Char
Isothermal TG
Oxy-fuel combustion
Kinetics models
Entrained flow reactor

ABSTRACT

The thermal reactivity and kinetics of four coal chars (HVN, UM, SAB and BA) in an oxy-fuel combustion atmosphere (30%O_2–70%CO_2) were studied using a thermobalance. The coal chars were obtained by devolatilization in an entrained flow reactor (EFR) at 1000 °C for 2.5 s under 100% N_2 and CO_2 atmospheres. The reactivity tests were carried out by isothermal thermogravimetric analysis at different temperatures in a kinetically controlled regime. Three *n*th-order representative gas–solid models – the volumetric model (VM), the grain model (GM) and the random pore model (RPM) – were employed in order to describe the reactive behaviour of the chars during oxy-fuel combustion. From these models, the kinetic parameters were determined. The RPM model was found to be the best for describing the reactivity of the HVN, UM and BA chars, while VM was the model that best described the reactivity of the SAB char. The reactivities of the chars obtained in N_2 and CO_2 in an oxy-fuel combustion atmosphere with 30% of oxygen were compared using the kinetic parameters, but no differences were observed between the two devolatilization atmospheres. The apparent volatile yield after the coal devolatilization under CO_2 in the EFR was greater than under N_2 for all the coals studied. According to the scanning electron microscopy (SEM) images of the chars, those obtained in the CO_2 atmosphere experienced a greater degree of swelling, some particles showing partially reacted surfaces indicative of reaction between the char and CO_2.

© 2011 Elsevier Ltd. All rights reserved.

1. Introduction

The use of coal in power plants generates a large amount of CO_2, which is the chief contributor to global climate change. However, coal is the most abundant and geographically the most widely distributed fossil fuel. The stability of its supply and its relatively low cost will ensure its inclusion in the energy mix in the foreseeable future [1]. Several strategies for the reduction and capture of CO_2 from large-scale stationary power plants are being studied. The main problem is that the concentration of CO_2 in a conventional coal-air combustion flue gas stream is low (typically 15% by volume), rendering it unsuitable for direct sequestration in a supercritical state via compression which requires a high concentration of CO_2 [2]. As an alternative, the oxy-fuel combustion process has been proposed as a promising technology for CO_2 capture from fossil fuel power plants. This technology involves the combustion of coal in a mixture of oxygen (instead of air) and recycled flue gas (RFG), which consists mainly of CO_2 and H_2O [3]. In this process, the net volume of flue gas is reduced and a highly concentrated CO_2 (95%) flue gas is produced, which after purification [4,5] can be directly stored in a supercritical state by means of compression.

The combustion of coal in the O_2/CO_2 atmosphere of an oxy-coal combustion boiler can be expected to be different from that of an O_2/N_2 atmosphere of a conventional coal-air combustion boiler, because CO_2 has a larger specific molar heat than N_2, and the coal may be gasified by the CO_2 [6]. The use of CO_2 instead of N_2 may also cause a reduction in the propagation speed, stability of the flame and gas temperature profile or lead to an increase in the unburned carbon content. During the oxy-fuel combustion process, these problems can be overcome by increasing the oxygen concentration in the oxidizer (up to approximately 30%) in order to match the combustion performance achieved in air.

In addition, oxy-coal combustion can be used as retrofit technology in conventional pulverized coal boilers to capture and store carbon. However, the successful implementation of O_2/CO_2 technology in conventional pulverized coal boilers requires a full understanding of the changes that occur when N_2 is replaced by CO_2 in a combustion atmosphere [7]. A precise knowledge of char reactivity and kinetics under a CO_2 atmosphere is essential for designing and modelling oxy-fuel combustion at industrial scale. In modelling studies related to oxy-coal combustion, coal pyrolysis during oxy-coal combustion is usually assumed to be the same as in air [8]. According to Naredi and Pisupati [9], it is necessary to establish whether the pyrolysis of coal particles in CO_2 will produce different results from pyrolyzing them in an inert gas medium. Knowledge of coal pyrolysis under a CO_2 atmosphere is

* Corresponding author. Tel.: +34 985 118 975; fax: +34 985 297 662.
E-mail address: frubiera@incar.csic.es (F. Rubiera).

0306-2619/$ - see front matter © 2011 Elsevier Ltd. All rights reserved.
doi:10.1016/j.apenergy.2011.09.017

essential for understanding the process of oxy-fuel combustion [10].

The aim of the present work is to study the oxy-fuel combustion (30%O_2–70%CO_2) reactivity and kinetic behaviour of four coal chars obtained under N_2 and CO_2 atmospheres. For this purpose, three mathematical models – the volumetric model (VM), the grain model (GM) and the random pore model (RPM) – were used to determine the kinetic parameters which best represent the oxy-fuel combustion characteristics of the coal chars obtained in N_2 and CO_2 under an oxygen–carbon dioxide atmosphere. The morphology of the coal chars was compared by scanning electron microscopy (SEM).

2. Experimental

2.1. Fuel samples

Four coals of different rank were used: a semi-anthracite (HVN), a medium-volatile bituminous coal (UM) and two high-volatile bituminous coals (SAB and BA). The samples were ground and sieved to obtain a particle size fraction of 75–150 μm. The results of the proximate and ultimate analyses and high heating values of the samples are shown in Table 1.

2.2. Char preparation

The chars were prepared by devolatilizing the raw coals in an electrically heated entrained flow reactor (40 mm internal diameter, 1400 mm length) in streams of 100% N_2 or 100% CO_2 (4.79 N L min^{-1}). The experimental device has been described elsewhere [11,12]. The devolatilization experiments were carried out at a reactor temperature of 1000 °C and a particle residence time of 2.5 s. After the experiments, the chars were cooled down under a flow of nitrogen to room temperature. A water-cooled collecting probe was inserted into the reaction chamber from below to collect the char samples. The external morphology of the coal chars was examined by means of scanning electron microscopy (SEM).

2.3. Oxy-fuel combustion reactivity tests of the chars

Thermogravimetric analysis (TGA) is one of the most commonly used techniques to investigate and compare thermal events and kinetics during the combustion and pyrolysis of solid raw materials, such as coal and woods [13–17]. The reactivity tests were conducted in a thermobalance (Setaram TAG24) at atmospheric pressure. Approximately 5 mg of char sample was placed in a crucible of height 2 mm with a circular base 5 mm in diameter. A thermocouple was located close to the platinum basket to monitor the temperature and to close the control loop. In this work, all the experiments were performed under isothermal conditions at different temperatures (400–600 °C). These temperatures were chosen in order to avoid diffusion problems and consequently apply the Arrhenius plot for calculating the kinetic parameters. The total flow rate of the reactive gas introduced into the thermobalance during the oxy-fuel combustion experiments was 50 N mL min^{-1}, the gas consisting of 30% O_2 and 70% CO_2. The char conversion, X, and the reaction rate, dX/dt, were calculated.

Table 1
Proximate and ultimate analyses and high heating value of the coals.

Sample	HVN	UM	SAB	BA
Origin	Spain	Mexico	South Africa	Spain
Rank	sa	mvb	hvb	hvb
Proximate analysis[a]				
Moisture content (wt.%)	1.1	0.4	2.4	1.2
Ash (wt.%, db)	10.7	21.1	15.0	6.9
VM (wt.%, db)	9.2	23.7	29.9	33.9
FC (wt.%, db)[b]	80.1	55.2	55.1	59.2
Ultimate analysis (wt.%, daf)[a]				
C	91.7	86.2	80.8	88.5
H	3.5	5.5	5.0	5.5
N	1.9	1.6	2.0	1.9
S	1.6	0.8	0.9	1.1
O[b]	1.3	5.9	11.3	3.0
HHV (MJ/kg, db)	31.8	27.8	27.8	33.1

sa: Semi-anthracite; mvb: medium-volatile bituminous coal; hvb: high-volatile bituminous coal.
db: Dry basis and daf: dry and ash free bases.
[a] The proximate analysis was conducted in a LECO TGA-601, and the ultimate analysis in a LECO CHNS-932.
[b] Calculated by difference.

3. Kinetic models

A general kinetic expression for the overall reaction rate in gas–solid reactions can be expressed as follows [18]:

$$dX/dt = k(P_g, T)f(X) \quad (1)$$

where k is the apparent combustion reaction rate, which includes the effect of temperature (T) and the effect of the reactive gas partial pressure (P_g), and where $f(X)$ describes the changes in the physical or chemical properties of the sample as the combustion proceeds. Assuming that the partial pressure of the reactive gas remains constant during the process, the apparent combustion reaction rate will be dependent on the temperature and can be expressed using the Arrhenius equation, as follows:

$$k = k_0 \exp^{-E/RT} \quad (2)$$

where k_0 and E are the pre-exponential factor and activation energy, respectively.

In this work, three nth-order models were applied in order to describe the reactivity of the chars studied: the volumetric model (VM), the grain model (GM) and the random pore model (RPM). These models give different formulations of the term $f(X)$, with X representing the degree of char conversion on a dry ash-free basis.

The VM assumes a homogeneous reaction throughout the particle and a linearly decreasing reaction surface area with conversion [19]. The overall reaction rate is expressed by:

$$dX/dt = k_{VM}\ (1 - X) \quad (3)$$

The GM or shrinking core model, proposed by Szekely and Evans [20], assumes that a porous particle consists of an assembly of uniform nonporous grains and that the reaction takes place on the surface of these grains. The space between the grains constitutes the porous network. The shrinking core behaviour applies to each of these grains during the reaction. In a regime of chemical kinetic control and, assuming that the grains have a spherical shape, the overall reaction rate can be expressed as:

$$dX/dt = k_{GM}\ (1 - X)^{2/3} \quad (4)$$

This model predicts a monotonically decreasing reaction rate and surface area because the surface area of each grain is receding during the reaction.

The RPM model considers the overlapping of the pore surfaces, which reduces the area available for reaction [21]. The basic equation for this model is:

$$dX/dt = k_{RPM}\ (1 - X)[1 - \psi \ln(1 - X)]^{1/2} \quad (5)$$

This model is able to predict a maximum value of reactivity as the reaction proceeds, as it considers the competing effects of pore growth during the initial stages of combustion and the destruction of the pores due to the coalescence of neighbouring pores during the reaction. The RPM model employs two parameters, the

apparent combustion reaction rate, k_{RPM}, and ψ, which is utilized to represent the pore structure of the unreacted sample and was used as a fitting parameter.

In order to evaluate these models using the experimental results, Eqs. (3)–(5) were linearized, giving Eqs. (6)–(8), respectively:

$$-\ln(1-X) = k_{VM}t \tag{6}$$

$$3[1-(1-X)^{1/3}] = k_{GM}t \tag{7}$$

$$(2/\psi)[(1-\psi\ln(1-X))^{1/2}-1] = k_{RPM}t \tag{8}$$

The values of the apparent combustion reaction rates (k_{VM}, k_{GM}, k_{RPM}) and ψ were calculated using the experimental data obtained in the isothermal thermogravimetric runs, from the slope of the plots of Eqs. (6)–(8). The Arrhenius plot ($\ln k$ vs. $1/T$) was then employed to calculate the activation energy, E, and the pre-exponential factor, k_0, for each of the char samples and models according to Eq. (2).

The conversion-time relationships for the three models are:

$$X = 1-\exp(-k_{VM}t) \tag{9}$$

$$X = 1-(1-k_{GM}t/3)^3 \tag{10}$$

$$X = 1-\exp[-k_{RPM}t(1+k_{RPM}t\psi/4)] \tag{11}$$

The k values were calculated by introducing the estimated E and k_0 values into Eq. (2). $X_{calc,i}$ was obtained by introducing the k values, and the ψ value in the case of the RPM model, into Eqs. (9)–(11). The X calculations were performed in order to assess the quality of the fit and verify the capacity of the kinetic models to describe the degree of char conversion. By comparing the experimental and calculated X values, the kinetic model may be further tested and verified. The deviation (DEV) between the experimental and calculated curves was calculated using the following expression:

$$\text{DEV } X\ (\%) = 100\left[\sum_{i=1,N}(X_{exp,i}-X_{calc,i})^2/N\right]^{1/2} \Big/ \max X_{exp} \tag{12}$$

where $X_{exp,i}$ and $X_{calc,i}$ represent the experimental and calculated data of X, N is the number of data points, and max X_{exp} is the highest absolute value of the experimental curve.

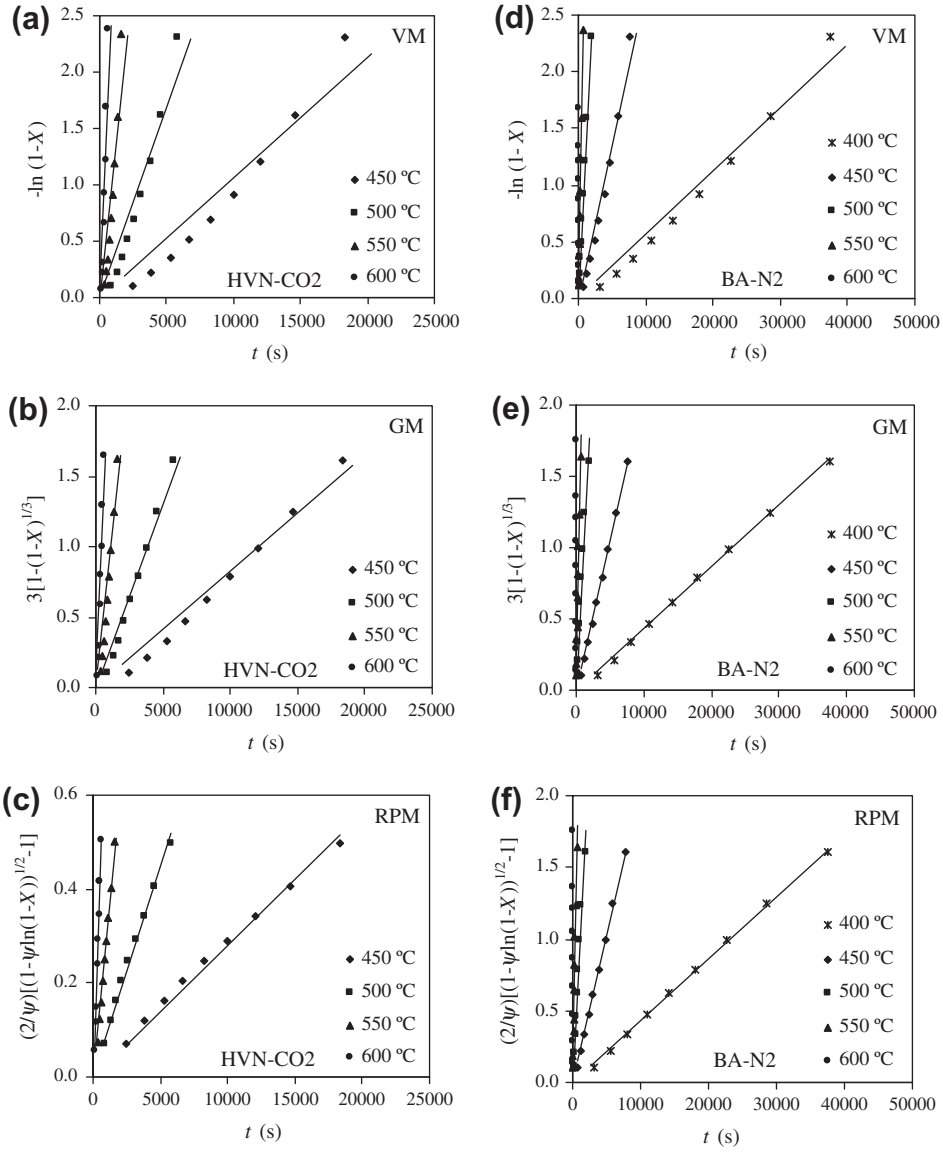

Fig. 1. VM, GM and RPM linearized models for the HVN-CO_2 (a–c) and BA-N_2 (d–f) char samples during oxy-fuel combustion at different temperatures.

In order to compare the oxy-fuel combustion reactivity of the chars obtained under the N_2 and CO_2 atmospheres, the reactivity index at 500 °C, R_{500}, was calculated as follows:

$$R_{500} = 0.5/\tau_{0.5} \quad (13)$$

where $\tau_{0.5}$ represents the time required to reach 50% of carbon conversion. High reactivity indices indicate high reactivities.

4. Results and discussion

4.1. Kinetic parameters

The linearized form of the three models studied, Eqs. (6)–(8), was used to represent the experimental data obtained during oxy-fuel combustion at all the temperatures studied in order to find the parameters k_{VM}, k_{GM}, k_{RPM} and ψ of best fit. As an example, the plots of the VM, GM and RPM linearized models for the HVN-CO_2 and BA-N_2 char samples are shown in Fig. 1. The parameter ψ was calculated assuming that its value is constant for each char sample at all the temperatures, since it is related to the initial pore structure.

The Arrhenius plot ($\ln k$ vs. $1/T$) was then employed to calculate the activation energy, E, and the pre-exponential factor, k_0, for each of the char samples (Eq. (2)). As an example, Fig. 2 shows the Arrhenius plots for the HVN-N_2, HVN-CO_2, BA-N_2 and BA-CO_2 char samples, using the reaction rates calculated with the three models studied. Only the results obtained under the chemical controlled regime were included in the calculations. The change from chemical to diffusion-controlled regime can be detected from the change in slope on the Arrhenius plots.

Table 2 shows the values of the activation energy, E, and the pre-exponential factor, k_0, that allow the best fit of the experimental data to the different models. In the case of the RPM model, the ψ value was also included.

In order to assess the ability of the kinetic models to predict conversion during oxy-fuel combustion, the experimental conversion values, $X_{exp,i}$, were compared with the calculated values,

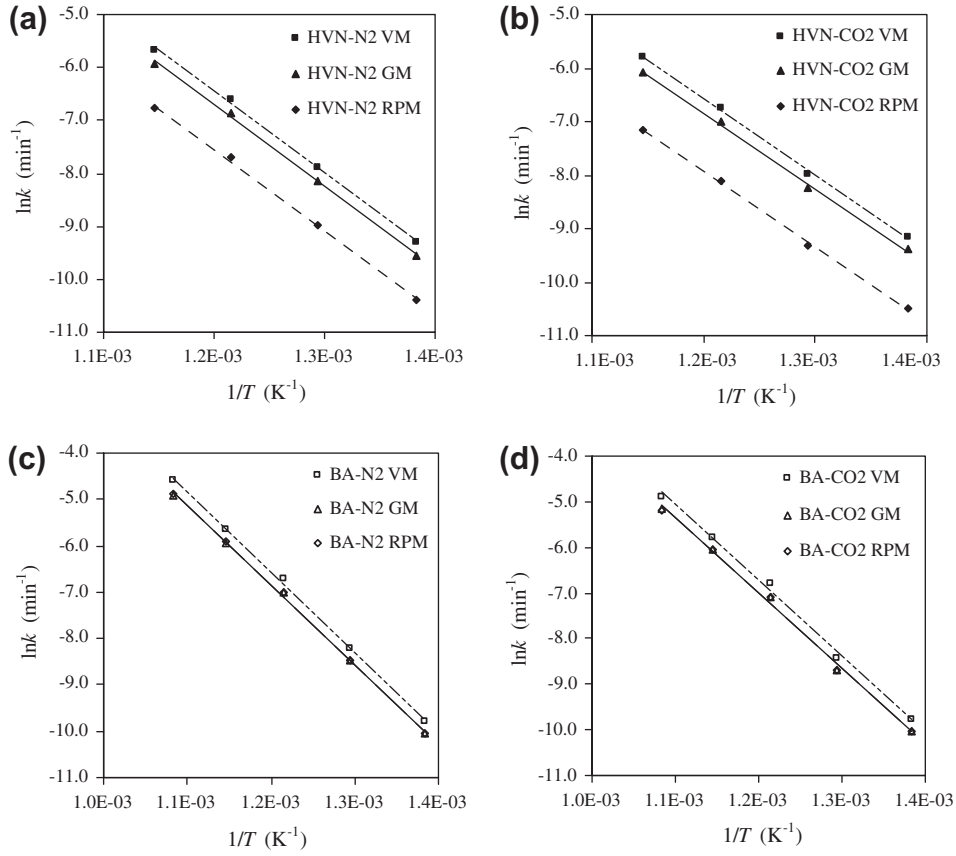

Fig. 2. Arrhenius plot for the VM, GM and RPM models of the HVN-N_2 (a), HVN-CO_2 (b), BA-N_2 (c) and BA-CO_2 (d) coal chars during oxy-fuel combustion.

Table 2
Kinetic parameters that allow the best fit of the experimental data from oxy-fuel combustion (30%O_2–70%CO_2) to the VM, GM and RPM models.

Char	Volumetric model (VM)		Grain model (GM)		Random pore model (RPM)		
	E (kJ mol^{-1})	k_0 (s^{-1})	E (kJ mol^{-1})	k_0 (s^{-1})	E (kJ mol^{-1})	k_0 (s^{-1})	ψ
HVN-N_2	128	1.64E+05	128	1.21E+05	127	5.09E+04	15.9
HVN-CO_2	118	3.55E+04	118	2.51E+04	117	8.10E+03	29.4
UM-N_2	125	1.90E+05	123	1.12E+05	123	5.89E+04	6.7
UM-CO_2	121	9.1E+04	120	5.76E+04	119	2.14E+04	16.4
SAB-N_2	121	1.36E+05	120	8.15E+04	120	9.48E+04	0.7
SAB-CO_2	125	2.50E+05	125	1.88E+05	125	2.31E+05	0.2
BA-N_2	127	4.09E+05	126	2.66E+05	126	2.82E+05	0.9
BA-CO_2	122	1.57E+05	121	1.10E+05	121	1.11E+05	1.0

$X_{calc,i}$, at the different temperatures selected. The calculated conversion values of the chars during oxy-fuel combustion were obtained by introducing the previously estimated k (calculated from k_0 and E) and ψ values into Eqs. (9)–(11). As an example, the results for the HVN-N_2, HVN-CO_2, BA-N_2 and BA-CO_2 char samples are shown in Fig. 3. In addition, the errors produced by the kinetic models in predicting the values of conversion were quantified by means of Eq. (12), which compares the experimental and calculated X values taking into account the deviation, DEV X (%), between the experimental and calculated curves. Table 3 shows the results of the average deviation for all the char samples.

The best model for describing the reactivity of the HVN, UM and BA coal chars proved to be RPM, which presented the lowest deviation values. VM was the model that best described the reactivity of the SAB chars, although in this case the DEV X value was similar to that of RPM model. This was due to the ψ value being very close to zero and, when this occurs, the RPM model predicts an almost constant decrease in reactivity with conversion, like the VM model, which assumes a homogeneous reaction throughout the particle [19].

Using the models of best fit, the activation energy for the coal chars under oxy-fuel atmosphere (30% O_2) was 117–127 kJ mol^{-1} (Table 2). Niu et al. [22] obtained activation energy values for pulverized coals in an oxy-fuel atmosphere (20% O_2) that ranged between 109 and 248 kJ mol^{-1}. Similarly, Liu [6] achieved activation energy values for coal chars in an oxy-fuel atmosphere (10% O_2) that ranged between 115 and 147 kJ mol^{-1}.

Table 4 shows the reactivity index, R_{500}, calculated from Eq. (13). As can be seen, the reactivity index values obtained for the coal chars in N_2 and CO_2 were similar, although there is a slight trend towards higher reactivity values in the case of the N_2-chars. Table 2 shows that the activation energy values and pre-exponential factors for the chars obtained under CO_2 and N_2 are also very similar. From these data, it can be concluded that no differences in the kinetic parameters are produced by using these different devolatilization atmospheres. The reaction rate of a char under an oxygen atmosphere is usually very high and in the present study the reactivity was measured in a high oxygen content (30%) atmosphere, which may have concealed possible differences in reactivity between both chars and may explain why no differences were observed between the chars obtained under N_2 or CO_2. The results obtained by Naredi and Pisupati [9] also suggest that the reactivity of the coal char generated in CO_2 was similar to that of the coal char generated in an Ar gas medium. These authors were led to conclude that the properties of the char obtained in both atmospheres differed only at high temperatures (>1300 °C), which they attributed to the effect of char gasification resulting from the reaction between the char and CO_2.

4.2. Properties of the chars

The apparent volatile yields of the four coals studied after devolatilization in N_2 and CO_2 at 1000 °C in an entrained flow reactor are presented in Table 5. The apparent volatile yields (V^*) of the UM, SAB and BA coals calculated from the EFR experiments were higher than their respective volatile matter contents (VM) obtained by proximate analysis, indicating an enhanced devolatilization at the higher temperature and heating rate in the entrained flow reactor. However, in the case of the HVN coal, the V^* yields measured after coal devolatilization in N_2 and CO_2 in the EFR were lower than the coal VM content, probably due to the high rank of this coal together with the short residence time in the EFR during the devolatilization experiments compared to that of the proximate analysis.

Furthermore, the apparent volatile yields measured after coal devolatilization under CO_2 were greater than those obtained under N_2 for all the coals studied (Table 4). The greater mass loss observed under CO_2 was probably caused by char-CO_2 gasification occurring at high temperatures during the devolatilization experiments in the EFR. Rathnam et al. [2] and Li et al. [23] also observed higher apparent volatile yields under CO_2 than under N_2 after

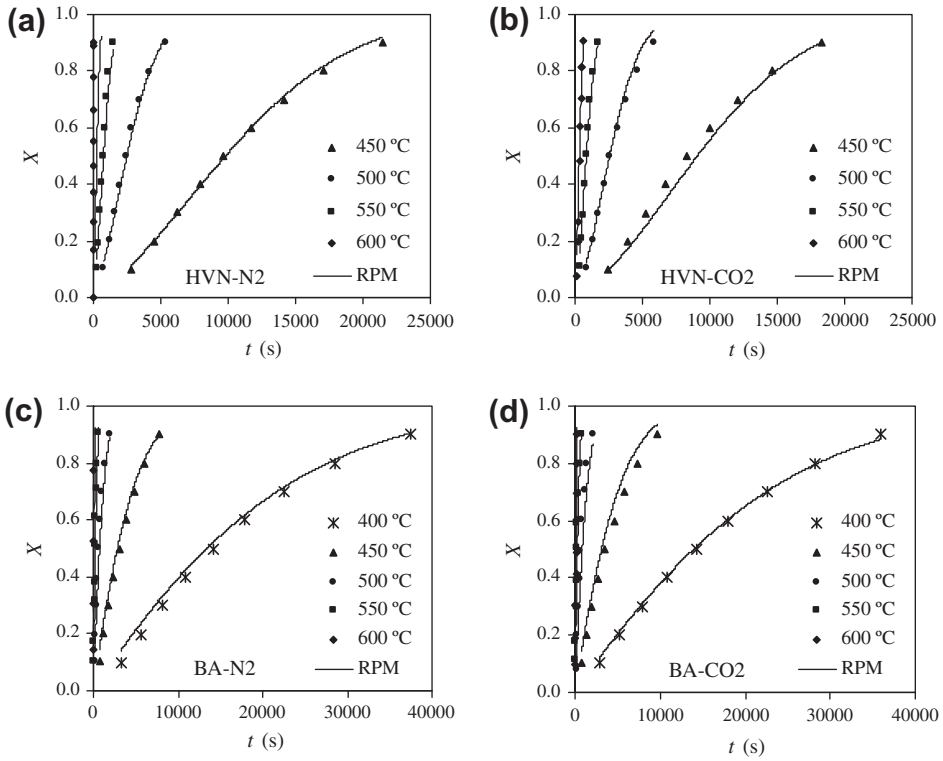

Fig. 3. Experimental conversion curves for HVN-N_2 (a), HVN-CO_2 (b), BA-N_2 (c) and BA-CO_2 (d) coal chars and those calculated with the RPM model during oxy-fuel combustion at different temperatures.

Table 3
Average deviation (%) between the experimental and calculated conversion (X) data.

Char	DEV X (%)		
	VM	GM	RPM
HVN-N_2	8.5	5.7	2.5
HVN-CO_2	9.3	6.4	2.9
UM-N_2	8.5	5.5	3.8
UM-CO_2	10.8	8.7	6.1
SAB-N_2	6.2	7.4	6.4
SAB-CO_2	5.1	5.9	5.2
BA-N_2	5.3	4.9	4.0
BA-CO_2	6.8	7.2	5.8

Table 4
Reactivity index at 500 °C of the coal chars obtained in N_2 and CO_2.

	HVN		UM		SAB		BA	
	N_2	CO_2	N_2	CO_2	N_2	CO_2	N_2	CO_2
R_{500} (h^{-1})	0.76	0.69	1.25	1.19	2.68	2.08	2.94	2.78

Table 5
Apparent volatile yield of the coal chars obtained under N_2 and CO_2 in entrained flow reactor experiments at 1000 °C.

	HVN	UM	SAB	BA
VM proximate analysis (wt.%, daf)	10.3	30.1	35.2	36.4
V^* (N_2)	6.0	40.6	44.9	49.9
V^* (CO_2)	7.2	65.3	53.1	62.2

daf: Dry and ash free bases.

devolatilization in a drop tube furnace. These authors attributed the higher values to the gasification of the chars by CO_2. Jamil et al. [24] observed a lower char yield in CO_2 than in He after the pyrolysis of a brown coal at 900 °C in a wire-mesh reactor, which they attributed to gasification of the char by CO_2. In contrast, Brix et al. [25] noted that the devolatilization of coal in N_2 and CO_2 in an entrained flow reactor gave rise to a similar char morphology and volatile yield. Naredi and Pisupati [9] reported a higher weight loss during pyrolysis in CO_2 than in Ar in a drop tube reactor at temperatures above 900 °C, which they also ascribed to the reaction between char and CO_2. Gasification of the coal would seem a reasonable explanation for the higher volatile yield in CO_2 in the present study in view of the residence time and temperature used. Brix et al. [25] concluded that at high temperatures (>1227 °C) the low residence times required for devolatilization to occur limit the access of CO_2 to the surface of the particle. These authors did not observe any differences between devolatilization in N_2 and CO_2 at temperatures over 1300 °C when the heating and devolatilization process was completed between 150 and 200 ms.

The chars obtained from coal devolatilization under N_2 and CO_2 in the entrained flow reactor were also examined using a scanning electron microscope (SEM), images of which are shown in Figs. 4–7. It can be observed that the HVN-N_2 coal consists of solid particles with an external angular profile, whereas the HVN-CO_2 char is composed of solid particles with a more rounded shape (Fig. 4). Both types of char particle have a similar mean particle size.

Both the UM-N_2 and the UM-CO_2 char particles show significant signs of swelling after devolatilization, but both have a similar particle size distribution and external appearance (Fig. 5). They also have a network-type char structure (Fig. 5b, c and f), although the proportion of this type of char is lower in the case of UM-CO_2, while the proportion of thick-walled particles with wide blow holes (Fig. 5g) is higher in the UM-CO_2 char than in the UM-N_2 char. The particles exhibited intense bubbling and grew larger during the plastic stage to form larger and more hollow char particles due to the growth of the bubbles. These bubbles grow thanks to the generation of volatiles and, if they swell to a sufficiently large extent, the particles appear almost transparent. On the other hand, the bubbles may rupture at an early stage and the holes may not close again if the release of volatiles through the holes is intense [26]. This might explain the larger amount of char particles with large blow-holes on their surface in UM-CO_2 (Fig. 5g), resulting from more intense release of volatiles under CO_2 than under N_2.

A more noticeable swelling is observed in the case of the SAB-CO_2 and BA-CO_2 particles than in the case of the chars obtained under N_2, since the mean particle size of the SAB-CO_2 and BA-CO_2 char particles is larger than that of the SAB-N_2 and BA-N_2 chars, respectively (Figs. 6 and 7). The SAB-N_2 char exhibits both solid and irregular particles with very small holes, while the SAB-CO_2 particles are more spherical with wider holes and thick walls. This could be due to the high vitrinite content (43.5 wt.% mineral-matter-free basis) in the SAB coal. In general, particles containing liptinites or vitrinites generate a porous char, while those containing inertinites generate relatively dense char structures [26].

The BA-N_2 char has both solid particles and particles with holes, while the BA-CO_2 char exhibits more spherical particles with thinner walls, bigger holes and a network structure (Fig. 7). This diversity in morphology in the case of the BA char particles seems to indicate a multiplicity of maceral components, possibly due to

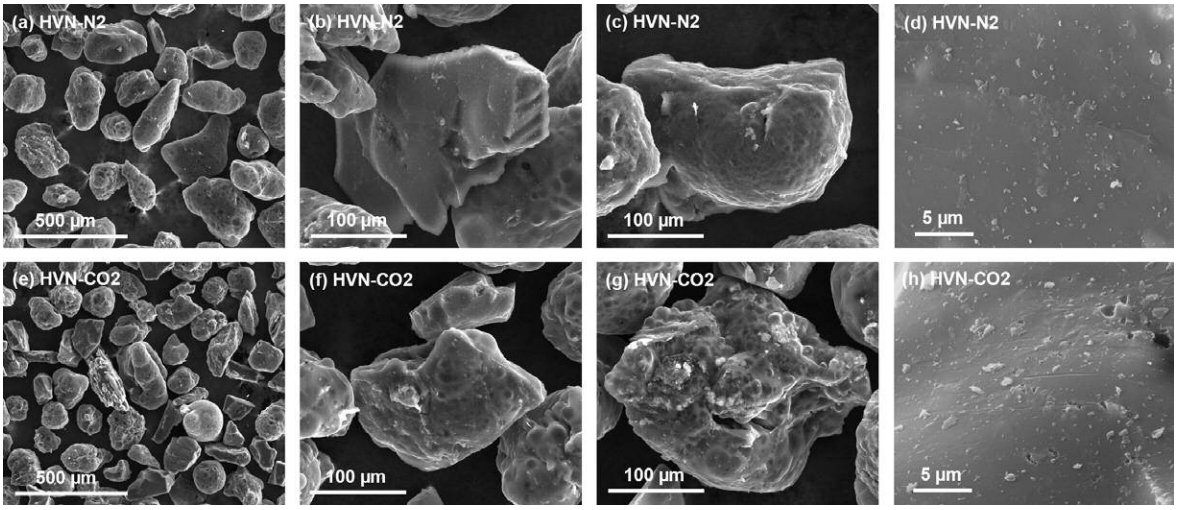

Fig. 4. SEM images of the HVN coal char particles obtained under N_2 (a–d) and CO_2 (e–h) in an entrained flow reactor (EFR) at 1000 °C.

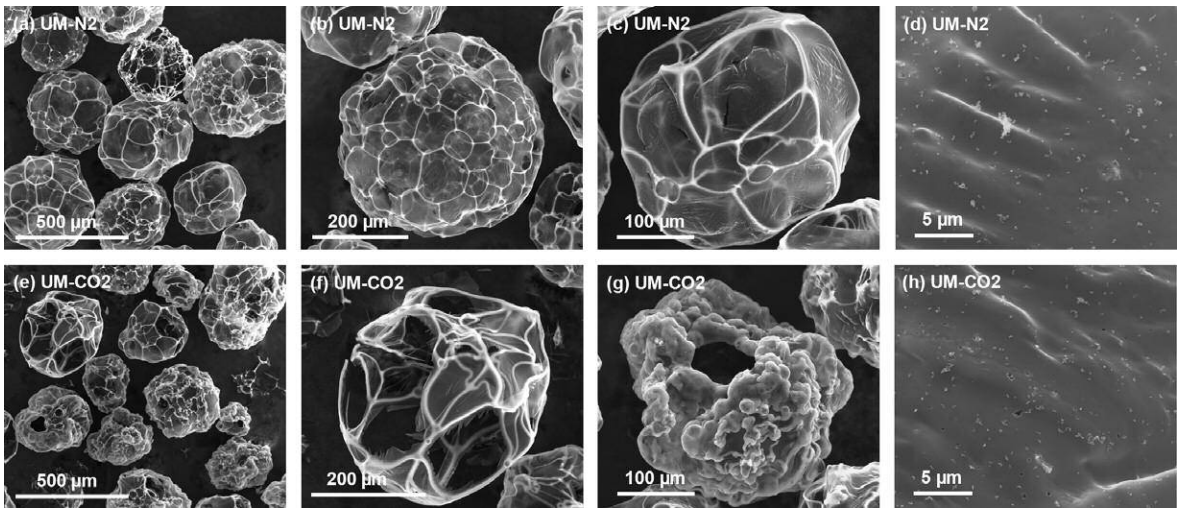

Fig. 5. SEM images of the UM coal char particles obtained under N_2 (a–d) and CO_2 (e–h) in an entrained flow reactor (EFR) at 1000 °C.

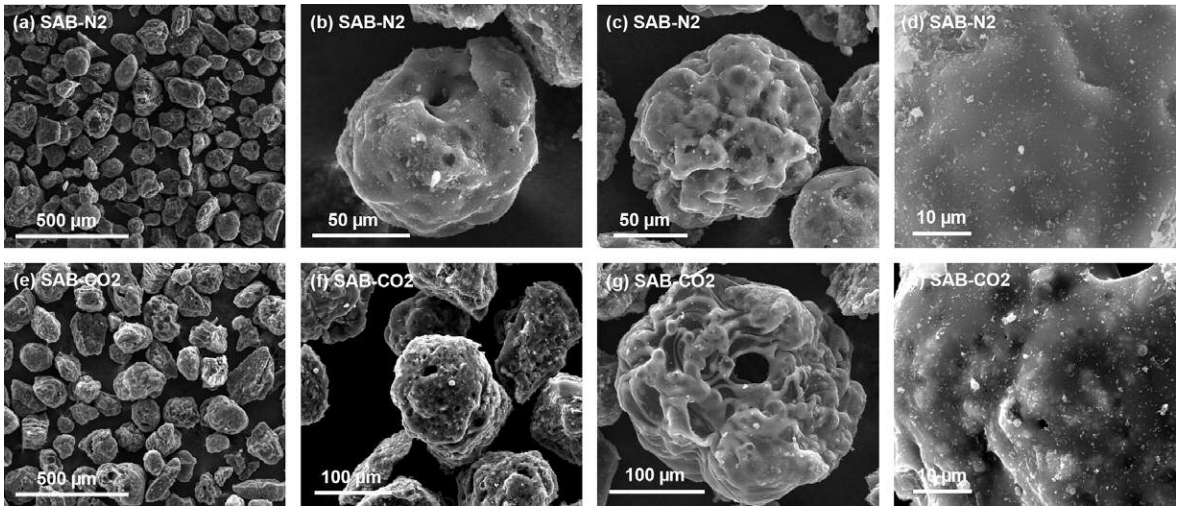

Fig. 6. SEM images of the SAB coal char particles obtained under N_2 (a–d) and CO_2 (e–h) in an entrained flow reactor (EFR) at 1000 °C.

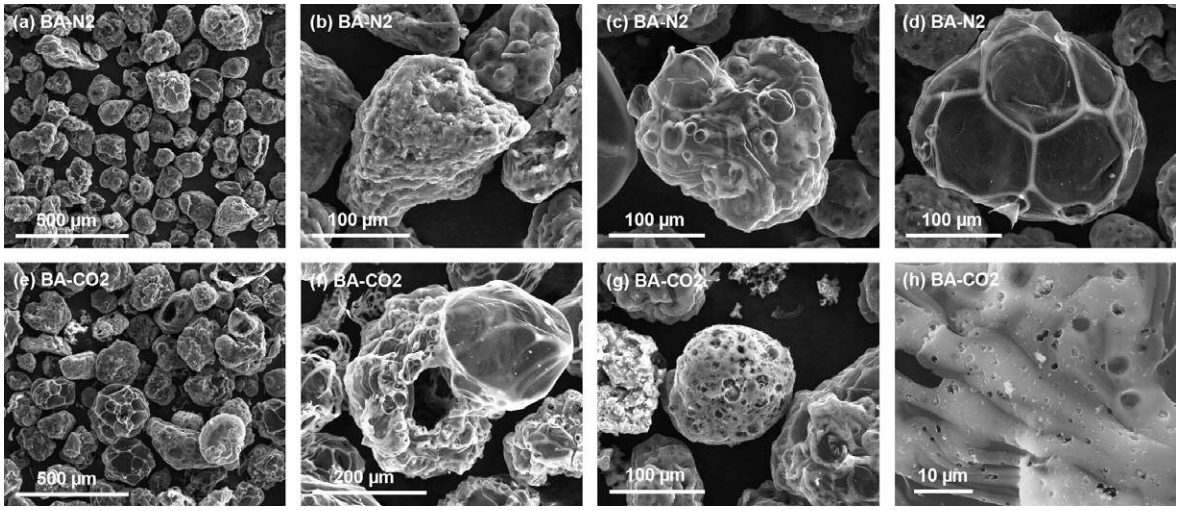

Fig. 7. SEM images of the BA coal char particles obtained under N_2 (a–d) and CO_2 (e–h) in an entrained flow reactor (EFR) at 1000 °C.

the fact that the BA coal is a mixture of bituminous coals and anthracites (>90% high-volatile bituminous coal).

In general, from the SEM images (Figs. 4–7) of the coal chars, it can be concluded that devolatilization under CO_2 causes a more pronounced swelling in the char particles than under N_2. Furthermore, some particles in the UM and BA CO_2-chars show partially reacted surfaces (Figs. 5h and 7h), which could be indicative of a reaction between the char and CO_2. This would accord with the higher volatile yield obtained after CO_2-devolatization.

5. Conclusions

Chars obtained from four coals were subjected to oxy-fuel combustion in a thermobalance in order to evaluate their thermal reactivity and kinetics under a 30%O_2–70%CO_2 atmosphere. The isothermal thermogravimetric technique was employed at different temperatures in a kinetically controlled regime to analyze the gas–solid reactions and three models – the volumetric model (VM), the grain model (GM) and the random pore model (RPM) – were applied to describe the reactive behaviour of the chars during oxy-fuel combustion. The best model for describing the char oxy-fuel combustion of the HVN, UM and BA coals was found to be the RPM model, whereas the most efficient model for describing SAB char reactivity was VM. The kinetic parameters did not show an evidence of the chars obtained under CO_2 and N_2 showing different reactivities in a typical oxy-fuel combustion atmosphere (30%O_2–70%CO_2). The reactivity indices would appear to indicate a slightly higher reactivity in the case of the N_2-chars over the CO_2-chars. Finally, the comparatively higher apparent volatile yields and certain features in the SEM images of the chars obtained under CO_2 may indicate that the char has undergone gasification by CO_2, which would accord with the lower reactivity displayed by the CO_2-chars.

Acknowledgements

This work was carried out with financial support from the Spanish MICINN (Project PS-120000-2005-2) co-financed by the European Regional Development Fund. M.V.G. and L.A. acknowledge funding from the CSIC JAE-Pre and CSIC JAE-Doc programs, respectively, co-financed by the European Social Fund. J.R. acknowledges funding from the Government of the Principado de Asturias (Severo Ochoa program).

References

[1] Buhre BJP, Elliott LK, Sheng CD, Gupta RP, Wall TF. Oxy-fuel combustion technology for coal-fired power generation. Prog Energy Combust Sci 2005;31:283–307.
[2] Rathnam RK, Elliott LK, Wall TF, Liu Y, Moghtaderi B. Differences in reactivity of pulverised coal in air (O_2/N_2) and oxy-fuel (O_2/CO_2) conditions. Fuel Process Technol 2009;90:797–802.
[3] Hu Y, Yan J. Characterization of flue gas in oxy-coal combustion processes for CO_2 capture. Appl Energy 2011. doi: 10.1016/j.apenergy.2011.03.005.
[4] Liu H, Shao Y. Predictions of the impurities in the CO_2 stream of an oxy-coal combustion plant. Appl Energy 2010;87:3162–70.
[5] Li H, Yan J, Yan J, Anheden M. Impurity impacts on the purification process in oxy-fuel combustion based CO_2 capture and storage system. Appl Energy 2009;86:202–13.
[6] Liu H. Combustion of coal chars in O_2/CO_2 and O_2/N_2 mixtures: a comparative study with non-isothermal thermogravimetric analyzer (TGA) tests. Energy Fuels 2009;23:4278–85.
[7] Molina A, Shaddix CR. Ignition and devolatilization of pulverized bituminous coal particles during oxygen/carbon dioxide coal combustion. Proc Combust Inst 2007;31:1905–12.
[8] Chui EH, Douglas MA, Tan YW. Modeling of oxy-fuel combustión for a western Canadian sub-bituminous coal. Fuel 2003;82:1201–10.
[9] Naredi P, Pisupati S. Effect of CO_2 during coal pyrolysis and char burnout in oxy-coal combustion. Energy Fuels 2011;25:2452–9.
[10] Duan L, Zhao C, Zhou W, Qu C, Chen X. Investigation on coal pyrolysis in CO_2 atmosphere. Energy Fuels 2009;23:3826–30.
[11] Álvarez L, Gharebaghi M, Pourkashanian M, Willians A, Riaza J, Pevida C, et al. CFD modelling of oxy-coal combustion in an entrained flow reactor. Fuel Process Technol 2011;92:1489–97.
[12] Álvarez L, Riaza J, Gil MV, Pevida C, Pis JJ, Rubiera F. NO emissions in oxy-coal combustion with the addition of steam in an entrained flow reactor. Greenhouse Gas Sci Technol 2011;1:180–90.
[13] Arenillas A, Rubiera F, Pis JJ, Jones JM, Williams A. The effect of the textural properties of bituminous coal chars on NO emissions. Fuel 1999;78:1779–85.
[14] Rubiera F, Arenillas A, Fuente E, Miles N, Pis JJ. Effect of the grinding behaviour of coal blends on coal utilisation for combustion. Powder Technol 1999;105:351–6.
[15] Arenillas A, Rubiera F, Pis JJ, Cuesta MJ, Iglesias MJ, Jiménez A, et al. Thermal behaviour during the pyrolysis of low rank perhydrous coals. J Anal Appl Pyrol 2003;68–69:371–85.
[16] Xiao H, Ma X, Lai Z. Isoconversional kinetic analysis of co-combustion of sewage sludge with straw and coal. Appl Energy 2009;86:1741–5.
[17] Muthuraman M, Namioka T, Yoshikawa K. Characteristics of co-combustion and kinetic study on hydrothermally treated municipal solid waste with different rank coals: a thermogravimetric analysis. Appl Energy 2010;87:141–8.
[18] Lu GQ, Do DD. Comparison of structural models for high-ash char gasification. Carbon 1994;32:247–63.
[19] Ishida M, Wen CY. Comparison of zone-reaction model and unreacted-core shrinking model in solid-gas reactions – I isothermal analysis. Chem Eng Sci 1971;26:1031–41.
[20] Szekely J, Evans JW. A structural model for gas–solid reactions with a moving boundary. Chem Eng Sci 1970;25:1091–107.
[21] Bhatia SK, Perlmutter DD. A random pore model for fluid-solid reactions: I. Isothermal, kinetic control. AIChE J 1980;26:379–86.
[22] Niu SL, Lu CM, Han KH, Zhao JL. Thermogravimetric analysis of combustion characteristics and kinetic parameters of pulverized coals in oxy-fuel atmosphere. J Therm Anal Calorim 2009;98:267–74.
[23] Li X, Rathnam RK, Yu J, Wang Q, Wall T, Meesri C. Pyrolysis and combustion characteristics of an Indonisian low-rank coal under O_2/N_2 and O_2/CO_2 conditions. Energy Fuels 2010;24:160–4.
[24] Jamil K, Hayashi J, Li C-Z. Pyrolysis of a Victorian brown coal and gasification of nascent char in CO_2 atmosphere in a wire-mesh reactor. Fuel 2004;83:833–43.
[25] Brix J, Jensen PA, Jensen AD. Coal devolatilization and char conversion under suspension fired conditions in O_2/N_2 and O_2/CO_2 atmospheres. Fuel 2000;89:3373–80.
[26] Yu J, Lucas JA, Wall TF. Formation of the structure of chars during devolatilization of pulverized coal and its thermoproperties: a review. Prog Energy Combust Sci 2007;33:135–70.

4.4.2 Publicación IV

Kinetic models for the oxy-fuel combustion of coal and coal/biomass blend chars obtained in N_2 and CO_2 atmospheres.

M.V. Gil, J. Riaza, L. Álvarez, C. Pevida, J.J. Pis, F. Rubiera.
Energy
2012. 48 (1) pp. 510–518.
doi:10.1016/j.energy.2012.10.033

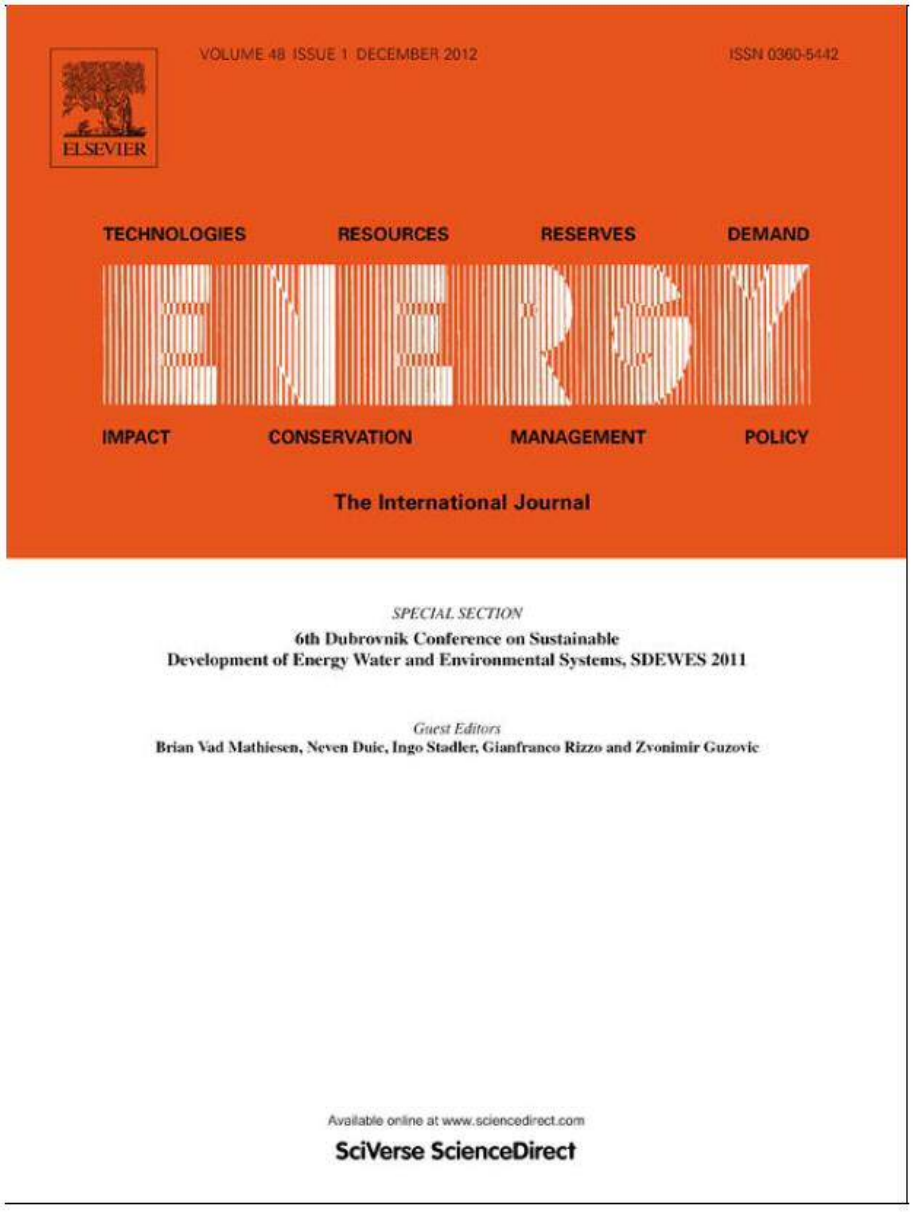

Energy 48 (2012) 510–518

Contents lists available at SciVerse ScienceDirect

Energy

journal homepage: www.elsevier.com/locate/energy

Kinetic models for the oxy-fuel combustion of coal and coal/biomass blend chars obtained in N_2 and CO_2 atmospheres

M.V. Gil, J. Riaza, L. Álvarez, C. Pevida, J.J. Pis, F. Rubiera*

Instituto Nacional del Carbón, INCAR-CSIC, Apartado 73, 33080 Oviedo, Spain

ARTICLE INFO

Article history:
Received 30 May 2012
Received in revised form
17 October 2012
Accepted 21 October 2012
Available online 8 November 2012

Keywords:
Coal
Biomass
Non-isothermal TG
Oxy-fuel combustion
Kinetic models
Entrained flow reactor

ABSTRACT

The thermal reactivity and kinetics of five coal chars, a biomass char, and two coal/biomass char blends in an oxy-fuel combustion atmosphere (30%O_2–70%CO_2) were studied using the non-isothermal thermogravimetric method at three heating rates. Fuel chars were obtained by devolatilization in an entrained flow reactor at 1273 K under N_2 and CO_2 atmospheres. Three *n*th-order representative gas–solid models – the volumetric model (VM), the grain model (GM) and the random pore model (RPM) – were employed to describe the reactive behaviour of the chars. The RPM model was found to be the best for describing the reactivity of the high rank coal chars, while VM was the model that best described the reactivity of the bituminous coal chars, the biomass char and the coal-biomass blend char. The kinetic parameters of the chars obtained in N_2 and CO_2 in an oxy-fuel combustion atmosphere with 30% of oxygen were compared, but no relevant differences were observed. The behaviour of the blend of the bituminous coal (90%wt.) and the biomass (10%wt.) chars resembled that of the individual coal concealing the effect of the biomass. Likewise, no interaction was detected between the high rank coal and the biomass chars during oxy-fuel combustion of the blend.

© 2012 Elsevier Ltd. All rights reserved.

1. Introduction

Whereas power generation from CO_2-neutral renewable fuels is being promoted, coal utilization is expected to continue in the future, as the reserves of coal are abundant and its cost is relatively low [1]. However, the use of coal in power plants generates a large amount of CO_2, which is the chief contributor to global climate change. One of the promising technologies being developed to facilitate carbon capture and storage (CCS) from fossil-fuel-fired power plants is the oxy-fuel combustion. The oxy-coal combustion together with carbon sequestration is a strategy that has received considerable attention as a viable, cost-effective technology for power production and that can be used as a retrofit on existing coal-fired power plants. This technology involves the combustion of pulverized coal in a mixture of oxygen and recycled flue gas (RFG), which consists mainly of CO_2 and H_2O [2]. In this process, the net volume of flue gas is reduced and a CO_2 volume fraction in the flue gas of 95% or higher is provided, which after purification can be directly stored in a supercritical state by means of compression.

The oxy-coal combustion is expected to be different from the coal combustion under an O_2/N_2 atmosphere as the CO_2 has higher specific molar heat capacity and varying radiation properties compared to those of N_2. Previous research studies have focused on the fact that the use of CO_2 instead of N_2 may cause a reduction in the propagation speed, flame stability and gas temperature profile or lead to an increase in the unburned carbon content. Thus, Liu et al. [3] concluded that during the oxy-fuel combustion process, these problems can be overcome by increasing the oxygen concentration in the oxidizer (up to approximately 30%) to match the combustion performance achieved in air. However, the reaction models and kinetics to describe coal combustion in O_2/CO_2 atmosphere have been scarcely studied. The knowledge of the effect of the CO_2 atmosphere on the reactivity of coal is needed for evaluating the kinetic parameters required for computational fluid dynamics (CFD) calculations [4], which will be useful for designing and modelling oxy-fuel combustion at industrial scale. There are a few recent studies on the calculation of the kinetic parameters of the combustion of coal in an oxy-fuel atmosphere. Niu et al. [5,6] carried out the coal combustion in O_2/CO_2 mixtures on a thermogravimetric analyzer and calculated the kinetic parameters which describe the combustion process by linearization using the Coats–Redfern method. Wang et al. [7] compared the combustion of coals and chars in oxy-fuel atmosphere applying the non-isothermal

* Corresponding author. Tel.: +34 985 118 975; fax: +34 985 297 662.
E-mail address: frubiera@incar.csic.es (F. Rubiera).

0360-5442/$ – see front matter © 2012 Elsevier Ltd. All rights reserved.
http://dx.doi.org/10.1016/j.energy.2012.10.033

thermogravimetric analysis, but these authors claimed that insufficient information exits on the effect of char preparation atmosphere on the char reactivity.

Thermogravimetric analysis (TGA) is a common technique used to investigate and compare thermal events and determine kinetic parameters during the combustion, pyrolysis and gasification of solid raw materials, such as coal, wood, etc. [8–14]. Moreover, quantitative methods can be applied to TGA curves to obtain kinetic parameters of the thermal events. Miura and Silveston [15] showed the validity of the temperature-programmed reaction (TPR) technique for the analysis of noncatalytic gas–solid reactions. This technique appears to provide more kinetic information than what is obtainable from the same number of experiments performed at constant temperature. Kasaoka et al. [16] also stated that in an isothermal experiment, a tedious repetition of experimental runs is required to determine the kinetic parameters of the Arrhenius equation.

On the other hand, with the EU announcing that it intends to supply 20% of its overall energy needs from renewable sources by 2020, interest in biomass as a renewable source is growing [17]. This source of energy is considered carbon neutral because the carbon dioxide released during biomass utilization is recycled as an integral part of the carbon cycle. Co-combustion of biomass and coal has generated widespread interest because of the reduced emissions of gases such as CO_2, SO_2 and NO_x compared to those emitted by the combustion of coal [18]. The cofiring of biomass with coal is advantageous since biomass has higher volatile matter content and lower devolatilization temperature, which can aid the ignition and combustion characteristics of the blend [19]. Lai et al. [20] compared the combustion behaviour of lignocellulosic materials in CO_2/O_2 and N_2/O_2 atmospheres and calculated the kinetic parameters considering three parallel reactions during the combustion. A few studies have been published on the oxy-fuel combustion of coal and biomass blends [21–23], but reactivity and kinetic studies of biomass and coal/biomass blends under oxy-fuel combustion needs to be carried out.

The aim of the present work was to study the oxy-fuel combustion ($30\%O_2$–$70\%CO_2$) reactivity and kinetic behaviour of five coal chars and a biomass char obtained under $100\%N_2$ and $100\%CO_2$ atmospheres, as well as the coal/biomass char blends. For this purpose, the temperature-programmed reaction (TPR) technique at three different heating rates was used. Three mathematical models – the volumetric model (VM), the grain model (GM) and the random pore model (RPM) – were used to determine the kinetic parameters which best represent the oxy-fuel combustion characteristics of the coal char, biomass char and coal/biomass char blends under an oxygen–carbon dioxide atmosphere.

2. Experimental

2.1. Fuel samples

Five coals were used in this work: an anthracite (AC), a semi-anthracite (HVN) and three high-volatile bituminous coals (DAB, M6N and NZ). A type of biomass, torrefacted pine sawdust (TPIN), was also employed. The coal and biomass samples were ground, sieved and the resulting 75–150 μm size fraction was used for the devolatilization tests. The results of the proximate and ultimate analyses and high heating values of the coal and biomass samples are shown in Table 1.

The torrefaction of the biomass was carried out to improve its properties for pulverised systems [24]. To obtain the TPIN sample, a raw pine sawdust sample was ground and sieved to obtain a particle size fraction of 75–212 μm. Then, the torrefaction of this sample was performed using a vertical quartz reactor with a diameter of 20 mm and a length of 50 mm, where 10–15 g of biomass was kept at a temperature of 513 K for 1 h under a nitrogen flow rate of 50 NmL min^{-1}.

Table 1
Proximate and ultimate analyses and high heating value of the samples.

Sample	AC	HVN	DAB	M6N	NZ	PIN	TPIN
Origin	Spain	Spain	China	Mexico	New Zealand	Spain	Spain
Rank	an	sa	hvb	hvb	hvb		
Proximate analysis[a]							
Moisture (wt.%)	2.3	1.1	2.9	1.8	11.5	6.8	–
Ash (wt.%, db)	14.2	10.7	10.9	30.2	2.9	3.8	4.2
V.M. (wt.%, db)	3.6	9.2	28.8	30.6	47.9	79.8	75.5
F.C. (wt.%, db)[b]	82.2	80.1	60.3	39.2	49.2	16.4	20.3
Ultimate analysis (wt.%, daf)[a]							
C	94.7	91.7	81.9	76.7	67.5	45.9	51.2
H	1.6	3.5	5.0	6.2	5.3	6.1	5.7
N	1.0	1.9	1.1	1.6	1.0	0.7	0.9
S	0.7	1.6	1.2	1.2	0.2	0.0	0.0
O[b]	2.0	1.3	10.8	14.3	26.0	47.3	42.2
HHV (MJ/kg, db)	29.2	31.8	28.8	23.1	27.9	18.9	20.2

an: anthracite; sa: semi-anthracite; hvb: high-volatile bituminous coal.
db: dry basis; daf: dry and ash-free bases.
[a] The proximate analysis was conducted in a LECO TGA-601, and the ultimate analysis in a LECO CHNS-932.
[b] Calculated by difference.

2.2. Char preparation

The chars were prepared by devolatilizing the raw fuels in an electrically heated entrained flow reactor (40 mm internal diameter, 1400 mm length) in streams of $100\%N_2$ and $100\%CO_2$ (4.79 NL min^{-1}). The experimental device has been described elsewhere [25,26]. The devolatilization experiments were carried out at a reactor temperature of 1273 K and a particle residence time of 2.5 s. After the experiments, the chars were cooled down under a flow of nitrogen to room temperature and a water-cooled collecting probe was inserted into the reaction chamber from below to collect the char samples. The obtained coal and biomass char samples were used for the oxy-fuel combustion reactivity experiments. Moreover, two blends, AC + TPIN and DAB + TPIN, composed of 10wt% of biomass char TPIN-CO_2 and 90wt% of coal char AC-CO_2 or DAB-CO_2, respectively, were prepared. The components of the mixtures were blended in the adequate proportions and manually homogenized.

2.3. Oxy-fuel combustion reactivity tests of the chars

The reactivity tests were conducted in a thermobalance (Setaram TAG24) at atmospheric pressure. Approximately 5 mg of sample was placed in a crucible of 2 mm height with a circular base of 5 mm diameter. A small amount of sample and slow heating rates were used to avoid heat transfer limitations and to minimize mass transfer effects. A thermocouple was located close to the platinum basket to monitor the temperature and to close the oven control loop. In this work, all the experiments were performed under non-isothermal conditions from room temperature to 1273 K at three different heating rates: 2, 3 and 5 K min^{-1}. For the NZ samples, the heating rates used were: 1, 2 and 3 K min^{-1}. The total flow rate of the gas introduced into the thermobalance during the oxy-fuel combustion experiments was 50 NmL min^{-1}, the gas consisting of $30\%O_2$ and $70\%CO_2$. The char conversion, X, and the reaction rate, dX/dt, were calculated. The TG reactivity tests were firstly performed for the coal and biomass chars separately, and then for the coal/biomass char blends.

3. Kinetic models

A general kinetic expression for the overall reaction rate in gas–solid reactions is written as follows [27]:

$$dX/dt = k(P_g, T)f(X) \quad (1)$$

where k is the apparent combustion reaction rate, which includes the effect of temperature (T) and the effect of the reactive gas partial pressure (P_g), and $f(X)$ describes the changes in the physical or chemical properties of the sample during reaction. X represents the loss in mass fraction or mass conversion ratio, which can be calculated by the following relationship:

$$X = (m_0 - m_t)/(m_0 - m_f) \quad (2)$$

where m_0 is the initial mass of the char sample, m_t the mass of the char sample at time t and m_f the final mass of the char sample.

Assuming that the partial pressure of the reactive gas remains constant during the process, the apparent combustion reaction rate will be dependent on the temperature and can be expressed using the Arrhenius equation, as follows:

$$k = k_0 e^{-E/RT} \quad (3)$$

where k_0 and E are the pre-exponential factor and activation energy, respectively.

In this work, three nth-order models were applied to describe the reactivity of the chars studied: the volumetric model (VM), the grain model (GM) and the random pore model (RPM). These models give different formulations of the term $f(X)$, with X representing the degree of char conversion on a dry ash-free basis.

The VM assumes a homogeneous reaction throughout the particle and a linearly decreasing reaction surface area with conversion [28]. The overall reaction rate is expressed by:

$$dX/dt = k_{VM}(1 - X) \quad (4)$$

The GM or shrinking core model, proposed by Szekely and Evans [29], assumes that a porous particle consists of an assembly of uniform nonporous grains and that the reaction takes place on the surface of these grains. The space between the grains constitutes the porous network. The shrinking core behaviour applies to each of these grains during the reaction. In the regime of chemical kinetic control and, assuming the grains have a spherical shape, the overall reaction rate can be expressed as:

$$dX/dt = k_{GM}(1 - X)^{2/3} \quad (5)$$

This model predicts a monotonically decreasing reaction rate and surface area because the surface area of each grain is receding during the reaction.

The RPM model considers the overlapping of pore surfaces, which reduces the area available for reaction [30]. The basic equation for this model is:

$$dX/dt = k_{RPM}(1 - X)[1 - \psi \ln(1 - X)]^{1/2} \quad (6)$$

This model is able to predict a maximum value of reactivity as the reaction proceeds, as it considers the competing effects of pore growth during the initial stages of combustion and the destruction of the pores due to the coalescence of neighbouring pores during the reaction. The RPM model employs two parameters, the apparent combustion reaction rate constant, k_{RPM}, and ψ, which is related to the pore structure of the unreacted sample, although Miura and Silveston [15] suggested that the ψ parameter should be considered as an adjustable parameter.

The non-isothermal thermogravimetric method or temperature-programmed reaction (TPR) technique involves heating the samples at a constant rate, a. The temperature, T, is related to time, t, by:

$$T = T_0 + at \quad (7)$$

where T_0 is the temperature at which heating is started, which can be set equal to 0 provided that T_0 is low enough for the reaction rate to be practically zero when heating is initiated.

By means of Eq. (7), Eq. (4) can be integrated to give:

$$X = 1 - \exp\left(-\frac{k_0 E}{aR} p(u)\right) \quad (8)$$

where

$$p(u) = \frac{e^{-u}}{u} - \int_X^\infty \frac{e^{-u}}{u} du \quad (9)$$

$$u = E/RT \quad (10)$$

From the literature, several proposed approximations for $p(u)$ can be found. In this study the one employed has been [15,31,32]:

$$p(u) = e^{-u}/u^2 \quad (11)$$

This approximation is valid for $u > 10$, which is fulfilled by these fuels when burned in the studied oxy-fuel atmosphere. Eq. (8) can then be written as:

$$X = 1 - \exp\left[-\frac{RT^2}{aE} k_0 e^{\frac{-E}{RT}}\right] \quad (12)$$

Similarly, Eqs. (5) and (6) can be integrated with the above approximation, to give Eqs. (13) and (14) respectively:

$$X = 1 - \left[1 - \frac{RT^2}{3aE} k_0 e^{\frac{-E}{RT}}\right]^3 \quad (13)$$

$$X = 1 - \exp\left[-\frac{RT^2}{aE} k_0 e^{\frac{-E}{RT}}\left(1 + \frac{\psi}{4}\left(\frac{RT^2}{aE}\right) k_0 e^{\frac{-E}{RT}}\right)\right] \quad (14)$$

Eqs. (12)–(14) can be utilized to determine k_0 and E values from X experimental data sets by employing nonlinear least-squares fitting methods. According to Miura and Silveston [15], the determination of the kinetic parameters from a single TPR run may lead to unreliable rate parameters and, furthermore, the fitting of data by a model may not validate the model if just one TPR run is used. These authors claimed that at least three TPR runs at different heating rates are required to estimate reliable parameters and accurate activation energies.

In this study the kinetic parameters were determined from three TPR runs, each one performed at a different heating rate. The nonlinear least-squares method was employed to fit the experimental data of $1-X$ vs. temperature, T, to the three models by means of Eqs. (12)–(14), and to estimate the k_0 and E values which minimize the objective function, OF:

$$OF = \sum_{i=1,N} \left[(1 - X)_{exp,i} - (1 - X)_{calc,i}\right]^2 \quad (15)$$

where $(1-X)_{exp,i}$ is the experimental point corresponding to the ith temperature, T_i, $(1-X)_{calc,i}$ is the value calculated at T_i, and N is the number of data points.

According to Várhegyi [33], the method of least-squares can work better in non-isothermal kinetics than other methods requiring simpler computer programming or less computational time, since this technique aims directly at the description of the experimental data in a wide range of experimental conditions.

To assess the quality of the fit and verify the capacity of the kinetic models to describe the degree of char conversion, X (or $1-X$), the deviation (DEV) between the experimental and calculated curves was obtained using the following expression:

$$\mathrm{DEV}(1-X)(\%) = 100\left[\sum_{i=1,N}\left((1-X)_{\mathrm{exp},i} - (1-X)_{\mathrm{calc},i}\right)^2/N\right]^{1/2}/\max(1-X)_{\mathrm{exp}} \quad (16)$$

where $(1-X)_{\mathrm{exp},i}$ and $(1-X)_{\mathrm{calc},i}$ represent the experimental and calculated data of $1-X$, N is the number of data points, and $\max(1-X)_{\mathrm{exp}}$ is the highest absolute value of the experimental curve. The best fitting kinetic parameters and model were chosen from the highest R^2 value obtained from the results which proved to be statistically significant, together with the lowest value of DEV $(1-X)$.

4. Results and discussion

4.1. Kinetic parameters

Table 2 shows the kinetic parameters (E, k_0 and ψ) determined from the data obtained at three heating rates (1, 2 and 3 K min^{-1} for the NZ coal char and 2, 3 and 5 K min^{-1} for the rest of samples) together with the coefficients of determination, R^2, for each model and sample. R^2 shows the variation in the dependent variable, $1-X$, which is explained by the model. Table 2 also presents the statistically significant model fittings.

The RPM model fits the experimental data better than the other two models for coal chars AC-N_2 ($R^2 = 0.999$), AC-CO_2 ($R^2 = 0.999$), HVN-N_2 ($R^2 = 0.998$) and HVN-CO_2 ($R^2 = 0.998$), since it displayed a significant fit and presented the highest R^2 value (Table 2). In the case of the DAB, M6N and NZ char samples, as well as the DAB + TPIN blend, the ψ value obtained from the RPM model is a meaningless negative value, which indicates that the best fit to the experimental data is obtained with a ψ value of zero. For the TPIN samples, the ψ value obtained from the RPM model is close to zero and the fits were not significant. When the ψ value is close to zero, the RPM model predicts a nearly constant decrease in reactivity with conversion, as does the VM model. Therefore, it can be concluded that the model which best describes the reactivity of the DAB-N_2 ($R^2 = 0.998$), DAB-CO_2 ($R^2 = 0.998$), M6N-N_2 ($R^2 = 0.995$), M6N-CO_2 ($R^2 = 0.996$), NZ-N_2 ($R^2 = 0.998$), NZ-CO_2 ($R^2 = 0.996$), TPIN–N_2 ($R^2 = 0.998$) and TPIN–CO_2 ($R^2 = 0.996$) char samples, as well as the DAB + TPIN ($R^2 = 0.999$) blend, was the VM model (Table 2). On the other hand, the reactivity of the AC + TPIN blend has not been satisfactorily described by none of the considered models, since the oxy-fuel combustion process took place in two stages and it was not then possible to obtain a simple set of kinetic parameters for this sample.

The RPM model predicts a maximum in reaction rate as the reaction proceeds, as pore overlapping is considered. Pore shape is assumed cylindrical and supposed to grow radially while reaction proceeds, instead of keeping initial volume. Initially, the cylinder growth causes an increase in total reaction surface, which means higher reaction rate. Finally, reaction progress brings about a neighbouring pore intersection. Due to pore overlapping, the reaction surface area is lower and, consequently, the reaction rate decreases [34]. Conversely, the VM and GM models cannot describe a maximum in reaction rate but predict a constant decrease in the reaction rate with conversion. Therefore, from the results of the model fits it can be deduced that, in the case of the high rank coals used in this work, AC and HVN, the char reaction rate presents a maximum value during combustion. However, for the bituminous coals (DAB, M6N and NZ), the biomass sample (TPIN) and the coal/biomass blend (DAB + TPIN) the char reaction rate decreases linearly during the whole oxy-fuel combustion process under the conditions of the present study.

Figs. 1 and 2 show, for the three heating rates, the experimental $1-X$ data and the $1-X$ curves calculated (Eqs. (12)–(14)) using the parameters obtained from the data at the three heating rates for the meaningful and statistically significant models (Table 2). As example, the curves for the AC, HVN and DAB char samples obtained both in N_2 and CO_2 are shown in Fig. 1 and the curves for the biomass char, TPIN, and the blends, AC + TPIN and DAB + TPIN, are shown in Fig. 2. To quantify the errors produced by the kinetic models in predicting the values of conversion, the deviation (DEV) between the experimental and calculated $1-X$ curves was obtained using the Eq. (16). The results obtained from the significant models for all the char samples and the blend are summarised in Table 3. In accordance with the previous results (Table 2), the lowest deviation from the calculated values of the conversion rates was obtained using the RPM model for all the AC and HVN char samples and the VM model for all the DAB, M6N, NZ, TPIN and DAB + TPIN samples (Table 3). Saravanan et al. [4] and Gil et al. [35] have also studied the reactivity of coal chars during oxy-fuel combustion using the

Table 2
Kinetic parameters of the chars during oxy-fuel combustion (30%O_2–70%CO_2) determined with the TPR technique at three heating rates for VM, GM and RPM models.

Char	Volumetric model (VM)			Grain model (GM)			Random pore model (RPM)			
	E (kJ mol^{-1})	k_0 (s^{-1})	R^2	E (kJ mol^{-1})	k_0 (s^{-1})	R^2	E (kJ mol^{-1})	k_0 (s^{-1})	ψ	R^2
AC-N_2	260	4.45E+13	0.977[a]	194	1.83E+09	0.970[a]	137	1.43E+04	2955	0.999[a]
AC-CO_2	234	7.96E+11	0.987[a]	169	3.54E+07	0.980[a]	140	5.88E+04	490	0.999[a]
HVN-N_2	184	1.08E+09	0.995[a]	149	4.13E+06	0.994[a]	128	6.88E+04	19.1	0.998[a]
HVN-CO_2	190	2.75E+09	0.996[a]	157	1.25E+07	0.995[a]	116	7.72E+03	37.1	0.998[a]
DAB-N_2	146	8.10E+06	0.998[a]	113	2.95E+04	0.992[a]	152	2.03E+07	−0.2	0.999[a]
DAB-CO_2	152	1.82E+07	0.998[a]	117	5.27E+04	0.989[a]	160	7.25E+07	−0.2	0.999[a]
M6N-N_2	171	1.47E+09	0.995[a]	106	1.83E+04	0.970[a]	175	2.77E+09	−0.2	0.996[a]
M6N-CO_2	166	5.73E+08	0.996[a]	110	3.48E+04	0.973[a]	171	1.57E+09	−0.2	0.997[a]
NZ-N_2	131	1.13E+07	0.998[a]	76	2.81E+02	0.954[a]	134	2.17E+07	−0.2	0.999[a]
NZ-CO_2	141	1.37E+08	0.996[a]	63	2.78E+01	0.908[a]	142	1.60E+08	−0.1	0.996[a]
TPIN-N_2	118	9.60E+05	0.998[a]	96	1.31E+04	0.996[a]	112	2.68E+05	0.4	0.998
TPIN-CO_2	129	6.29E+06	0.996[a]	102	3.72E+04	0.992[a]	128	5.42E+06	0.03	0.996
DAB + TPIN	136	1.42E+06	0.999[a]	102	5.03E+03	0.991[a]	141	3.73E+06	−0.2	0.999[a]

[a] Statistically significant.

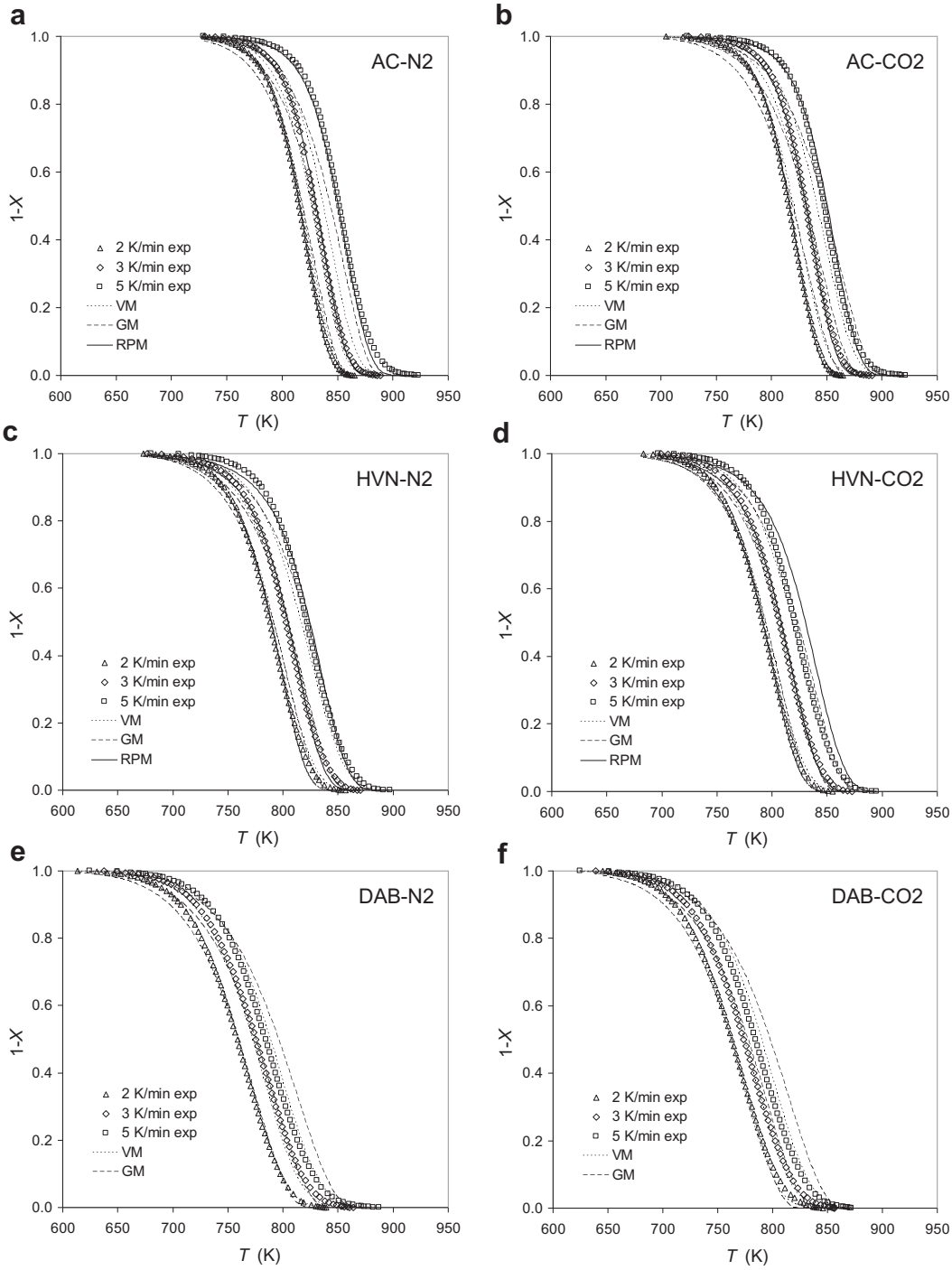

Fig. 1. Experimental conversion curves for AC-N_2 (a), AC-CO_2 (b), HVN-N_2 (c), HVN-CO_2 (d), DAB-N_2 (e) and DAB-CO_2 (f) coal chars during oxy-fuel combustion (30%O_2–70%CO_2) and those calculated with three nth-order reaction models (VM, GM and RPM) using parameters determined from heating rates at 2, 3 and 5 K min^{-1}.

random pore model. Gil et al. [35] found that RPM model was the best for describing the reactivity of coal chars.

Table 4 summarizes the activation energy values obtained for the char samples used in the present study, together with data from previous works on oxy-fuel combustion. In the present work, using the models of best fit, the activation energy for the coal chars under 30%O_2–70%CO_2 atmosphere was 116–171 kJ mol^{-1} (Table 2). In a previous study, Gil et al. [35] had calculated activation energy values for coal chars under oxy-fuel atmosphere with 30%O_2 of 117–127 kJ mol^{-1}. Niu et al. [5] obtained activation energy values for pulverized coals in an oxy-fuel atmosphere (20% O_2) that ranged between 109 and 248 kJ mol^{-1}. Similarly, Liu [36] achieved activation energy values for coal chars in an oxy-fuel atmosphere (10% O_2) which ranged between 115 and 147 kJ mol^{-1}. On the other hand, the activation energy for the TPIN biomass char under 30%O_2–70%CO_2 atmosphere was 118–129 kJ mol^{-1} (Table 2). In the case of the DAB + TPIN char blend, a value of the activation energy of 136 kJ mol^{-1} was obtained, which is an intermediate value between those of the individual components of the blend.

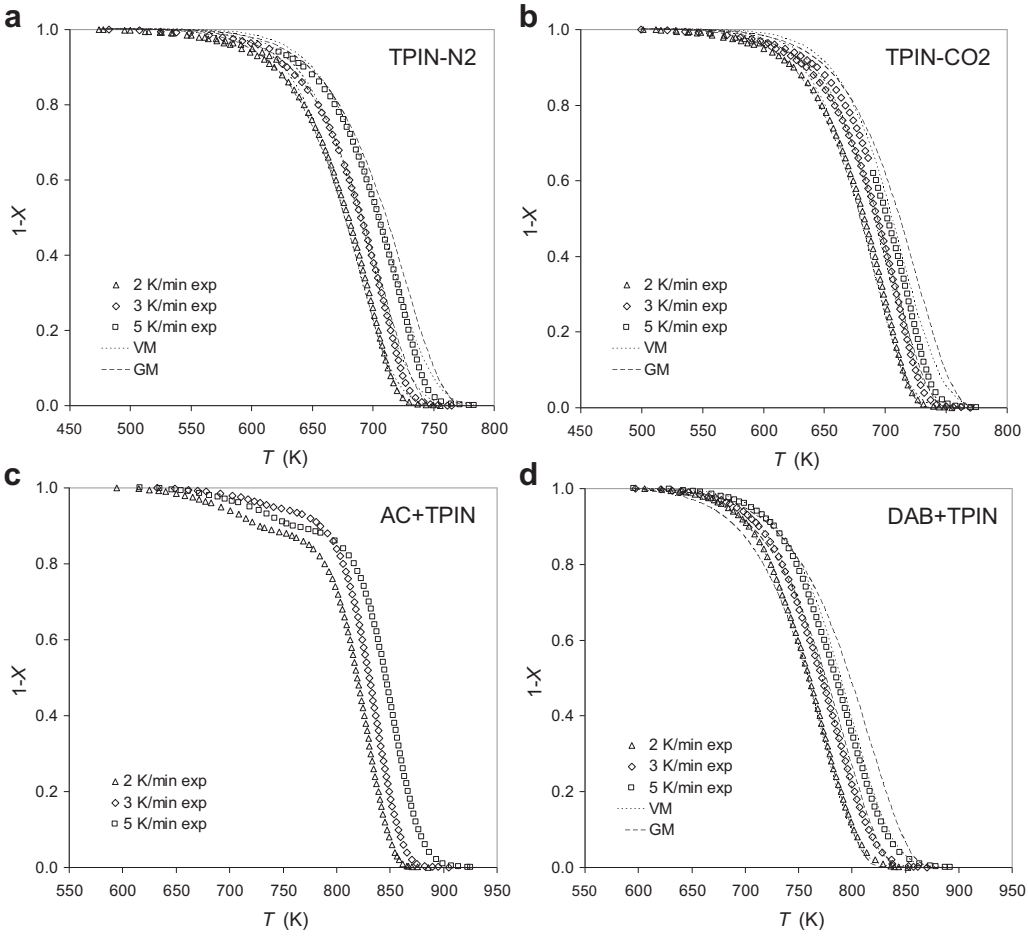

Fig. 2. Experimental conversion curves for TPIN-N_2 (a), TPIN-CO_2 (b), AC + TPIN (c) and DAB + TPIN (d) samples during oxy-fuel combustion (30%O_2–70%CO_2) and those calculated with three nth-order reaction models (VM, GM and RPM) using parameters determined from heating rates at 2, 3 and 5 K min^{-1}.

Table 2 shows that the activation energy values and pre-exponential factors for the two devolatilization atmospheres are very similar. From these data, it can be concluded that no differences in the kinetic parameters of oxy-fuel combustion under 30% O_2–70%CO_2 atmosphere are produced by using 100%N_2 and 100% CO_2 devolatilization atmospheres.

Wang et al. [7] studied the devolatilization of coal samples in 100%N_2 and 100%CO_2 by means of TGA and found that the TG and DTG curves in both atmospheres were almost superposing in the low temperature zone (up to ~1073 K), concluding that the pyrolysis reactivity is highly similar in N_2 and CO_2. At higher temperatures, however, in CO_2 atmosphere char-CO_2 gasification was observed, which is also in accordance with the results obtained by Rathnam et al. [37]. At the temperature used in the present study for obtaining the chars (1273 K), gasification process could therefore occur at some extent, which would affect the char characteristics. The additional char-CO_2 reaction could then increase the reactivity of the coal char obtained under CO_2 atmosphere. Nevertheless, the endothermic effect of char-CO_2 reaction could also play a negative role in the enhancement of the reactivity through reducing the coal particle temperature. Wang et al. [7] pointed out the necessity of studies to clarify the circumstances in which those opposite effects will preponderate the other. These authors concluded that char reactivity (in 21%O_2/79% CO_2) prepared in CO_2 is almost equivalent to that prepared in N_2 in a study where coal chars were obtained at low temperature (~1073 K) in a tubular furnace. Borrego et al. [38] studied the characteristics of the chars from various biomass materials generated at a high heating rate in a drop tube furnace (DTF) under N_2 and CO_2 atmospheres and they found that similar morphology, optical texture and specific surface area were shown by the biomass chars generated under both atmospheres.

The reaction rate of a char under an oxygen atmosphere is usually very high and in the present study the reactivity was

Table 3
Deviation (%) between the experimental and calculated conversion (1−*X*) data.

Char	DEV (1−*X*) (%)		
	VM	GM	RPM
AC-N_2	6.39	7.94	1.24
AC-CO_2	4.36	5.40	1.08
HVN-N_2	2.80	3.07	1.57
HVN-CO_2	2.30	2.72	1.41
DAB-N_2	1.53	3.45	–
DAB-CO_2	1.63	4.09	–
M6N-N_2	2.89	6.73	–
M6N-CO_2	2.52	6.11	–
NZ-N_2	1.63	8.01	–
NZ-CO_2	2.67	11.84	–
TPIN-N_2	1.82	2.16	–
TPIN-CO_2	2.30	3.18	–
DAB + TPIN	1.08	3.50	–

Table 4
Comparison of the activation energy values obtained in the present work and in previous oxy-fuel combustion studies.

Sample	Atmosphere	E (kJ mol^{-1})	Model	Reference
Coal chars	30%O_2–70%CO_2	116–171 kJ mol^{-1}	nth-order gas–solid models	Present study
Coal chars	30%O_2–70%CO_2	117–127 kJ mol^{-1}	nth-order gas–solid models	Gil et al. (2012) [35]
Pulverized coals	20%O_2–80%CO_2	109–248 kJ mol^{-1}	Coats–Redfern method	Niu et al. (2009) [5]
Coal chars	10%O_2–90%CO_2	115–147 kJ mol^{-1}	Isoconversional model-free methods	Liu (2009) [36]
Biomass chars	30%O_2–70%CO_2	118–129 kJ mol^{-1}	nth-order gas–solid models	Present study
Coal/biomass char blend	30%O_2–70%CO_2	136 kJ mol^{-1}	nth-order gas–solid models	Present study

measured in a high oxygen content (30%) atmosphere, which may have concealed possible differences in reactivity between both chars and may explain why no differences were observed between the chars obtained under N_2 or CO_2. Várhegyi et al. [39] studied the coal char kinetics in O_2/Ar and O_2/CO_2 atmospheres by non-isothermal thermogravimetry and concluded that the char reaction rate was proportional to the O_2 concentration of the ambient gas and was not influenced by the presence of high amounts of CO_2 since char-CO_2 reactions have much lower rates than char oxidation. Niu et al. [6] confirmed that for O_2 concentrations of 30–40% in oxy-fuel atmospheres, the reaction process is mainly dominated by the diffusion of the O_2 to the surface of the solid coal and the effect of the carrier gas is not very important.

The relative reactivity of O_2 with coal is much greater than CO_2 with coal, which suggests that the char oxidation in the present work was predominantly due to oxygen and a possible gasification reaction due to CO_2 during the reactivity experiments would have not existed under these conditions. It was also noted by Saravanan et al. [4] in their study about the reactivity of coal chars during oxy-fuel combustion under different concentrations of CO_2, who pointed out that the effect of CO_2 concentration on the char oxidation rate in the presence of oxygen might be only due to the bulk resistance offered by CO_2 during the char–oxygen reaction, although this fact would require more additional studies.

4.2. Comparison of isothermal and non-isothermal reactivity tests

In a previous study [35], a kinetic analysis of the oxy-fuel combustion of the HVN-N_2 and HVN-CO_2 char samples had been carried out by the authors at constant temperature. The results obtained using the TPR technique were then compared with those obtained from experiments performed at constant temperature. From the isothermal oxy-fuel combustion experiments, it was concluded that the best model for describing the behaviour of both HVN samples was RPM and the parameters estimated using this model by both techniques were therefore compared. Following the indications from Miura and Silveston [15], the values of $k_0e^{-E/RT}$ were calculated using the kinetic parameters in Table 2. They were plotted on an Arrhenius diagram (Fig. 3) and compared with those obtained in the isothermal experiments [34]. A good agreement can be observed between the $k_0e^{-E/RT}$ values estimated by both methods, indicating that the TPR technique provides reliable kinetics parameters when data from the three heating rates are used.

4.3. Interactions between the components of the coal/biomass blends

Fig. 4 shows the experimental dX/dt curves for the coal/biomass blends (AC + TPIN and DAB + TPIN) under the oxy-fuel combustion atmosphere studied, together with the theoretical reaction rate curves calculated according to the additive rule from those of the individual components. The dX/dt curves for the individual components of the blends were also included. The theoretical and experimental dX/dt curves of the coal/biomass blends were compared to find out whether the components of the blends interacted during the oxy-fuel combustion process. As mentioned above, the theoretical dX/dt curves of the blends were calculated according to the additive rule of blends, i.e.:

$$(dX/dt)_{blend} = x_1(dX/dt)_{coal} + x_2(dX/dt)_{biomass} \quad (17)$$

where $(dX/dt)_{coal}$ and $(dX/dt)_{biomass}$ are the reaction rate of the individual fuels, and x_1 and x_2 are the proportions of coal and biomass in the blend, respectively.

Fig. 4a shows that when the AC high rank coal and the TPIN biomass are co-combusted under oxy-fuel atmosphere, two independent peaks are observed in the DTG curves of the blend. Furthermore, no significant deviations are appreciated between the experimental and theoretical dX/dt curves in the case of the AC + TPIN char blend at the three heating rates. This suggests that no significant interactions occur during char oxy-fuel combustion with 30% of oxygen, reflecting the additive behaviour of blend components during the combustion process. This means that it should be possible to predict the experimental reactivity curve of the blend, on the basis of the experimental reactivity curves of each individual component and their percentages in the blend. The absence of synergetic effects during the char oxy-fuel combustion

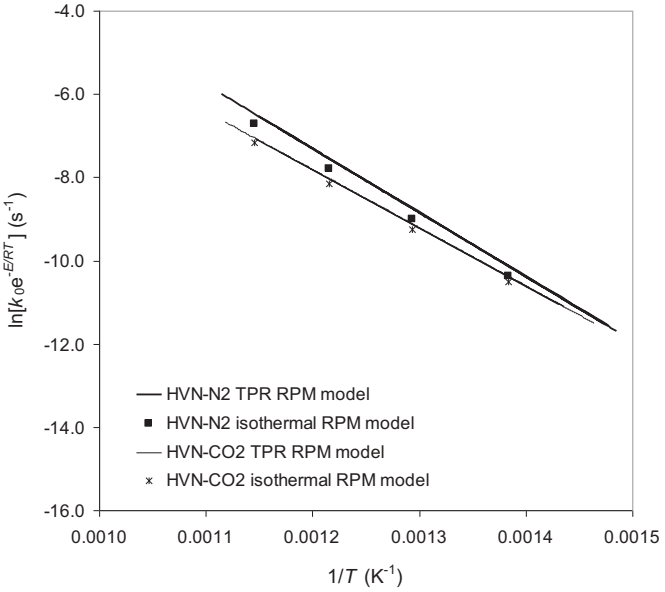

Fig. 3. Comparison between the apparent oxy-fuel combustion reaction rates for HVN-N_2 and HVN-CO_2 obtained from TPR data (at heating rates of 2, 3 and 5 K min^{-1}) and data obtained from isothermal experiments [35].

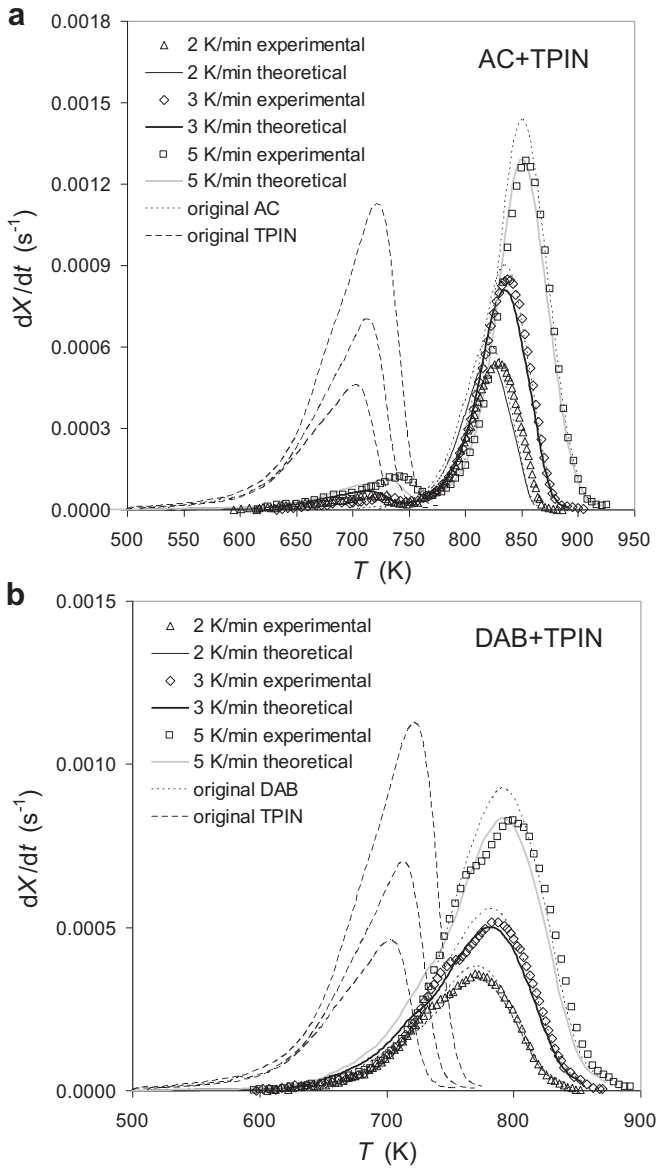

Fig. 4. Comparison between the experimental and theoretical (according to the additive rule from those of the individual components) reaction rate curves for the AC + TPIN (a) and DAB + TPIN (b) blends during non-isothermal (2, 3 and 5 K min^{-1}) oxy-fuel combustion.

process, indicates that the oxy-fuel combustion reactions of the coal char did not seem to be influenced by the presence of 10wt% of biomass char. Each component of the mixture behaved independently and did not interact with the other material.

When the experimental and theoretical dX/dt curves for the DAB + TPIN blend are compared (Fig. 4b), it can be seen that dX/dt curve of the blend closely resembled that of the coal char sample. This indicates that the addition of the TPIN biomass char to the DAB coal char, when added in a proportion of 10%, has very little effect on the behaviour of the individual coal char.

5. Conclusions

The chars from five coals (AC, HVN, DAB, M6N and NZ) and a torrefacted biomass (TPIN) obtained in N_2 or CO_2 atmospheres, as well as two coal/biomass blends (AC + TPIN and DAB + TPIN), were subjected to oxy-fuel combustion in a thermobalance to study their thermal reactivity. The temperature-programmed reaction technique employed in the analysis of noncatalytic gas–solid reactions was applied at three heating rates to estimate the kinetic parameters which best described the reactive behaviour of the chars during oxy-fuel combustion. The best model for describing the char oxy-fuel combustion of the AC and HVN high rank coals was found to be the RPM model, whereas the VM model better described the char reactivity of the DAB, M6N and NZ bituminous coals, the TPIN biomass and the DAB + TPIN blend under oxy-fuel conditions. The kinetic parameters showed that no differences in reactivity under a typical oxy-fuel combustion atmosphere (30%O_2–70%CO_2) exist between chars obtained under CO_2 and N_2. No significant interactions were detected between the components of the coals-biomass blends chars (90-10wt%) with 30% of oxygen.

Acknowledgements

This work was carried out with financial support from the Spanish MICINN (Project PS-120000-2005-2) co-financed by the European Regional Development Fund (ERDF). M.V.G. and L.A. acknowledge funding from the CSIC JAE-Pre and CSIC JAE-Doc programs, respectively, co-financed by the European Social Fund. J.R. acknowledges funding from the Government of the Principado de Asturias (Severo Ochoa program).

References

[1] Deutch J, Moniz J. The future of coal: options for a carbon-constrained world. Massachusetts Institute of Technology Interdisciplinary Study; 2007.
[2] Hu Y, Yan J. Characterization of flue gas in oxy-coal combustion processes for CO_2 capture. Appl Energy 2012;90:113–21.
[3] Liu H, Zailani R, Gibbs BM. Comparisons of pulverized coal combustion in air and in mixtures of O_2/CO_2. Fuel 2005;84:833–40.
[4] Saravanan V, Shivakumar R, Jayanti S, Ramakrishna Seetharamu S. Evaluation of the effect of the concentration of CO_2 on the overall reactivity of drop tube furnace derived Indian sub-bituminous coal chars during CO_2/O_2 combustion. Ind Eng Chem Res 2011;50:12865–71.
[5] Niu SL, Lu CM, Han KH, Zhao JL. Thermogravimetric analysis of combustion characteristics and kinetics parameters of pulverized coals in oxy-fuel atmosphere. J Therm Anal Calorim 2009;98:267–74.
[6] Niu SL, Han KH, Lu CM. Characteristic of coal combustion in oxygen/carbon dioxide atmosphere and nitric oxide release during this process. Energy Convers Manag 2011;52:532–7.
[7] Wang C, Zhang X, Liu Y, Che D. Pyrolysis and combustion characteristics of coals in oxyfuel combustion. Appl Energy 2012;97:264–73.
[8] Lai ZY, Ma XQ, Tang YT, Lin H. A study on municipal solid waste (MSW) combustion in N_2/O_2 and CO_2/O_2 atmosphere from the perspective of TGA. Energy 2011;36:819–24.
[9] Fermoso J, Arias B, Pevida C, Plaza MG, Rubiera F, Pis JJ. Kinetic models comparison for steam gasification of different nature fuel chars. J Therm Anal Calorim 2008;91:779–86.
[10] Skodras G, Grammelis P, Basinas P. Pyrolysis and combustion behaviour of coal-MBM blends. Bioresour Technol 2007;98:1–8.
[11] Wang C, Wang F, Yang Q, Liang R. Thermogravimetric studies of the behavior of wheat straw with added coal during combustion. Biomass Bioenergy 2009; 33:50–6.
[12] Arenillas A, Rubiera F, Pis JJ, Cuest MJ, Iglesias MJ, Jiménez A, et al. Thermal behaviour during the pyrolysis of low rank perhydrous coals. J Anal Appl Pyrol 2003;68–69:371–85.
[13] Yu YH, Kim SD, Lee JM, Lee KH. Kinetic studies of dehydration, pyrolysis and combustion of paper sludge. Energy 2002;27:457–69.
[14] Park SW, Jang CH. Effects of pyrolysis temperature on changes in fuel characteristics of biomass char. Energy 2012;39:187–95.
[15] Miura K, Silveston PL. Analysis of gas-solid reactions by use of a temperature-programmed reaction technique. Energy Fuels 1989;3:243–9.
[16] Kasaoka S, Sakata Y, Shimada M, Matsutomi T. A new kinetic model for temperature programmed thermogravimetry and its applications to the gasification of coal chars with steam and carbon dioxide. J Chem Eng Jpn 1985;18:426–32.
[17] European Commission Directive 2009/28/EC. Off J Eur Union L 2009;140(16):162.
[18] Kazanc F, Khatami R, Crnkovic PM, Levendis YA. Emissions of NO_x and SO_2 from coals of various ranks, bagasse, and coal-bagasse blends burning in O_2/N_2 and O_2/CO_2 environments. Energy Fuels 2011;25:2850–61.
[19] Sami M, Annamalai K, Wooldridge M. Co-firing of coal and biomass fuel blends. Prog Energy Combust Sci 2001;27:171–214.

[20] Lai ZY, Ma XQ, Tang YT, Lin H, Chen Y. Thermogravimetric analyses of combustion of lignocellulosic materials in N_2/O_2 and CO_2/O_2 atmospheres. Bioresour Technol 2012;107:444–50.
[21] Arias B, Pevida C, Rubiera F, Pis JJ. Effect of biomass blending on coal ignition and burnout during oxy-fuel combustion. Fuel 2008;87:2753–9.
[22] Gil MV, Riaza J, Álvarez L, Pevida C, Pis JJ, Rubiera F. A study of oxy-coal combustion with steam addition and biomass blending by thermogravimetric analysis. J Therm Anal Calorim 2012;109:49–55.
[23] Haykiri-Acma H, Turan AZ, Yaman S, Kucukbayrak S. Controlling the excess heat from oxy-combustion of coal by blending with biomass. Fuel Process Technol 2010;91:1569–75.
[24] Arias B, Pevida C, Fermoso J, Plaza MG, Rubiera F, Pis JJ. Influence of torrefaction on the grindability and reactivity of woody biomass. Fuel Process Technol 2008;89:169–75.
[25] Álvarez L, Gharebaghi M, Pourkashanian M, Willians A, Riaza J, Pevida C, et al. CFD modelling of oxy-coal combustion in an entrained flow reactor. Fuel Process Technol 2011;92:1489–97.
[26] Álvarez L, Riaza J, Gil MV, Pevida C, Pis JJ, Rubiera F. NO emissions in oxy-coal combustion with the addition of steam in an entrained flow reactor. Greenhouse Gas Sci Technol 2011;1:180–90.
[27] Lu GQ, Do DD. Comparison of structural models for high-ash char gasification. Carbon 1994;32:247–63.
[28] Ishida M, Wen CY. Comparison of zone-reaction model and unreacted-core shrinking model in solid-gas reactions – I Isothermal analysis. Chem Eng Sci 1971;26:1031–41.
[29] Szekely J, Evans JW. A structural model for gas-solid reactions with a moving boundary. Chem Eng Sci 1970;25:1091–107.
[30] Bhatia SK, Perlmutter DD. A random pore model for fluid-solid reactions: I. Isothermal, kinetic control. AIChE J 1980;26:379–86.
[31] Leroy V, Cancellieri D, Leoni E, Rossi JL. Kinetic study of forest fuels by TGA: model-free kinetic approach for the prediction of phenomena. Thermochim Acta 2010;497:1–6.
[32] Miura K, Nakagawa H, Nakai S, Kajitani S. Analysis of gasification reaction of coke formed using a miniature tubing-bomb reactor and a pressurized drop tube furnace at high pressure and high temperature. Chem Eng Sci 2004;59:5261–8.
[33] Várhegyi G. Aims and methods in non-isothermal reaction kinetics. J Anal Appl Pyrol 2007;79:278–88.
[34] Aranda A, Murillo R, García T, Callén MS, Mastral AM. Steam activation of tyre pyrolytic carbon black: kinetic study in a thermobalance. Chem Eng J 2007; 126:79–85.
[35] Gil MV, Riaza J, Álvarez L, Pevida C, Pis JJ, Rubiera F. Oxy-fuel combustion kinetics and morphology of coal chars obtained in N_2 and CO_2 atmospheres in an entrained flow reactor. Appl Energy 2012;91:67–74.
[36] Liu H. Combustion of coal chars in O_2/CO_2 and O_2/N_2 mixtures: a comparative study with non-isothermal thermogravimetric analyzer (TGA) tests. Energy Fuels 2009;23:4278–85.
[37] Rathnam RK, Elliott LK, Wall TF, Liu Y, Moghtaderi B. Differences in reactivity of pulverised coal in air (O_2/N_2) and oxy-fuel (O_2/CO_2) conditions. Fuel Process Technol 2009;90:797–802.
[38] Borrego AG, Garavaglia L, Kalkreuth WD. Characteristics of high heating rate biomass chars prepared under N_2 and CO_2 atmospheres. Int J Coal Geol 2009; 77:409–15.
[39] Várhegyi G, Szabó P, Jakab E, Till F. Mathematical modeling of char reactivity in Ar-O_2 and CO_2-O_2 mixtures. Energy Fuels 1996;10:1208–14.

5. Ignición y combustión de carbón en atmósferas de oxicombustión en reactor de flujo en arrastre

Durante la oxicombustión el carbón se quema con una mezcla de oxígeno y gases de combustión (CO_2 y H_2O) recirculados, siendo la concentración de oxígeno mayor que la del aire. El objetivo de este trabajo ha consistido en la evaluación del efecto de la atmósfera de combustión ($O_2/CO_2/H_2O$ y aire como referencia) sobre las propiedades de ignición, combustibilidad y emisiones producidas en carbones de distinto rango. Para ello, se han realizado experimentos de ignición y combustión en el reactor de flujo en arrastre descrito en el Apartado 2.3. En el presente Capítulo se presentan los resultados correspondientes a ensayos de ignición y combustión de una semiantracita y un carbón bituminoso alto en volátiles en el reactor de flujo en arrastre, en atmósferas de aire y de oxicombustión con reciclo húmedo y seco.

Los gases de salida del proceso de oxicombustión están compuestos por CO_2, vapor de agua y hasta un 5 % de oxígeno como componentes mayoritarios. En un proceso a escala real los gases de combustión se someten a una etapa de control y retención de las partículas de cenizas, procesos para la desulfuración y desnitrificación de los humos así como la condensación del vapor de agua. Durante la oxicombustión la toma de gases para la recirculación de los humos de salida puede realizarse en distintos puntos del proceso, variando consecuentemente la proporción de sustancias recirculadas como SO_x y NO_x así como la proporción de vapor de agua en el reciclo.

La recirculación de los humos puede tener lugar tras la condensación del vapor siendo entonces el reciclo seco aunque todavía con una cierta cantidad de vapor de agua. En otros casos el reciclo puede realizarse previamente a la condensación del vapor, reciclo húmedo. El hecho de cómo afectará este vapor a los procesos de ignición y combustión que experimenta el carbón es un aspecto que ha sido poco investigado hasta la fecha. La proporción de vapor presente en un reciclo a nivel industrial dependerá de las características de diseño de la planta así como del combustible empleado; se trata de un parámetro que presenta gran incertidumbre hasta la fecha, ya que no existen instalaciones de oxicombustión a escala comercial.

En este trabajo inicialmente se plantearon reciclos con unos contenidos de 0, 5 y 10 % de vapor de agua en la corriente oxidante. Dada la baja influencia que reportó la presencia de estas concentraciones de vapor se aumentó la proporción de vapor de agua introducida en la

corriente de los gases reaccionantes hasta un 20%. Este valor de concentración es muy similar al obtenido en algunos estudios que simularon la oxicombustión de mezclas de carbón y biomasa [Jurado, 2013], así como de ensayos realizados a escala de planta piloto [Beisheima, 2013].

En los dos artículos que se incluyen en este Capítulo se ha estudiado el efecto que ejerce la adición de vapor de agua, a los gases de entrada al reactor de flujo en arrastre, en lo que respecta a la ignición de los carbones empleados, el grado de quemado obtenido y las emisiones gaseosas producidas durante la oxicombustión.

5.1 Ignición y Oxicombustión

La ignición de un combustible es importante dado que influye en la estabilidad, forma y longitud de la llama. En la práctica, el comportamiento en la ignición de los combustibles sólidos es crucial para determinar la posición óptima de los quemadores en las calderas de carbón pulverizado. El aumento de la proporción de reciclo en los procesos de oxicombustión produce un empeoramiento de la ignición [Strömberg, 2009]. La geometría de los quemadores está diseñada para producir turbulencia tanto en el interior de la llama como en la zona perimetral. Según lo observado por Khare et al. [Khare, 2008] debido a la recirculación de CO_2 en oxicombustión, cuando un quemador trabaja con flujos bajos y por tanto menores velocidades, existe la posibilidad de que las llamas, que son normalmente del tipo 2, pasen a ser llamas de tipo 0. Ello implicaría un desplazamiento de la turbulencia hacia posiciones más alejadas del quemador y sin reflujo interno. Este efecto se puede evitar mediante un diseño adecuado que asegure la turbulencia y que restablezca las llamas de tipo 2, comúnmente empleadas en las aplicaciones industriales.

Se ha observado en experimentos de oxicombustión a escala de planta piloto, un empeoramiento de la ignición por lo que se ha tenido que ajustar el grado de turbulencia y la concentración de oxígeno en los quemadores para tener una ignición adecuada y una llama estable. Por esta razón es necesario un estudio detallado del fenómeno de ignición en atmósferas de oxicombustión. Taniguchi et al. [Taniguchi, 2011a] desarrollaron un modelo para predecir la forma de la llama y la velocidad de propagación del frente de llama en aire. El modelo puede ser empleado para analizar los efectos de las propiedades del carbón, el tamaño de partícula y la composición del gas circundante. El modelo ha sido adaptado para el diseño de quemadores de oxicombustión a escala piloto [Taniguchi, 2011b].

Smart et al. [Smart, 2010] evaluaron el efecto de los gases de oxicombustión en las características de la llama, mediante imágenes digitales tomadas en un sistema experimental de un quemador de carbón pulverizado de 0,5 MWth. En los ensayos realizados se observó que la elevada proporción de CO_2 en la corriente de gases recirculados retardaba la ignición y la combustión era más inestable.

Khatami et al. [Khatami, 2012] determinaron el retraso del inicio de la ignición para dos lignitos y un carbón bituminoso, en atmósferas de O_2/N_2 y O_2/CO_2 con proporciones de O_2 entre 20 y 100 %. Los experimentos se llevaron a cabo en el dispositivo descrito en el Apartado 3.2. Estos autores observaron un retraso en la ignición de todos los carbones en las atmósferas de CO_2 respecto a las de N_2 con la misma concentración de O_2. Para ambas atmósferas el aumento de la concentración de oxígeno supone un adelanto de la ignición. Zhang et al. [Zhang, 2010] obtuvieron unos resultados similares al quemar un carbón bituminoso en atmósferas de aire y O_2/CO_2 con concentraciones de O_2 entre 21 y 27 %. Al aumentar la concentración de CO_2 se producía un retraso en la ignición de los carbones y como una parte de los volátiles permanecían inquemados en el contorno de la partícula, se favorece la oxidación parcial y la reacción de gasificación del *char* por la presencia de elevadas concentraciones de CO_2.

5.2 *Emisiones de NO_x*

El nitrógeno presente en los humos de combustión en forma de óxidos tiene dos orígenes. Una parte proviene de la combustión de las partículas del combustible, ya que el nitrógeno está presente en su composición, y otra parte es el llamado NO_x de origen térmico. La proporción de los óxidos de nitrógeno procedentes del combustible, estará determinada por la cantidad de nitrógeno en la composición del combustible. Los NO_x de origen térmico se producen por la oxidación del nitrógeno del aire a temperaturas elevadas. En los procesos de oxicombustión la presencia de N_2 en la atmósfera de combustión será debida únicamente a infiltraciones en la cámara de combustión y las etapas de molienda, así como a las impurezas del O_2 introducido en los gases de entrada. Por tanto, la formación de NO_x térmico será muy reducida.

La formación de óxidos de nitrógeno está muy influenciada por la atmósfera de combustión, según sean las condiciones oxidantes o se encuentren zonas reductoras. En condiciones de baja concentración de oxígeno con gran concentración de hidrocarburos de cadena corta y CO, la formación de NO será muy baja. A medida que aumenta el exceso de oxígeno la formación de NO se ve favorecida. Esto se ha corroborado en los experimentos realizados con diferentes excesos de oxígeno.

5.3 Compendio de resultados:

Se ha estudiado en un reactor de flujo en arrastre, el efecto de distintas atmósferas de oxicombustión sobre las propiedades de ignición y de combustión de carbones de distinto rango. Los resultados obtenidos indican un empeoramiento en las propiedades de ignición en la atmósfera 21%O_2/79%CO_2 en comparación con la ignición en aire. La ignición se ve retrasada al sustituir N_2 por CO_2 para la misma concentración de O_2 (21 %) debido a la mayor capacidad calorífica del CO_2 y a la menor difusividad del O_2 en CO_2. Sin embargo, al aumentar la concentración de O_2 se produce un descenso en la temperatura de ignición, y para una concentración del 30 % de O_2 se obtuvo una temperatura de ignición menor que en aire.

En condiciones de oxicombustión con recirculación húmeda de gases, se observó un ligero aumento en la temperatura de ignición con la presencia de vapor de agua en las atmósferas de oxicombustión, es decir, un retardo en la ignición de los carbones estudiados. Sin embargo la presencia de vapor de agua no ejerce efectos muy apreciables en la evolución de los gases durante la ignición de los carbones.

En lo referente al proceso de combustión global del carbón, se estudió el efecto de la sustitución de N_2 por CO_2 para la misma concentración de oxígeno (21 %), sobre el grado de conversión. Se observó una disminución en el grado de conversión, debido a las diferencias en las propiedades físicas de ambos gases. A medida que la concentración de O_2 aumenta, el tiempo de quemado de las partículas disminuye y esto se tradujo en un aumento del grado de quemado en los experimentos realizados en el reactor de flujo en arrastre.

Los volátiles liberados durante la combustión del carbón bituminoso alto en volátiles reaccionan rápidamente, alcanzando temperaturas elevadas en los primeros instantes de la combustión que sumado a la mayor reactividad del *char* respecto a los carbones de alto rango, permite obtener valores de grado de quemado muy elevados. La semiantracita tiene un menor contenido en volátiles y es menos reactiva, por lo que este carbón requiere mayor exceso de oxígeno para alcanzar niveles de quemado elevados, en el mismo tiempo de residencia que el carbón bituminoso.

Al aumentar la concentración de oxígeno por encima del 30 % mejora el grado de quemado, pero también aumenta la producción de óxidos de nitrógeno. No obstante, la cantidad de NO por gramo de carbón quemado (o unidad de energía producida) sigue siendo menor que la producida en aire. La atmósfera 30%O_2/70%CO_2 es la que muestra un balance más equilibrado entre grado de conversión alcanzado y cantidad de NO producido por unidad de energía.

La presencia de vapor de agua en las atmósferas de oxicombustión no ejerce efectos muy apreciables durante la combustión de los carbones. Se observó un menor grado de quemado

en las atmósferas con 10 y 20 % de vapor de agua, únicamente para el caso de concentraciones de oxígeno bajas.

Las emisiones de NO son menores en las atmósferas de oxicombustión que en aire, incluso en las atmósferas con mayor concentración de oxígeno. La presencia de concentraciones elevadas de CO en las atmósferas de oxicombustión propicia la reducción de NO para formar N_2. Este hecho, unido a la ausencia de NO de origen térmico, produce un descenso notable en las emisiones de NO. Las emisiones de NO en las atmósferas de oxicombustión en presencia de vapor disminuyeron ligeramente, debido a que el vapor podría interactuar con compuestos intermedios actuando como agente reductor de NO. Por tanto, el efecto de la presencia de vapor de agua en las condiciones experimentales empleadas es muy limitado, sin embargo sería deseable evaluar el efecto que pudiera ejercer en condiciones de temperaturas superiores a 1.200-1.300 °C.

5.4 Publicaciones relacionadas:

V **Effect of oxy-fuel combustion with steam addition on coal ignition and burnout in an entrained flow reactor,**
J. Riaza, L. Álvarez, M.V. Gil, C. Pevida, J.J. Pis, F. Rubiera, Energy 2011. 36 (8) pp. 5314 – 5319. doi:10.1016/j.energy.2011.06.039

VI **NO Emissions in oxy-coal combustion with addition of steam in an entrained flow reactor.**
L. Álvarez, J. Riaza, M.V. Gil, C. Pevida, J.J. Pis, F. Rubiera**.** Greenhouse Gases: Science and Technology 2011. 1 (2) pp. 180-190. doi:10.1002/ghg.016

5.4.1 *Publicación V*

Effect of oxy-fuel combustion with steam addition on coal ignition and burnout in an entrained flow reactor,

J. Riaza, L. Álvarez, M.V. Gil, C. Pevida, J.J. Pis, F. Rubiera,
Energy
2011. 36 (8) pp. 5314 – 5319.
doi:10.1016/j.energy.2011.06.039

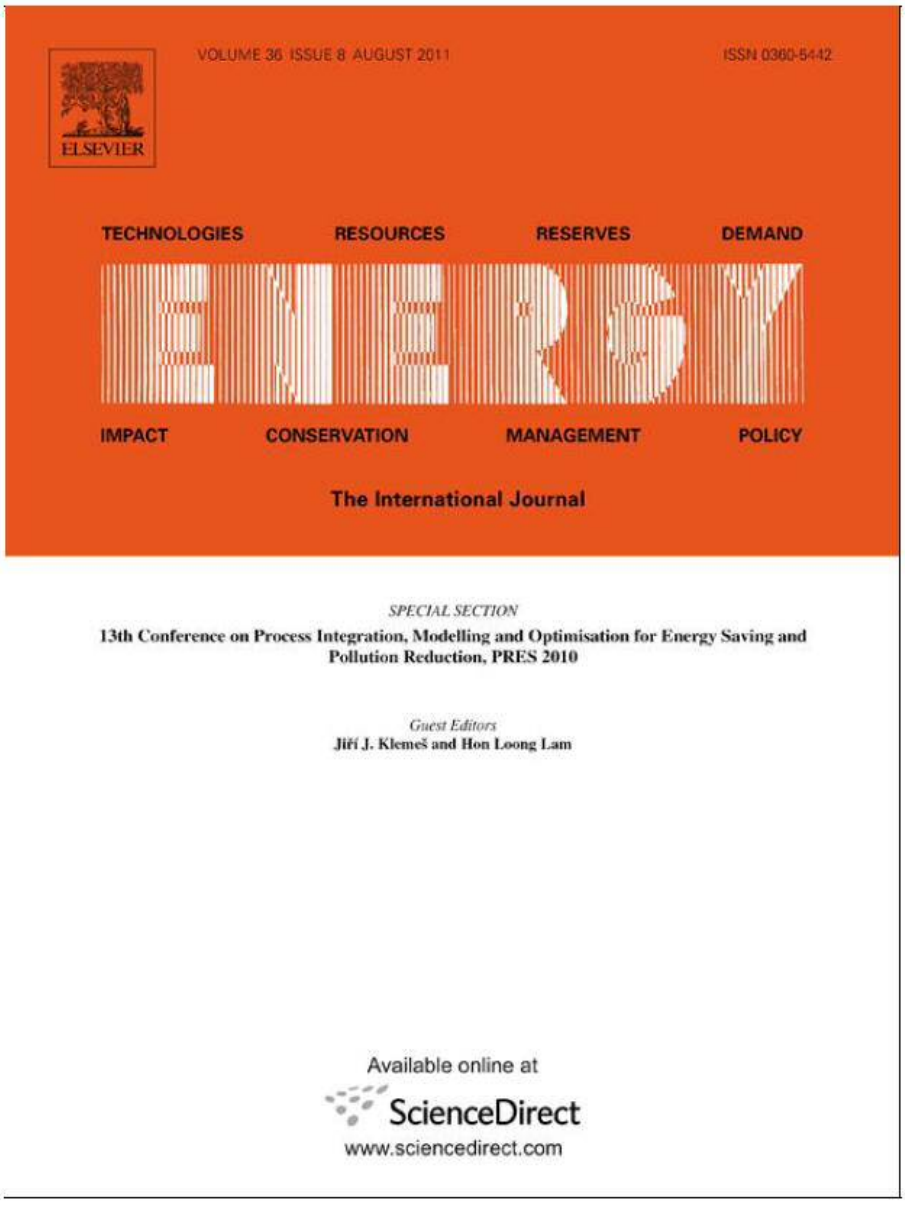

Energy 36 (2011) 5314–5319

Contents lists available at ScienceDirect

Energy

journal homepage: www.elsevier.com/locate/energy

Effect of oxy-fuel combustion with steam addition on coal ignition and burnout in an entrained flow reactor

J. Riaza, L. Álvarez, M.V. Gil, C. Pevida, J.J. Pis, F. Rubiera*

Instituto Nacional del Carbón, INCAR-CSIC, Apartado 73, 33080 Oviedo, Spain

ARTICLE INFO

Article history:
Received 10 February 2011
Received in revised form
10 June 2011
Accepted 18 June 2011
Available online 20 July 2011

Keywords:
Oxy-fuel combustion
Pulverized coal
Steam addition
Ignition
Burnout
Entrained flow reactor

ABSTRACT

The ignition temperature and burnout of a semi-anthracite and a high-volatile bituminous coal were studied under oxy-fuel combustion conditions in an entrained flow reactor (EFR). The results obtained under oxy-fuel atmospheres (21%O_2–79%CO_2, 30%O_2–70% O_2 and 35%O_2–65%CO_2) were compared with those attained in air. The replacement of CO_2 by 5, 10 and 20% of steam in the oxy-fuel combustion atmospheres was also evaluated in order to study the wet recirculation of flue gas. For the 21%O_2–79% CO_2 atmosphere, the results indicated that the ignition temperature was higher and the coal burnout was lower than in air. However, when the O_2 concentration was increased to 30 and 35% in the oxy-fuel combustion atmosphere, the ignition temperature was lower and coal burnout was improved in comparison with air conditions. On the other hand, an increase in ignition temperature and a worsening of the coal burnout was observed when steam was added to the oxy-fuel combustion atmospheres though no relevant differences between the different steam concentrations were detected.

© 2011 Elsevier Ltd. All rights reserved.

1. Introduction

The use of coal in power plants generates a large amount of CO_2, which is the chief contributor to global climate change. However, coal is the most abundant and geographically the most widely distributed fossil fuel. The stability of its supply and its relatively low cost ensure its inclusion in the energy mix in the foreseeable future [1].

Several strategies for the reduction and capture of CO_2 from large-scale stationary power plants are being considered. The main problem is that the concentration of CO_2 in conventional coal-air combustion flue gas is low (typically 14–16%) and its direct storage is not economically feasible [2]. As an alternative, the oxy-fuel combustion process has been proposed as a new promising technology for CO_2 capture from fossil fuel power plants. This technology entails the combustion of coal in a mixture of oxygen (instead of air) and recycled flue gas (RFG), which mainly contains CO_2 and H_2O. The net volume of flue gas is reduced and a highly concentrated CO_2 (95%) flue gas is produced, which can be directly stored in a supercritical state by means of compression.

The combustion of coal in the O_2/CO_2 atmosphere of an oxy-coal combustion boiler can be expected to be different from that of an O_2/N_2 atmosphere of a conventional coal-air combustion boiler, because CO_2 has a larger specific molar heat than N_2, and the coal can be gasified by the CO_2 [3]. The replacement of N_2 by CO_2 may affect the operation parameters of the combustion furnace. The propagation speed and stability of the flame and the gas temperature profile may decrease or the unburned carbon content may increase. During the oxy-fuel combustion process, this problem can be overcome by increasing the oxygen concentration in the oxy-fuel combustion atmosphere (up to approximately 30%) in order to match the combustion performance achieved in air, in relation to flame temperature, ignition time, heat transfer, gas temperature profile and char burnout. This would also contribute to the overall efficiency of the oxy-fuel process [4]. The flexibility acquired by adjusting the O_2 concentration in the feed gas to control the heat flux and flame temperature would have an additional advantage in that it would allow a more flexible selection of fuels, especially for coal-fired power plants [5].

One of the advantages of this technology is that it would prevent the formation of thermal NO_x due to the absence of nitrogen. It has been shown that a reduction in NO_x emissions can be achieved with oxy-fuel combustion compared to air-firing [6–8].

In addition, oxy-coal combustion allows the capture and storage of carbon as a retrofit technology in conventional pulverized coal boilers.

Although oxy-fuel recycle combustion requires that some modifications are carried out in the existing pulverized coal

* Corresponding author. Tel.: +34 985 118 975; fax: +34 985 297 662.
E-mail address: frubiera@incar.csic.es (F. Rubiera).

0360-5442/$ – see front matter © 2011 Elsevier Ltd. All rights reserved.
doi:10.1016/j.energy.2011.06.039

combustion technology that has well-proven reliability and industrial acceptance, it is a promising approach for continued use of coal for electric power production [9]. However, the successful implementation of O_2/CO_2 technology in conventional pulverized coal boilers requires a full understanding of the changes that occur when N_2 is replaced by CO_2 in the combustion atmosphere [10]. The ignition of coal particles is an important preliminary step in the coal combustion process due to its influence on flame stability, the formation and emission of pollutants and flame extinction [11]. Thus, the study of the reactivity and the minimum gas temperature for the ignition of coal particles will be very important when designing the boiler and for controlling the combustion process [12].

Although previous work has already dealt with the oxy-fuel combustion process in entrained flow reactors (EFR) [9] or drop tube furnaces (DTF) [13,14], and simulation studies have been published [15–17], the presence of steam in the oxidizer stream has not received significant consideration [18,19]. Recently, Smart et al. [20] showed that the combustion of coal in an $O_2/CO_2/H_2O$ atmosphere, in relation to ignition, burnout, flame stability and emissions, requires further clarification.

In this work, an entrained flow reactor was used in order to study the effect of replacing N_2 with CO_2 and of enhanced levels of O_2 in an oxy-fuel combustion atmosphere upon coal ignition temperature and burnout. The addition of steam has also been evaluated in order to study the effect of the wet recirculation of flue gas.

2. Experimental

2.1. Coals

Two coals of different rank were used: a semi-anthracite from the Hullera Vasco-Leonesa in León, Spain (HVN), and a high-volatile bituminous coal from the Batán coal washing plant in Asturias, Spain (BA). The samples were ground and sieved to obtain a particle size fraction of 75–150 μm. The results of the proximate and ultimate analyses and higher heating values of the samples are shown in Table 1.

2.2. Experimental device and procedure

An entrained flow reactor was used to study the ignition and the oxy-fuel combustion characteristics of the coal at high heating rates and short residence times. A diagram of the experimental device used is shown in Fig. 1. The reactor has a reaction zone with a maximum length of 1700 mm and an internal diameter of 40 mm. The EFR is electrically heated and is able to work at a maximum temperature of 1100 °C. The coal samples were fed in from a hopper and the mass flow was controlled using a mechanical feeding system. The samples were introduced through an air-cooled injector to ensure that their temperature did not exceed 100 °C before entering the reaction zone. The gases were preheated to the oven temperature before being introduced into the reactor through flow straighteners. The flow rates of N_2, CO_2 and O_2 from the gas cylinders were controlled by mass flow controllers. The steam was generated by a vaporizer, in which water was heated up to 250 °C. A high performance liquid chromatography (HPLC) pump was used to control the flow rate of water towards the vaporizer. The steam was mixed with the inlet gases before they were introduced into the preheater. A water-cooled collecting probe was inserted into the reaction chamber from below. Nitrogen was introduced at the top of the probe to quench the reaction products. Particles were removed by means of a cyclone and a filter, and the exhaust gases were monitored using a battery of analysers (O_2, CO_2, CO, NO and SO_2).

During the ignition tests, the reactor was heated at 15 °C min^{-1} from 400 to 800 °C. The gas flow used in these tests ensured a particle residence time of 2.5 s at 500 °C, and the excess oxygen (defined as the O_2 supplied in excess of that required for the stoichiometric combustion of coal) was fixed at a value of 25%. Ignition is the initiation stage of combustion and it is defined as the temperature at which the heat generated by the reactions exceeds the heat losses by various mechanisms of heat transfer. The criterion for determining the ignition temperature was based on the first derivative temperature curves of the gases produced. The ignition temperature was taken as the temperature at which the first derivative temperature curve, normalized by the maximum derivative value, reached a value of 10% [12].

On the other hand, the combustion experiments were carried out at a reactor temperature of 1000 °C and a particle residence time of 2.5 s. The burnout is defined as the loss of mass of a fuel during its combustion and it is expressed as the ratio of mass loss during combustion to total mass in the input coal.

Four binary mixtures of O_2/N_2 and O_2/CO_2 and several ternary mixtures of $O_2/N_2/H_2O(v)$ and $O_2/CO_2/H_2O(v)$ were employed to study the behaviour of the coals. Thus, for the ignition and combustion tests, air (21%O_2–79%N_2) was taken as reference and three binary mixtures of O_2 and CO_2 were compared: 21%O_2–79%CO_2, 30%O_2–70%CO_2 and 35%O_2–65%CO_2. The addition of 5, 10 and 20% of steam was also evaluated for all the air and the oxy-fuel combustion atmospheres, as a substitute for N_2 or CO_2 respectively, in order to study the effect of the wet recirculation of flue gas upon coal ignition and oxy-fuel combustion.

Table 1
Proximate and ultimate analyses and high heating value of the coals.

Sample	HVN	BA
Origin	Spain	Spain
Rank	sa	hvb
Proximate Analysis[a]		
Moisture content (wt.%)	1.1	1.2
Ash (wt.%, db)	10.7	6.9
V.M. (wt.%, db)	9.2	33.9
F.C. (wt.%, db)[b]	80.1	59.2
Ultimate Analysis (wt.%, daf)[a]		
C	91.7	88.5
H	3.5	5.5
N	1.9	1.9
S	1.6	1.1
O[b]	1.3	3.0
High heating value (MJ/kg, db)	31.8	33.1

sa: semi-anthracite; hvb: high-volatile bituminous coal; db: dry basis; daf: dry and ash free bases.
[a] The proximate analysis was conducted in a LECO TGA-601, and the ultimate analysis in a LECO CHNS-932.
[b] Calculated by difference.

3. Results and discussion

3.1. Ignition tests

The ignition temperatures of coal BA and semi-anthracite HVN under the different atmospheres studied are shown in Fig. 2. The ignition of HVN took place at higher temperatures than that of BA in all the atmospheres studied, in accordance with coal rank (Table 1). The reactivity of the high-volatile bituminous coal, BA, was higher than that of the semi-anthracite, HVN, which caused the heat to be released earlier and led to a reduction in the ignition temperatures.

In the case of HVN, when N_2 (21%O_2–79%N_2) was replaced by CO_2 (21%O_2–79%CO_2), the ignition temperature increased (Fig. 2a). This can be attributed to the higher specific molar heat of CO_2 compared to that of N_2. Before ignition, the coal particles were

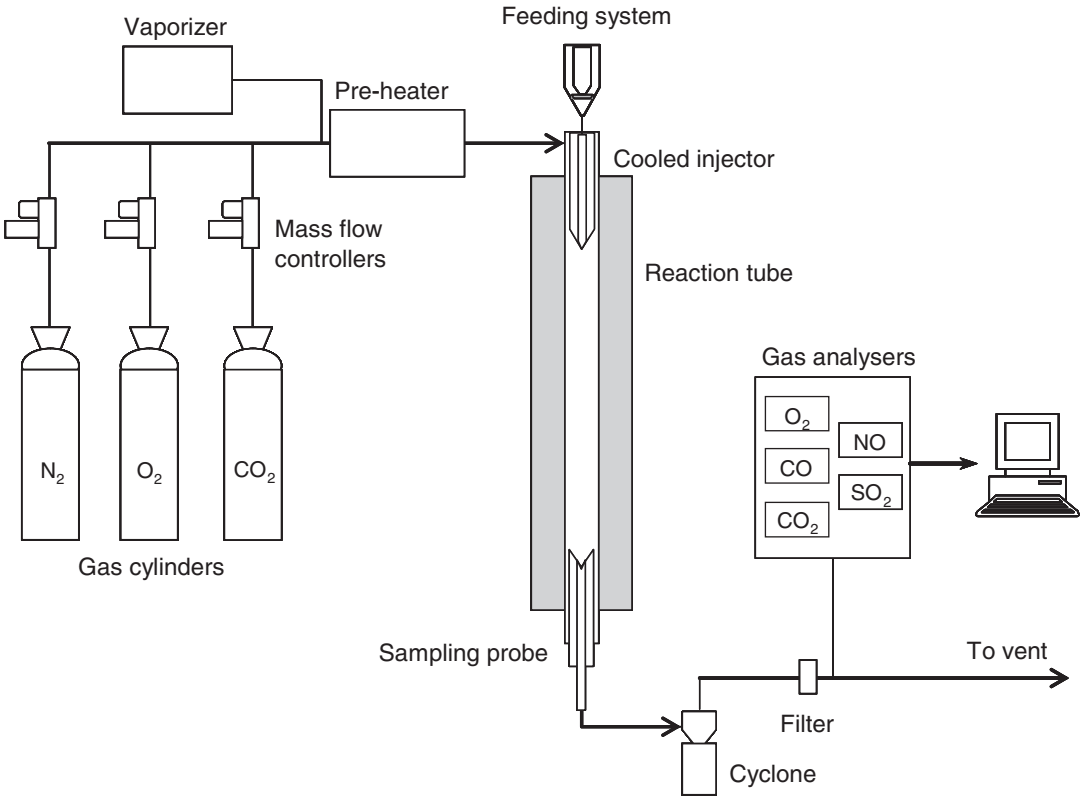

Fig. 1. Schematic diagram of the entrained flow reactor (EFR) used in the experiments.

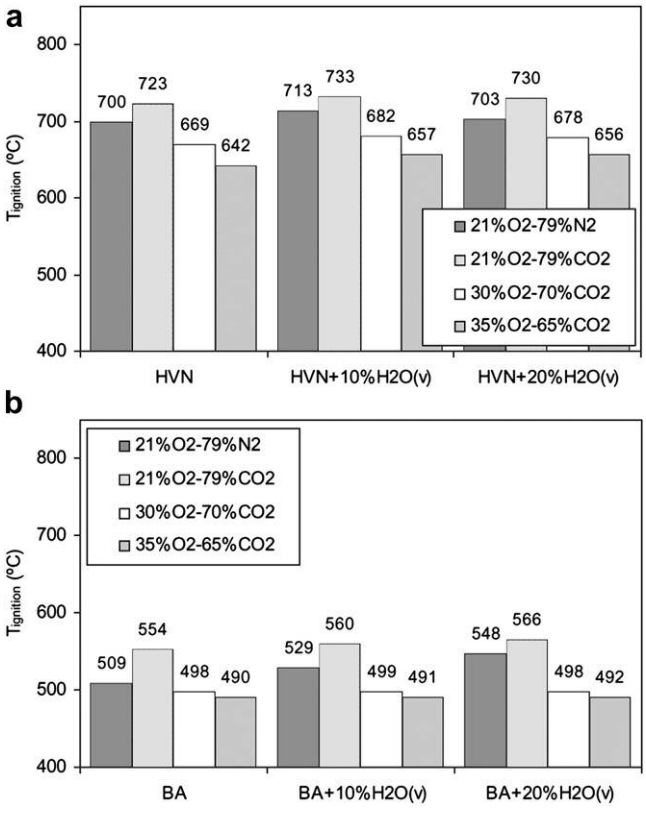

Fig. 2. Ignition temperature of HVN (a) and BA (b) coals under different atmospheres (the $H_2O(v)$ is added as a substitute for N_2 or CO_2).

heated up by the ambient environment, after which the release of coal volatiles occurred, the radiant heat from the particles causing an increase in the gas temperature. The fact that the specific molar heat of CO_2 is higher than that of N_2 would produce a comparatively lower gas temperature and, therefore, a reduction in coal particle temperature during oxy-fuel combustion in comparison to combustion in air at the same oxygen concentration (21%). The result of this would be a decrease in the burning rate and a delay in the ignition of volatiles and char under a 21%O_2–79%CO_2 atmosphere, as pointed out by Liu et al. [21] and Molina and Shaddix [10].

However, when the oxygen concentration was increased (30% O_2–70%CO_2 and 35%O_2–65%CO_2), the ignition temperature decreased to below that of the air conditions (Fig. 2a). If the O_2 concentration increases, the mass flux of O_2 to the coal surface particles, the rate of devolatilization and the oxidation rate of volatiles will increase. This shortens the coal particle auto-ignition time considerably [14]. In contrast a reduction in oxygen concentration retards the ignition of volatile matter and char [22].

Fig. 2b shows the ignition temperatures for coal BA under the different atmospheres studied. It can be observed that, when N_2 was replaced by CO_2 in the atmosphere with 21% O_2, the ignition temperature also increased, indicating a delay in ignition under this oxy-fuel combustion atmosphere due to the lower gas temperatures caused by the higher specific molar heat of CO_2. It should be noted that a marked difference was observed in the ignition temperatures under both atmospheres, possibly due to the high-volatile content of coal BA (Table 1), since CO_2 decreases the rate of devolatilization because of the lower mass diffusivity of the volatiles in CO_2 mixtures [9].

On the other hand, when the oxygen concentration was increased, the ignition temperature decreased to lower values than that in air (Fig. 2b). Nevertheless, it can be seen that the

ignition temperatures of coal BA (without steam addition) under the 30%O_2–70%CO_2 and 35% O_2–70%CO_2 atmospheres were very close to that reached under air conditions. The high-volatile content of coal BA may have caused a substantial accumulation of volatiles in the vicinity of the particles prior to their ignition, which in turn may have affected the availability of oxygen [14]. If the cloud of volatiles persisted on the char surface for a long time, this would cause O_2 depletion on the char surface, decreasing the rate of devolatilization and delaying the ignition process. Stanmore et al. [23] also observed serious oxygen depletion in the volatile cloud during coal combustion in a drop tube furnace. This behaviour was observed in this work after N_2 was replaced with CO_2 at different O_2 concentrations for the HVN and BA samples both with and without steam addition (Fig. 2).

On the other hand, Fig. 2 shows that the replacement of N_2 or CO_2 by steam caused a slight increase in the ignition temperatures in all the atmospheres for HVN, but no significant differences were observed between the atmospheres with 10 and 20% of steam. In the case of the BA coal, the ignition temperatures increased after the addition of steam to the atmospheres with 21% of O_2, whereas no differences were observed when steam was added to the oxy-fuel atmospheres with 30 and 35% of O_2. Nozaki et al. [18] found that the flame temperatures were lower when a wet recycle flue gas (16% of H_2O) was used compared to a dry recycle flue gas, and they concluded that drying the gas improved ignition stability. In our work, it was the addition of steam that probably led to lower temperatures, causing an increase in the ignition temperatures under atmospheres containing significant water vapour content.

3.2. Combustion tests: burnout

Coals HVN and BA were burned under different levels of excess oxygen for each atmosphere studied. The fuel ratio, defined as the ratio between the coal mass flow rate and the stoichiometric value, was used to determine the excess oxygen during combustion.

The HVN and BA burnouts, with and without steam addition, are shown in Figs. 3 and 4, respectively. The coal burnout decreased as the fuel ratio increased due to the lower availability of oxygen at higher fuel ratio values. At low fuel ratio values (high oxygen excess), the BA burnout curves showed an asymptotic approach towards a value of 100% (Fig. 4). However, the HVN burnout showed an almost linear dependence on the fuel ratio in both air and oxy-fuel conditions (Fig. 3). Even at low values of fuel ratio (high excess oxygen), the HVN coal showed low burnout values, reflecting the lower reactivity of high rank coals.

For the HVN coal (Fig. 3), both with and without steam addition, the burnout obtained under the 21%O_2–79%CO_2 atmosphere was lower than that reached under 21%O_2–79%N_2 conditions. Liu et al. [21] observed that, when air was replaced by 21%O_2–79%CO_2, gas temperatures dropped significantly. As mentioned above, CO_2 has a higher specific molar heat than N_2, which implies that when N_2 is replaced by CO_2 the heat capacity of the gases increases, leading to lower flame and gas temperatures. According to Zhang et al. [14], the specific heat capacity of diluent gas is one of the principal factors affecting char surface temperature for any given O_2 fraction. Therefore, the particle temperature during the 21%O_2–79%CO_2 atmosphere can be expected to be lower, causing the combustion rate of the char and the coal burnout value to fall [24]. Bejarano and

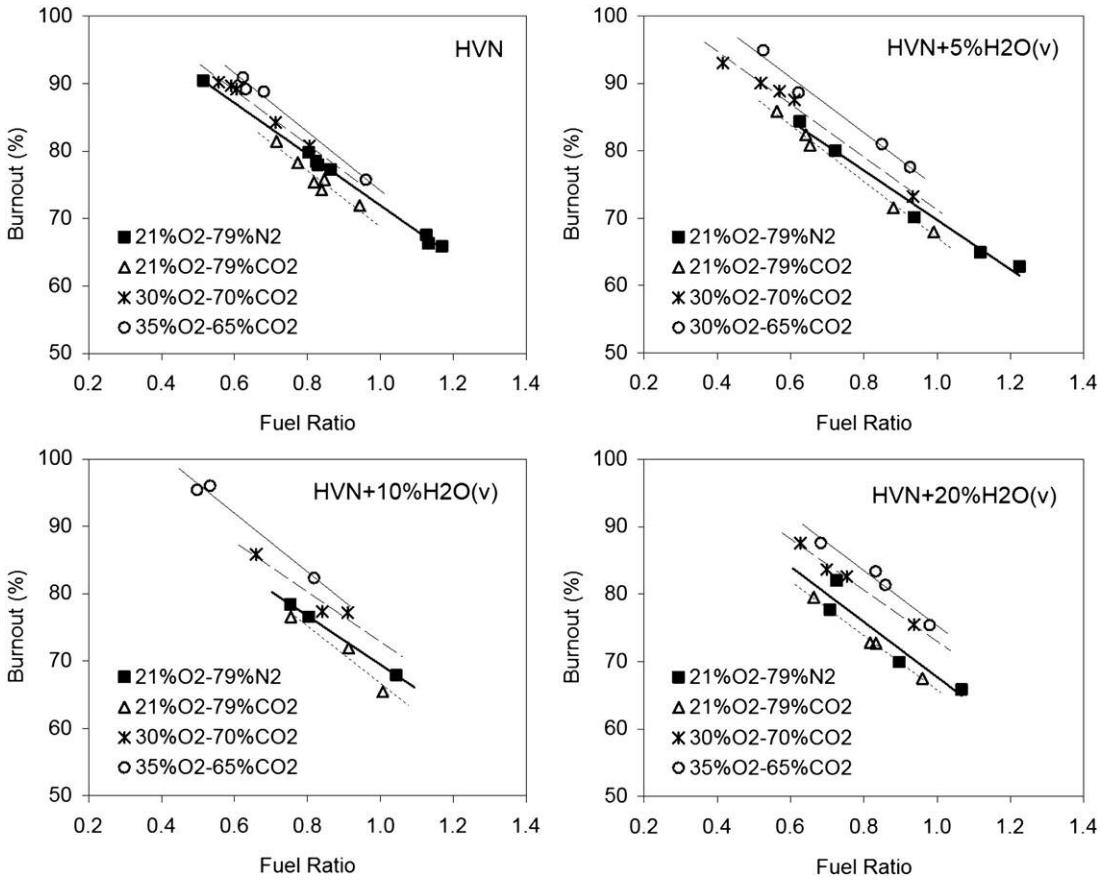

Fig. 3. Burnout of HVN coal under different atmospheres at different fuel ratios (the H_2O(v) is added as a substitute for N_2 or CO_2).

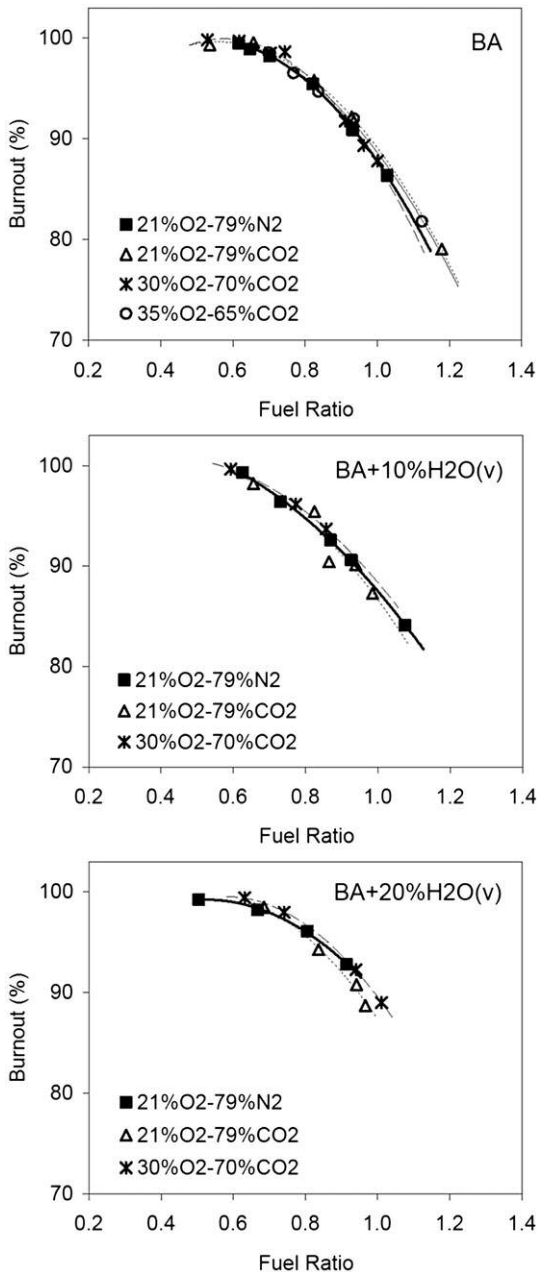

Fig. 4. Burnout of BA coal under different atmospheres at different fuel ratios (the $H_2O(v)$ is added as a substitute for N_2 or CO_2).

Levendis [4], when performing combustion experiments in a drop tube furnace, found that coal particles burned at higher temperatures and shorter combustion times in O_2/N_2 than in O_2/CO_2 environments for equivalent oxygen fractions. In the present work, the ignition temperature under the 21%O_2–79%CO_2 atmosphere was higher than in air, resulting in delayed ignition and a longer combustion time.

Li et al. [13] studied coal combustion characteristics under oxy-fuel and air conditions using a drop tube furnace. These authors attributed the different behaviours under both atmospheres to the fact that the lower diffusivity of O_2 in CO_2 than in N_2 affects the transport of O_2 to the surface of the particles, leading to a reduced combustion of the volatile matter released from the coal particle and reduced char combustion rates under oxy-fuel conditions. Furthermore, once a coal is ignited, the flame formed provides a vast heat release that consumes the extra volatiles evolved and the char particles. However, the diffusivity of the fuel vapour or small hydrocarbons throughout the volatile cloud and CO_2 boundary layer would be retarded when the N_2 is replaced by CO_2, thereby reducing the rate at which the volatiles are consumed [14].

Under the 30%O_2–70%CO_2 and 35%O_2–65%CO_2 atmospheres, the burnout of HVN was higher than in air (Fig. 3), since the higher oxygen concentration produced an increase in the char combustion rate. Though the gas temperature increases only slightly when the O_2 fraction in bulk gas is increased, it is likely that the increase in the mass flux rate of O_2 from the bulk gas to the coal surface at higher O_2 concentrations promotes the consumption rate of the volatiles [9], providing extra heat feedback to the coal particle to enhance its devolatilization, ignition and combustion [24]. Liu et al. [21] found that coal combustion in 30%O_2–70%CO_2 matched the gas temperature profile of coal combustion in air but that it showed a better char burnout.

Increasing the O_2 fraction in CO_2 up to 30% is still insufficient to match the specific heat capacity of air. However, coal burnout in the 30%O_2–70%CO_2 atmosphere reached a higher value than in air, which means that another parameter must have changed to offset the negative effect of the specific heat capacity of the gas. According to Zhang et al. [14], in atmospheres containing CO_2, the extra CO derived from char-CO_2 gasification increases the reactivity of the local mixture of fuel and oxidizer gas, which may account for the explanation of the increase in the coal burnout. Homogeneous oxidation of the gasification-derived CO would generate extra heat, which would in turn increase the adiabatic flame temperature and the oxidation of both the volatiles and the char. Zhang et al. [14] underlined the importance of the extra CO and its homogeneous oxidation in the vicinity of the char particle, as it would enhance thermal feedback to the char particles, in the same way as volatile oxidation does. The char gasification reaction would also be beneficial for coal conversion.

For coal BA (Fig. 4), both with and without the addition of steam, no significant differences can be observed between the different atmospheres studied because BA reached a very high burnout under all conditions due to its high reactivity.

In order to facilitate the comparison of the behaviours of these coals under air and oxy-fuel atmospheres both with and without steam addition, the burnouts were interpolated at a fuel ratio of 0.8 using the curves shown in Figs. 3 and 4. The results for both coals, HVN and BA, are shown in Fig. 5a and b, respectively. It can be seen that the burnout of HVN in air and under an oxy-fuel atmosphere with 21% of oxygen, decreased slightly after the addition of steam, but no relevant differences were found between the three steam concentrations (Fig. 5a). The lower burnout observed after the addition of steam seems to indicate the combustion temperature under these atmospheres was lower. The higher specific molar heat of $H_2O(v)$ compared to N_2 would explain the decrease in burnout after the addition of steam to the air atmosphere. However, under oxy-fuel atmospheres, although the specific molar heat of water vapour is lower than that of CO_2, no increase in burnout was observed when steam was added to the 21%O_2–79%CO_2 atmosphere. This suggests that other factors must have influenced oxy-fuel combustion with the addition of steam. Thus, enhancements in thermal radiation or endothermic radical formation (O, OH, H, etc.) might explain the reduction in combustion temperature [25]. High proportions of H_2O in the furnace gases may have resulted in higher gas emissivities due to the high emission capacity of water vapour via radiative heat transfer. Wall et al. [26] estimated that total emissivity due to the joint emission of the gas and the particulate was higher under wet oxy-fuel conditions than under a dry oxy-fuel atmosphere, and it presented the lowest value in air. Nozaki et al. [18] found that drying the flue gas increased the gas temperature near the burner by about 150 °C for the same volumetric gas flow

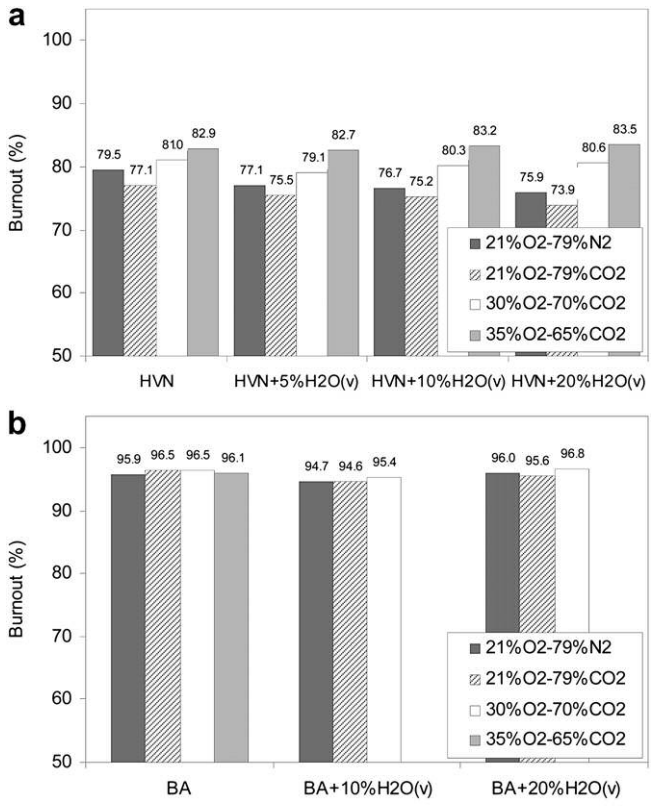

Fig. 5. Burnout of HVN (a) and BA (b) coals under different atmospheres at a fuel ratio of 0.8 (the $H_2O(v)$ is added as a substitute for N_2 or CO_2).

rate and thus helped to stabilize the flame by improving ignition stability. Zhou and Moyeda [19] by means of a computational fluid dynamics (CFD) simulation showed that the wet flue gas recycle led to a lower flame temperature than the dry flue gas recycle.

Under the oxy-fuel combustion atmospheres with 30 and 35% of oxygen, the addition of steam did not significantly affect coal burnout (Fig. 5a), which was due to the fact that more oxygen was available. As a result, the burnout of HVN was less affected by the presence of low concentrations of steam.

For the BA coal, no different burnout values can be observed between the atmosphere with and without steam (Fig. 5b), because of the high reactivity of this coal.

4. Conclusions

The ignition temperature and burnout of a semi-anthracite and a high-volatile bituminous coal were studied under oxy-fuel combustion conditions in an entrained flow reactor (EFR). The results showed that the ignition temperature was higher under a 21%O_2–79%CO_2 atmosphere than in air conditions, whereas the burnout was lower. This was due to the higher specific molar heat of CO_2 compared to N_2 and the lower diffusivity of O_2 in CO_2 than in N_2. However, when the O_2 concentration was increased to 30 and 35% in the oxy-fuel combustion atmosphere, the ignition temperature was lower than in air, whereas the burnout value was increased above that reached under air-firing. It was due to an increase in the mass flux of O_2 to the coal particles. Finally, higher ignition temperatures and lower coal burnout values were observed after the addition of steam in oxy-fuel combustion atmospheres under the experimental conditions of this study, but no relevant differences were observed between the different steam concentrations. This could have been due to higher losses of heat by thermal radiation.

Acknowledgements

This work was carried out with financial support from the Spanish MICINN (Project PS- 120000-2005-2) co-financed by the European Regional Development Fund. L.A. and J.R. acknowledge funding from the CSIC JAE program, co-financed by the European Social Fund, and the Government of the Principado de Asturias (Severo Ochoa program), respectively.

References

[1] Buhre BJP, Elliott LK, Sheng CD, Gupta RP, Wall TF. Oxy-fuel combustion technology for coal-fired power generation. Prog Energy Combust Sci 2005; 31:283–307.
[2] Davidson RM, Santos SO. Oxyfuel combustion of pulverised coal. London: IEA Clean Coal Centre; 2010. CCC/168.
[3] Liu H. Combustion of coal chars in O_2/CO_2 and O_2/N_2 mixtures: a comparative study with non-isothermal thermogravimetric analyzer (TGA) tests. Energy Fuels 2009;23:4278–85.
[4] Bejarano PA, Levendis YA. Single-coal-particle combustion in O_2/N_2 and O_2/CO_2 environments. Combust Flame 2008;153:270–87.
[5] Tan Y, Croiset E, Douglas MA, Thambimuthu KV. Combustion characteristics of coal in a mixture of oxygen and recycled flue gas. Fuel 2006;85:507–12.
[6] Andersson K, Normann F, Johnsson F, Leckner B. NO emission during oxy-fuel combustion of lignite. Ind Eng Chem Res 2008;47:1835–45.
[7] Croiset E, Thambimuthu KV. NO_x and SO_2 emissions from O_2/CO_2 recycle coal combustión. Fuel 2001;80:2117–21.
[8] Stadler H, Christ D, Habermeh M, Heil P, Kellermann A, Ohiger A, et al. Experimental investigation of NO_x emissions in oxycoal combustion. Fuel 2011;90:1604–11.
[9] Shaddix CR, Molina A. Particle imaging of ignition and devolatilization of pulverized coal during oxy-fuel combustion. Proc Combust Inst 2009;32:2091–8.
[10] Molina A, Shaddix CR. Ignition and devolatilization of pulverized bituminous coal particles during oxygen/carbon dioxide coal combustion. Proc Combust Inst 2007;31:1905–12.
[11] Faúndez J, Arias B, Rubiera F, Arenillas A, García X, Gordon AL, et al. Ignition characteristics of coal blends in an entrained flow furnace. Fuel 2007;86: 2076–80.
[12] Faúndez J, Arenillas A, Rubiera F, García X, Gordon AL, Pis JJ. Ignition behaviour of different rank coals in an entrained flow reactor. Fuel 2005;84:2172–7.
[13] Li X, Rathnam RK, Yu J, Wang Q, Wall T, Meesri C. Pyrolysis and combustion characteristics of an Indonesian low-rank coal under O_2/N_2 and O_2/CO_2 conditions. Energy Fuels 2010;24:160–4.
[14] Zhang L, Binner E, Qiao Y, Li C- Z. In situ diagnostics of Victorian brown coal combustion in O_2/N_2 and O_2/CO_2 mixtures in drop-tube furnace. Fuel 2010; 89:2703–12.
[15] Hong J, Chaudhry G, Brisson JG, Field R, Gazzino M, Ghoniem AF. Analysis of oxy-fuel combustion power cycle utilizing a pressurized coal combustor. Energy 2009;34:1332–40.
[16] Liszka M, Ziębik A. Coal-fired oxy-fuel power unit – process and system analysis. Energy 2010;35:943–51.
[17] Chui EH, Majeski AJ, Douglas MA, Tan Y, Thambimuthu KV. Numerical investigation of oxy-coal combustion to evaluate burner and combustor design concepts. Energy 2004;29:1285–96.
[18] Nozaki T, Takano S, Kiga T, Omata K, Kimura N. Analysis of the flame formed during oxidation of pulverized coal by an O_2-CO_2 mixture. Energy 1997;22: 199–205.
[19] Zhou W, Moyeda D. Process evaluation of oxy-fuel combustion with flue gas recycle in a conventional utility boiler. Energy Fuels 2010;24:2162–9.
[20] Smart JP, O'Nions P, Riley GS. Radiation and convective heat transfer, and burnout in oxy-coal combustion. Fuel 2010;89:2468–76.
[21] Liu H, Zailani R, Gibbs BM. Comparisons of pulverized coal combustion in air and in mixtures of O_2/CO_2. Fuel 2005;84:833–40.
[22] Huang X, Jiang X, Han X, Wang H. Combustion characteristics of fine-and miro-pulverized coal in the mixture of O_2/CO_2. Energy Fuels 2008;22: 3756–62.
[23] Stanmore BR, Choi Y-C, Gadiou R, Charon O, Gilot P. Pulverised coal combustion under transient cloud conditions in a drop tube furnace. Combust Sci Technol 2000;159:237–53.
[24] Arias B, Pevida C, Rubiera F, Pis JJ. Effect of biomass blending on coal ignition and burnout during oxy-fuel combustion. Fuel 2008;87:2753–9.
[25] Toftegaard MB, Brix J, Jensen PA, Glarborg P, Jensen AD. Oxy-fuel combustion of solid fuels. Prog Energy Combust Sci 2010;36:581–625.
[26] Wall T, Liu Y, Spero C, Elliott L, Khare S, Rathnam R, et al. An overview on oxyfuel coal combustion-State of the art research and technology development. Chem Eng Res Des 2009;87:1003–16.

5.4.2 *Publicación VI*

NO Emissions in oxy-coal combustion with addition of steam in an entrained flow reactor.

L. Álvarez, J. Riaza, M.V. Gil, C. Pevida, J.J. Pis, F. Rubiera.
Greenhouse Gases: Science and Technology
2011. 1 (2) pp. 180-190.
doi:10.1002/ghg.016

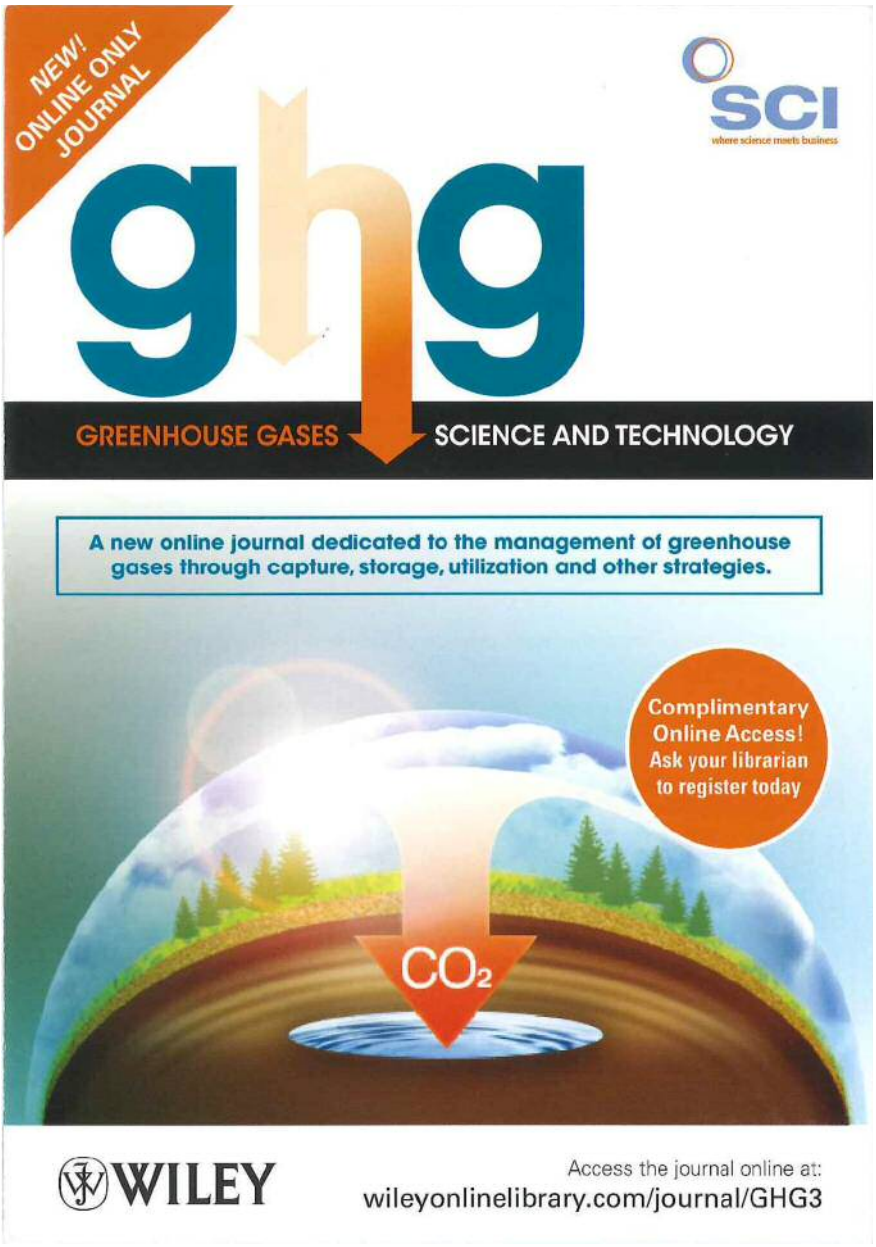

Short Communication

GREENHOUSE GASES SCIENCE AND TECHNOLOGY

NO emissions in oxy-coal combustion with the addition of steam in an entrained flow reactor

Lucia Álvarez, Juan Riaza, Maria V. Gil, Covadonga Pevida, José J. Pis and Fernando Rubiera,
Instituto Nacional del Carbón, CSIC, Oviedo, Spain

Abstract: The NO emissions of a semi-anthracite and a high-volatile bituminous coal were studied under oxy-fuel combustion conditions in an entrained flow reactor (EFR). The results obtained under oxy-fuel atmospheres (21%O_2–79%CO_2, 30%O_2–70% O_2 and 35%O_2–65%CO_2), were compared with those produced in air. The replacement of CO_2 by 5, 10, and 20% of steam in the oxy-fuel combustion atmospheres was also evaluated in order to study the wet recirculation of flue gas. The NO emissions during oxy-fuel combustion were lower than those in air-firing, and a slight increasing trend in NO emissions was observed as O_2 concentrations in the oxy-fuel atmospheres increased. Similarly, the NO concentration was reduced by the addition of steam, both under air and under oxy-fuel atmospheres, but no relevant differences between the different steam concentrations were observed.
© 2011 Society of Chemical Industry and John Wiley & Sons, Ltd

Keywords: entrained flow reactor; NO emissions; oxy-fuel combustion; pulverized coal; steam addition

Introduction

The combustion of fossil fuels results in the formation of nitrogen oxides (NO_x), either via the fixation of atmospheric nitrogen (thermal or prompt mechanisms), or by the conversion of nitrogen-containing structures in the fuel (fuel-bound nitrogen oxidation). Coal is a cheaper and more abundant resource than other fossil fuels, such as oil and natural gas, while at the same time being a reliable fuel for power production.[1] Coal is part of the greenhouse problem, since the main emissions from coal combustion are sulfur dioxide, nitrogen oxides, particulates, and CO_2.[2] The mechanisms behind the formation and destruction of NO_x have been the subject of extensive investigations for a long time.[3]

In recent years, the oxy-fuel combustion process, which consists of the burning of fuel in a mixture of oxygen and recycled flue gases (mainly CO_2 and H_2O), has come to be regarded as a very promising technology for capturing CO_2 from fossil fuel power plants. The exhaust flue gas consists of approximately 95% of CO_2 on a dry basis, the remaining part being mainly excess oxygen from combustion, nitrogen and, to a lesser extent, pollutants, such as nitrogen oxides (NO_x) and sulfur oxides (SO_x) (approximately 0.1–0.2%). Control of these contaminants is required for emissions into the environment, since NO_x causes acid rain and formation of ground level ozone, and potentially for CO_2 storage.[4] In oxy-firing, nitrogen is excluded from the combustion and the volume of flue gas is reduced by around 80% compared to air-firing.

Correspondence to: F. Rubiera, Instituto Nacional del Carbón, CSIC, Apartado 73, 33080 Oviedo, Spain. E-mail: frubiera@incar.csic.es
Received February 15, 2011; revised March 7, 2011; accepted March 7, 2011
Published online at Wiley Online Library (wileyonlinelibrary.com) DOI: 10.1002/ghg.016

Table 1. Proximate and ultimate analyses and high heating value of the coals

Sample	HVN	BA
Origin	Spain	Spain
Rank	sa	hvb
Proximate Analysis[a]		
Moisture content (wt.%)	1.12	1.20
Ash (wt.%, db)	10.64	6.91
V.M. (wt.%, db)	9.22	33.86
F.C. (wt.%, db)[b]	80.14	59.23
Ultimate Analysis (wt.%, daf)[a]		
C	91.68	88.44
H	3.49	5.48
N	1.91	1.93
S	1.58	1.12
O[b]	1.34	3.03
High heating value (MJ kg^{-1}, db)	31.78	33.08

sa: semi-anthracite; hvb: high-volatile bituminous coal.
db: dry basis; daf: dry and ash free bases.
[a] The proximate analysis was conducted in a LECO TGA-601, and the ultimate analysis in a LECO CHNS-932.
[b] Calculated by difference.

Furthermore, most of the flue gas is extracted for storage and only around 10% of the gas generated is emitted to the atmosphere.[4]

It has been shown that a significant reduction of NO_x can be achieved with oxy-fuel combustion in relation to air-firing.[5,6] This substantial NO_x reduction is partly due to the suppression of thermal NO formation due first to the absence of atmospheric N_2 and, second, because recycled NO is reduced to molecular nitrogen after being introduced into the flame zone. Nitrogen oxides include nitric oxide (NO) and nitrogen dioxide (NO_2). NO is the most important nitrogen-oxygen product of combustion, but it could be further oxidized to NO_2 at low temperatures.

A number of previous works have already dealt with NO emissions under oxy-fuel combustion conditions,[6–9] in which it is shown that lower emissions can be achieved with oxy-fuel combustion than with air-firing. However, the use of steam in the oxidizer stream has only occasionally been mentioned.[10,11] Recently, Smart *et al.*[12] pointed out that the combustion of coal in an $O_2/CO_2/H_2O$ atmosphere (including ignition, burnout, flame stability, and emissions) was a topic worthy of study.

In the present work, an entrained flow reactor (EFR) was used in order to study the effect of replacing N_2 with CO_2 in a combustion atmosphere, and the effect of enhanced levels of O_2 in an oxy-fuel combustion atmosphere upon NO emissions from coal combustion. The addition of steam was evaluated in order to study the effect of the wet recirculation of flue gas.

Experimental

Coals

Two coals of different rank were used in this work: a semi-anthracite (HVN) and a high-volatile bituminous coal (BA). The samples were ground and sieved to obtain a particle size fraction of 75–150 μm. The results of the proximate and ultimate analyses and the high heating values of the samples are presented in Table 1.

Experimental facility and operation procedures

An entrained flow reactor was used to study the NO emissions in oxy-coal combustion at high heating rates and short residence times. A diagram of the experimental device used is shown in Fig. 1. The reactor has a reaction zone with a maximum length of 1.7 m and an internal diameter of 0.04 m. The EFR is electrically heated and is able to work at a maximum

© 2011 Society of Chemical Industry and John Wiley & Sons, Ltd

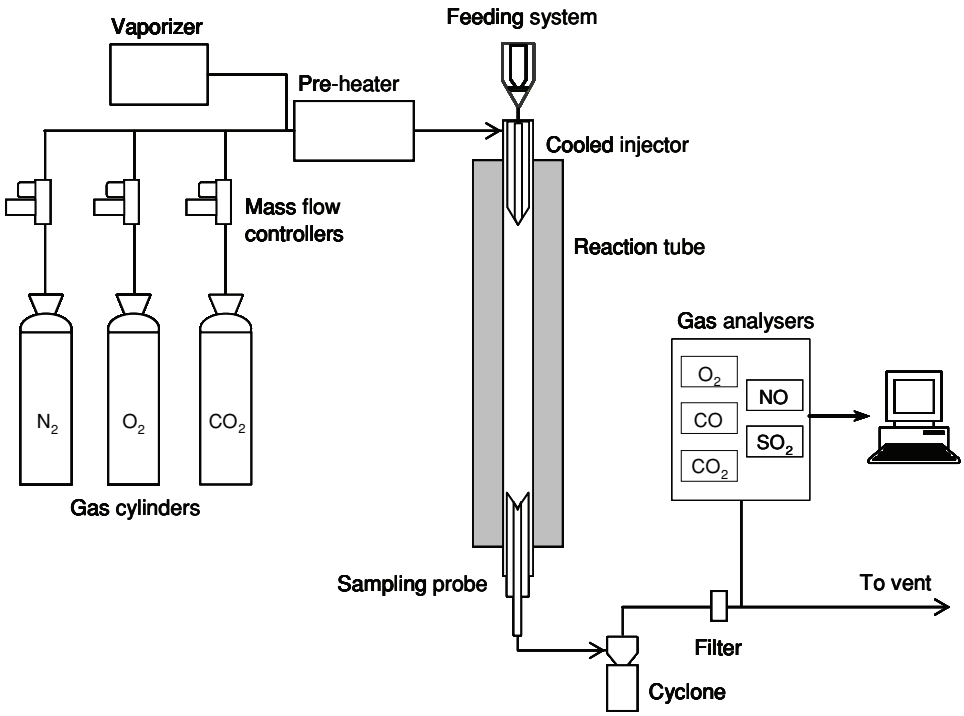

Figure 1. Schematic diagram of the entrained flow reactor (EFR) used in the experiments.

temperature of 1100 °C. Coal samples were fed from a hopper and the mass flow was controlled using a mechanical feeding system. The samples were introduced through an air-cooled injector to ensure that the temperature did not exceed 100 °C before entering the reaction zone. The gases were pre-heated to the oven temperature before being introduced into the reactor through flow straighteners. The flow rates of N_2, CO_2 and O_2 from the gas cylinders were controlled by mass flow controllers. The steam was generated by a vaporizer, in which water was heated up to 250 °C. A high performance liquid chromatography (HPLC) pump was used to control the flow rate of water toward the vaporizer. The steam was then mixed with the inlet gases before they were introduced into the pre-heater. A water-cooled collecting probe was inserted into the reaction chamber from below. Nitrogen was introduced at the top of this probe to quench the reaction products. Particles were removed by means of a cyclone and a filter, and the exhaust gases were monitored using a battery of analyzers (O_2, CO_2, CO, NO and SO_2). The experimental errors in the measurements were around 5%. During the combustion experiments, the reactor was kept at a temperature of 1000 °C and a particle residence time of 2.5 s was employed.

Four binary mixtures of O_2, N_2 and CO_2 and several ternary mixtures of O_2, N_2, CO_2 and H_2O(v) were used to study the behavior of the coals. Thus, air ($21\%O_2$–$79\%N_2$) was used as reference and three binary mixtures of O_2 and CO_2 were compared ($21\%O_2$–$79\%CO_2$, $30\%O_2$–70% O_2 and $35\%O_2$–$65\%CO_2$). Moreover, the addition of 5, 10, and 20% of steam to the air and the oxy-fuel combustion atmospheres, as a replacement for N_2 or CO_2, respectively, was evaluated in order to study the effect of the wet recirculation of flue gas on NO emissions from the oxy-fuel combustion of coal.

Results and discussion

Coals HVN and BA were burned under different levels of excess oxygen for each atmosphere studied. The fuel ratio, defined as the ratio between the coal mass flow rate and the stoichiometric value, was used to assess the excess oxygen during combustion. The NO concentrations (mg NO/mg burned coal) of coals HVN and BA under the different atmospheres employed, both with and without the addition of steam, are shown in Figs 2 and 3, respectively. A decrease in NO concentration was observed as the fuel ratio increased, since the lesser amount of

© 2011 Society of Chemical Industry and John Wiley & Sons, Ltd

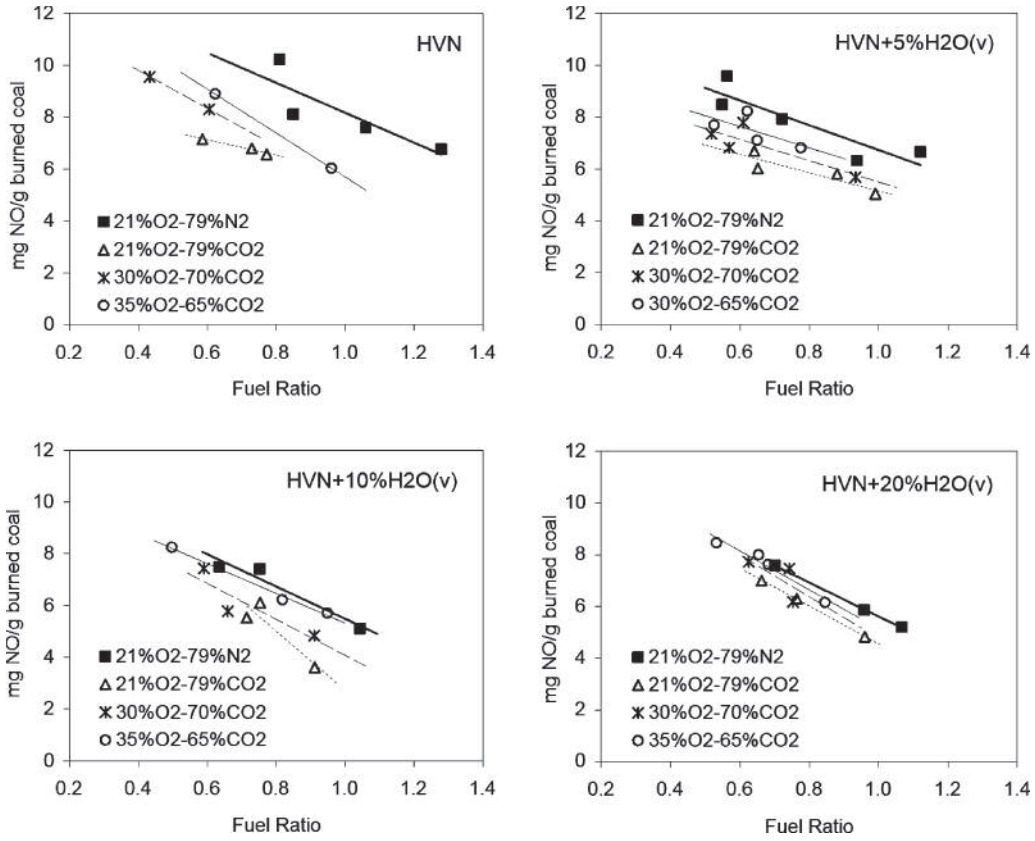

Figure 2. NO concentration of the HVN coal under different atmospheres at different fuel ratios.

oxygen available at higher fuel ratios would reduce coal burnout.

For a better comparison, the behavior of coals under air and oxy-fuel atmospheres, NO concentrations were interpolated at a fuel ratio of 0.8 using the graphs shown in Figs 2 and 3. The results for both coals, HVN and BA, are presented in Fig. 4. For HVN, the NO concentration (mg NO/mg burned coal) obtained under the 21%O_2–79%CO_2 atmosphere was lower than that achieved under 21%O_2–79%N_2 conditions. In the 30%O_2–70%CO_2 and 35%O_2–65%CO_2 atmospheres, the NO concentration for HVN was slightly higher than that in the oxy-fuel atmosphere containing 21% of O_2, since higher oxygen concentrations increase the burnout value. However, the NO concentration in all the oxy-fuel atmospheres still remained lower than that in air. Therefore, only small differences in the reduction of NO in relation to the O_2 concentration in the three oxy-fuel combustion atmospheres were observed. Nevertheless, a slight tendency for the NO concentration to increase was detected as the O_2 increased. For coal BA, the differences in NO emissions between the different atmospheres studied were not as great, but a slight decrease in such emissions after oxy-fuel combustion was detected.

In order to facilitate a comparison of the behavior of the coals under air and oxy-fuel atmospheres both with and without the addition of steam, NO concentrations (mg NO/mg burned coal) interpolated at a fuel ratio of 0.8 are shown in Fig. 5. It can be seen that the NO concentration of HVN in air and under oxy-fuel atmospheres decreased slightly after the addition of steam. There were however small differences between each of the three steam concentrations (Fig. 5(a)). For coal BA, the differences in NO concentration values for the different atmospheres were smaller (Fig. 5(b)).

Under air conditions, the thermal formation of NO resulting from the reaction between molecular N_2 and O_2 may occur at high temperatures (>1500 °C). In this study, this route would make only an insignificant contribution to the formation of NO due to

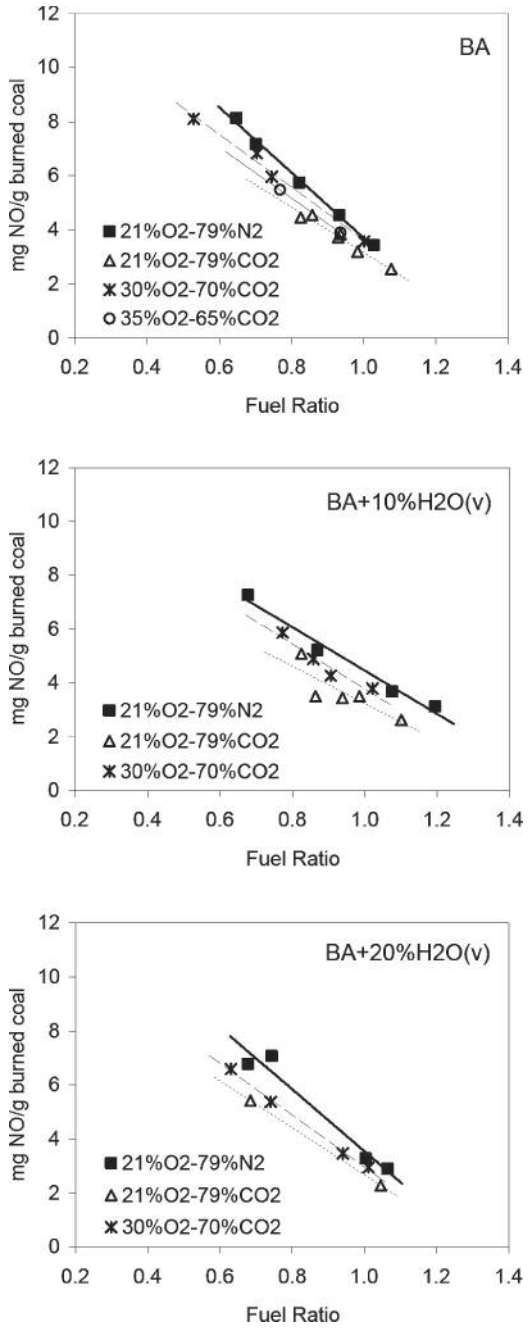

Figure 3. NO concentration of the BA coal under different atmospheres at different fuel ratios.

experimental temperature conditions. Under oxy-fuel conditions, the thermal formation of NO would be impossible due to the absence of N_2. Therefore, fuel-N would actually be the main source of NO emissions in the conditions established in these experiments.

Nitrogen in coal is converted to volatile nitrogen and char nitrogen during devolatilization. Thus, the fate of volatile-N and char-N becomes crucial for the formation of NO, and, hence, for determining the concentrations of NO in coal combustion systems. The volatile-N is transformed into either NO or N_2, while char-N reacts through a set of heterogeneous reactions as the char is oxidized.

On the other hand, two opposed mechanisms affect NO concentrations during coal combustion: first, the oxidation of fuel-N by oxygen and other oxidizing agents and, second, the reduction of the NO already produced by reducing agents.[10] Consequently, the nitrogen product distribution will be largely dependent on the competition between the mechanisms of NO formation and destruction.[13]

As already mentioned, at the experimental temperatures used in this work, the predominant source of NO will be the nitrogen bound in the organic structures. A significant proportion of this coal-bound nitrogen will be released during the initial stages of combustion (devolatilization) as tars and as light gases such as HCN, NH_3, and HNCO.[14] Evolved HCN is considered to be one of the most important volatile N-containing species formed during coal devolatilization at high temperatures because it is one of the main precursors of nitrogen oxides. In the presence of oxygen, the oxidation of HCN via NCO produces NO:

$$HCN + O_2 \rightarrow NCO + OH \quad (R1)$$

$$NCO + OH \rightarrow NO + CO + H \quad (R2)$$

NH_3 may be formed by direct release from the solid matrix or from the hydrogenation of HCN on the char surface. Thus, by adding water vapour to the combustion reaction gas, Schäfer and Bonn[15] found a parallel conversion route through the hydrolysis of HCN into NH_3 (temperature > 650 °C) (R3), followed by a subsequent oxidation reaction (R4):

$$HCN + H_2O \rightarrow NH_3 + CO \quad (R3)$$

$$2NH_3 + 5/2O_2 \rightarrow 2NO + 3H_2O \quad (R4)$$

However, the same authors also found that the parallel formation of NH_3 by hydrolysis (R3) not only led to the formation of NO (R4) at medium temperatures (650–800 °C), but also to the decomposition of NO at elevated temperatures (800–1100 °C) (R5), according to the following reaction:

© 2011 Society of Chemical Industry and John Wiley & Sons, Ltd

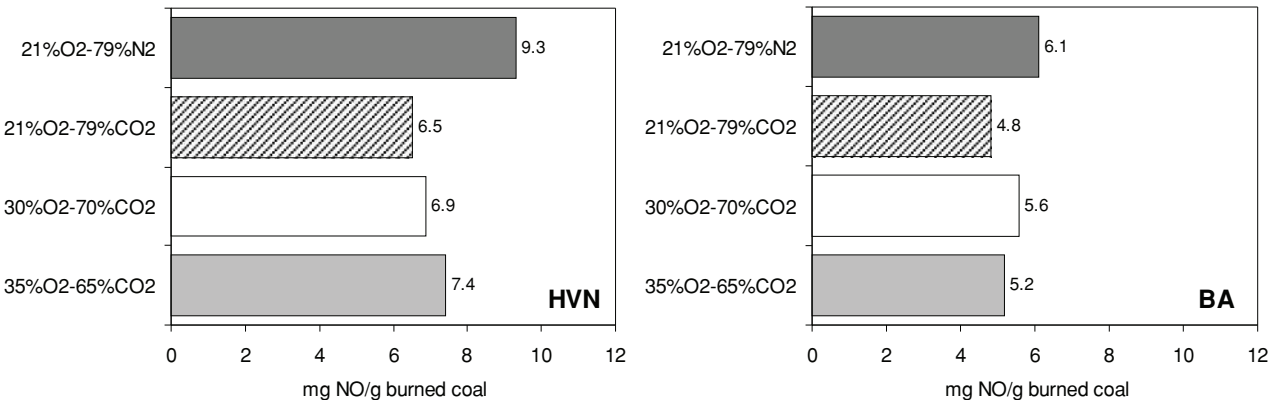

Figure 4. Comparison of NO emissions of the HVN and BA coals under air and oxy-fuel combustion atmospheres at a fuel ratio of 0.8.

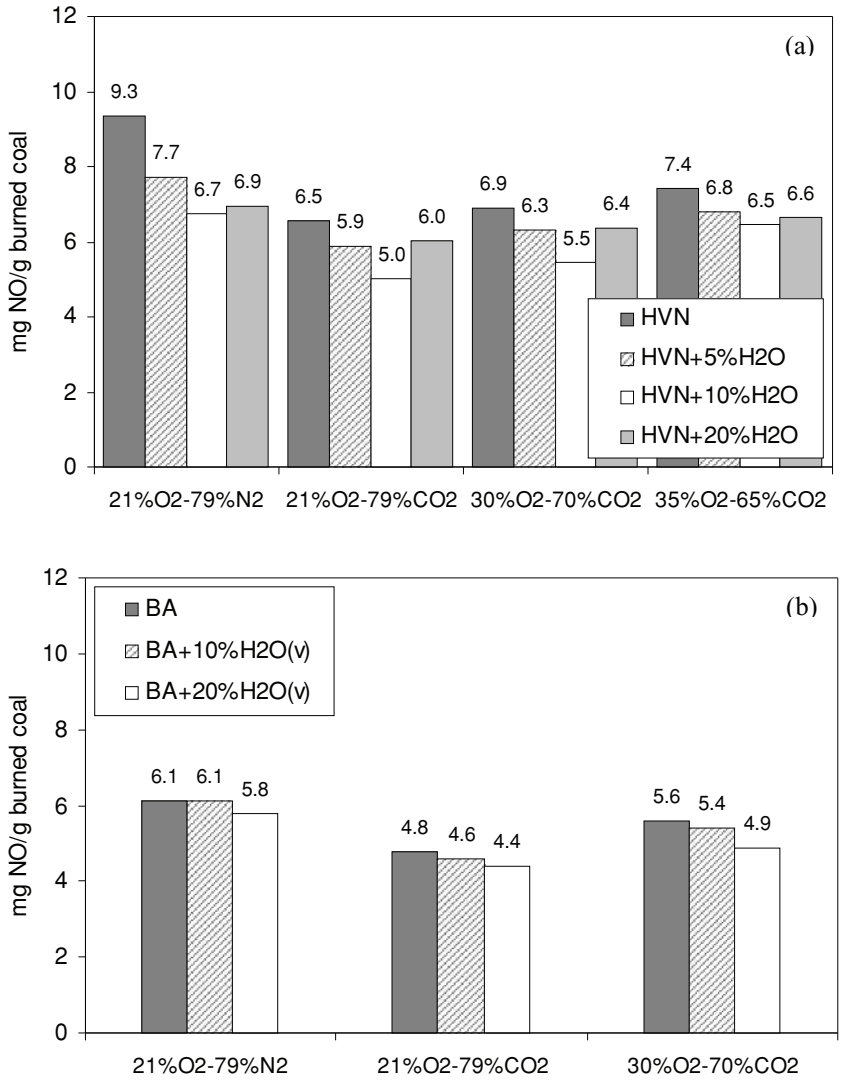

Figure 5. Comparison of NO emissions of the HVN (a) and BA (b) coals under different atmospheres with and without steam at a fuel ratio of 0.8 (the $H_2O(v)$ is added as a substitute for N_2 or CO_2).

© 2011 Society of Chemical Industry and John Wiley & Sons, Ltd

$$NH_3 + NO + 1/4O_2 \rightarrow N_2 + 3/2H_2O \quad (R5)$$

According to Normann *et al.*,[4] HCN and NH_3 react in a series of reactions and finally end up as NH and N, while subsequent reactions, which determine whether NO or N_2 is formed, are heavily dependent on the O/OH/H radical pool, which is related to flame conditions (stoichiometry, temperature, and composition).[3] The oxidation of HCN is controlled primarily by the HCN + OH reaction in case of increasing H_2O concentration. The oxidation of HCN starts at lower temperatures and the conversion of HCN to NO is inhibited by increase in H_2O concentration.[16]

In addition to volatile-N, varying amounts of coal N are retained in the char matrix and only released during the burning of the char. A full understanding of the reaction pathways for the conversion of char-N has not yet been achieved and is still an area of ongoing research.[1] Park *et al.*[17] studied the chemistry of char-N release and its conversion to nitrogen-containing products after reacting with different reactant gases: O_2, CO_2, and H_2O. These authors found that if char-N reacted with O_2, the major species formed were N_2 and NO. NO would be the primary product via the oxidation of the inherent nitrogen char surface species, C(N), (R6), whereas N_2 would result from the subsequent interaction of NO with the char surface (R8), as shown below:

$$C(N) + O_2 \rightarrow NO + CO \text{ and/or } C(O) \quad (R6)$$

Meanwhile, new nitrogen surface species, C(N), would be formed by the reaction of NO with the carbon char surface:

$$2C + NO \rightarrow C(N) + CO \text{ and/or } C(O) \quad (R7)$$

Finally, N_2 would be formed by reaction with the gas-phase NO:

$$C(N) + NO \rightarrow N_2 + CO \text{ and/or } C(O) \quad (R8)$$

Aihara *et al.*[18] and Ashman *et al.*[13] proposed the above reaction mechanism for the formation of N_2 during coal char oxidation. Glarborg *et al.*[3] added that under kinetic control the reaction of char-N with O_2 (R6) is much faster than with NO (R8), whereas at high temperatures the reaction of char-N with O_2 becomes diffusion-limited, favoring the reaction of char-N with NO.

On the other hand, Park *et al.*[17] found that the reaction of char-N with CO_2 mainly produced N_2 with a very high selectivity. During the reaction with CO_2 char-N may be released as NO at short contact times, but this NO would rapidly be reduced to N_2 by reaction with CO (R10), which would be produced from the reaction of the char-C with CO_2 (gasification reaction) (R9):

$$C + CO_2 \rightarrow 2CO \quad (R9)$$

$$NO + CO \rightarrow 1/2N_2 + CO_2 \quad (R10)$$

Park *et al.*[17] also found that if the reactant gas was H_2O, the major species formed were HCN and NH_3, with lower concentrations of N_2. HCN would be the primary product from the reaction of char-N with H_2O, and the other products would result from reactions or interactions of the HCN with the char surface. Therefore, HCN may be released not only from coal devolatilization, but also from char-N when H_2O is added to the reactant gas, since the fate of the char surface nitrogen, C(N), will depend on the availability of hydrogen on the char surface. According to Park *et al.*[17], hydrogen may come from H atoms on the char surface, C(H), or it may be provided by gas phase H_2, gas phase H atoms or steam:

$$C(N) + C(H) \rightarrow C(H,N) \rightarrow HCN \quad (R11)$$

$$C(N) + 1/2H_2 \text{ or } H \rightarrow C(H,N) \rightarrow HCN \quad (R12)$$

The exact nature and structure of the C(H,N) species still requires further elucidation. The formation of HCN becomes greater at higher reaction temperatures; above 900 °C.[19] The fate of the HCN formed from char-N will be determined later by the reactions R3–R5.

On the other hand, the NO may be reduced to form molecular nitrogen in an environment of low oxygen content in which the reduction of NO may occur. The reactants most likely to react with the NO in a reducing environment would be the hydrocarbon radicals formed from the released volatiles (reburning) or char-C. Andersson *et al.*[5] pointed out that the char could play an important role as a catalyst for the destruction of NO, either directly, or by reaction with CO or H_2. The surface-catalyzed reaction between NO and CO was illustrated above by R10.

© 2011 Society of Chemical Industry and John Wiley & Sons, Ltd

Moreover, in the high-temperature regime, the reduction of NO on the char surface may be enhanced by an increase in the concentration of CO, since CO may contribute by removing oxides from the surface of the carbon as follows:[20]

$$C(O) + CO \rightarrow CO_2 + C^* \quad (R13)$$

where C(O) represents a surface carbon oxide and C* a 'free' site, active in the reduction of NO. CO could result from the gasification reaction of coal char with CO_2 (R9), or alternatively the char may also interact with H_2O to form H_2 and additional CO (gasification reaction) (R14):

$$C + H_2O \rightarrow CO + H_2 \quad (R14)$$

In this work, a significantly lower NO concentration was obtained under an oxy-fuel atmosphere with 21% of O_2 than under air conditions (Fig. 4). This was the case both in the steam and steamless atmospheres (Fig. 5), probably due to a higher NO reduction under oxy-fuel conditions as a result of the reaction of NO with CO (R10). Andersson *et al.*[5] found that the formation of NO from fuel-N in oxy-fuel combustion was the same as, or even slightly higher than, in air-firing conditions, whereas the destruction of NO was about 50% greater in oxy-combustion. It can be inferred therefore that the NO emissions during oxy-fuel combustion were lower than those of air-firing due to the increased destruction of NO formed under the O_2/CO_2 atmosphere. Okazaki and Ando[8] also concluded that the reduction of NO to molecular N_2 due to chemical reactions in the combustion zone under oxy-fuel conditions was the main reason for the overall decrease (50–80%) in NO concentration. Liu *et al.*[7] found that the higher CO concentrations inside the oxy-fuel combustion zone and within the vicinity of the combustion particles resulted in a further reduction of NO.

Moreover, Mendiara and Glarborg[21] reported that an increase in the CO_2 concentration affected the concentrations of radicals (O/H/OH), and increased the probability of formation of N_2 from NH_3 (R5) instead of NO (R4). On the other hand, Giménez-López *et al.*[22] concluded that high levels of CO_2 compete with O_2 for atomic hydrogen, through the $CO_2 + H \leftrightarrow CO + OH$ reaction, thereby reducing the formation of chain carriers via $O_2 + H \leftrightarrow O + OH$, thus inhibiting HCN oxidation. These authors also observed a lower HCN combustion in the CO_2 atmosphere, accompanied by a higher level of CO formation and lower NO concentrations than under air combustion.

In our work, gasification of the char with CO_2 (R9) may have contributed to the increase in the production of CO during oxy-fuel combustion. Alternatively, in the flame zone under oxy-fuel conditions, CO_2 may dissociate into CO and O_2 via a strong endothermic reaction as follows:

$$CO_2 \leftrightarrow CO + 1/2O_2 \quad (R15)$$

However, as Toftegaard *et al.*[1] pointed out, there is a difference of opinion among researchers as to whether thermal dissociation (R15) or the gasification reaction (R9) is responsible for the significant increase in CO concentration in oxy-fuel combustion compared to air-firing.

Figure 6 shows the CO concentrations (mg CO/mg burned coal) at the outlet under the different atmospheres studied (at a fuel ratio of 0.8) corresponding to the HVN and BA coals. It can be seen that the CO concentration was higher under the $21\%O_2$–$79\%CO_2$ oxy-fuel atmosphere than under air conditions, surely due to the larger amount of CO produced from reactions R9 and/or R15. Hecht *et al.*[23] showed that CO may be formed by the char reacting with CO_2 in an oxy-combustion environment. If that was the case, the CO produced under oxy-fuel conditions would have reacted with NO (R10), since a lower NO concentration was found under the oxy-fuel atmosphere with 21% of O_2 than under air conditions. It is also possible that incomplete combustion occurred at the lower gas temperatures under oxy-fuel conditions ($21\%O_2$–$79\%CO_2$) leading to the production of additional CO. This would be explained by the high CO concentration observed under the $21\%O_2$–$79\%CO_2$ atmosphere (Fig. 6).

In the presence of steam, the reactions R3 and R15 form additional CO. However, in general, no important differences were found in the CO concentrations after the addition of steam, either under the air or oxy-fuel combustion conditions for the HVN coal (Fig. 6(a)). The differences between the CO concentrations under the different atmospheres studied were also very small for the BA coal (Fig. 6(b)). In fact, the CO reacts with water according to the water gas shift reaction (R17), which probably happened to the CO formed in the atmospheres with steam:[15]

© 2011 Society of Chemical Industry and John Wiley & Sons, Ltd

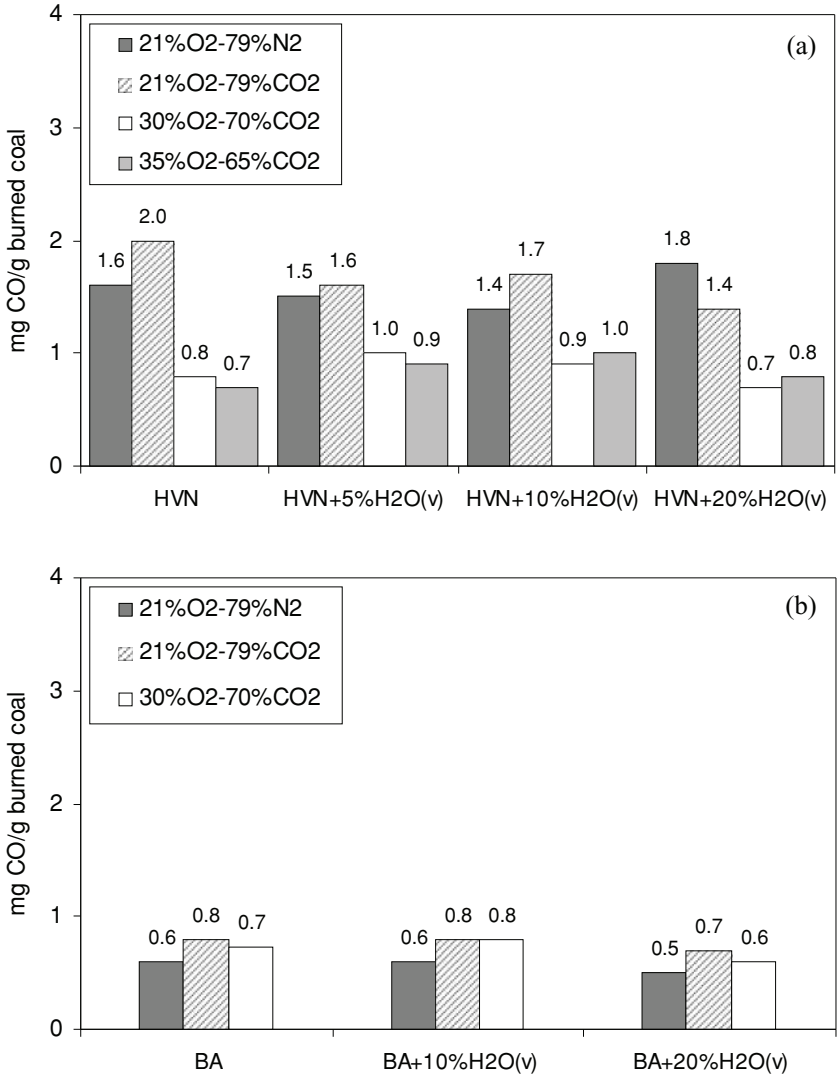

Figure 6. CO emissions of the HVN (a) and BA (b) coals under different atmospheres with and without steam at a fuel ratio of 0.8 (the H_2O(v) is added as a substitute for N_2 or CO_2).

$$CO + H_2O \leftrightarrow H_2 + CO_2 \quad \text{(R16)}$$

Although Figs 4 and 5 show only small differences in the NO concentrations under the oxy-fuel atmospheres with increasing O_2 concentrations, the NO emissions seem to increase slightly with the O_2 concentration. The conversion of fuel-N to NO is expected to grow with the increase in O_2 in the feed gas due to the fact that a higher oxygen concentration in the feed gas causes a significant rise in temperature. Andersson *et al.*[5] found that NO emissions per unit of fuel energy supplied fell under oxy-fuel combustion with 25% of O_2 compared to air-fired conditions. However, they found only small differences in the reduction of NO with the different O_2 concentrations in the feed gas (25, 27, and 29%) under oxy-fuel atmospheres.

As for the addition of water vapor, both under the air and oxy-fuel combustion atmospheres, a decrease in the NO concentration was observed for HVN when steam was added, even though no relevant differences were observed between different steam concentrations (Fig. 5(a)). In the case of the BA coal (Fig. 5(b)), the differences between the NO concentrations under the different atmospheres were very small.

© 2011 Society of Chemical Industry and John Wiley & Sons, Ltd

The lower NO concentration after steam was added would be due to the formation of additional HCN in the presence of H_2O (R12) followed by the formation of NH_3 from HCN (R3), which in turn was due to the presence of H_2O, and subsequent destruction of NO at high temperatures (R5). In the presence of O_2, the HCN and NH_3 produced from H_2O could also have been transformed (R1, R2, and R4) to NO in the gas phase.[5] However, Schäfer and Bonn[15] observed that the rate of NO formation from HCN is delayed at temperatures above 710 °C. Likewise, these authors stated that the reaction of NO with NH_3, formed as an intermediate from HCN, could contribute to the release of N_2 (R5), since NH_3 may lead to an additional formation of NO at medium temperatures but to an additional decomposition of NO at elevated temperatures (800–1100 °C).

In our study, therefore, the NH_3 formed from HCN could have contributed to the reduction of NO concentration under the atmospheres with steam. Moreover, if char gasification with H_2O (R14) had occurred, H_2 had been formed, contributing to the reduction of NO concentration in atmospheres with steam. However, it is thought that this effect was only minor, since no relevant increase in burnout was observed after the addition of steam.

Cao *et al.*,[24] by means of computational fluid dynamics modeling, showed that a high concentration of nitrogen intermediates in the combustion zone – which can be achieved by wet recycling due to the presence of H_2O – favors the reduction of NO. Payne *et al.*[25] observed that the reduction of NO through reburning appeared to be greater in a wet recycle than in a dry one. Stadler *et al.*[10] found lower NO_x emissions in wet oxy-fuel conditions than in dry oxy-fuel combustion after the numerical simulation of the NO behavior. This is because less fuel-N is converted to NO in wet oxy-fuel conditions, as water vapour prevents the oxidation of intermediates from forming NO, and favors the reduction of NO from these intermediates. These authors also found that an increased oxygen concentration could undermine the positive effect that the increased water concentration would have on the NO emissions, as it is suggested in our study. The findings of our work also showed that the addition of CO_2 was more effective in reducing NO emissions than H_2O, in agreement with the results of Park *et al.*[26]

Conclusions

NO emissions were lower during oxy-fuel combustion than in air-firing due to a higher reduction of NO by reaction with CO. A slight increasing trend in NO emissions was observed as the O_2 concentration increased in the oxy-fuel atmospheres. However, the NO concentration fell when steam was added, both under the air and under the oxy-fuel atmospheres, but no relevant differences between the different steam concentrations were observed. This would be due to the lower formation of NO, since steam prevents the oxidation of intermediates from forming NO, and the higher reduction of NO by reaction with these intermediates, whose formation increases in the presence of steam.

Acknowledgements

Work carried out with financial support from the Spanish MICINN (Project PS- 120000-2005-2) co-financed by the European Regional Development Fund. L.A. and J.R. acknowledge funding from the CSIC JAE program, co-financed by the European Social Fund, and the Asturias Regional Government (PCTI program), respectively.

References

1. Toftegaard MB, Brix J, Jensen PA, Glarborg P and Jensen AD, Oxy-fuel combustion of solid fuels. *Prog Energ Combust* **36**:581–625 (2010).
2. Balat M, Influence of coal as an energy source on environmental pollution. *Energy Sources Part A-Recovery Util Environ Eff* **29**:581–589 (2007).
3. Glarborg P, Jensen AD and Johnsson JE, Fuel nitrogen conversion in solid fuel fired systems. *Prog Energ Combust* **29**:89–113 (2003).
4. Normann F, Andersson K, Leckner B and Johnsson F, Emission control of nitrogen oxides in the oxy-fuel process. *Prog Energ Combust* **35**:385–397 (2009).
5. Andersson K, Normann F, Johnsson F and Leckner B, NO emission during oxy-fuel combustion of lignite. *Ind Eng Chem Res* **47**:1835–1845 (2008).
6. Croiset E and Thambimuthu KV, NO_x and SO_2 emissions from O_2/CO_2 recycle coal combustion. *Fuel* **80**:2117–2121 (2001).
7. Liu H, Zailani R and Gibbs BM, Comparisons of pulverized coal combustion in air and in mixtures of O_2/CO_2. *Fuel* **84**:833–840 (2005).
8. Okazaki K and Ando T, NO_x reduction mechanism in coal combustion with recycled CO_2. *Energy* **22**:207–215 (1997).
9. Tan Y, Croiset E, Douglas MA and Thambimuthu KV, Combustion characteristics of coal in a mixture of oxygen and recycled flue gas. *Fuel* **85**:507–512 (2006).
10. Stadler H, Christ D, Habermeh M, Heil P, Kellermann A, Ohiger A *et al.*, Experimental investigation of NO_x emissions in oxycoal combustion. *Fuel* **90**:1604–1611 (2011).

© 2011 Society of Chemical Industry and John Wiley & Sons, Ltd

11. Le Cong T and Dagaut P, Experimental and detailed modeling study of the effect of water vapor on the kinetics of combustion of hydrogen and natural gas, impact on NO*x*. *Energ Fuel* **23**:725–734 (2009).
12. Smart JP, O'Nions P and Riley GS, Radiation and convective heat transfer, and burnout in oxy-coal combustion. *Fuel* 89:2468–2476 (2010).
13. Ashman PJ, Haynes BS, Nicholls PM and Nelson PF, Interactions of gaseous NO with char during the low-temperature oxidation of coal chars. *Proc Combust Inst* **28**:2171–2179 (2000).
14. Wargadalam VJ, Löffler G, Winter F and Hofbauer H, Homogeneous formation of NO and N_2O from the oxidation of HCN and NH_3 at 600–1000 °C. *Combust Flame* **120**:465–478 (2000).
15. Schäfer S and Bonn B, Hydrolysis of HCN as an important step in nitrogen oxide formation in fluidised combustion. Part 1: Homogeneous reactions. *Fuel* **79**:1239–1246 (2000).
16. Shoji M, Yamamoto T, Tanno S and Aoki H, Miura T, Modeling study of homogeneous NO and N_2O formation from oxidation of HCN in a flow reactor. *Energy* **30**:337–345 (2005).
17. Park D-C, Day SJ and Nelson PF, Nitrogen release during reaction of coal char with O_2, CO_2 and H_2O. *Proc Combust Inst* **30**:2169–2175 (2005).
18. Aihara T, Matsuoka K, Kyotani T and Tomita A, Mechanism of N_2 formation during coal char oxidation. *Proc Combust Inst* **28**:2189–2195 (2000).
19. Orikasa H, Matsuoka K, Kyotani T and Tomita A, HCN and N_2 formation mechanism during NO/char reaction. *Proc Combust Inst* **29**:2283–2289 (2002).
20. Aarna I and Suuberg EM, A review of the kinetics of the nitric oxide-carbon reaction. *Fuel* **76**:475–491 (1997).
21. Mendiara T and Glarborg P, Ammonia chemistry in oxy-fuel combustion of methane. *Combust Flame* **156**:1937–1949 (2009).
22. Giménez-López J, Millera A, Bilbao R and Alzueta MU, HCN oxidation in an O_2/CO_2 atmosphere: An experimental and kinetic modeling study. *Combust Flame* **157**:267–276 (2010).
23. Hecht ES, Shaddix CR, Molina A, Haynes BS, Effect of CO_2 gasification reaction on oxy-combustion of pulverized coal char. *Proc Combust Inst* **33**:1699–1706 (2011).
24. Cao H, Sun S, Liu Y and Wall TF, Computational fluid dynamics modelling of NO_x reduction mechanism in oxy-fuel combustion. *Energ Fuel* **24**:131–135 (2010).
25. Payne R, Chen SL, Wolsky AM and Richter WF, CO_2 recovery via coal combustion in mixtures of oxygen and recycled flue gas. *Combust Sci Technol* **67**:1–16 (1989).
26. Park J, Kim S-G, Lee K-M and Kim TK, Chemical effect of diluents on flame structure and NO emission characteristic in methane-air counterflow diffusion flame. *Int J Energy Res* **26**:1141–1160 (2002).

Juan Riaza

Juan Riaza is a mining engineer and has an MSc in Energy Engineering from the University of Oviedo. He has recently been awarded a PhD grant to conduct his thesis on the subject of co-combustion of coal and biomass under oxyfuel conditions.

Lucía Álvarez

Lucía Álvarez received her MSc in Chemical Engineering from the University of Oviedo in 2008. She is undertaking her PhD studies at INCAR-CSIC in Oviedo. Her research interests involve oxy-fuel combustion modelling by means of Computational Fluid Dynamics techniques.

Victoria Gil

Victoria Gil received her PhD in Environmental Sciences from the University of León, Spain, in 2007. She has been working as a postdoctoral researcher at the INCAR-CSIC since 2009. Her research interests embrace energy production from renewable and fossil fuels, and the gasification of coal and biomass.

José J. Pis

José J. Pis was awarded a PhD from Oviedo University in 1976. He joined the INCAR-CSIC in 1979. He was Head of Department, and also Vice Director until 1995. In 1999, he became a Research Professor. His research involves from the characterization of carbon materials and the design and optimization of pilot scale reactors.

Covadonga Pevida

Covadonga Pevida graduated with a PhD from Oviedo University in 2004. Following her postdoctoral work at the Universities of Lyon and Nottingham, she secured a position as Tenured Scientist at the INCAR-CSIC in 2008. Her main lines of research involve carbon capture by adsorption processes and oxycoal combustion.

Fernando Rubiera

Fernando Rubiera received his PhD from Oviedo University in 1991. He is currently a Research Scientist and Head of the Department of Energy & Environment at the INCAR-CSIC. His main research interests embrace the co-utilization of coal and biomass, and pre- and post-combustion carbon capture from coal.

© 2011 Society of Chemical Industry and John Wiley & Sons, Ltd

6. Efecto de la adición de biomasa en oxicombustión

La biomasa es un combustible que puede sustituir parcialmente al carbón con modificaciones menores en las calderas convencionales, siendo por tanto viable la cocombustión también en oxicombustión. El combustible biomásico suele tener menor poder calorífico que la mayoría de los carbones, por tanto la energía liberada en la caldera por masa de combustible alimentado es menor. Esto puede dar lugar a una menor potencia de la caldera si no se modifica adecuadamente el sistema de alimentación.

Por otra parte la biomasa libera gran cantidad de volátiles. Como se ha indicado en el Capítulo 3, la combustión de los volátiles de la biomasa requiere tiempos más largos que la combustión del *char*, lo que constituye la diferencia más importante entre la combustión de carbón y biomasa. La biomasa presenta además un rendimiento en volátiles mucho mayor que los carbones, en condiciones de elevadas velocidades de calentamiento y elevadas temperaturas. Esto condiciona la velocidad de reacción global. La liberación de una mayor cantidad de volátiles debido a la adición de biomasa, provoca cambios en los fenómenos de ignición y en el transcurso de las reacciones de combustión, lo que repercutirá en la estabilidad de la llama, la temperatura, el grado de quemado y las emisiones contaminantes. Además, la reactividad del *char* de biomasa es también mayor que la del carbón. Los estudios de cocombustión en aire así como algunos trabajos previos llevados a cabo en nuestro Grupo de Investigación [Arias, 2008] alentaron a profundizar en los efectos que induce la adición de biomasa durante la oxicombustión con carbón.

En los tres artículos que conforman este Capítulo se presentan los resultados correspondientes a experimentos de oxicombustión de mezclas de carbón y biomasa en distintos dispositivos experimentales (termobalanza y reactor de flujo en arrastre). Se han llevado a cabo estudios de ignición y combustión de carbones individuales y sus mezclas con biomasa en distintas proporciones, y se ha evaluado el efecto inducido sobre el grado de quemado y las emisiones de NO.

En el primer artículo (Publicación VII) se ha aplicado la termogravimetría para evaluar el efecto de la adición de vapor durante experimentos de oxicombustión de mezclas de carbón y biomasa. El efecto combinado de la biomasa y el vapor de agua es muy novedoso ya que no se encuentran estudios en la bibliografía donde se haya evaluado su efecto de manera conjunta en atmósferas de oxicombustión.

El segundo artículo (Publicación VIII) de este Capítulo describe la ignición de mezclas de carbón y biomasa en atmósferas de oxicombustión. Este estudio se realizó en el reactor de

flujo en arrastre. Se realiza un estudio de la ignición por métodos indirectos, mediante el seguimiento de los gases a la salida del reactor. Este método fue descrito por Essenhigh [Essenhigh, 1989] para la ignición de partículas de carbón en flujo de aire, sin embargo, es perfectamente extrapolable a las atmósferas de oxicombustión. Esta metodología fue empleada también en este mismo reactor en estudios de combustión en aire de carbones de distinto rango [Faúndez, 2005].

El tercer artículo (Publicación IX) que compone este Capítulo expone los resultados de la oxicocombustión de mezclas de carbón y biomasa, en el reactor de flujo en arrastre. Este estudio se realizó determinando el grado de quemado y las emisiones de NO, para diferentes excesos de oxígeno, con proporciones de biomasa en la alimentación de 0, 10 y 20 % en masa. El grado de conversión alcanzado en la combustión depende del tiempo de residencia del combustible en las zonas de altas temperaturas y del tamaño de partícula. En los experimentos realizados, estos parámetros se mantuvieron constantes, por lo que el único parámetro que afectará al grado de conversión será el porcentaje de biomasa en la mezcla y el exceso de oxígeno. A medida que aumenta el exceso de oxígeno, aumenta la disponibilidad de O_2 y consecuentemente el grado de quemado o *burnout*.

Las emisiones de NO_x tienen relevancia en oxicombustión no solamente por su posible emisión a la atmósfera que podría ser evitada con los sistemas de control de NO_x, sino también por su efecto corrosivo en los sistemas de transporte de CO_2. El perjuicio en bombas y tuberías de transporte e inyección hace que su concentración deba ser controlada y evitada. En ausencia de aire, el nitrógeno del combustible será la principal fuente para formación de NO_x y, por tanto, se denota un acusado descenso de las emisiones respecto al aire. Sin embargo la cantidad de nitrógeno presente en el combustible no es el único parámetro influyente. Este hecho se comprobó en la Publicación VI, en la que el carbón bituminoso, con una mayor proporción de nitrógeno que la semiantracita, dio lugar a unas concentraciones menores de NO en todas las atmósferas de oxicombustión. Esto se debe a la diferente distribución del nitrógeno entre los volátiles y el *char*, y su liberación en la forma de NH_3 y HCN. Esta distribución es muy distinta en los combustibles biomásicos y presentan un elevado potencial de reducción de las emisiones de NO cuando se mezclan con carbón.

6.1 Compendio de resultados

El análisis térmico es muy útil, ya que es relativamente sencillo y de rápida aplicación, y sólo se necesita una pequeña cantidad de muestra. De esta forma, se han podido llevar a cabo comparaciones en cuanto a las propiedades de combustibilidad, de distintos carbones y sus mezclas con biomasa en distintas atmósferas de combustión, aire y $O_2/CO_2/H_2O_{(V)}$. Los resultados obtenidos a partir de los ensayos realizados en termobalanza han permitido concluir que la adición de biomasa da lugar a una mejora en la combustibilidad, respecto a la combustión del carbón, tanto en aire como en las atmósferas de oxicombustión.

Todos los carbones y sus mezclas con biomasa mostraron un empeoramiento en sus propiedades de combustibilidad al sustituir N_2 por CO_2, para la misma concentración de oxígeno (21 %). Sin embargo, se observó una mejora en atmósferas O_2/CO_2 con un contenido en oxígeno del 30 %, con respecto a lo observado en aire.

El efecto de la presencia de vapor de agua en la corriente oxidante, en los ensayos llevados a cabo en termobalanza, se traduce en un ligero aumento de la combustibilidad, con un incremento en la velocidad de pérdida de masa, y un acortamiento en los tiempos de quemado. Sin embargo, no se observan grandes diferencias entre proporciones del 10 y 20 % de vapor de agua. Estas observaciones al sustituir CO_2 por vapor de agua en condiciones de oxicombustión, se contraponen a los resultados obtenidos en la combustión en reactor de flujo en arrastre mostrados en la Publicación V. Esto es debido, fundamentalmente, a que las condiciones en la termobalanza difieren mucho de las del reactor de flujo en arrastre, que son más cercanas a las existentes en una caldera industrial en lo referente a velocidades de calentamiento, transmisión de calor o tiempos de residencia. Por otro lado, estas divergencias confirman que el efecto del vapor en la oxicombustión se relaciona con diferencias en la transmisión de calor más que con reacciones de gasificación para las condiciones estudiadas.

La termogravimetría sigue siendo una técnica muy útil a la hora de realizar un análisis preliminar del comportamiento de distintos combustibles en condiciones de oxicombustión, pero es necesario llevar a cabo experimentos en otros dispositivos, que puedan reproducir de forma más adecuada las condiciones de operación de una caldera industrial. Por ello, se han realizado experimentos en un reactor de flujo en arrastre, el cual reproduce de forma más adecuada algunas de las condiciones existentes en una caldera de carbón pulverizado.

El efecto de distintas atmósferas de oxicombustión sobre las propiedades de ignición y de combustión de mezclas de carbones de distinto rango y biomasa, se ha estudiado en un reactor de flujo en arrastre. Al igual que en los experimentos de ignición del carbón, en las mezclas de carbón y biomasa se observó un empeoramiento en las propiedades de ignición en la atmósfera $21\%O_2/79\%CO_2$, en comparación con la ignición en aire. Estas propiedades mejoran con respecto a la ignición en aire, al aumentar la concentración de oxígeno en la

mezcla O_2/CO_2 por encima del 30 %, con la misma tendencia observada para los carbones individuales.

La sustitución del 10 y 20 % de carbón por biomasa produce un descenso en la temperatura de ignición tanto en aire como en todas las atmósferas de oxicombustión respecto al carbón.

En lo referente al proceso de combustión global de las mezclas de carbón y biomasa, se estudió la sustitución de N_2 por CO_2 para la misma concentración de oxígeno (21 %), sobre el grado de conversión. Se observó una disminución en el grado de conversión, debido a las diferencias en las propiedades físicas de ambos gases. La biomasa libera gran cantidad de volátiles, produciendo un efecto positivo en la combustión del carbón; adelantando el inicio de la combustión de la mezcla y aumentando la temperatura de las partículas. De este modo se facilita la combustión del *char* y se obtienen conversiones más elevadas.

Este efecto es más notable en el carbón de alto rango que en el carbón bituminoso de alto contenido en volátiles, ya que este alcanza un grado de quemado elevado antes de la adición de biomasa.

Asimismo, se observó una disminución en las emisiones de NO, debido a la reducción heterogénea de NO a N_2, favorecida por el aumento en la concentración de CO en la atmósfera de oxicombustión. Al aumentar la concentración de oxígeno por encima del 30 % mejora el grado de quemado, pero también aumenta la producción de óxidos de nitrógeno. No obstante, la cantidad de NO por gramo de combustible quemado (o unidad de energía producida) sigue siendo menor que la producida en aire.

6.2 Publicaciones relacionadas

VII **A study of oxy-coal combustion with steam addition and biomass blending by thermogravimetric analysis.**
M.V. Gil, J. Riaza, L. Álvarez, C. Pevida, J.J. Pis, F. Rubiera. Journal of Thermal Analysis and Calorimetry 2012. 109 (1) pp. 49 – 55. doi:10.1007/s10973-011-1342-y

VIII **Ignition behaviour of coal and biomass blends under oxyfiring conditions with steam additions.**
J. Riaza, , L. Álvarez, M.V. Gil, R. Khatami, Y.A. Levendis, J.J. Pis, C. Pevida, F. Rubiera. Greenhouse Gases: Science and Technology 2013. 3 (5), pp. 397-414. doi:10.1002/ghg.1368

IX **Oxy-fuel combustion of coal and biomass blends.**
J. Riaza, M.V. Gil, L. Álvarez, C. Pevida, J.J. Pis, F. Rubiera. Energy 2012. 41 (1) pp. 429 – 435. doi: 10.1016/j.energy.2012.02.057

6.2.1 *Publicación VII*

A study of oxy-coal combustion with steam addition and biomass blending by thermogravimetric analysis.

M.V. Gil, J. Riaza, L. Álvarez, C. Pevida, J.J. Pis, F. Rubiera.
Journal of Thermal Analysis and Calorimetry
2012. 109 (1) pp. 49 – 55.
doi:10.1007/s10973-011-1342-y

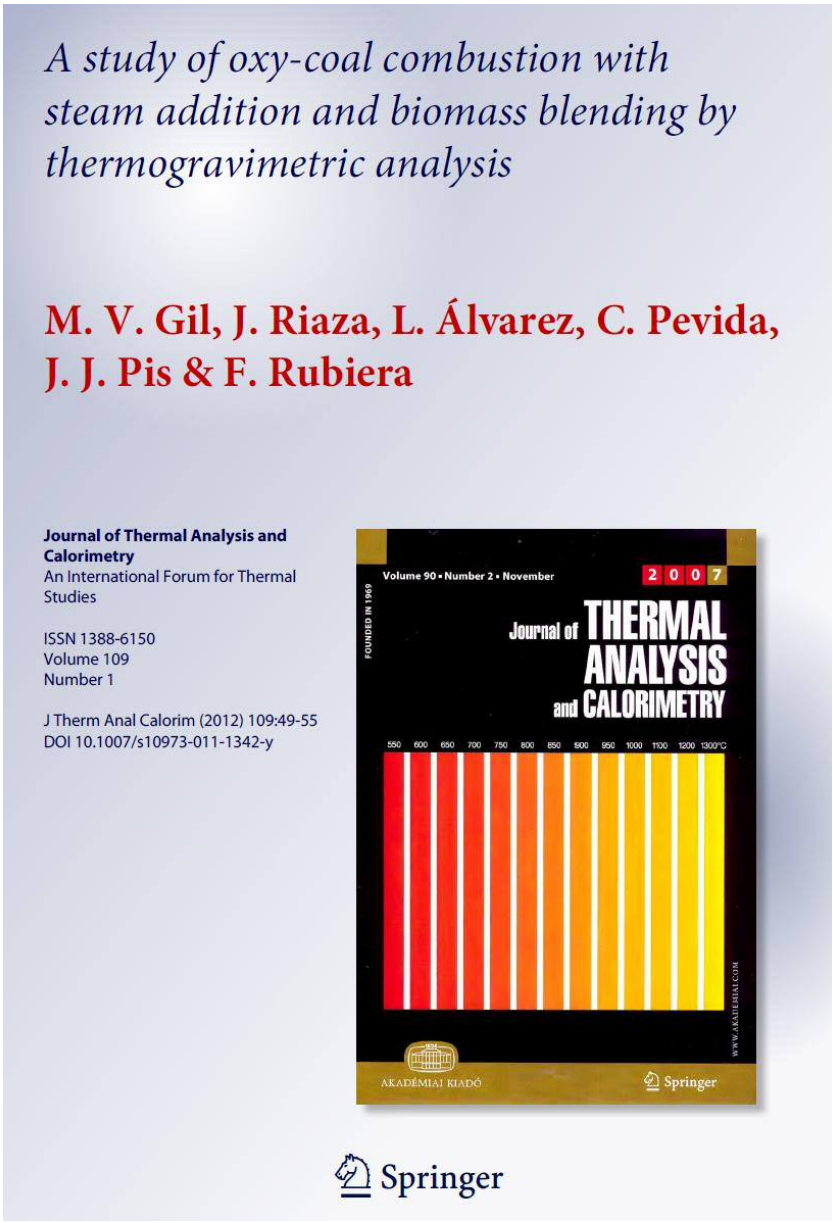

J Therm Anal Calorim (2012) 109:49–55
DOI 10.1007/s10973-011-1342-y

A study of oxy-coal combustion with steam addition and biomass blending by thermogravimetric analysis

M. V. Gil · J. Riaza · L. Álvarez · C. Pevida · J. J. Pis · F. Rubiera

Received: 23 November 2010 / Accepted: 11 January 2011 / Published online: 12 February 2011
© Akadémiai Kiadó, Budapest, Hungary 2011

Abstract The thermal characteristics of pulverized coal have been studied under oxy-fuel combustion conditions using non-isothermal thermogravimetric analysis (TG). The atmospheres used were 21%O_2/79%N_2, 21%O_2/79%CO_2, 30%O_2/70%O_2, and 35%O_2/65%CO_2. Coal blends of coal with 10 and 20% of biomass were also studied under these atmospheres. The addition of 10 and 20% of steam was evaluated for the oxy-fuel combustion atmospheres with 21 and 30% of O_2 in order to study the effect of the wet recirculation of flue gas. The results obtained were similar for all the different rank coals and indicated that replacing N_2 by CO_2 in the combustion atmosphere with 21% of O_2 caused a slight decrease in the rate of mass loss and delayed the burning process of the coal, biomass and coal/biomass blend samples. When the O_2 concentration was increased to 30 and 35% in the oxy-fuel combustion atmosphere, the rate of mass loss increased, the burning process occurred at lower temperatures and it was shorter in duration. An increase in the rate of mass loss and a reduction in burning time and temperature were observed after the addition of steam to the oxy-fuel combustion atmosphere. No relevant differences between the 10 and 20% steam concentrations were observed.

Keywords Oxy-fuel combustion · Pulverized coal · Biomass · Steam · TG

M. V. Gil · J. Riaza · L. Álvarez · C. Pevida · J. J. Pis · F. Rubiera (✉)
Instituto Nacional del Carbón, CSIC, Apartado 73, 33080 Oviedo, Spain
e-mail: frubiera@incar.csic.es

Introduction

Interest in coal as an energy source for the future has recently been revived due to the stability of its supply and it is relatively low cost. For these reasons, it is likely that coal will occupy an important position in the energy mix in the foreseeable future [1, 2]. However, the emissions of greenhouse gas carbon dioxide from coal-fired power plants are very high and their effect on global climate change has been acknowledged worldwide. Various strategies for their reduction and sequestration are under study, including improvements in the efficiency of existing power plants, the introduction of advanced combined cycle power plants and the capture and storage of CO_2 [3].

Carbon capture and storage (CCS) is considered one of the most realistic options for reducing CO_2 emissions from fossil fuel use, particularly from large-scale stationary power plants. The main problem, however, is that the combustion of fossil fuel in air leads to a diluted concentration of CO_2 in the flue gas stream (typically 15% by volume), rendering it unsuitable for direct sequestration in a supercritical state by compression, a process which requires a high concentration of CO_2 [4, 5].

As an alternative, oxy-fuel combustion is considered as a promising new approach for CO_2 capture. Oxy-fuel combustion technology involves the combustion of pulverized coal in a mixture of oxygen (as opposed to air) and recirculated flue gas (mainly CO_2 and H_2O). The advantages of this approach are that it offers a way of avoiding the excessively high flame temperatures characteristic of fuel combustion in oxygen, carries the heat through the boiler, reduces the net volume of flue gas and substantially increases the concentration of carbon dioxide in the flue gas. A flue gas consisting mainly of CO_2 (80–95% by volume) and water vapour is then generated. The water

vapour can be easily removed by condensation, making it easier to purify the remaining CO_2 [6].

The successful implementation of O_2/CO_2 technology in conventional pulverized coal boilers depends on a full understanding of the changes that result from replacing N_2 with CO_2 in the oxidizer stream [7]. Although many published works have focused on the oxy-fuel combustion process [8–12], the effect of adding steam to the oxy-fuel combustion atmosphere has hardly been studied [13].

Alternatively, biomass is a renewable fuel which can be used for reducing CO_2 emissions. This source of energy is considered carbon neutral because the carbon dioxide released during biomass utilization is recycled as an integral part of the carbon cycle. The combination of oxy-fuel combustion with biomass could be used as a sink for CO_2, and therefore more knowledge about cofiring coal and biomass under oxy-fuel conditions is needed [14].

Thermogravimetric analysis (TG) is one of the most common techniques used to rapidly investigate and compare thermal events during the combustion and pyrolysis of solid raw materials, such as coal, woods, etc. [15–22]. Although extrapolation to other devices at a larger scale cannot be performed directly, the information obtained from the combustion profiles in the TG could be used for an initial evaluation of the behaviour of the combustion on an industrial scale [23]. This would contribute to an understanding of coal combustion behaviour and prove very useful both from a fundamental viewpoint and for the comparison of samples [24].

In this work, TG was used in order to study the effect of replacing N_2 with CO_2 in a combustion atmosphere and of enhanced levels of O_2 in an oxy-fuel combustion atmosphere upon the thermal characteristics of different rank coals and coal/biomass blends. Oxy-fuel combustion with steam addition was also evaluated in order to study the effect of the wet recirculation of flue gas.

Materials and methods

Materials

Ten coals of different rank [25] were used in this work: an anthracite (AC), a semi-anthracite (HVN), two medium-volatile bituminous coals (UM and SAA), and six high-volatile bituminous coals (DAB, SAB, M6N, BA, CAB, and NZ). A biomass, olive waste (OW), was also employed. The samples were ground and sieved to obtain a particle size fraction of 75–150 μm. The proximate analysis and the high heating value of the samples are presented in Table 1.

Apparatus and procedure

The techniques employed in this study were TG and derivative thermogravimetry (DTG). Non-isothermal TG was performed using a Setaram TAG24 analyser. Approximately, 5 mg of sample was used for each experiment. A small amount of sample and a slow heating rate were used to avoid heat transfer limitations and to minimize mass transfer effects. The samples were heated at a heating rate of 15 °C min^{-1} in different atmospheres from room temperature to 1000 °C. The simulated air combustion atmosphere was 21%O_2/79%N_2. Three O_2/CO_2 oxy-fuel combustion conditions were used (21, 30, and 35% of O_2). The addition of 10 and 20% of steam (as a replacement for CO_2) to an oxy-fuel combustion atmosphere containing 21 and 30% of O_2 was also evaluated in order to

Table 1 Proximate analysis and high heating value of the coals

Sample	AC	HVN	UM	SAA	DAB	SAB	M6N	BA	CAB	NZ	OW
Origin	Spain	Spain	Mexico	South Africa	China	South Africa	Mexico	Spain	Colombia	New Zealand	Spain
Rank	an	sa	mvb	mvb	hvb	hvb	hvb	hvb	hvb	hvb	–
Proximate analysis[a]											
Moisture content/wt%	2.3	1.1	0.4	2.6	2.9	2.4	1.8	1.2	4.3	11.5	9.2
Ash/wt%, db	14.2	10.7	21.1	14.9	10.9	15.0	30.2	6.9	4.4	2.9	7.6
V.M./wt%, db	3.6	9.2	23.7	25.6	28.8	29.9	30.6	33.9	39.6	47.9	71.9
F.C./wt%, db[b]	82.2	80.1	55.2	59.5	60.3	55.1	39.2	59.2	56.0	49.2	20.5
High heating value/kJ kg^{-1}, db	29160	31818	27826	27952	28825	27780	23057	33081	30965	27943	19905

an anthracite, *sa* semi-anthracite, *mvb* medium-volatile bituminous coal, *hvb* high-volatile bituminous coal, *db* dry basis

[a] The proximate analysis was conducted in a LECO TGA-601

[b] Calculated by difference

study the effect of the wet recirculation of flue gas. The total flow rate of all the mixtures of gases was 150 cm^3 min^{-1}. The steam generator consisted of a CEM® (Controlled Evaporator and Mixer), in which water and O_2/CO_2 were mixed and heated up to 175 °C. Liquid and mass flow controllers were used to control the flow rates of the water, O_2, CO_2, and N_2. The derivative curves (DTG) of the samples were represented as a function of temperature.

Determination of the combustion parameters

From the combustion profiles, the following thermal parameters were calculated for characterizing the combustion process: initial temperature (T_i), final temperature (T_f), peak temperature (T_{peak}), temperature corresponding to a conversion degree of 50% (T_{50}), maximum rate of mass loss (DTG_{max}), average rate of mass loss (Average DTG), and coal reactivity index (R_C). The initial temperature (T_i) and the final temperature (T_f) were taken as the temperature values (after the initial loss of moisture) at which the rate of mass loss was 1% min^{-1}. The peak temperature (T_{peak}) corresponds to the temperature at which maximum rate of mass loss occurs [26]. The temperature value at the maximum rate of mass loss is usually considered inversely proportional to the reactivity and combustibility of the sample [27], whereas the maximum rate of mass loss is considered directly proportional to the reactivity of the sample [28]. The average rate of mass loss (Average DTG) is the ratio between the burnout fraction and time during the temperature range of initial to final temperature. The coal reactivity index (R_C) was used to evaluate the burning performance of pulverized coal, defined as:

$$R_C = 1/m_0(dm/dt)_{max} \quad (1)$$

where $(dm/dt)_{max}$ is the maximum combustion rate, and m_0 is the initial mass of ash free sample. It should be noted that the greater the R_C value, the higher the combustion reactivity.

Results and discussion

Combustion characteristics of pulverized coal under air and O_2/CO_2 atmospheres

DTG curves for the AC, HVN, DAB, and NZ coal samples under the different combustion and oxy-fuel combustion atmospheres are shown as example in Fig. 1. The DTG curves for the other coals (not represented) showed similar behaviour. From the combustion profiles (Fig. 1), it can be seen that coal combustion in the O_2/N_2 atmosphere differed from that in the O_2/CO_2 atmosphere at the same oxygen concentration (21%). For all the coals studied in the $21\%O_2/79\%CO_2$ atmosphere, the curves of mass loss rate shifted to higher temperatures in relation to those in the $21\%O_2/79\%N_2$ conditions. This implies that there was a delay in the burning process, which may have been due to the higher specific heat of CO_2 compared to N_2, leading to comparatively lower gas temperatures and in turn to a reduction of the fuel particle temperatures during oxy-fuel combustion in comparison to combustion in air. Li et al. [6] found lower rates of mass loss and higher burning times for a bituminous coal after replacing N_2 with CO_2 from an air atmosphere, indicating that the devolatilization rate of coal was lower under a CO_2 atmosphere than under a N_2 atmosphere. These authors thus concluded that replacing N_2 with CO_2 was unfavourable to coal combustion.

On the other hand, if the oxygen concentration was increased under the oxy-fuel combustion atmospheres ($30\%O_2/70\%CO_2$ and $35\%O_2/65\%CO_2$), the DTG curves moved to lower temperatures, and the rate of mass loss increased whereas the burning time decreased in comparison to the values achieved in the $21\%O_2/79\%N_2$

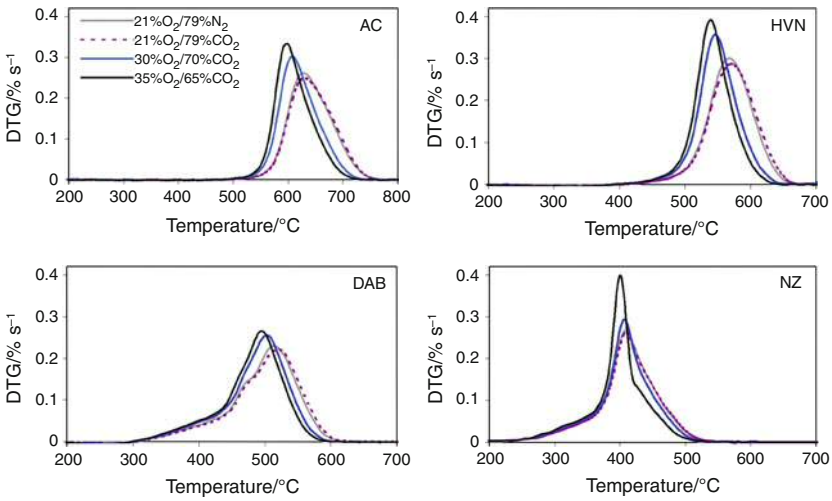

Fig. 1 DTG curves for coal combustion under different atmospheres

combustion atmosphere (Fig. 1). This may be because a higher oxygen concentration enhances the devolatilization and combustion of coal samples. Under a lower oxygen concentration, the ignition of both the volatile matter and char would be retarded [8].

Table 2 summarizes the combustion parameters for the AC, HVN, DAB, and NZ coals, whose results are similar to those of the other coals studied. It can be seen that the initial temperature, T_i, for the coal samples was similar or slightly higher under oxy-fuel combustion atmosphere with 21% of O_2 compared to air. However, T_i decreased as the O_2 concentration increased in the O_2/CO_2 atmosphere. The same tendency is observed for the final temperature, T_f, the peak temperature, T_{peak}, and the temperature corresponding to a conversion degree of 50%, T_{50}. In contrast, the Average DTG and DTG_{max} values followed the opposite tendency. They were slightly lower under the air atmosphere than under the oxy-fuel atmosphere containing 21% of O_2, but they increased as the O_2 concentration increased in the O_2/CO_2 atmosphere. Table 2 also shows that, in general, the coal reactivity index (R_C) in the 21%O_2/79%CO_2 atmosphere was slightly lower than that in the 21%O_2/79%N_2 atmosphere, but was higher in the 30%O_2/70%CO_2 and 35%O_2/65%CO_2 atmospheres, these two atmospheres showing similar values of coal reactivity.

If the characteristic temperatures for all the different rank coals are compared, the order is the following: AC > HVN > UM = BA > SAB = SAA ≥ DAB > CAB ≥ M6N > NZ. This order approximately coincides with that of coal rank (Table 1).

Combustion characteristics of biomass and coal/biomass blends under air and O_2/CO_2 atmospheres

Figure 2 shows the DTG curves for the biomass sample, OW, and the coal/biomass blends under the oxy-fuel combustion atmospheres. From the combustion profiles (Fig. 2), it can be seen that the combustion of the OW, 90%HVN + 10%OW, and 80%HVN + 20%OW samples in the O_2/N_2 atmosphere differed from that of the O_2/CO_2 atmosphere at the same oxygen concentration (21%). As in the case of the coals, in the 21%O_2/79%CO_2 atmosphere, the curves of mass loss rate shifted to higher temperatures in relation to those in the 21%O_2/79%N_2 conditions, indicating that there was a delay in the combustion process. However, for the biomass and coal/biomass blend samples, when the oxygen concentration was increased under the oxy-fuel combustion atmospheres (30%O_2/70%CO_2 and 35%O_2/65%CO_2), the DTG curves moved to lower temperatures, the rate of mass loss increased and the burning time decreased with respect to the corresponding parameters in the 21%O_2/79%N_2 combustion atmosphere.

Figure 2 also shows that an initial mass loss occurred between 25–105 °C for all the samples, due to moisture evaporation, after which two mass loss stages occurred in the OW and blend samples, compared to a one stage mass loss for the HVN sample (Fig. 1). The second mass loss stage in the OW sample was possibly due to the release of volatiles and their combustion, while the final mass loss may have been due to char oxidation. In the case of the blends, the second mass loss was very small, due to the low

Table 2 Combustion parameters of the coals under different atmospheres

Sample	Atmosphere	T_i/°C	T_f/°C	T_{peak}/°C	T_{50}/°C	DTG_{max}/% s^{-1}	Average DTG/% s^{-1}	R_C/% kg^{-1} s^{-1}
AC	21%O_2/79%N_2	560	732	625	634	0.261	0.141	53996
	21%O_2/79%CO_2	561	734	633	636	0.248	0.139	50849
	30%O_2/70%CO_2	545	707	608	613	0.303	0.146	65117
	35%O_2/65%CO_2	540	696	600	603	0.333	0.154	71177
HVN	21%O_2/79%N_2	482	644	567	566	0.301	0.149	60252
	21%O_2/79%CO_2	484	650	570	569	0.287	0.147	55352
	30%O_2/70%CO_2	470	627	547	547	0.358	0.157	78894
	35%O_2/65%CO_2	465	616	540	539	0.392	0.163	77706
DAB	21%O_2/79%N_2	357	588	516	499	0.229	0.105	48817
	21%O_2/79%CO_2	360	593	520	503	0.222	0.103	45983
	30%O_2/70%CO_2	351	576	501	490	0.255	0.109	55768
	35%O_2/65%CO_2	346	567	495	483	0.265	0.111	56410
NZ	21%O_2/79%N_2	293	504	410	405	0.267	0.104	49585
	21%O_2/79%CO_2	294	506	411	405	0.260	0.103	49821
	30%O_2/70%CO_2	288	497	406	400	0.293	0.105	57537
	35%O_2/65%CO_2	283	486	395	393	0.399	0.107	73462

T_i initial temperature, T_f final temperature, T_{peak} peak temperature, T_{50} temperature corresponding to a conversion degree of 50%, DTG_{max} maximum rate of mass loss, *Average DTG* average rate of mass loss, R_C coal reactivity index

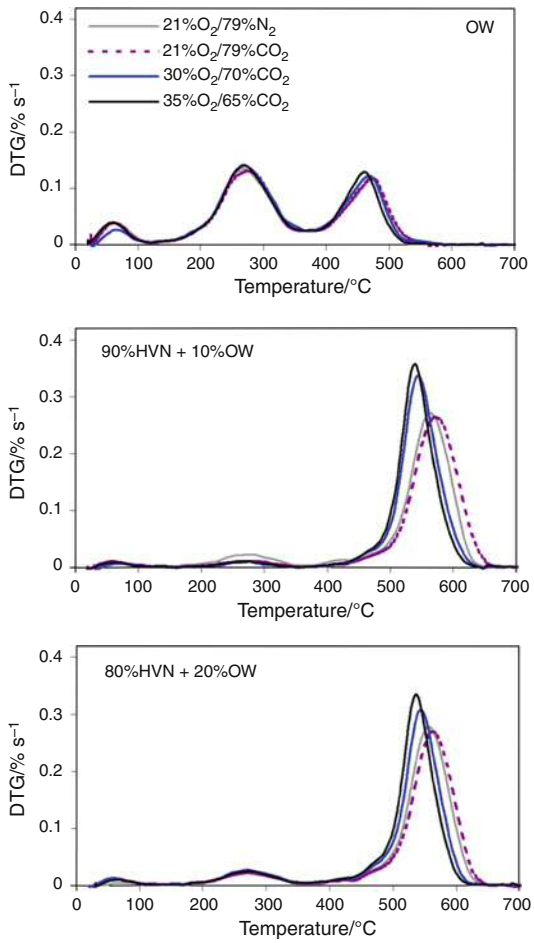

Fig. 2 DTG curves for the combustion of biomass and coal/biomass blends under different atmospheres

proportion of biomass in the blend, the last peak closely resembling that of the coal sample, presumably because coal was the predominant component of the blend.

The combustion parameters for these samples are summarized in Table 3. In the case of the OW and blend samples, the parameters were calculated only taking into consideration the last mass loss stage, so that they could be then compared with those of the HVN coal sample. For all the combustion and oxy-fuel combustion atmospheres, it can be observed that the highest values of T_i, T_f, T_{50}, DTG_{max} and Average DTG corresponded to the HVN samples, followed by those of the 90%HVN + 10%OW and the 80%HVN + 20%OW samples in that order. Small differences were found in the T_{peak} and R_C values of the samples. The addition of biomass to the coal caused a decrease in the combustion and oxy-fuel combustion temperatures. Biomass is a fuel with high reactivity and high volatile matter content (Table 1), which can lead to a faster reaction and to an improvement in the combustion behaviour of a coal in agreement with the results of other works [18, 29, 30].

Effects of steam addition upon the oxy-fuel combustion characteristics of pulverized coal

Figure 3 compares the DTG curves for the AC, HVN, DAB, and NZ coal samples under the 21%O_2/79%CO_2 and 30%O_2/70%CO_2 oxy-fuel combustion atmospheres with those corresponding to the same atmosphere after the replacement of CO_2 with 10 and 20% of steam. It can be observed that the addition of steam shifted the DTG curves

Table 3 Combustion parameters of the biomass and the coal/biomass blends under different atmospheres

Atmosphere	Sample	T_i/°C	T_f/°C	T_{peak}/°C	T_{50}/°C	DTG_{max}/% s^{-1}	Average DTG/% s^{-1}	R_C/% kg^{-1} s^{-1}
21%O_2/79%N_2	HVN	482	644	567	566	0.301	0.149	60252
	90%HVN-10%OW	465	641	565	561	0.282	0.132	62291
	80%HVN-20%OW	455	623	559	546	0.278	0.129	58044
	OW	367	520	475	302	0.118	0.064	24636
21%O_2/79%CO_2	HVN	484	650	570	569	0.287	0.147	55352
	90%HVN-10%OW	469	645	570	564	0.264	0.130	54590
	80%HVN-20%OW	460	628	565	552	0.269	0.127	55948
	OW	370	522	475	305	0.118	0.064	23807
30%O_2/70%CO_2	HVN	470	627	547	547	0.358	0.157	78894
	90%HVN-10%OW	453	619	545	542	0.337	0.142	69394
	80%HVN-20%OW	452	608	545	535	0.308	0.131	61221
	OW	371	514	467	308	0.122	0.067	31640
35%O_2/65%CO_2	HVN	465	616	540	539	0.392	0.163	77706
	90%HVN-10%OW	453	611	540	536	0.358	0.145	76386
	80%HVN-20%OW	448	601	535	529	0.335	0.137	65442
	OW	365	509	461	302	0.129	0.067	25639

T_i initial temperature, T_f final temperature, T_{peak} peak temperature, T_{50} temperature corresponding to a conversion degree of 50%, DTG_{max} maximum rate of mass loss, *Average DTG* average rate of mass loss, R_C coal reactivity index

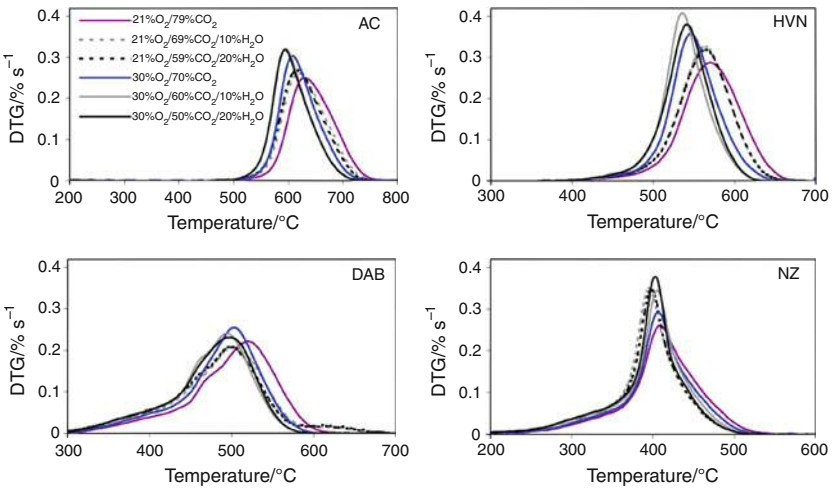

Fig. 3 DTG curves for coal combustion under oxy-fuel atmospheres with 21 and 30% of O_2 containing steam

to lower temperatures and generally caused an increase in the rate of mass loss and a decrease in combustion time with respect to those in the 21%O_2/79%CO_2 or 30%O_2/70%CO_2 oxy-fuel combustion atmospheres, probably due to the fact that the specific heat capacity of H_2O is lower than that of CO_2 [31], as a result of which the combustion stage was brought forward. However, no relevant differences were observed from the addition of 10 and 20% of steam (Fig. 3).

Conclusions

The different coals studied exhibited different combustion behaviours under O_2/CO_2 oxy-fuel conditions with respect to air combustion conditions. The coal, biomass, and coal/biomass blend samples showed slightly higher reactivities under air compared to oxy-fuel conditions at the same O_2 level, since the replacement of O_2 by CO_2 caused the rate of mass loss to decrease and the burning process occurred at higher temperatures. However, once the O_2 concentration had been increased to 30 and 35% in the oxy-fuel combustion atmosphere, the rate of mass loss rose and the burning process was brought forward and shortened. The addition of biomass to coal caused a decrease in the combustion and oxy-fuel combustion temperatures. The replacement of 10 and 20% of CO_2 with steam in the oxy-fuel combustion atmosphere of the coal resulted in an increase in the rate of mass loss and a decrease in the burning time, no significant differences being observed between the two steam concentrations.

Acknowledgements This study was carried out with financial support from the Spanish MICINN (Project PS-120000-2005-2) co-financed by the European Regional Development Fund. L.A. and J.R. acknowledge funding from the CSIC JAE program, which was co-financed by the European Social Fund, and the Asturias Regional Government (PCTI program), respectively.

References

1. BP 2009. BP statistical review of world energy June 2009. http://www.bp.com. Accessed 22 Nov 2010.
2. Buhre BJP, Elliott LK, Sheng CD, Gupta RP, Wall TF. Oxy-fuel combustion technology for coal-fired power generation. Prog Energy Combust Sci. 2005;31:283–307.
3. Bejarano PA, Levendis YA. Single-coal-particle combustion in O_2/N_2 and O_2/CO_2 environments. Combust Flame. 2008;153:270–87.
4. Rathnam RK, Elliott LK, Wall TF, Liu Y, Moghtaderi B. Differences in reactivity of pulverised coal in air (O_2/N_2) and oxy-fuel (O_2/CO_2) conditions. Fuel Process Technol. 2009;90:797–802.
5. Toftegaard MB, Brix J, Jensen PA, Glarbor P, Jensen AD. Oxy-fuel combustion of solid fuels. Prog Energy Combust Sci. 2010;36:581–625.
6. Li Q, Zhao C, Chen X, Wu W, Li Y. Comparison of pulverized coal combustion in air and in O_2/CO_2 mixtures by thermogravimetric analysis. J Anal Appl Pyrolysis. 2009;85:521–8.
7. Molina A, Shaddix CR. Ignition and devolatilization of pulverized bituminous coal particles during oxygen/carbon dioxide coal combustion. Proc Combust Inst. 2007;31:1905–12.
8. Huang X, Jiang X, Han X, Wang H. Combustion characteristics of fine- and miro-pulverized coal in the mixture of O_2/CO_2. Energy Fuels. 2008;22:3756–62.
9. Li X, Rathnam RK, Yu J, Wang Q, Wall T, Meesri C. Pyrolysis and combustion characteristics of an Indonesian Low-Rank Coal under O_2/N_2 and O_2/CO_2 conditions. Energy Fuels. 2010;24:160–4.
10. Liu H, Zailani R, Gibbs BM. Comparisons of pulverized coal combustion in air and in mixtures of O_2/CO_2. Fuel. 2005;84:833–40.
11. Várhegyi G, Szabó P, Jakab E, Till F. Mathematical modeling of char reactivity in Ar-O_2 and CO_2–O_2 mixtures. Energy Fuels. 1996;10:1208–14.
12. Zhang L, Binner E, Qiao Y, Li C-Z. In situ diagnostics of Victorian brown coal combustion in O_2/N_2 and O_2/CO_2 mixtures in drop-tube furnace. Fuel. 2010;89:2703–12.
13. Nozaki T, Takano S, Kiga T, Omata K, Kimura N. Analysis of the flame formed during oxidation of pulverized coal by an O_2-CO_2 mixture. Energy. 1997;22:199–205.
14. Arias B, Pevida C, Rubiera F, Pis JJ. Effect of biomass blending on coal ignition and burnout during oxy-fuel combustion. Fuel. 2008;87:2753–9.
15. Pis JJ, de la Puente G, Fuente E, Morán A, Rubiera F. A study of the self-heating of fresh and oxidized coals by differential thermal analysis. Thermochim Acta. 1996;279:93–101.

16. Rubiera F, Morán A, Martínez O, Fuente E, Pis JJ. Influence of biological desulphurisation on coal combustion performance. Fuel Process Technol. 1997;52:165–73.
17. Niu SL, Lu CM, Han KH, Zhao JL. Thermogravimetric analysis of combustion characteristics and kinetic parameters of pulverized coals in oxy-fuel atmosphere. J Therm Anal Calorim. 2009;98:267–74.
18. Arenillas A, Rubiera F, Pis JJ, Jones JM, Williams A. The effect of the textural properties of bituminous coal chars on NO emissions. Fuel. 1999;78:1779–85.
19. Jiang XM, Cui ZG, Han XX, Yu HL. Thermogravimetric investigation on combustion characteristics of oil shale and high sulphur coal mixture. J Therm Anal Calorim. 2006;85:761–4.
20. Buryan P, Staff M. Pyrolysis of the waste biomass. J Therm Anal Calorim. 2008;93:637–40.
21. Mothé CG, de Miranda IC. Characterization of sugarcane and coconut fibers by thermal analysis and FTIR. J Therm Anal Calorim. 2009;97:661–5.
22. Slovák V, Taraba B. Effect of experimental conditions on parameters derived from TG-DSC measurements of low-temperature oxidation of coal. J Therm Anal Calorim. 2010;101:641–6.
23. Cumming JW, McLaughlin J. The thermogravimetric behaviour of coal. Thermochim Acta. 1982;57:253–72.
24. Rubiera F, Arenillas A, Arias B, Pis JJ. Modification of combustion behaviour and NO emissions by coal blending. Fuel Process Technol. 2002;77:111–7.
25. ASTM Standard D 388. Standard classification of coals by rank; 2005.
26. Rubiera F, Arenillas A, Fuente E, Miles N, Pis JJ. Effect of the grinding behaviour of coal blends on coal utilisation for combustion. Powder Technol. 1999;105:351–6.
27. Haykırı-Açma H. Combustion characteristics of different biomass materials. Energy Convers Manage. 2003;44:155–62.
28. Zheng JA, Koziński JA. Thermal events occurring during the combustion of biomass residue. Fuel. 2000;79:181–92.
29. Gil MV, Casal D, Pevida C, Pis JJ, Rubiera F. Thermal behaviour and kinetics of coal/biomass blends during co-combustion. Bioresour Technol. 2010;101:5601–8.
30. Kastanaki E, Vamvuka D. A comparative reactivity and kinetic study on the combustion of coal-biomass char blends. Fuel. 2006;85:1186–93.
31. Khare SP, Wall TF, Farida AZ, Liu Y, Moghtaderi B, Gupta RP. Factors influencing the ignition of flames from air-fired swirl pf burners retroffited to oxy-fuel. Fuel. 2008;87:1042–9.

6.2.2 *Publicación VIII*

Ignition behaviour of coal and biomass blends under oxyfiring conditions with steam additions.

J. Riaza, , L. Álvarez, M.V. Gil, R. Khatami, Y.A. Levendis, J.J. Pis, C. Pevida, F. Rubiera. Greenhouse Gases: Science and Technology
2013. 3 (5), pp. 397-414.
doi:10.1002/ghg.1368

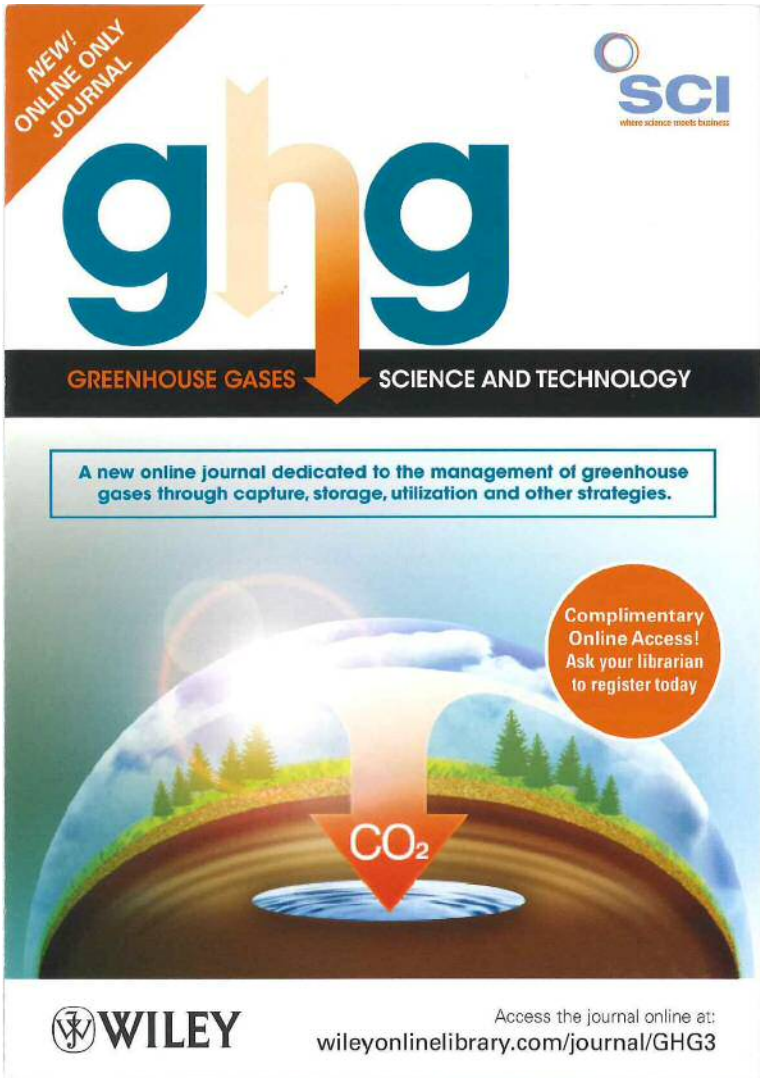

Short Communication

GREENHOUSE GASES SCIENCE AND TECHNOLOGY

Ignition behavior of coal and biomass blends under oxy-firing conditions with steam additions

Juan Riaza, Lucía Álvarez, and María V. Gil, Instituto Nacional del Carbón, INCAR-CSIC, Oviedo, Spain
Reza Khatami and Yiannis A. Levendis, Northeastern University, Boston, MA, USA
José J. Pis and Covadonga Pevida and Fernando Rubiera, Instituto Nacional del Carbón, INCAR-CSIC, Oviedo, Spain

Abstract: The ignition behavior of coal and biomass blends was assessed in air and oxy-firing conditions in an entrained flow reactor. Four coals of different rank, an anthracite, a semi-anthracite, and two high-volatile bituminous coals, were tested in air and O_2/CO_2 (21-35% O_2) environments. For all the coals, deterioration in ignition properties was observed in the 21%O_2/79%CO_2 atmosphere in comparison with air. However, the ignition properties were enhanced when the oxygen concentration in the O_2/CO_2 mixture was increased. Coal and biomass blends of a semi-anthracite and a high-volatile bituminous coal with 10 and 20 wt% of olive residue were also used in the ignition experiments under air and oxy-firing conditions. The ignition behavior of the coals improved as the additions of biomass increased both in air and oxy-firing conditions. In particular, the effect of biomass blending was more noticeable in the ignition of the high rank coal. Since industrial oxy-coal combustion with a wet recycle would result in higher concentrations of H_2O(v), the effect of steam addition on ignition behavior was also studied. A worsening in ignition behavior was observed when steam was added to the oxy-fuel combustion atmospheres, although an increase in the steam concentration from 10 to 20% did not produce any significant difference in the ignition characteristics of the fuels.
© 2013 Society of Chemical Industry and John Wiley & Sons, Ltd

Keywords: biomass; coal; ignition behavior; oxy-combustion; steam

Introduction

The use of coal in power plants generates a large amount of CO_2 which is the chief cause of global climate change. A diverse power generation portfolio including carbon capture and storage (CCS) technologies and renewable energies is needed to reduce atmospheric CO_2 to below 1990 levels.[1,2] During oxy-coal combustion, coal is burnt in a mixture of oxygen and recycled flue gas (RFG), mainly CO_2 and water vapor, to yield a rich CO_2 stream, which after purification is ready for sequestration.[3] In addition, biomass is a source of energy which is considered carbon neutral as the carbon dioxide

Correspondence to: Fernando Rubiera,Instituto Nacional del Carbón, INCAR-CSIC, Apartado 73, 33080 Oviedo, Spain.
E-mail: frubiera@incar.csic.es
Received July 2, 2013; revised August 5, 2013; accepted August 5, 2013
Published online at Wiley Online Library (wileyonlinelibrary.com). DOI: 10.1002/ghg.1368

released during its combustion is recycled as an integral part of the carbon cycle. The combination of oxy-coal combustion with biomass co-firing can help to increase CO_2 capture efficiency.[4] However, the successful implementation of the oxyfuel technology in pulverized coal boilers depends on fully understanding the differences that may result from replacing N_2 with a mixture of CO_2 and water vapor in the oxidizer stream. In oxy-firing conditions, due to the higher concentrations of CO_2 and $H_2O_{(v)}$, compared to conventional air combustion, several aspects such as heat transfer, flame ignition, pollutant formation, and volatile matter and char combustion are affected.[5–9] The use of biomass in existing coal power plants requires only minor modifications compared to the construction of new biomass-only fired power plants, making the co-firing of coal and biomass an easy and cheap way to obtain biomass energy.[10]

The application of the oxy-combustion technology has been implemented at a higher scale in Vattenfall's 30 MW_{th} oxyfuel pilot plant in Schwarze Pumpe, Germany,[11] which was constructed in order to investigate the oxyfuel firing process. The combustion investigations have focused on the radiation heat flux behavior, NO_x formation, as well as combustion performance and reaction rates between air and oxyfuel operation modes. Details on the operation with three different burners (one combined jet-swirl burner and one swirl burner both from Alstom, and one swirl DST-burner delivered by Hitachi) have been provided and it was found that the operation of the oxyfuel boiler with the three burners tested so far has proven to be very reliable and a good flame ignition and high stability over the entire load range has been achieved.[12]

The recycling of flue gas and the injection of the oxygen add more complexity to the design and operation of the oxyfuel burners and boilers.[13] Under oxyfuel conditions, the burner geometry has to be modified in order to achieve a stable flame attached to the burner quarl at oxygen contents in the O_2/RFG mixture close to that in air. In this regard a series of test runs was performed at the oxycoal test facility at RWTH Aachen University with the aim to achieve an experimentally confirmed database needed for development of a swirl burner able to operate at a wide range of O_2 concentrations (from18 to 34% vol. O_2) under oxy-firing conditions. Thus, a new burner concept based on aerodynamic stabilization of an oxyfuel swirl flame has been developed.[14]

The ignition of solid fuel particles is an important preliminary step in the overall combustion process due to its influence on the stability, shape, and length of the flame, and on the formation of pollutants. In practice, the ignition behavior of solid fuels may be decisive for identifying the optimal location for injecting them into industrial pulverized fuel burners. The ignition and combustion behavior of pulverized coal particles are not inherent properties of the coals, as they are dependent on the operating conditions.[15] In the oxy-fuel combustion of pulverized coal, poor ignition quality has often been observed during pilot-scale burning trials when operating with substantial flue gas recirculation.[16] Several efforts have been made recently to understand the fundamentals of ignition (i.e. particle ignition, flame propagation and flammability) in oxy-firing conditions when designing combustion systems.[17,18]

The present work studies the influence of fuel type, CO_2 dilution and oxygen concentration on the temperature and ignition mechanisms for a wide number of coals and coal/biomass blends (up to 20%wt biomass). It needs to be appreciated that, when blending different fuels, certain aspects such as ignition behavior, burnout or NO emissions cannot always be estimated from the behavior of the individual fuels.[19] As Smart *et al*.[20] have pointed out, another important aspect to consider is the effect of wet recycling in oxy-firing conditions on coal ignition and flame stability. In the present work, the effect of adding 10 and 20% of steam on the ignition characteristics, under air and oxy-firing conditions, was also studied.

Experimental

Materials

Four coals of different rank were used in this work: an anthracite from Cangas del Narcea, in Asturias, Spain (AC), a semi-anthracite from the Hullera Vasco-Leonesa in León, Spain (HVN), a South African high-volatile bituminous coal from the Aboño power plant in Asturias, Spain (SAB), and a washed coal supplied by the Batán coal preparation plant in Asturias, Spain (BA). A biomass, olive residue (OR) was also employed. This biomass is the wet solid residue that remains after the process of pressing and extraction of the olive oil. The coal and biomass samples were ground and sieved to obtain a particle size fraction of 75–150 μm. The proximate and ultimate analyses

© 2013 Society of Chemical Industry and John Wiley & Sons, Ltd

Table 1. Proximate and ultimate analyses and high heating value of the fuel samples.

Sample	AC	HVN	SAB	BA	OR
Origin	Spain	Spain	S. Africa	Spain	Spain
Rank	an	sa	hvb	hvb	-
Proximate Analysis (wt.%, db)					
Ash	14.2	10.7	15.0	6.9	7.6
V.M.	3.6	9.2	29.9	33.9	71.9
F.C.[a]	82.2	80.1	55.1	59.2	20.5
Ultimate Analysis (wt.%, daf)					
C	94.7	91.7	81.5	88.5	54.3
H	1.6	3.5	5.0	5.5	6.6
N	1.0	1.9	2.1	1.9	1.9
S	0.7	1.6	0.9	1.1	0.2
O[a]	2.0	1.3	10.5	3.0	37.0
High heating value (MJ kg^{-1}, db)	29.2	31.8	27.8	33.1	19.9

an: anthracite; sa: semi-anthracite; hvb: high-volatile bituminous coal
db: dry basis; daf: dry and ash free bases
[a]Calculated by difference

together with the high heating values of the samples are presented in Table 1.

Experimental device and procedure

The ignition characteristics of the coals and coal/biomass blends were studied in an entrained flow reactor (EFR), which has been described in detail elsewhere.[8] Briefly, the reactor has a reaction zone 140 cm in length and an internal diameter of 40 mm. It is electrically heated and is capable of reaching a maximum temperature of 1100 °C. Fuel samples were introduced through a cooled injector before entering the EFR reaction zone. The gases were preheated up to the reactor temperature before being introduced into the EFR, where they passed through two flow straighteners. The reaction products were quenched by aspiration in a stream of nitrogen using a water-cooled probe. The probe was inserted into the reaction chamber from below. Particles were removed by means of a cyclone and a filter. The exhaust gases were monitored using a battery of analyzers (O_2, CO, CO_2, SO_2, and NO).

During the ignition tests, the reactor was heated at 15 °C min^{-1} from 400 to 900 °C. The gas flow used in these tests ensured a particle residence time of 2.5 s. Air (21%O_2/79%N_2) and three binary mixtures of O_2/CO_2 (21%O_2/79%CO_2, 30%O_2/70%CO_2 and 35%O_2/65%CO_2) were employed to study the ignition characteristics of the coals and coal/biomass blends. Also, several ternary mixtures of $O_2/N_2/H_2O_{(v)}$ and $O_2/CO_2/H_2O_{(v)}$ were employed. The addition of 10 and 20% of steam was evaluated for all the air and oxy-fuel combustion atmospheres as a substitute for N_2 or CO_2 in order to study the effect of the wet recirculation of flue gas on coal ignition properties.

Results and discussion

Effect of the coal rank

Faúndez *et al.*[21] have stated that ignition is characterized by a rapid decrease in CO production, a significant consumption of O_2, and an increase in the production of CO_2 and NO. Prior to ignition, at low temperatures, the production of CO increases due to the release of volatiles and incomplete char combustion. The production of CO_2 and NO shows only a slight increase, and there is some O_2 consumption due to the evolution and subsequent combustion of coal volatiles at low temperatures. The criterion for determining the ignition temperature was based on the first derivative temperature curves of the gases produced. The ignition temperature was taken as the temperature at which the first derivative curve, normalized from the maximum derivative value, reached an absolute value of 10%.[21] The ignition temperatures, derived from derivative curves of the gases, for coals AC, HVN, SAB,and BA are shown in Table 2. As can be seen, coals SAB and BA tend to ignite at lower temperatures than coals AC and HVN. This may be due to their higher volatiles content (which enhances subsequent char combustion), and to their higher reactivity.[22]

Wall *et al.*[23] tracked the changes in gas composition during the ignition of pulverized coal in air in a laboratory scale drop-tube reactor, and associated these changes with the homogeneous ignition of volatiles and heterogeneous char combustion. In general, two types of mechanisms have been observed for coal particle ignition:[24] gas mode ignition (ignition of the volatiles in an enveloping flame that surrounds a devolatilizing char particle), heterogeneous mode ignition (which often signifies char ignition) or a

© 2013 Society of Chemical Industry and John Wiley & Sons, Ltd

Table 2. Ignition temperatures (°C) of coals AC, HVN, SAB and BA under air and O_2/CO_2 (21–35 vol.% O_2).

Coal	21%O_2/79%N_2	21%O_2/79%CO_2	30%O_2/70%CO_2	35%O_2/65%CO_2
AC	757	782	767	761
HVN	700	723	669	642
SAB	543	565	524	498
BA	509	554	498	490

combination of both. The ignition mechanism is closely related with the particle combustion mode. In a recent paper by Khatami *et al*.,[25] the authors employed the term two-mode combustion to signify events where the gas-phase (homogeneous) combustion of volatiles in an enveloping flame that surrounds a char particle, is distinct from the ensuing heterogeneous combustion of the solid char, as it occurs in homogeneous ignition. On the other hand, the term one-mode combustion was used to refer to events where either (i) the combustion of devolatilized char takes place or (ii) the combustion of the volatiles in the proximity of the char surface occurs with, presumably, simultaneous burning of the char, as in heterogeneous ignition. In the present paper, the ignition mode was elucidated from the gas evolution profiles. Examples in the air atmosphere are provided for a better comparison between coal samples.

The evolution of the gases during the ignition tests in air conditions for anthracite coal AC is shown in Fig. 1. The CO concentration increases up to a value of ~750 ppm. At around 760 °C there is a reduction in CO concentration, which is accompanied by a drastic reduction in O_2 and a sudden increase in NO and CO_2 corresponding to the ignition of the char. This is confirmed by the continued decrease in CO after the ignition event. The coal ignites heterogeneously as a result of the direct attack of oxygen on the surface of the char. For the ignition mode of various coal ranks, see also Fig. 2. As can be seen in the cinematographic observations, most of the AC coal particles burn heterogeneously, there being no evidence of the burning of the volatiles.

The gas emissions during semi-anthracite coal HVN ignition in air can be seen in Fig. 3. Above 400 °C there is an increase in the CO concentration due to coal devolatilization (the major devolatilization products are CH_4, CO and CO_2). Two changes in the CO profile and its derivative value can be observed: an initial decrease in CO concentration takes place at around 625 °C, which corresponds to the combustion of volatiles. The second change involves another decrease in CO concentration which takes place at around 670 °C. This is accompanied by a sudden decrease in O_2 concentration and an increase in NO and CO_2. These latter events correspond to char ignition, which is confirmed by the constant increase in the CO_2 produced after the ignition event. The ignition mechanism of this coal is the most difficult to unravel, i.e. it seems to be homogenous since the ignition of volatiles and char took place sequentially. Coal HVN is a physical blend of approx. 90% anthracitic and 10% low volatile bituminous coal from the same mine. For the ignition mode of semi-anthracite HVN coal, see also Fig. 2. As observed in the cinematographic records, some of the semi-anthracite HVN particles burn heterogeneously, but for other particles a small surrounding flame is observed corresponding to the combustion of volatiles. This enveloping flame burns up prior to the heterogeneous combustion of the char. However, in the EFR it is not possible to appreciate the ignition of single particles, it can only be seen that, globally, the stream of HVN particles burned homogenously (although much less volatile matter was released in comparison with hvb coals (Fig. 4)).

The gas evolution profiles for the SAB ignition tests in air are shown in Fig. 4. Above 400 °C there is a significant increase in CO concentration (due to the higher volatile matter content of SAB, the amount of CO released is much higher than for anthracitic coals). Also a continuous decrease in O_2 concentration is observed, which suggests that part of the volatiles released are oxidized. At a temperature of 530 °C the CO concentration starts to decrease, which suggests that coal devolatilization has ended, and that more CO is being consumed than formed. From Fig. 4 it can be inferred that the ignition of the char takes place at around 545 °C (i.e. there is a sudden decrease in the concentration of CO and O_2, and an increase in NO and CO_2). This suggests that the ignition of high-volatile coals takes place via a homogeneous mechanism,

© 2013 Society of Chemical Industry and John Wiley & Sons, Ltd

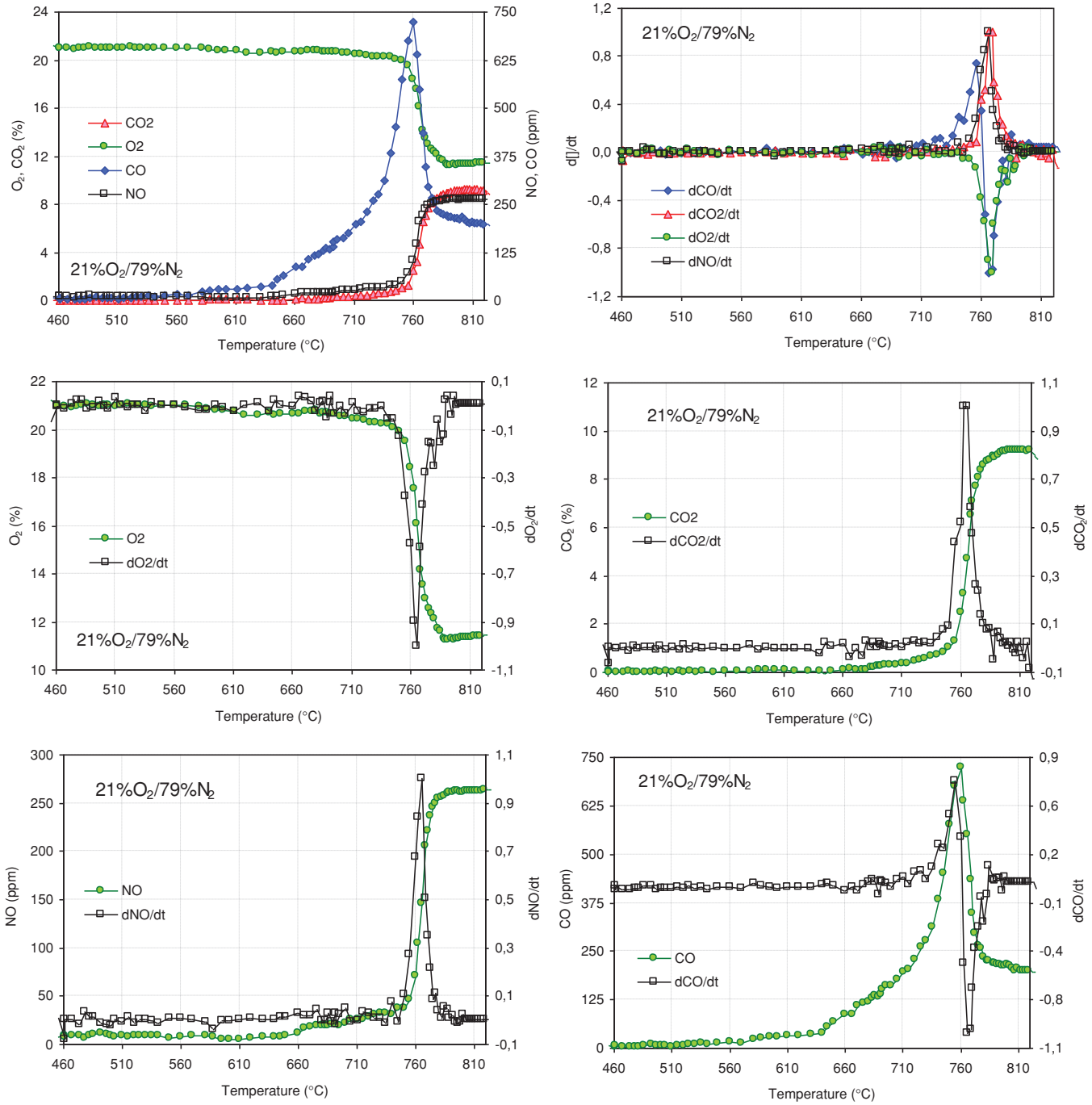

Figure 1. Gas emissions and normalized derivative curves of gas concentration during ignition tests in air for anthracite coal AC.

with the sequential ignition of volatiles and char. However, the ignition delay between the extinction of the volatiles and char combustion is much shorter than in the case of semi-anthracite coal HVN. For the ignition mode of bituminous coal SAB, see also Fig. 2. As can be seen from the cinematographic records, the combustion of coal SAB includes particle devolatilization with ignition and combustion of the volatiles in a flame that surrounds the particle, followed by the ignition and combustion of the resulting char.

Coal BA is a high-volatile bituminous coal whose ignition mechanism is also homogeneous. Since its

© 2013 Society of Chemical Industry and John Wiley & Sons, Ltd

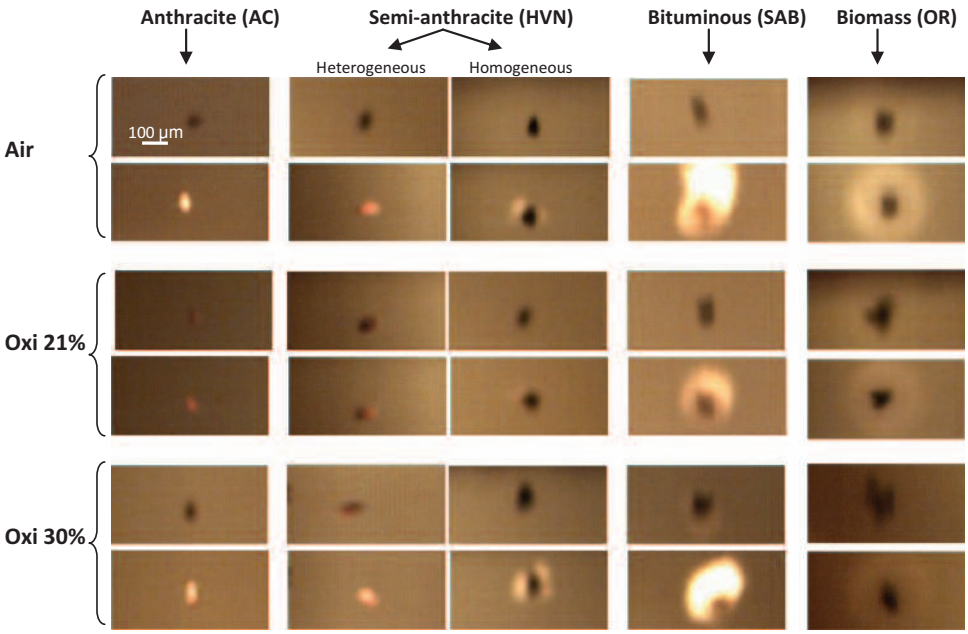

Figure 2. High-speed, high-magnification cinematographic images of single particles (75–150µm) of various coals (anthracite AC, semi-anthracite HVN, a bituminous SAB) and a biomass (olive residue OR) in air and in two different simulated oxy-fuel conditions (21%O_2–79CO_2 and 30%O_2–70%CO_2). In each case, a particle is shown prior and after ignition takes place. Different coal ranks experience different ignition modes.

gas evolution profiles are very similar to those of coal SAB, they are not shown in this paper.

Effect of the O_2/CO_2 atmosphere

In order to evaluate the effect of the presence of CO_2 in large concentrations, ignition tests were conducted in both O_2/N_2 and O_2/CO_2 environments. As can be seen in Table 2 higher ignition temperatures are required when N_2 (21%O_2/79%N_2) is replaced by CO_2 (21%O_2/79%CO_2). Stivers *et al.*[26] and Khatami *et al.*[27] observed a delay in ignition in an O_2/CO_2 environment compared to an O_2/N_2 environment with identical O_2 concentration. They attributed the longer ignition delay partly to the effect of the volumetric heat capacity of the gas mixtures. The temperature rise during ignition is inversely proportional to the heat capacity of the surrounding gas and, since the heat capacity of CO_2 is higher than that of N_2, a reduction in gas temperature occurs. However, the heat capacity and temperature of the surrounding gas are not the only factors that affect ignition properties; the oxygen concentration, the heating rate of the gas and devolatilization rates of particles, and the coal volatiles content also have a considerable influence.[15,25]

It should be noted that in this study the highest increase in ignition temperature was observed for coal BA, the coal with the highest volatile matter content, due to the lower mass diffusivity of the volatiles in the CO_2 mixture.[28] It can also be observed that for semi-anthracite and bituminous coals HVN, SAB and BA and for oxygen concentrations up to 30% or 35%, the ignition temperature is lower than in air, even though the heat capacity of the gas atmospheres with O_2 concentrations up to 30–35% are still higher than the heat capacity of the air. In the case of anthracite coal AC – which has the lowest volatile matter content- increasing the oxygen concentration to 35% was not enough to compensate for the negative effects of CO_2 on ignition temperature.

From the values of the ignition temperatures it is difficult to determine whether the worsening of the ignition properties under oxy-fuel conditions is due to the reactions affecting the char, the reactions involving the volatiles, changes in heat transfer or a combination of all three factors. For this reason the ignition

© 2013 Society of Chemical Industry and John Wiley & Sons, Ltd

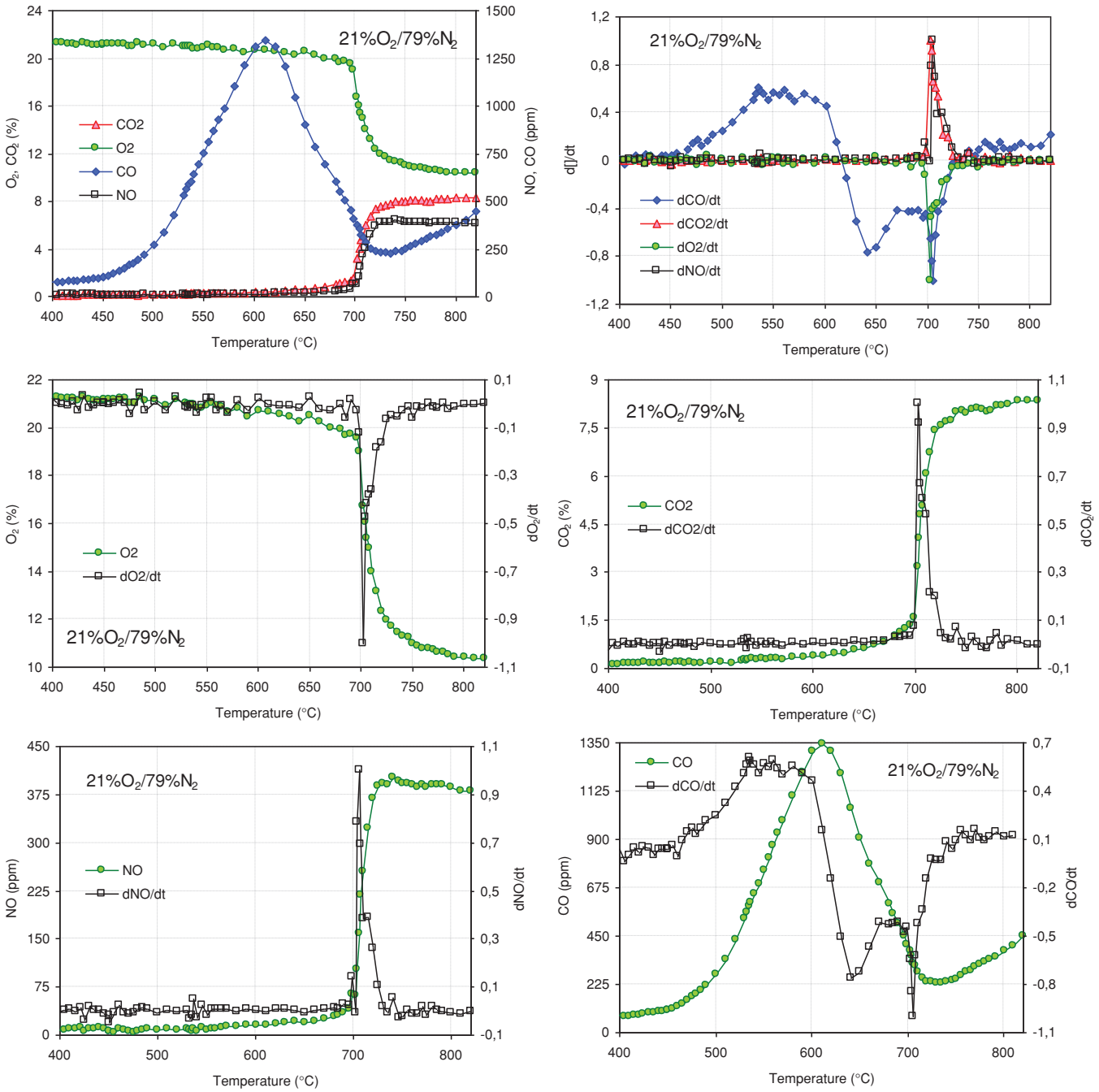

Figure 3. Gas emissions and normalized derivative curves of gas concentration during ignition tests in air for semi-anthracite coal HVN.

mechanism of the different coals was inferred from the evolution curves of the gases.

The gas evolution during the ignition of anthracite coal AC in two of the oxy-firing conditions studied ($21\%O_2/79\%CO_2$ and $35\%O_2/65\%CO_2$) is shown in Fig. 5. The ignition mechanism is the same as that observed under air-firing conditions; i.e. the char ignites heterogeneously due to the direct attack of oxygen. The only difference between the air and oxy-fuel atmospheres is the larger amount of CO formed, which may be attributed to char-CO_2 reactions. Pyrolysis experiments for the coals studied in the N_2 and CO_2 atmospheres at 1000 °C have been carried out previously in the EFR.[22] The results for

© 2013 Society of Chemical Industry and John Wiley & Sons, Ltd

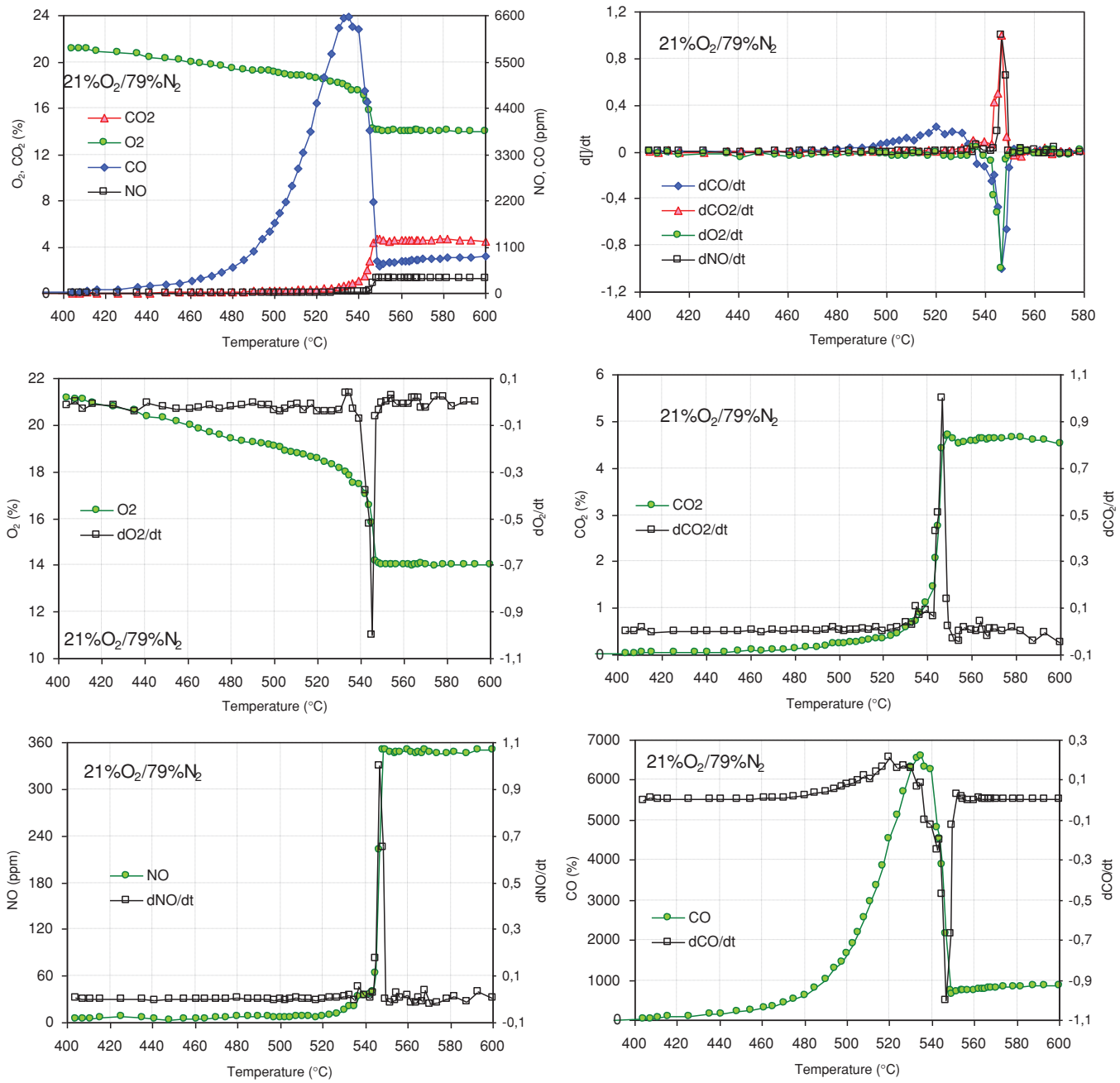

Figure 4. Gas emissions and normalized derivative curves of gas concentration during ignition tests in air for bituminous coal SAB.

volatile yields are presented in Table 3, and they show that the volatile yield is enhanced in a CO_2 atmosphere, as the CO_2 reacts with the resulting chars. The high amounts of CO which persist as a thick protective sheath, even with oxygen contents of 35%, prevent particle ignition.

The gas evolution profiles for semi-anthracite coal HVN in oxy-fuel conditions are shown in Fig. 6. An increase in CO concentration occurs due to the devolatilization of HVN at temperatures above 400 °C. In the 21%O_2/79%CO_2 atmosphere the combustion of part of these volatiles takes place above 625 °C, as in air-firing conditions. The ignition of the char (i.e. a marked reduction in O_2 concentration and a marked increase in CO_2 and NO) occurs at around 725 °C. The ignition mechanism is the same as that of

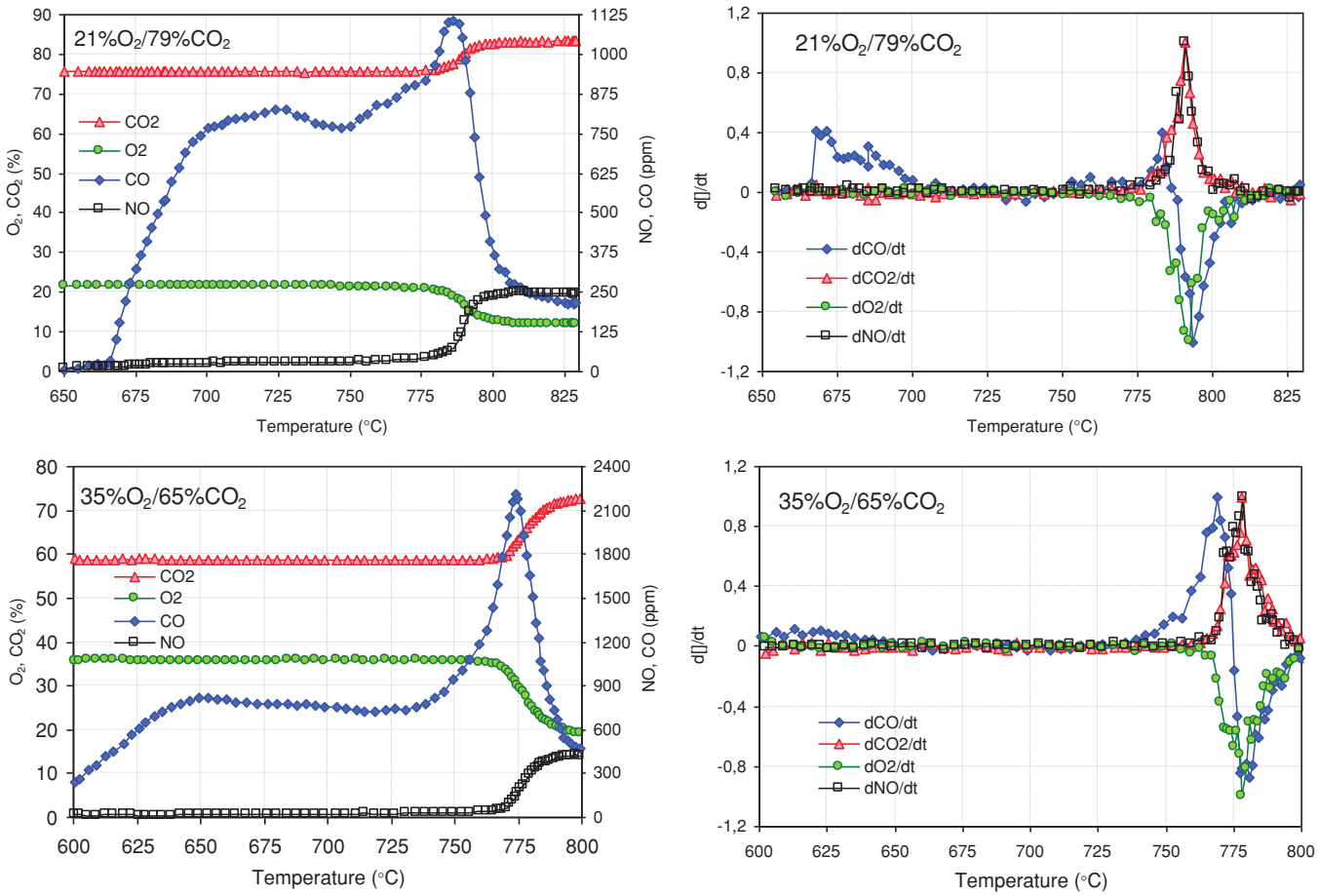

Figure 5. Gas emissions and normalized derivative curves of gas concentration during ignition tests in oxy-firing conditions for anthracite coal AC.

air ignition. However, higher CO concentrations are obtained. These higher CO concentrations contribute to the deterioration in ignition properties, via the formation of a persistent cloud around the particle that prevents the oxygen from gaining access to the surface of the particle. As other authors have observed[25,29] in a 21%O_2/79%CO_2 atmosphere, the volatiles released remain partially unburnt and form a thick envelope cloud. Also, higher concentrations of CO are formed, partly due to the incomplete combustion of the volatiles, and partly as a result of char gasification by CO_2. To compare the intensity and brightness of the burning coal particles in air and CO_2 atmospheres see also Fig. 2. From the cinematographic records, when N_2 is replaced by CO_2 for the same oxygen concentration, the burning particles appeared dim, which is indicative of slow oxidation. The brightness and intensity of the coal combustion increases drastically with oxygen in the O_2/CO_2 environments. The combustion images of the 30%O_2/70%CO_2 atmosphere resemble those of air.

Since the gas evolution profiles corresponding to 30%O_2/70%CO_2 and 35%O_2/65%CO_2 are similar, only those for the 35%O_2/65%CO_2 atmosphere are shown in Fig. 6. At temperatures above 400 °C the process of coal devolatilization starts with the consequent

Table 3. Experimental devolatilization yields at 1000 °C in the EFR under N_2 and CO_2 atmospheres.

Coal	Volatile yield-N_2 (%)	Volatile yield-CO_2 (%)
AC	3.6	4.2
HVN.	6.0	7.2
SAB	44.9	53.1
BA	49.9	62.2

© 2013 Society of Chemical Industry and John Wiley & Sons, Ltd

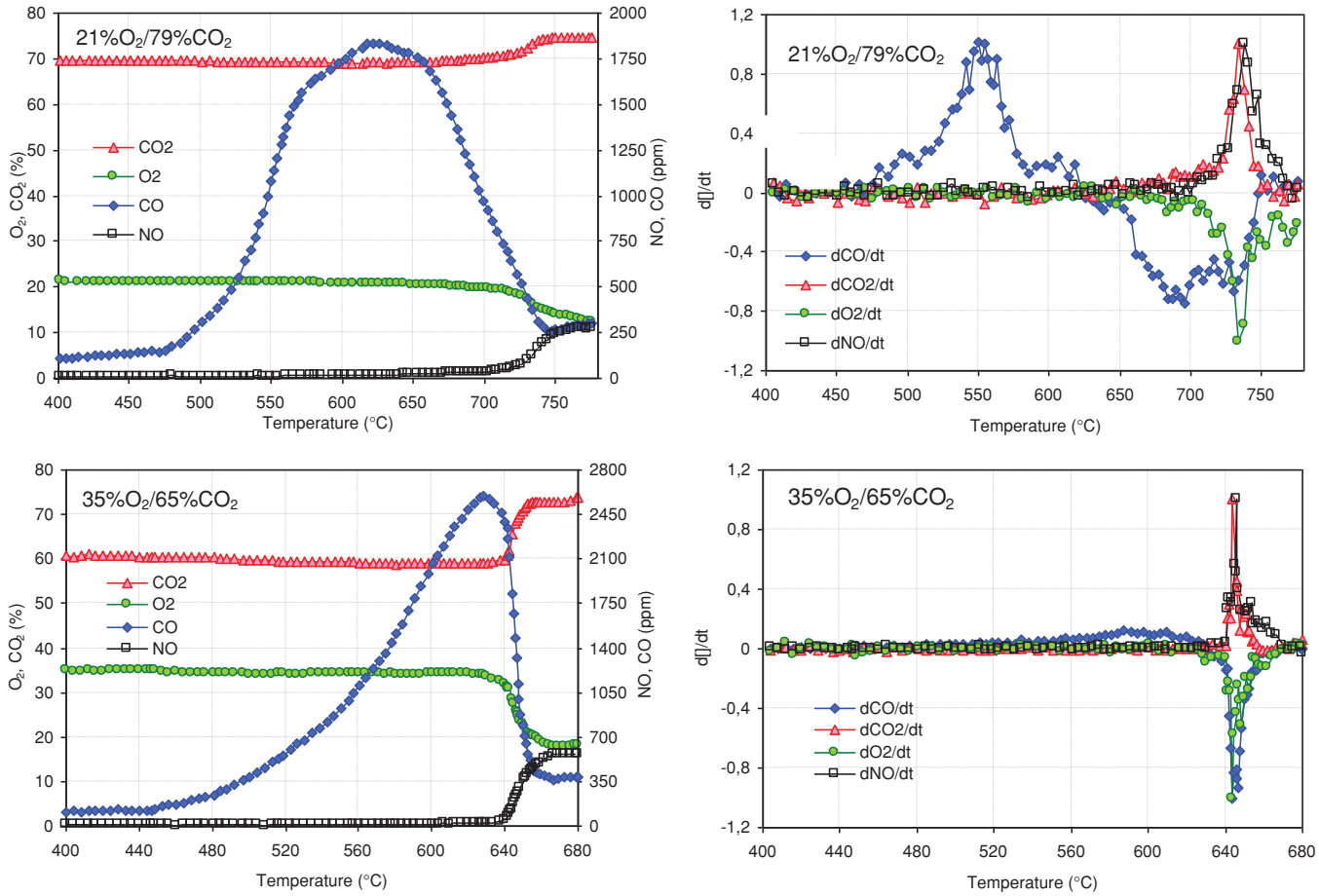

Figure 6. Gas emissions and normalized derivative curves of gas concentration during ignition tests in oxy-firing conditions for semi-anthracite coal HVN.

increase in CO concentration. As in the case of the N_2 and CO_2 atmospheres with a 21% oxygen content, the CO starts to oxidize above 625 °C. The ignition of the char occurs at 642 °C. Thus, in these cases ignition also takes place with the sequential ignition of volatiles and char. However, the time delay between volatiles and char combustion decreases as the oxygen concentration increases and ignition occurs at a lower temperature than in air. Khatami *et al.*[25,27] have also observed that the ignition delay in O_2/CO_2 atmospheres becomes smaller as O_2 increases. The ignition and combustion of volatiles provide extra heat that enhances the ignition of the char. However, this effect is not observed for coal AC due to its low volatile matter content. Also, when there is sufficient oxygen, the combustion of CO to form CO_2 provides extra heat.

The gas evolution of bituminous coal SAB during its ignition in oxy-firing conditions is shown in Fig. 7. High amounts of CO are released during coal devolatilization, which are later oxidized at temperatures of around 545 °C. Subsequently, char ignition takes place. The ignition mechanism is therefore homogeneous with the sequential ignition of volatiles and chars. However, the time delay between them is much shorter than in the case of semi-anthracite coal HVN, and becomes even shorter with increasing oxygen concentrations. Also larger amounts of CO are produced under oxy-firing conditions. It can be observed in Table 3 that the volatile yield in CO_2 for coal SAB is much higher than in N_2 in comparison with coals AC and HVN. These findings are in accordance with those reported by Zhang *et al.*[29] who have found that the replacement of N_2 by CO_2 enhanced coal particle pyrolysis prior to ignition, as CO_2 reacted with the resulting char to form additional combustible gases, i.e. CO, in the vicinity of the particle. The cinematographic records showed an increase in both char and volatile burning times in

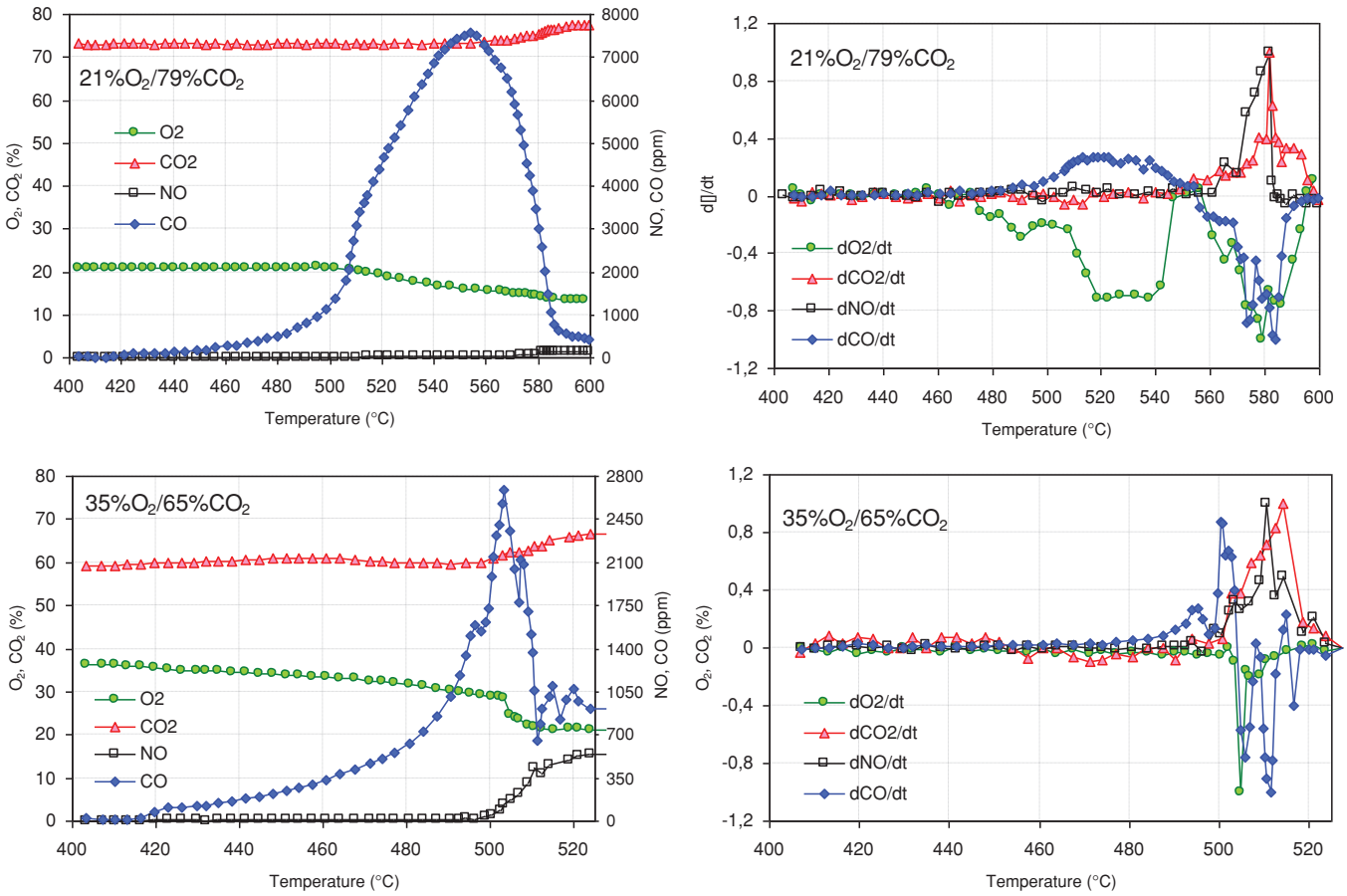

Figure 7. Gas emissions and normalized derivative curves of gas concentration during ignition tests in oxy-firing conditions for bituminous coal SAB.

the 21%O_2/79%CO_2 atmosphere in comparison with air-firing conditions. Also, there is a decrease on burning times in the O_2/CO_2 environments with increasing oxygen concentrations, and a decrease in the time delay between the extinction of the volatiles and char ignition.

Bituminous coal BA experiences the highest ignition delay, when N_2 is replaced by CO_2 for the same oxygen concentration, of all the coals under study. As for coal SAB, during its ignition in 21%O_2/79%CO_2, the CO concentration remains very high over a wide range of temperatures, preventing the oxygen from gaining access to the surface of the particle and causing a big delay in ignition. In a recent paper by Khatami *et al.*[27] the authors observed coal and char particle ignition in O_2/N_2 and O_2/CO_2 atmospheres. They found that in a N_2 atmosphere the presence of volatiles accelerated the ignition process, as the coals ignited faster than the chars, whereas in CO_2 the chars ignited faster than the coals, because the presence of a thick cloud of volatiles appeared to have impeded the ignition process. In the present study, coal BA has the highest content of volatiles, and therefore it releases more CO than the other coals. Also, as can be seen from Table 3, it shows the highest volatile yield in a CO_2 atmosphere (not shown). When the oxygen concentration is increased to 30% or 35%, the oxidation of CO to CO_2 is favored and, as a consequence, ignition takes place at lower temperatures.

Effect of the addition of biomass

The effect of blending coals and biomass on ignition behavior was studied under air and O_2/CO_2 (21-35% O_2) conditions. Two coals of different rank, the semi-anthracite HVN and the high volatile bituminous coal SAB, were blended with the olive residue OR. The ignition temperatures are shown in Table 4. It can be observed that the addition of olive residue, OR, causes a significant reduction in the ignition

© 2013 Society of Chemical Industry and John Wiley & Sons, Ltd

Table 4. Ignition temperatures (ºC) for blends HVN-OR and SAB-OR in air and O_2/CO_2 (21–35 vol.% O_2).

	21%O_2/79%N_2	21%O_2/CO_2	30%O_2/CO_2	35%O_2/CO_2
HVN	700	723	669	642
90HVN-10OR	636	662	615	567
80HVN-20OR	574	612	551	503
SAB	543	565	524	498
90SAB-10OR	510	532	491	455
90SAB-20OR	461	478	444	425

temperature of both coals in all the atmospheres studied. This decrease is proportional to the amount of biomass in the blend and is more pronounced for the HVN-OR blends.

As can be seen in Fig. 8, the ignition mechanism of the HVN-OR blends in air is homogeneous (i.e., with the sequential ignition of char and volatiles). For the case of oxy-fuel combustion, the addition of biomass does not affect the ignition mechanism because it remains homogeneous, so their gas evolution profiles are not shown in this paper.

In any case, a significant reduction in ignition temperature is observed in both the air and oxy-fuel atmospheres when coal is blended with biomass. Biomass is a highly reactive fuel and has much higher volatile matter content than coal. The

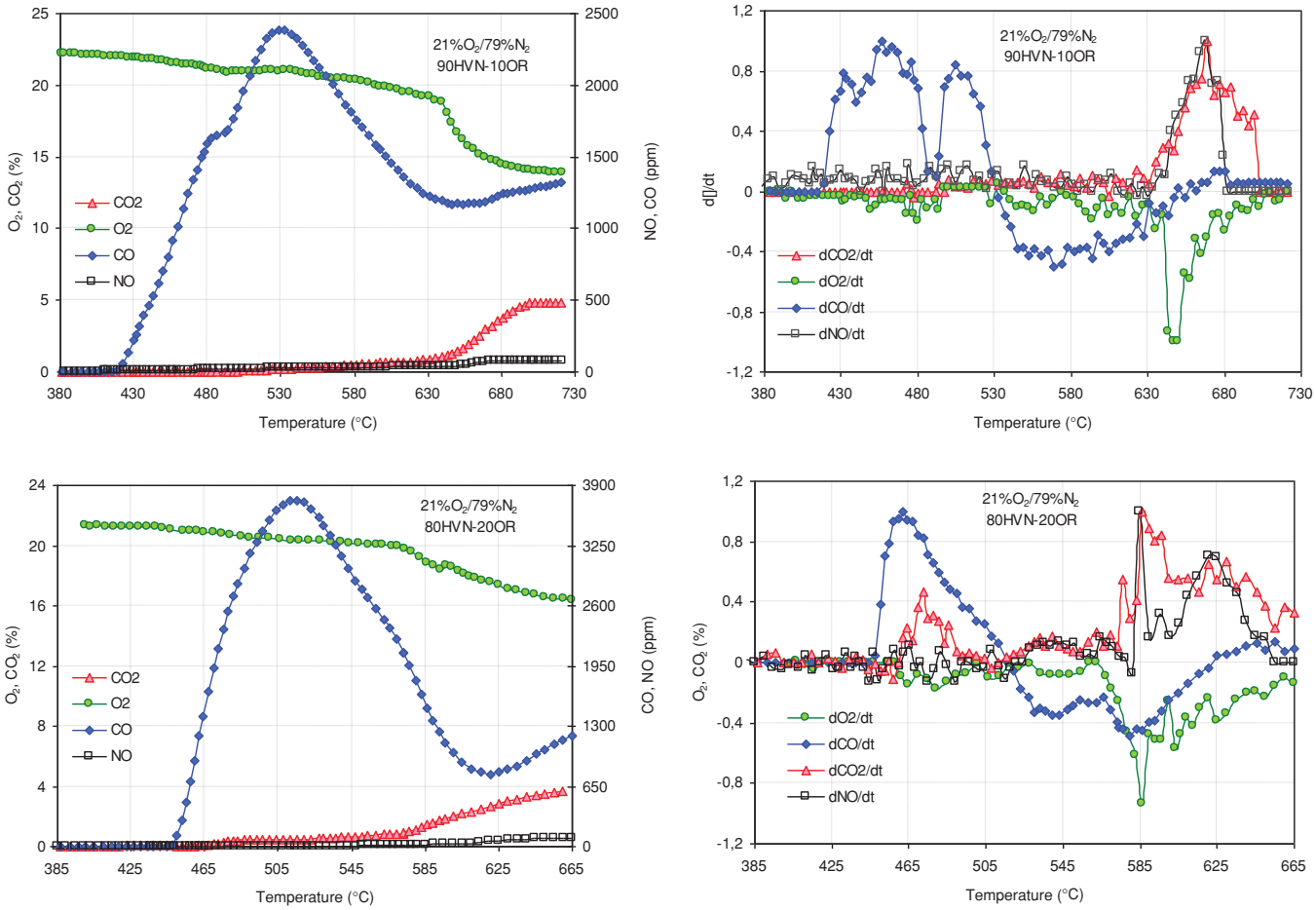

Figure 8. Gas emissions and normalized derivative curves of gas concentration during ignition tests in air-firing conditions for blends HVN-OR.

© 2013 Society of Chemical Industry and John Wiley & Sons, Ltd

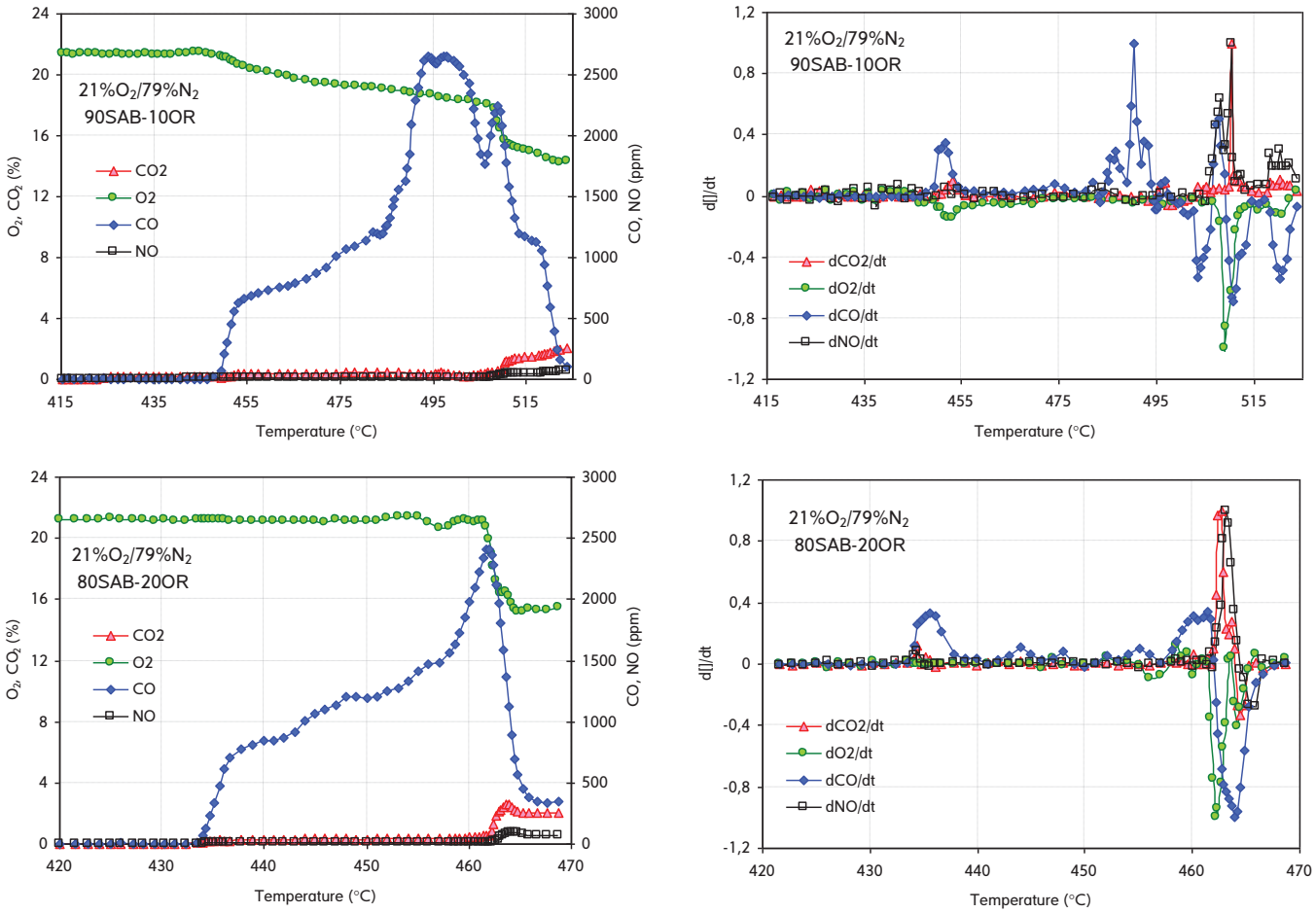

Figure 9. Gas emissions and normalized derivative curves of gas concentration during ignition tests in air-firing conditions for blends SAB-OR.

biomass OR will release far more volatiles when it is devolatilized than coal HVN, and this is reflected in the higher CO concentrations observed in the coal/biomass blends. As mentioned before, the ignition of the volatiles and char takes place sequentially. For coal HVN the ignition of the volatiles occurs at around 600 °C (Fig. 3), whereas for blends 90HVN-10OR and 80HVN-20OR it takes place at around 530 °C and 510 °C, respectively; whereas the combustion of char occurs at 636 °C and 575 °C. In summary, the addition of increasing quantities of biomass leads to a reduction in the ignition temperatures and in the delay between the ignition of the volatiles and char.

From Fig. 9 it can be seen that the ignition mechanism of the SAB-OR blends in air is homogeneous, as in the case of the individual coal SAB. The ignition mechanism for oxy-fuel conditions is also homogeneous (figures not shown). Furthermore ignition occurs at lower temperatures as the biomass content in the blends increases. For coal SAB the volatiles ignite at around 530 °C and the char at 543 °C (Fig. 4); whereas for blend 90SAB-10OR the ignition temperatures are of 500 °C and 510 °C, respectively. In the case of blend 80SAB-20OR there is a marked reduction in ignition delay between the volatiles and char ignition almost to the point where they seem to happen simultaneously at around 461 °C.

Although there is a decrease in ignition temperatures for both char and volatiles when increasing the biomass percentage in the SAB-OR blends, these decreases are less influenced by the addition of biomass than in the case of HVN-OR blends. This suggests that the effect of the addition of biomass on the ignition temperature of coal is more marked for high rank coals. When two fuels are fired as a blend, the ignition properties of the blend may be different to those exhibited when each component is

© 2013 Society of Chemical Industry and John Wiley & Sons, Ltd

ignited individually.[30] The ignition properties of high rank coals, which have far fewer volatiles and are less reactive than low rank coals, will be more easily enhanced by the addition of biomass. Faúndez *et al.*[19] have observed that, when blending fuels with different volatile matter contents, the ignition of the higher volatile component of the blend enhances the ignition of the lower volatile component. However, when both fuels have similar volatile contents, they compete for the oxygen available. As was shown by Khatami *et al.*[25] when biomass particles are burned, large volatile flames are formed. This also happens when burning low rank coals. The simultaneous burning of biomass and low rank coals leads to a competition for oxygen and in some zones oxygen depletion will result. Consequently, the enhancement of ignition properties will be less marked than when biomass is blended with high rank coals.

In summary, the ignition mechanism of high rank and low rank coals does not change when they are blended with biomass (up to 20% by mass). However, the addition of biomass improves their ignition properties, i.e. the coal and biomass blends ignite at lower temperatures than the individual coals.

Effect of the addition of steam

In order to study the effect of wet recirculation of flue gas, ignition tests were performed under air and oxy-firing conditions with the addition of steam as a substitute for N_2 or CO_2, respectively. Two coals of different rank, a semi-anthracite (HVN) and a high volatile bituminous coal (BA), were chosen for the ignition experiments. The ignition temperatures are shown in Table 5. The partial replacement of N_2 or CO_2 by steam causes a slight increase in the ignition temperatures, but no significant differences are observed between the results for 10 and 20% of steam. It should be noted that in the case of coal BA no significant differences were observed when steam was added to the oxy-fuel atmosphere with 30 or 35% oxygen content.

Figure 10 shows the gas evolution curves during the ignition of coal HVN under air and oxy-firing conditions with 20% steam addition. Similar gas evolution curves were obtained for 10% steam addition (not shown). The addition of steam does not affect the ignition mechanism of coal HVN. However, higher CO concentrations are observed with the addition of water vapor. In the atmospheres with lower oxygen content (21%), the CO concentrations are higher and they remain higher over a wider range of temperatures. The reasons for these high CO concentrations with the addition of steam are not yet clear. They may be partly due to unburnt volatiles. Binner *et al.*[31,32] observed that the ignition of a volatile flame was delayed during wet coal combustion, as well as a decrease in particle temperature. The same authors also observed that steam gasification of the char could take place to some extent. As was observed for oxy-firing conditions without the addition of steam, the CO preferentially remains in the vicinity of the particle surface, forming a thick protective sheath. If the CO remains on the char surface for a long time, this will result in O_2 depletion on the char surface, delaying the ignition process. When the oxygen concentration is increased, the combustion of CO to form CO_2 is favored and, the ignition of the coal particles is enhanced.

A similar conclusion can be drawn from the evolution of gases during the ignition of coal BA in air and oxy-firing conditions with steam addition. The ignition mechanism remains homogeneous for air and oxy-fuel conditions, both in wet and dry conditions.

Table 5. Ignition temperatures (ºC) for coals HVN and BA in air and O_2/CO_2 (21–35 vol.% O_2) with steam addition (the $H_2O_{(v)}$ is added as a substitute of N_2 or CO_2).

	21%O_2/N_2	21%O_2/CO_2	30%O_2/CO_2	35%O_2/CO_2
HVN	700	723	669	642
HVN+10%$H_2O_{(v)}$	713	733	682	657
HVN+20%$H_2O_{(v)}$	703	730	678	656
BA	509	554	498	490
BA+10%$H_2O_{(v)}$	529	560	499	491
BA+20%$H_2O_{(v)}$	548	566	498	492

© 2013 Society of Chemical Industry and John Wiley & Sons, Ltd

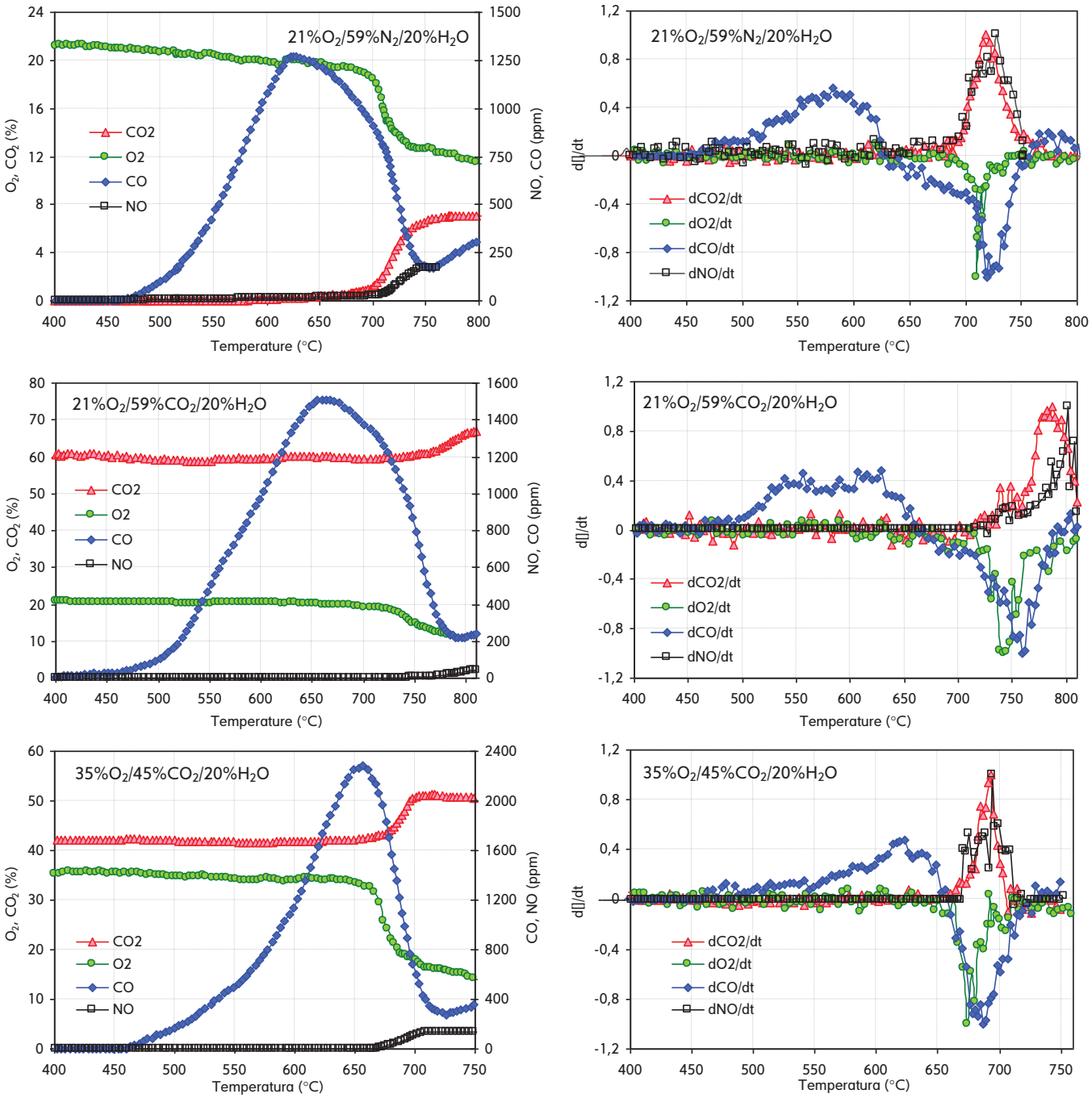

Figure 10. Gas emissions and normalized derivative curves of gas concentration during ignition tests for semi-anthracite coal HVN in air and O_2/CO_2 (21–35%O_2) with steam addition (the $H_2O_{(v)}$ is added as a substitute of N_2 or CO_2).

Also higher CO concentrations are observed with increasing steam addition.

Conclusions

The aim of this work was to study the ignition characteristics of coal and biomass blends in oxy-firing conditions with and without steam addition. The most important conclusions of this work are as follows:

(a) A significant increase in ignition temperature was observed when N_2 was replaced by CO_2, for the same oxygen concentration for the four coals studied (an anthracite, a semi-anthracite, and two

© 2013 Society of Chemical Industry and John Wiley & Sons, Ltd

high-volatile bituminous coals). This increase is not only due to the higher heat capacity of the background gas, but also due to the persistence of a thick cloud of volatiles around each particle which prevents its ignition. Not all the coals are affected in the same way by the background gases. In the O_2/CO_2 with low oxygen content (i.e. 21%) coals with a higher volatile matter content experience higher ignition delays due to the larger concentrations of volatiles and CO formed around the particle. The anthracite coal ignites in a heterogeneous mode in both air and oxy-firing conditions, semi-anthracite coal partially ignite heterogeneously whereas the bituminous coals ignite in a homogeneous mode.

(b) Co-firing coal (a semi-anthracite and a high-volatile bituminous coal) and biomass results in an improvement in the ignition properties of the blend in both air and oxy-firing conditions. However, this improvement is more significant in the case of the blends with the semi-anthracite. The ignition properties of the bituminous coal seem to be less affected by the addition of biomass.

(c) A worsening of ignition properties is observed when N_2 or CO_2 is partially replaced by $H_2O_{(v)}$ for both semi-anthracite and high-volatile bituminous coals. Higher CO concentrations are observed when the $H_2O_{(v)}$ concentrations are increased. The effect of steam addition is less noticeable in atmospheres with a high oxygen content.

Acknowledgements

This work was carried out with financial support from the Spanish MICINN (Project PS-120000-2005-2) co-financed by the European Regional Development Fund. L.A. and M.V.G. acknowledge funding from the CSIC JAE programs, co-financed by the European Social Fund. J.R. acknowledges funding from the Government of the Principado de Asturias (Severo Ochoa program). Support from the CSIC (PIE 201080E09) is gratefully acknowledged.

References

1. IEA, *World Energy Outlook*, IEA, Paris, France (2011).
2. Rubiera F and Pevida C, Progress in pilot, large-scale projects as an inducement for CCUS deployment. *Greenhouse Gases: Sci Technol* **3**:97–98 (2013)
3. Wall T, Liu Y, Spero C, Elliott L, Khare S, Rathnam R *et al.,* An overview on oxyfuel coal combustion – state of the air research and technology development. *Chem Eng Res Des* **87**:1003–1016 (2009).
4. Wall TF, Stanger R and Santos S, Demonstrations of coal-fired oxy-fuel technology for carbon capture and storage and issues with commercial deployment. *Int Greenhouse Gas Control* **5S:**S5–S15 (2011).
5. Smart JP, Patel R and Riley GS, Oxy-fuel combustion of coal and biomass, the effect on radiative and convective heat transfer and burnout. *Combust Flame* **157**:2230–2240 (2010).
6. Shaddix CR and Molina A, Fundamental investigation of NOx formation during oxy-fuel combustion of pulverized coal. *Proc Combust Inst* **33**:1723–1730 (2011).
7. Álvarez L, Riaza J, Gil MV, Pevida C, Pis JJ and Rubiera F, NO emissions in oxy-coal combustion with the addition of steam in an entrained flow reactor. *Greenhouse Gases: Sci Technol* **1**:180–190 (2011).
8. Riaza J, Álvarez L, Gil MV, Pevida C, Rubiera F and Pis JJ, Effect of oxy-fuel combustion with steam addition on coal ignition and burnout in an entrained flow reactor. *Energy* **36**:5314–5319 (2011).
9. Andersen J, Rasmussen CL, Giselsson T and Glarborg P, Global combustion mechanisms for use in CFD modeling under oxy-fuel conditions. *Energy Fuel* **23**:1379–1389 (2009).
10. Demirbas A, Potential applications of renewable energy sources, biomass combustion problems in boiler power systems and combustion related to environmental issues. *Prog Energy Combust Sci* **31**:171–192 (2005).
11. Anheden M, Burchhardt U, Ecke H, Faber R, Jidinger O, Giering R *et al.,* Overview of operational experience and results from test activities in Vattenfall's 30 MW_{th} oxyfuel pilot plant in Schwarze Pumpe. *Energy Procedia* **4**:941–950 (2011).
12. Rehfeldt S, Kuhr C, Schiffer F-P, Weckes P, Bergins C, First test results of oxyfuel combustion with Hitachi's DST-burner at Vattenfall's 30 MWth Pilot Plant at Schwarze Pumpe. *Energy Procedia* **4**:1002–1009 (2011).
13. IEAGHG. Oxyfuel combustion of pulverized coal. 2010/07. IEA, Paris, France (2010).
14. Habermehl M, Erfurth J, Toporov D, Förster M and Kneer R, Experimental and numerical investigations on a swirl oxycoal flame. *Appl Therm Eng* **49**:161–169 (2012).
15. Chen L, Yong SZ and Ghoniem AF, Oxy-fuel combustion of pulverized coal: Characterization, fundamentals, stabilization and CFD modelling. *Prog Energy Combust Sci* **38:**156–214 (2012).
16. Strömberg L, Lindgren G, Jacoby J, Giering R, Anheden M, Burchhardt U *et al.,* Update on Vattenfall's 30 MWth oxyfuel pilot plant in Schwarze Pumpe. *Energy Procedia* **1**:581–589 (2009).
17. Taniguchi M, Shibata T and Kobayashi H, Prediction of lean flammability limit and flame propagation velocity for oxy-fuel fired pulverized coal combustion. *Proc Combust Inst* **33**:3391–3398 (2011).
18. Taniguchi M, Yamamoto K, Okazaki T, Rehfeldt S and Kuhr C, Application of lean flammability limit and large eddy simulation to burner development for an oxy-fuel combustion system. *Int J Greenhouse Gas Control* **5S**:S111–S119 (2011).
19. Faúndez J, Arias B, Rubiera F, Arenillas A, García X, Gordon AL *et al*., Ignition characteristics of coal blends in an entrained flow reactor. *Fuel* **86**:2076–2080 (2007).

© 2013 Society of Chemical Industry and John Wiley & Sons, Ltd

20. Smart JP, O'Nions P and Riley GS, Radiative and convective heat transfer, and burnout in oxy-coal combustion. *Fuel* **89**:833–840 (2010).
21. Faúndez J, Arenillas A, Rubiera F, García X, Gordon AL and Pis JJ, Ignition behaviour of different rank coals in an entrained flow reactor. *Fuel* **84**:2172–2177 (2005).
22. Gil MV, Riaza J, Álvarez L, Pevida C, Pis JJ and Rubiera F, Oxy-fuel combustion kinetics and morphology of coal chars obtained in N_2 and CO_2 atmospheres in an entrained flow reactor. *Appl Energy* **91**:67–74 (2012).
23. Wall TF, Phong-Anant D, Gururajan VS, Wibberley LJ, Tate A and Lucas J, Indicators of ignition for clouds of pulverized coal. *Combust Flame* **72**:111–118 (1988).
24. Essenhigh RH, Misra MK and Shaw DW, Ignition of coal particles: a review. *Combust Flame* **77**:3–30 (1989).
25. Khatami R, Stivers C, Joshi K, Levendis YA and Sarofim AF, Combustion behavior of single particles from three different coal ranks and from sugar cane bagasse in O_2/N_2 and O_2/CO_2 atmospheres. *Combust Flame* **159**:1253–1271 (2012).
26. Stivers C and Levendis YA, Ignition of single coal particles in $O_2/N_2/CO_2$ atmospheres. In: The 35th International Technical Conference on Clean Coal & Fuel Systems. Clearwater, FL, June 7–10 (2010).
27. Khatami R, Stivers C and Levendis YA, Ignition characteristics of single coal particles from three different ranks in O_2/N_2 and O_2/CO_2 atmospheres. *Combust Flame* **159**:3554–3568 (2012).
28. Shaddix CR and Molina A, Ignition and devolatilisation of pulverized coal during oxygen/carbon dioxide coal combustion. *Proc Combust Inst* **32**:2091–2098 (2009).
29. Zhang L, Binner E, Qiao Y and Li C-Z, *In situ* diagnostics of Victorian brown coal combustion in O_2/N_2 and O_2/CO_2 mixtures in a drop tube furnace. *Fuel* **89**:2703–2712 (2010).
30. Arias B, Pevida C, Rubiera F and Pis JJ, Effect of biomass blending on coal ignition and burnout during oxy-fuel combustion. *Fuel* **87**:2753–2759 (2008).
31. Binner E, Zhang L, Li C-Z and Bhattacharya S, *In-situ* observation of the combustion of air-dried and wet Victorian brown coal. *Proc Combust Inst* **33**:1739–1746 (2011).
32. Binner E, Zhang L and Bhattacharya S, Investigation of the effect of inherent water content on the combustion characteristics of Victorian brown coal in air an under oxy-fuel conditions, *26th International Pittsburgh Coal Conference*. Pittsburgh, PA, September 20–23 (2009).

Juan Riaza

Juan Riaza is a Mining Engineer and has an MSc in Energy Engineering from the University of Oviedo. He is undertaking his PhD studies at INCAR-CSIC in Oviedo on the co-combustion of coal and biomass blends under oxyfuel conditions.

Lucía Álvarez

Lucía Álvarez graduated with a PhD in Chemical Engineering from Oviedo University in 2012. She is currently working as a postdoctoral researcher at the INCAR-CSIC. Her research interests involve oxy-fuel combustion modelling by means of Computational Fluid Dynamics techniques. She has established strong international collaborations with prestigious institutions on this subject.

Victoria Gil

Victoria Gil received her PhD in Environmental Sciences from the University of León, Spain, in 2007. She has been working as a postdoctoral researcher at the INCAR-CSIC since 2009. Her research interests embrace energy production from renewable and fossil fuels, and the co-gasification of coal and biomass.

Reza Khatami

Reza Khatami obtained his MSc degree in Mechanical Engineering from Sharif University of Technology in Tehran, Iran in 2005. He worked for the NRI research institute and for oil and gas and metal production industries (IRITEC, ITOK) in Tehran before joining Northeastern University in 2008 to pursue his PhD. His current research focuses on the single particle ignition and combustion of different coal ranks and biomasses in oxy-fuel environments.

Yiannis A. Levendis

Yiannis A. Levendis received his PhD degree in Environmental Engineering Science from Caltech, in the USA, in 1988. He joined the Northeastern University faculty in 1988, and he is currently a College of Engineering Distinguished Professor in the Department of Mechanical and Industrial Engineering. His current research is dealing with conventional and oxy-combustion, alternative energy sources, air pollution and acid rain prevention.

© 2013 Society of Chemical Industry and John Wiley & Sons, Ltd

José J. Pis

José J. Pis was awarded a PhD from Oviedo University in 1976. He joined the INCAR-CSIC in 1979. He was Head of Department, and also Vice-director until 1995. In 1999 he became a Research Professor. His research involves from the characterization of carbon materials to the design and optimization of pilot scale reactors.

Covadonga Pevida

Covadonga Pevida graduated with a PhD from Oviedo University in 2004. Following her postdoctoral work at the Universities of Lyon and Nottingham, she got a position as Tenured Scientist at the INCAR-CSIC in 2008. She is currently Head of the Department of Energy & Environment at the INCAR-CSIC. Her main lines of research involve carbon capture by adsorption processes and oxycoal combustion.

Fernando Rubiera

Fernando Rubiera received his PhD from Oviedo University in 1991. He is currently a Research Scientist and Vice-director at the INCAR-CSIC. His main research interests embrace the co-utilisation of coal and biomass, and pre- and post-combustion carbon capture from coal.

© 2013 Society of Chemical Industry and John Wiley & Sons, Ltd

6.2.3 *Publicación IX*

Oxy-fuel combustion of coal and biomass blends.

J. Riaza, M.V. Gil, L. Álvarez, C. Pevida, J.J. Pis, F. Rubiera.
Energy
2012. 41 (1) pp. 429–435.
doi: 10.1016/j.energy.2012.02.057

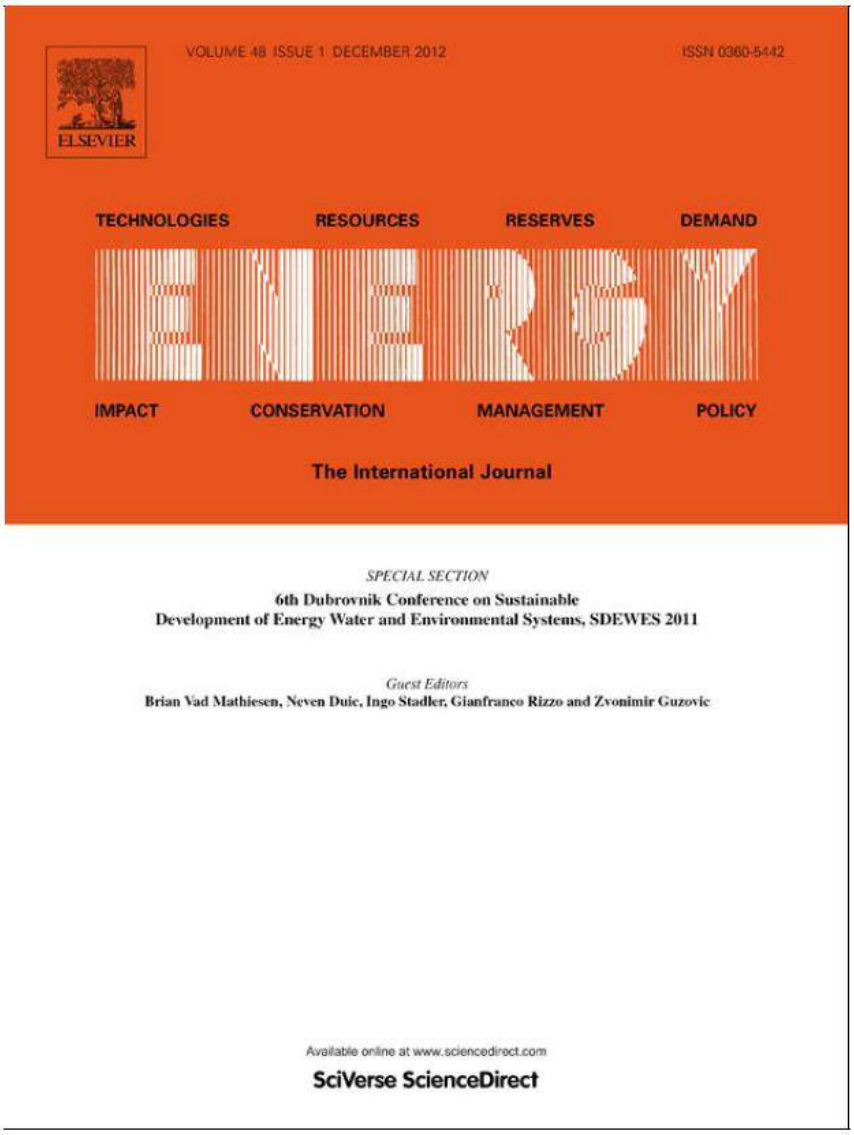

Energy 41 (2012) 429–435

Contents lists available at SciVerse ScienceDirect

Energy

journal homepage: www.elsevier.com/locate/energy

Oxy-fuel combustion of coal and biomass blends

J. Riaza, M.V. Gil, L. Álvarez, C. Pevida, J.J. Pis, F. Rubiera*

Instituto Nacional del Carbón, INCAR-CSIC, Apartado 73, 33080 Oviedo, Spain

ARTICLE INFO

Article history:
Received 14 October 2011
Received in revised form
23 February 2012
Accepted 25 February 2012
Available online 28 March 2012

Keywords:
Coal
Biomass
Oxy-fuel combustion
Ignition
Burnout

ABSTRACT

The ignition temperature, burnout and NO emissions of blends of a semi-anthracite and a high-volatile bituminous coal with 10 and 20 wt.% of olive waste were studied under oxy-fuel combustion conditions in an entrained flow reactor (EFR). The results obtained under several oxy-fuel atmospheres (21%O_2–79%CO_2, 30%O_2–70%CO_2 and 35%O_2–65%CO_2) were compared with those attained in air. The results indicated that replacing N_2 by CO_2 in the combustion atmosphere with 21% of O_2 caused an increase in the temperature of ignition and a decrease in the burnout value. When the O_2 concentration was increased to 30 and 35%, the temperature of ignition was lower and the burnout value was higher than in air conditions. A significant reduction in ignition temperature and a slight increase in the burnout value was observed after the addition of biomass, this trend becoming more noticeable as the biomass concentration was increased. The emissions of NO during oxy-fuel combustion were lower than under air-firing. However, they remained similar under all the oxy-fuel atmospheres with increasing O_2 concentrations. Emissions of NO were significantly reduced by the addition of biomass to the bituminous coal, although this effect was less noticeable in the case of the semi-anthracite.

© 2012 Elsevier Ltd. All rights reserved.

1. Introduction

The role of coal as an energy source has attracted renewed interest due to the stability of its supply and its relatively low cost, which will probably guarantee its inclusion in the energy mix in the foreseeable future [1]. Until renewable energy sources can reliably produce significant amounts of energy, the immediate energy demand is likely to be met by conventional fossil fuel combustion, such as coal. However, coal combustion produces a large amount of CO_2, which is the chief contributor to global climate change. To meet future targets for the reduction of greenhouse gas (GHG) emissions, CO_2 must be captured and stored. Several strategies for the reduction and capture of CO_2 from large-scale stationary power plants are currently being studied.

The oxy-fuel combustion of coal with recycled flue gas is considered as a promising option to ensure the continued use of coal for electric power production [2–5]. Conventional pf coal-fired boilers use air for combustion and the nitrogen in the air (approximately 79% by volume) has the effect of diluting the concentration of CO_2 in the flue gas, which is present in concentrations of 14–16% in air-firing conditions. However, during oxy-fuel combustion, fuel is burnt in a mixture of oxygen and recycled flue gas to yield a rich CO_2 (95%) and water vapour stream, which after purification and compression is ready for sequestration [6]. An important advantage of this technology is that it avoids the formation of thermal NO_x due to the absence of nitrogen gas in the combustion atmosphere, with the result that NO_x emissions are reduced. The amount of NO_x released also decreases because the NO_x in the recycled flue gas decomposes as it comes into contact with the flame-generated hydrocarbons and the reducing atmosphere near the flame, a mechanism to which Scheffknecht et al. [7] attach considerable importance.

In addition, the oxy-combustion of coal makes it possible to capture and sequester carbon using technology already available in conventional pulverized coal boilers, and to capitalize on the enormous quantities of money invested in existing boilers. What is more, oxy-fuel recycle combustion requires only a slight modification of the existing pulverized coal combustion technology that has already demonstrated its reliability and won widespread industrial acceptance [5].

The combustion of coal in the O_2/CO_2 atmosphere of an oxy-coal combustion boiler may be expected to be different to that of an O_2/N_2 atmosphere of a conventional coal-air combustion boiler, because the CO_2 gas is denser and has a higher specific heat capacity than N_2 and because coal may be gasified by the CO_2. Consequently, the replacement of N_2 by CO_2 will decrease the speed of propagation and stability of the flame and gas temperature, while increasing the unburned carbon content. It is for this reason that a high oxygen concentration in an oxy-fuel combustion atmosphere (up to approximately 30%) is generally used in order to match the combustion performance achieved in air in relation to

* Corresponding author. Tel.: +34 985 118 975; fax: +34 985 297 662.
E-mail address: frubiera@incar.csic.es (F. Rubiera).

0360-5442/$ – see front matter © 2012 Elsevier Ltd. All rights reserved.
doi:10.1016/j.energy.2012.02.057

flame temperature, ignition time, heat transfer, gas temperature profile and char burnout.

On the other hand, biomass is a renewable fuel which can be used to reduce CO_2 emissions. This source of energy is considered carbon neutral because the carbon dioxide released during its combustion is recycled as an integral part of the carbon cycle. The co-firing of biomass with coal is an environmentally friendly method of coal utilization since it reduces harmful emissions and provides an alternative to land filling [8]. One of the main advantages of co-firing biomass and coal is its relatively easy and cheap application in existing pulverized coal power plants, that requires only minor modifications compared to the costly construction of new biomass-only fired power plants [9]. The combination of oxy-fuel combustion with biomass could afford a method of disposal for CO_2 that has only partially been studied. Preliminary works have been carried out employing thermogravimetric analysis [8,10] and an entrained flow reactor [11] with the aim of studying the co-firing of coal and biomass under oxy-fuel conditions, but more research is required in order to introduce this practise at industrial scale.

In this work, a biomass derived from the olive oil production process, olive waste (OW), was utilized. It is the wet solid waste that remains after the process of pressing and extraction of the olive oil. The objective was to study the co-firing of coal with this biomass under oxy-fuel combustion conditions in an entrained flow reactor. Air conditions were used for comparison. The ignition temperature, burnout and NO emissions from various coal/biomass blends under air and oxy-fuel environments were determined and, in this way, the effect of adding biomass upon the oxy-fuel combustion of coal was evaluated.

2. Materials and methods

2.1. Materials

Two coals of different rank were used in this work: a semi-anthracite from the Hullera Vasco-Leonesa in León (Spain), HVN, and a South African high-volatile bituminous coal from the Aboño power plant in Asturias (Spain), SAB. A biomass, olive waste (OW), was also employed. The coal and biomass samples were ground and sieved to obtain a particle size fraction of 75–150 μm. The proximate and ultimate analyses together with the higher heating values of the samples are presented in Table 1.

Table 1
Proximate and ultimate analyses and higher heating value of the fuel samples.

Sample	HVN	SAB	OW
Origin	Spain	South Africa	Spain
Rank	sa	hvb	–
Proximate Analysis[a]			
Moisture content (wt.%)	1.1	2.4	9.2
Ash (wt.%, db)	10.7	15.0	7.6
V.M. (wt.%, db)	9.2	29.9	71.9
F.C. (wt.%, db)[b]	80.1	55.1	20.5
Ultimate Analysis (wt.%, daf)[a]			
C	91.7	81.5	54.3
H	3.5	5.0	6.6
N	1.9	2.1	1.9
S	1.6	0.9	0.2
O[b]	1.3	10.5	37.0
Higher heating value (MJ/kg, db)	31.8	27.8	19.9

sa: semi-anthracite; hvb: high-volatile bituminous coal. db: dry basis; daf: dry and ash free bases.

[a] The proximate analysis was conducted in a LECO TGA-601, and the ultimate analysis in a LECO CHNS-932.

[b] Calculated by difference.

2.2. Experimental device and procedure

The ignition and oxy-fuel combustion characteristics of the coals and coal/biomass blends at high heating rates and short residence times were studied in an entrained flow reactor (EFR), which has been described in detail elsewhere [12,13]. Briefly, the reactor has a reaction zone of length 1400 mm and internal diameter 40 mm which is electrically heated and is capable of reaching a maximum temperature of 1100 °C. Fuel samples are fed in from a hopper through an air-cooled injector to ensure that the temperature does not exceed 100 °C before entering the reaction zone and the mass flow is controlled by means of a mechanical feeding system. The gases are preheated to the oven temperature before being introduced into the reactor through flow straighteners. The flow rates of N_2, CO_2 and O_2 from the gas cylinders are controlled by mass flow controllers. A water-cooled collecting probe is inserted into the reaction chamber from below. Nitrogen is introduced at the top of this probe to quench the reaction products. Particles are removed by means of a cyclone and a filter, and the exhaust gases are monitored using a battery of analysers (O_2, CO_2, CO, NO and SO_2).

During the ignition tests carried out in the present study, the reactor was heated at 15 °C min^{-1} from 400 to 800 °C. The gas flow used in the tests ensured a particle residence time of 2.5 s at 500 °C, and excess oxygen (defined as the O_2 supplied in excess of that required for the stoichiometric combustion of coal) was set at a value of 25%. The criterion for determining the ignition temperature was based on the first derivative temperature curves of the gases produced. The ignition temperature was taken as the temperature at which the first derivative temperature curve, normalized by the maximum derivative value, reached a value of 10% [14].

On the other hand, the combustion tests were carried out at a reaction temperature of 1000 °C employing a particle residence time of 2.5 s. In order to check the constant gas temperature over the reactor height, a temperature profile along the reactor was measured with a fine wire type K thermocouple, while the gas was flowing, and it was found to be 1000 ± 10 °C. Burnout is defined as the loss of mass of a fuel during its combustion and is expressed as the ratio of mass loss during combustion to the total mass in the input coal. Fuel mass loss during the experiments was determined by the ash tracer method. The experimental errors in the burnout and NO measurements were 4 and 5% respectively.

Four binary mixtures of O_2/N_2 and O_2/CO_2 were employed to study the combustion behaviour of the coals and coal/biomass blends. Thus, for the ignition and combustion tests, air (21%O_2–79%N_2) was taken as reference and three binary mixtures of O_2 and CO_2 were compared: 21%O_2–79%CO_2, 30%O_2–70%CO_2 and 35%O_2–65%CO_2. The addition of 10 and 20 wt.% of olive waste to the coals was evaluated for all of the air and the oxy-fuel combustion atmospheres, in order to study the effect of adding biomass on the ignition temperature, burnout value and NO emissions.

3. Results and discussion

3.1. Ignition temperature

The ignition temperature of the semi-anthracite HVN and the bituminous coal SAB, as well as their blends with OW, under the different atmospheres studied is presented in Fig. 1. Both coals showed the same behaviour in relation to the combustion atmosphere. However, the ignition of the HVN coal took place at much higher temperatures than that of the SAB coal in all of the atmospheres studied, in accordance with its rank (Table 1). The reactivity of the high-volatile bituminous coal, SAB, is greater than that of the

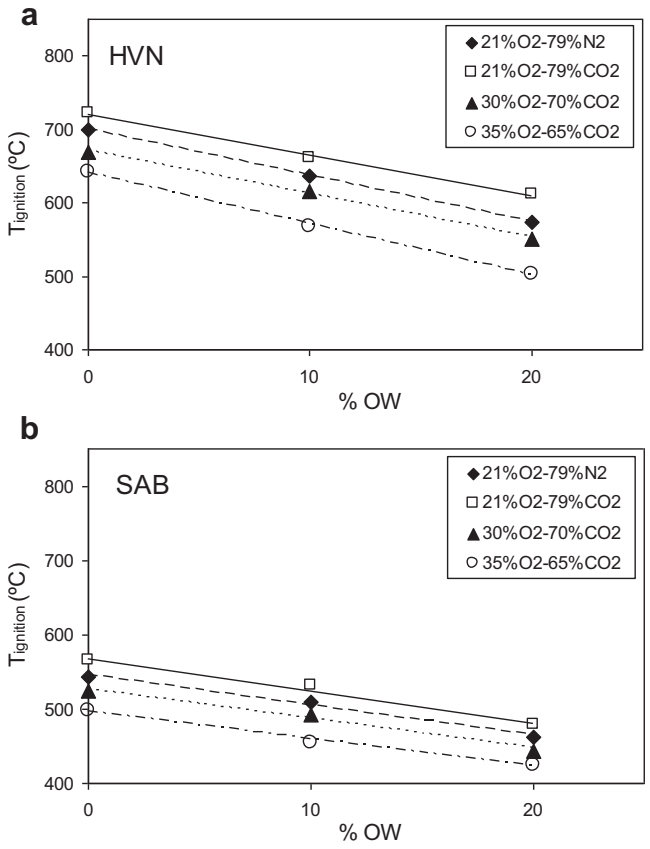

Fig. 1. Ignition temperatures of the HVN (a) and SAB (b) coals and their blends with olive waste (OW) under different atmospheres.

semi-anthracite, HVN, as a result of which one would expect heat to be released earlier and the ignition temperatures to be reduced.

The behaviour of the coal/biomass blends under the oxy-fuel combustion atmospheres was similar to that of the individual coals. Thus, when N_2 (21%O_2–79%N_2) was replaced by CO_2 (21%O_2–79%CO_2), the ignition temperature increased (Fig. 1). This may be attributed to the higher specific molar heat of CO_2 compared to N_2. Before ignition, the fuel particles are heated up by the ambient environment until the combustion occurs. The radiant heat from the particles then causes an increase in the temperature of the gas. Because of the higher specific molar heat of CO_2, more ambient heat is needed to increase the temperature under an oxy-fuel combustion atmosphere. This results in a comparatively lower gas temperature and, therefore, a reduction in the fuel particle temperature during oxy-fuel combustion in comparison to combustion in air at the same oxygen concentration [13]. This should lead to a delay in the ignition of volatiles and char under the 21%O_2–79%CO_2 atmosphere, as pointed out by Liu et al. [15] and Molina and Shaddix [16]. Liu et al. [17] observed a longer ignition delay under the CO_2 atmosphere than under N_2 in an entrained flow reactor, which they attributed to the higher volumetric heat capacity of CO_2 inhibiting the local thermal runaway. The reduced diffusivity of oxygen in CO_2 may also have contributed to the delay in ignition.

When the oxygen concentration was increased (30%O_2–70%CO_2 and 35%O_2–65%CO_2), the ignition temperature decreased to below that of the air conditions, both in the case of the coals and the coal/biomass blends (Fig. 1). If the O_2 concentration was increased, the mass flux of O_2 to the fuel surface particles, the rate of devolatilization and the oxidation rate of the volatiles will also increase. This will shorten the fuel particle auto-ignition time considerably [18]. Molina and Shaddix [16] observed in single particle experiments that the particle ignition and devolatilization properties in an atmosphere of 30%O_2 in CO_2 were similar to those of air.

Information on the effect of high levels of CO_2 on the ignition of coal/biomass particles is important both for understanding how to prepare existing burners that operate in air for operating in O_2/CO_2 mixtures, and for the CFD modelling of the performance of pulverized coal burners in O_2/CO_2 systems [7].

From Fig. 1 it can also be seen that the addition of olive waste, OW, caused a significant reduction in the ignition temperatures of both coals in all the atmospheres studied. This decrease became more pronounced as the biomass concentration in the blend was increased due to the fact that because biomass is a highly reactive fuel and has high-volatile matter content (Table 1), it will react faster and improve the ignition behaviour of the coal. As the percentage of biomass is increased, more heat will be released earlier leading to a greater reduction in the ignition temperature of the blend. Arias et al. [11] observed a substantial reduction in the ignition temperature of coal/biomass blends in air but only a small decrease under oxy-fuel combustion atmospheres. They explained this because biomass has a lower heating value than coal, and so less heat is generated during its oxidation in the ignition process, and CO_2 has a specific heat higher than N_2. Thus, when CO_2 is the major component in the surrounding gases, the heat released by the biomass present in the blend generates a small increase in the temperature of the gases and so the ignition properties of coal are less affected. However, in the present work, a reduction in the ignition temperature of coal/biomass blends occurred both in the air and oxy-fuel atmospheres, in agreement with the results of Gil et al. [10], who from a previous thermogravimetric analysis, observed that the addition of olive waste to the HVN coal caused a decrease in the combustion and oxy-fuel combustion temperatures.

Decreases in the ignition temperature of 75–54 °C and 139–111 °C were achieved when coal HVN was blended with 10 and 20 wt.% of OW, respectively. When the SAB coal was blended with 10 and 20 wt.% of OW, reductions of 43–33 °C and 87–73 °C, respectively, were achieved. These differences can be attributed to the different reactivities of these coals resulting in much lower ignition temperatures in the case of the SAB coal. The ignition temperature of coal SAB was therefore less affected by the addition of biomass than that of the HVN coal. These results suggest that the effect of the addition of biomass on the ignition temperature of coal is more significant in high rank coals, which have much lower reactivity values than the biomass.

3.2. Burnout

Coals HVN and SAB and their blends with biomass were burned at different levels of excess oxygen for each atmosphere studied. The fuel equivalence ratio, defined as the ratio between the fuel mass flow rate and the stoichiometric value, was used to determine the excess oxygen during combustion.

The burnout values of HVN and SAB, and their blends with olive waste (OW), are shown in Figs. 2 and 3, respectively. It can be seen that the burnout value decreased as the fuel equivalence ratio increased due to less oxygen being available at higher fuel equivalence ratio values. For coal HVN and its blends with OW, the burnout showed an almost linear dependence on the fuel equivalence ratio in both the air and oxy-fuel conditions (Fig. 2). Even at low values of fuel equivalence ratio (high excess oxygen), the samples showed low burnout values, reflecting the lower reactivity of this high rank coal. However, at low fuel equivalence ratio values (high oxygen excess), the burnout curves of SAB and its blends with

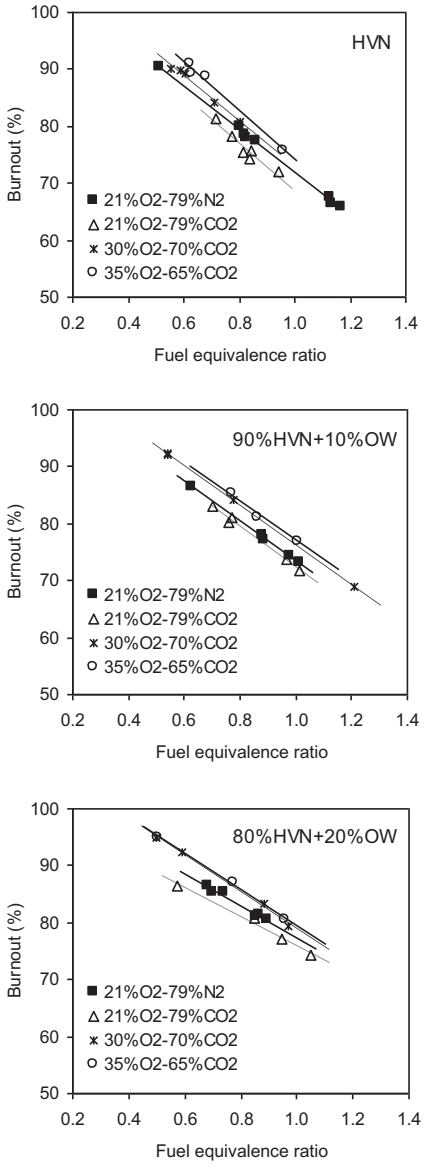

Fig. 2. Burnout values of the HVN coal and HVN + OW blends under different atmospheres at different fuel equivalence ratios.

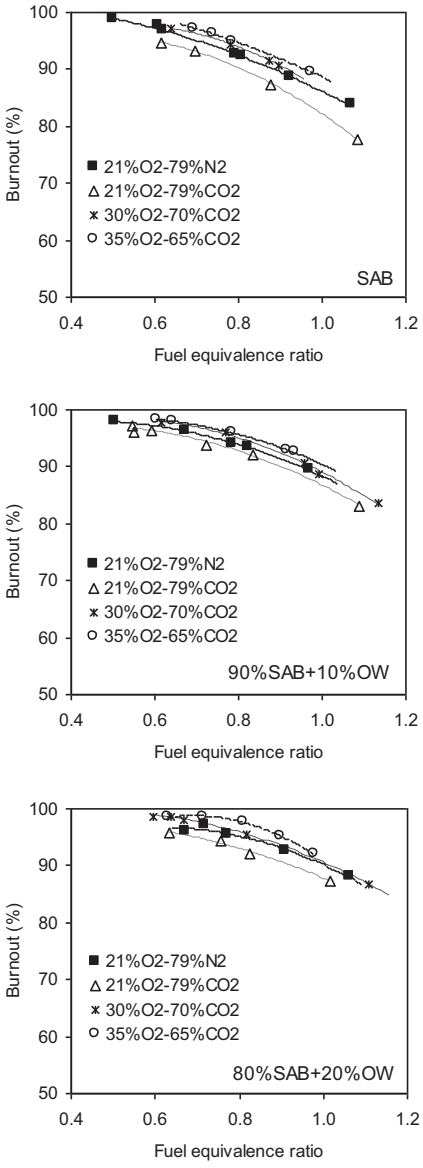

Fig. 3. Burnout values of the SAB coal and SAB + OW blends under different atmospheres at different fuel equivalence ratios.

biomass showed an asymptotic approach towards values close to 100% (Fig. 3) due to the high reactivity of this coal.

In order to facilitate a comparison of the behaviour of these coals and their blends with biomass under air and oxy-fuel atmospheres, the burnout values were interpolated at a fuel equivalence ratio of 0.8 using the curves shown in Figs. 2 and 3. The results for both, HVN and SAB, are presented in Fig. 4a and Fig. 4b, respectively. The burnout behaviour of the coal/biomass blends under the oxy-fuel combustion atmospheres in relation to the air atmosphere was similar to that of the individual coals.

For both coals and their blends with biomass (Fig. 4), the burnout value obtained under the 21%O_2–79%CO_2 atmosphere was lower than that reached under 21%O_2–79%N_2 conditions. Liu et al. [15] observed that, when air was replaced by 21%O_2–79%CO_2, the gas temperatures dropped significantly. Due to the higher specific molar heat of CO_2, the heating capacity of the surrounding gases will be higher, which in turn will lead to lower flame and gas temperatures under this atmosphere. According to Zhang et al. [18], the specific heat capacity of the diluent gas is one of the principal factors affecting char surface temperature for any given fraction of O_2. Therefore, particle temperature in a 21%O_2–79%CO_2 atmosphere can be expected to be lower, which will cause the combustion rate of the char and the fuel burnout value to fall [11]. In addition, Li et al. [19] attributed the different coal combustion behaviours under both atmospheres in a drop tube furnace to the lower diffusivity of O_2 in CO_2 than in N_2, impeding the transport of O_2 to the surface of the particles and reducing the combustion rate of the volatile matter and char in oxy-fuel conditions.

Under the 30%O_2–70%CO_2 and 35%O_2–65%CO_2 atmospheres, the burnout of the HVN and SAB coals and their blends with biomass was higher than in air (Fig. 4), which is explained because the higher oxygen concentration caused an increase in the char combustion rate, together with a decrease in the ignition temperature. The lower ignition temperature means a higher combustion time, which will lead to reach higher burnout values. Though the gas temperature increases only slightly when the O_2 fraction in bulk gas is increased, it is likely that the increase in the mass flux

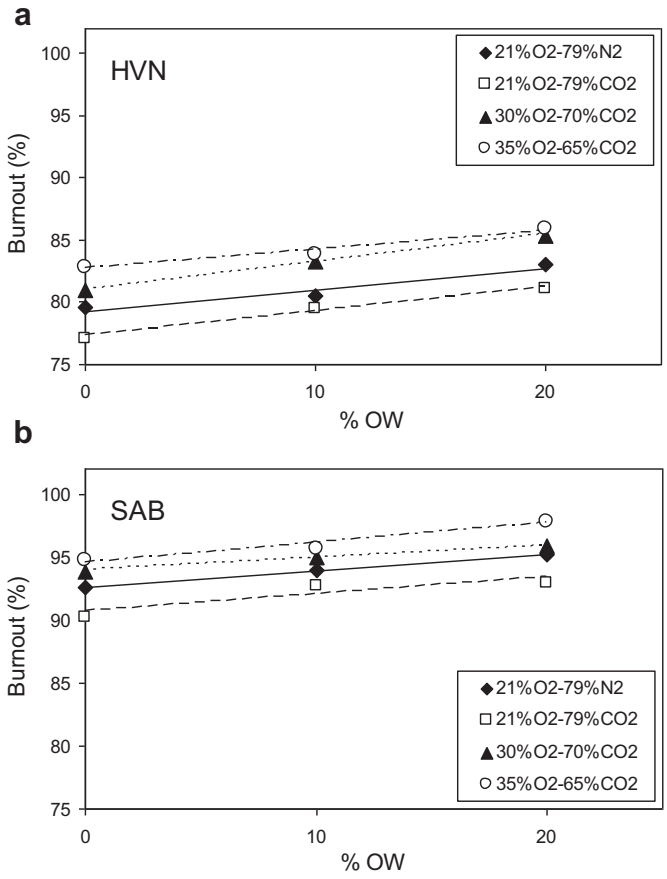

Fig. 4. Burnout values of the HVN (a) and SAB (b) coals and their blends with olive waste (OW) under different atmospheres at a fuel equivalence ratio of 0.8.

rate of O_2 to the particle surface at higher O_2 concentrations promotes the consumption rate of the volatiles [20] and provides extra heat feedback to the particle, enhancing devolatilization, ignition and combustion.

It can be seen that under the air and the three oxy-fuel combustion atmospheres studied, the addition of olive waste, OW, caused an increase in the burnout value of both coals, this increase becoming more pronounced as the biomass concentration increased. Smart et al. [21] also observed an improvement in burnout by co-firing coal and biomass (shea meal and sawdust) under both oxy-fuel and air-firing conditions.

Previous studies on the co-combustion of coal/biomass blends have also shown that the addition of biomass to coal can improve the burnout efficiency of coal to a certain degree [22]. Since biomass has a higher volatile matter content and a lower ash content, devolatilization and gaseous phase combustion can acquire more importance than in the case of the combustion of an individual coal. Munir et al. [23] studied shea meal and cotton stalk as potential fuels for co-combustion with coal and also concluded that the co-combustion of biomass with coal is beneficial from the point of view of burnout due to the greater reactivity of biomass char.

If the reactivities of two fuels which are burned as a blend are different, there will be differences in their combustion, as the more reactive fuel will react faster, thereby reducing oxygen concentration and increasing the temperature at the top of the reaction chamber. Any improvement in the burnout of the less reactive component will depend on the oxygen and temperature profiles in the reactor [11]. In this work, olive waste, OW, was more reactive than coals HVN and SAB and so the burnout of the blends was improved. This indicates that the coals were not negatively affected by the modification of the oxygen and temperature profiles due to the biomass combustion, i.e., the availability of oxygen was not restricted during the combustion of the blend.

The improvement in burnout after the addition of biomass, especially in the 20 wt.% biomass blends, was more noticeable in the case of HVN than SAB. This may be due to the fact that the individual SAB coal had already reached a high burnout degree before blending, so there was less margin for improvement by adding olive waste to this coal. The addition of 20% of biomass was therefore less effective.

From the results obtained, it can be concluded that the addition of biomass had a greater effect on the ignition temperature than on the burnout, especially with high biomass concentrations in the blend, all of which underlines the importance of the devolatilization and gaseous phase after the addition of biomass. On the other hand, since biomass has a lower calorific value and higher moisture content than coal, the flame temperature may be reduced and the radiative heat flux impeded if the concentration of biomass in the blend is too high. This would then reduce the oxidation rate as Smart et al. [21] suggested. However, these authors have shown that the positive effect of co-firing with biomass on burnout is dependent on the type of biomass and have observed significant improvements in burnout value when biomass with a high reactivity is used.

3.3. NO emissions

The NO concentration (mg NO/mg burned fuel) values interpolated at a fuel equivalence ratio of 0.8 for coals HVN and SAB and their blends with olive waste (OW) are shown in Fig. 5. For both coals, the NO concentration obtained under the $21\%O_2-79\%CO_2$ atmosphere was lower than that achieved under $21\%O_2-79\%N_2$ conditions. The lower NO concentrations in the oxy-fuel combustion atmospheres than in air are partly explained by the suppression of thermal NO formation since there is no nitrogen gas in the combustion atmosphere. However, under the experimental conditions of the present study, this explanation does not seem applicable. Under air conditions, the thermal formation of NO resulting from the reaction between molecular N_2 and O_2 occurs at high temperatures. In this work however, this route could make only a minor contribution to the formation of NO due to the temperature used (1000 °C).

It would appear, therefore, than the lower NO concentration obtained under the oxy-fuel atmosphere with 21% of O_2 than under air conditions was probably due to the greater NO reduction under oxy-fuel conditions resulting from the chemical reactions of NO with either CO or with nitrogen species (volatile-N) and hydrocarbon species released during devolatilization. Andersson et al. [24] found that the formation of NO from fuel-N in oxy-fuel combustion was the same as, or slightly higher than, in air-firing conditions, whereas the reduction of NO could be up to 50% greater in oxy-combustion. In the present experiments therefore the lower NO emissions during oxy-fuel combustion than under air-firing must have been due to the increased reduction of NO under the O_2/CO_2 atmosphere. Okazaki and Ando [25] also concluded that the reduction of NO to molecular N_2 due to chemical reactions in the combustion zone under oxy-fuel conditions was the main reason for the overall decrease in NO concentration. Al-Makhadmeh et al. [26] found that the reduction of NO is enhanced during combustion in O_2/CO_2 compared to combustion in O_2/N_2. Liu et al. [15] found that the higher CO concentrations inside the oxy-fuel combustion zone and within the vicinity of the combustion particles resulted in a further reduction of NO. Gasification of the

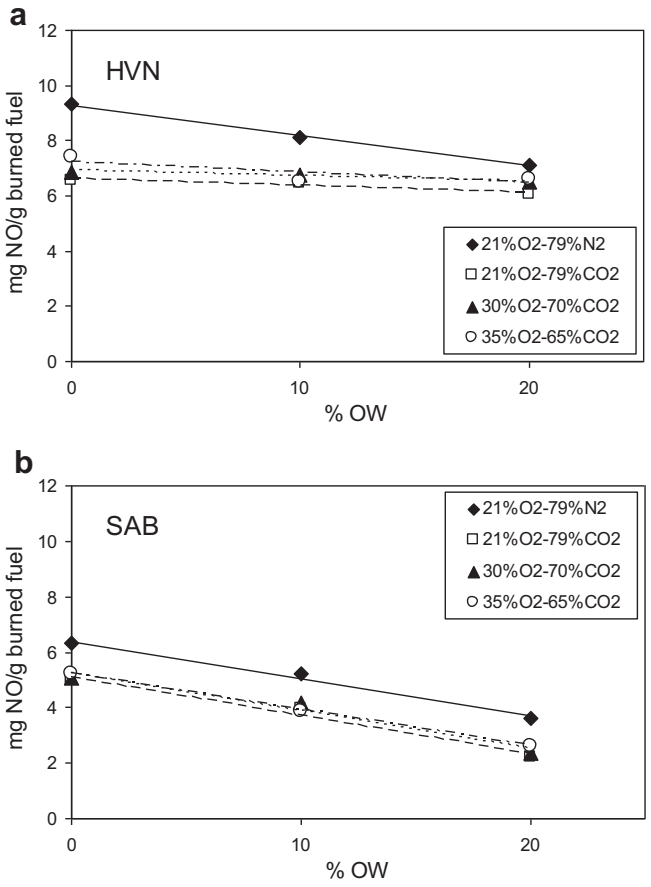

Fig. 5. NO emissions of the HVN (a) and SAB (b) coals and their blends with olive waste (OW) under different atmospheres at a fuel equivalence ratio of 0.8.

char with CO_2 may have contributed to an increase in the production of CO during oxy-fuel combustion. Furthermore, the recent results of experimental investigation on NO_x formation during the oxy-fuel combustion of pulverized coal published by Shaddix and Molina [5] and Sun et al. [27] lead to the conclusion that fuel-N conversion to NO in O_2/CO_2 is lower than in O_2/N_2, and that this may contribute to a lower NO concentration. Yoshiie et al. [28] found that the NO emissions and conversions of fuel nitrogen to NO under oxy-fuel combustion conditions were lower than that under air combustion conditions without adding NO in the fed atmosphere. Also, Jiang et al. [29] shown lower NO concentrations under oxy-fuel combustion atmospheres than in air without gas recirculation.

In the 30%O_2–70%CO_2 and 35%O_2–65%CO_2 atmospheres, the NO concentrations were similar to that of the oxy-fuel atmosphere containing 21% of O_2 (Fig. 5). In none of the oxy-fuel atmospheres did the NO concentration reach that of air. Only small differences in NO concentrations under the oxy-fuel atmospheres with increasing O_2 concentrations were found in the present study. Andersson et al. [25] found that NO emissions per unit of fuel energy supplied fell under oxy-fuel combustion with 25% of O_2 compared to air-firing conditions, but they found only small differences in the reduction of NO for different O_2 concentrations (25, 27 and 29%) in oxy-fuel atmospheres.

For the SAB coal (Fig. 5b), it can be seen that the NO concentration in air and under oxy-fuel atmospheres decreased after the addition of biomass, this decrease becoming greater as the biomass concentration was increased. For the HVN coal (Fig. 5a), the same tendency was observed, but the decrease in NO concentration values was smaller. The effect of co-firing biomass with pulverised coal on NO_x formation is highly complex and is dependent as much on the relative reactivities of the fuels as on the inherent nitrogen contents of the individual fuels [23,30].

Since the HVN coal and the biomass used in the present work showed similar values of nitrogen content (Table 1), the lower NO emissions during co-firing cannot be explained by the dilution of N in the mixed fuel because of the lower nitrogen content in the biomass. However, in the case of the SAB coal the dilution of N may have had an effect since the nitrogen content of SAB was slightly higher than that of the biomass OW (Table 1), which could have increased the differences in NO emissions after the addition of the biomass.

Skeen et al. [31] studied the NO emissions during coal/biomass combustion under air-fired and oxy-fuel conditions in a laboratory-scale combustor and found that NO emissions were reduced with the addition of biomass under air-firing conditions but not under oxy-fuel conditions.

A reasonable explanation for the decrease in NO emissions after the addition of biomass has been provided by Liu et al. [32] in their study on conventional co-combustion of coal and biomass. These authors believe that lower NO_x emissions may occur during co-combustion than with individual coals because most of the biomass is released as volatiles (about 75% at temperatures above 800 °C) and the fuel-N in the biomass is predominantly liberated as NH_3 which may on the one hand form NO_x, but also act as a reducing agent in further reactions with NO_x to form N_2. Since most of fuel-N in coal is retained in the char and is then oxidised to NO_x, the NH_3 originating from the biomass may lead to the reduction of NO_x, since the high amount of released volatile matter from the biomass combustion produces a fuel-rich condition in the atmosphere which would favour the reduction of NO [33]. Akpulat et al. [34] studied the co-combustion of coal and olive cake in a fluidized bed combustor and they attribute the decrease in NO_x concentrations to the percentage of olive cake in the fuel being increased by the higher amount of volatile matter evolved from the olive cake, and to the generation of high levels of hydrocarbon radicals and CO formation (reducing atmosphere) in the freeboard region.

In the case of the SAB coal, its higher volatile matter content may have contributed to the creation of a reducing atmosphere that favoured the consumption of NO, which would explain why the reduction in the concentration of NO was greater than in the HVN coal. In general, it seems that the effect of the addition of biomass on the NO emissions from coal is more noticeable in low rank coals, which have a higher volatile matter content.

4. Conclusions

The ignition temperature and burnout of a semi-anthracite and a high-volatile bituminous coal and their blends with biomass (olive waste) were studied under oxy-fuel combustion conditions in an entrained flow reactor (EFR). As in the case of the individual coals, the ignition temperature of the coal/biomass blends was higher under a 21%O_2–79%CO_2 atmosphere than in air conditions, whereas the burnout was lower due to the higher specific molar heat of CO_2 compared to N_2 and the lower diffusivity of O_2 in CO_2 than in N_2. However, when the O_2 concentration was increased to 30 and 35% in the oxy-fuel combustion atmosphere, the ignition temperature was lower than in air, while the burnout value was greater than that achieved under air-firing. This was due to an increase in the mass flux of O_2 to the surface of the coal particles. The addition of biomass to the coal improved the ignition temperatures and the burnout values in both the air and oxy-fuel combustion atmospheres under the experimental conditions of

this study, reflecting the higher volatile content and reactivity of the biomass. The addition of biomass had a more pronounced effect on the ignition temperature than on burnout. NO emissions were lower during oxy-fuel combustion than in air-firing, but only small differences in the reduction of NO in relation to the O_2 concentration in the three oxy-fuel combustion atmospheres were observed. The addition of biomass significantly reduced the NO emissions from the bituminous coal, both under air and under oxy-fuel atmospheres, this decrease being proportional to the concentration of biomass. However the reduction of NO emissions was less noticeable in the case of the semi-anthracite.

Acknowledgements

This work was carried out with financial support from the Spanish MICINN (Project PS-120000-2005-2) co-financed by the European Regional Development Fund. M.V.G. and L.A. acknowledge funding from the CSIC JAE-Doc and CSIC JAE-Pre programs, respectively, co-financed by the European Social Fund. J.R. acknowledges funding from the Government of the Principado de Asturias (Severo Ochoa program).

References

[1] Buhre BJP, Elliott LK, Sheng CD, Gupta RP, Wall TF. Oxy-fuel combustion technology for coal-fired power generation. Prog Energy Combust Sci 2005; 31:283–307.
[2] Hong J, Chaudhry G, Brisson JG, Field R, Marco Gazzino, Ghoniem AF. Analysis of oxy-fuel combustion power cycle utilizing a pressurized coal combustor. Energy 2009;34:1332–40.
[3] Liszka M, Ziębik A. Coal-fired oxy-fuel power unit - process and system analysis. Energy 2010;35:943–51.
[4] Pak PS, Lee YD, Ahn KY. Characteristics and economic evaluation of a power plant applying oxy-fuel combustion to increase power output and decrease CO_2 emission. Energy 2010;35:3230–8.
[5] Shaddix CR, Molina A. Fundamental investigation of NO_x formation during oxy-fuel combustion of pulverized coal. Proc Combust Inst 2011;33:1723–30.
[6] Wall T, Liu Y, Spero C, Elliott L, Khare S, Rathnam R, et al. An overview on oxyfuel coal combustion–State of the art research and technology development. Chem Eng Res Des 2009;87:1003–16.
[7] Scheffknecht G, Al-Makhadmeh L, Schnell U, Maier J. Oxy-fuel coal combustion-A review of the current stat-of-the-art. Int J Greenhouse Gas Control 2011;5S:S16–35.
[8] Yuzbasi NS, Selçuk N. Air and oxy-fuel combustion characteristics of biomass/lignite blends in TGA-FTIR. Fuel Process Technol 2011;92:1101–8.
[9] Syed AU, Simms NJ, Oakey JE. Fireside corrosion of superheaters: Effects of air and oxy-firing of coal and biomass. Fuel; 2011. doi:10.1016/j.fuel.2011.03.010.
[10] Gil MV, Riaza J, Álvarez L, Pevida C, Pis JJ, Rubiera F. A study of oxy-coal combustión with steam addition and biomass blending by thermogravimetric análisis. J Therm Anal Calorim; 2011. doi:10.1007/s10973-011-1342-y.
[11] Arias B, Pevida C, Rubiera F, Pis JJ. Effect of biomass blending on coal ignition and burnout during oxy-fuel combustion. Fuel 2008;87:2753–9.
[12] Álvarez L, Riaza J, Gil MV, Pevida C, Pis JJ, Rubiera F. NO emissions in oxy-coal combustion with the addition of steam in an entrained flow reactor. Greenhouse Gas Sci Technol 2011;1:180–90.
[13] Riaza J, Álvarez L, Gil MV, Pevida C, Pis JJ, Rubiera F. Effect of oxy-fuel combustion with steam addition on coal ignition and burnout in an entrained flow reactor. Energy 2011;36:5314–9.
[14] Faúndez J, Arenillas A, Rubiera F, García X, Gordon AL, Pis JJ. Ignition behaviour of different rank coals in an entrained flow reactor. Fuel 2005;84:2172–7.
[15] Liu H, Zailani R, Gibbs BM. Comparisons of pulverized coal combustion in air and in mixtures of O_2/CO_2. Fuel 2005;84:833–40.
[16] Molina A, Shaddix CR. Ignition and devolatilization of pulverized bituminous coal particles during oxygen/carbon dioxide coal combustion. Proc Combust Inst 2007;31:1905–12.
[17] Liu Y, Geier M, Molina A, Shaddix CR. Pulverized coal stream ignition delay under convencional and oxy-fuel combustión conditions. Int J Greenhouse Gas Control 2011;5S:S36–46.
[18] Zhang L, Binner E, Qiao Y, Li C- Z. In situ diagnostics of Victorian brown coal combustion in O_2/N_2 and O_2/CO_2 mixtures in drop-tube furnace. Fuel 2010; 89:2703–12.
[19] Li X, Rathnam RK, Yu J, Wang Q, Wall T, Meesri C. Pyrolysis and combustion characteristics of an Indonisian low-rank coal under O_2/N_2 and O_2/CO_2 conditions. Energy Fuels 2010;24:160–4.
[20] Shaddix CR, Molina A. Particle imaging of ignition and devolatilization of pulverized coal during oxy-fuel combustion. Proc Combust Inst 2009;32: 2091–8.
[21] Smart JP, Patel R, Riley GS. Oxy-fuel combustion of coal and biomass, the effect on radiative and convective heat transfer and burnout. Combust Flame 2010; 157:2230–40.
[22] Haykiri-Acma H, Yaman S. Effect of co-combustion on the burnout of lignite/biomass blends: a Turkish case study. Waste Manage 2008;28:2077–84.
[23] Munir S, Nimmo W, Gibbs BM. Shea meal and cotton stalk as potential fuels for co-combustion with coal. Bioresour Technol 2010;101:7614–23.
[24] Andersson K, Normann F, Johnsson F, Leckner B. NO emission during oxy-fuel combustion of lignite. Ind Eng Chem Res 2008;47:1835–45.
[25] Okazaki K, Ando T. NO_x reduction mechanism in coal combustion with recycled CO_2. Energy 1997;22:207–15.
[26] Al-Makhadmeh L, Maier J, Scheffknecht G. Coal pyrolysis and char combustion under oxy-fuel conditions. In: 34th International Technical conference on coal utilization & fuel systems, Clearwater, 2009.
[27] Sun S, Cao H, Chen H, Wang X, Qian J, Wall T. Experimental study of influence of temperature on fuel-N conversion and recycle NO reduction in oxyfuel combustion. Proc Combust Inst 2011;33:1731–8.
[28] Yoshiie R, Kawamoto T, Hasegawa D, Ueki Y, Naruse I. Gas-phase reaction of NO_x formation in oxyfuel coal combustion at low temperature. Energy Fuels 2011;25:2481–6.
[29] Jiang X, Huang X, Liu J, Han X. NO_x emission of fine- and superfine- pulverized coal combustion in O_2/CO_2 atmosphere. Energy Fuels 2010;24:6307–13.
[30] Arenillas A, Backreedy RI, Jones JM, Pis JJ, Pourkashanian M, Rubiera F, et al. Modelling of NO formation in the combustion of coal blends. Fuel 2002;81: 627–36.
[31] Skeen S, Kumfer BM, Axelbaum RL. Nitric oxide emissions during coal and coal/biomass combustion under air-fired and oxy-fuel conditions. Energy Fuels 2010;24:4144–52.
[32] Liu DC, Zhang CL, Mi B, Shen BK, Feng B. Reduction of N_2O and NO emissions by co-combustion of coal and biomass. J Inst Energy 2002;75:81–4.
[33] Li S, Wu A, Deng S, Pan W. Effect of co-combustion of chicken litter and coal on emissions in a laboratory-scale fluidized bed combustor. Fuel Process Technol 2008;89:7–12.
[34] Akpulat O, Varol M, Atimtay AT. Effect of freeboard extension on co-combustion of coal and olive cake in a fluidized bed combustor. Bioresour Technol 2010;101:6177–84.

7. Conclusiones

- Debido al elevado contenido en volátiles de la biomasa, la desvolatilización cobra proporcionalmente mayor relevancia en la combustión de la biomasa que en la del carbón. La combustión de los gases liberados durante la etapa de desvolatilización tiene una cinética mucho más rápida que la reacción de combustión del *char*, por tanto, los tiempos de combustión de partículas de biomasa se acortan en gran medida respecto a los del carbón. Además, el *char* de las biomasas estudiadas es más reactivo que el de los carbones lo que provocará una reducción de los inquemados.

- La sustitución de N_2 por CO_2 para una misma concentración de O_2 (21 %) conlleva un empeoramiento de la ignición, reactividad y grado de quemado. A medida que la concentración de oxígeno aumenta se produce una mejora de los parámetros anteriores, y para concentraciones de O_2 del 30 % se obtienen mejores resultados que en aire.

- El vapor de agua no ejerce un gran efecto sobre las combustibilidad de los carbones estudiados, aunque se han obtenido resultados contrapuestos en el reactor de flujo en arrastre, donde se retrasaba la ignición y descendía ligeramente el grado de quemado en algunos casos, con respecto a los obtenidos en termobalanza, que indicaban una leve mejora en la reactividad al adicionar vapor de agua. Dadas las condiciones empleadas en ambos dispositivos, los efectos observados parecen tener más relación con los mecanismos de transmisión de calor en el reactor de flujo en arrastre, que con posibles reacciones de gasificación del *char* con vapor de agua, que requerirían temperaturas superiores de 1.000 ^{0}C.

- Los experimentos de oxicombustión con adición de biomasa han dado lugar a mejoras en la combustibilidad de las mezclas, con respecto a los combustibles individuales. Esto se ha visto reflejado en distintos parámetros como son la temperatura de ignición, el grado de quemado y las emisiones de NO.

- En los experimentos llevados a cabo con carbones con elevado contenido de materia volátil y elevada reactividad, su mezcla con biomasa produce un efecto menor que en el caso de carbones de alto rango, en los que la adición de biomasa produce un aumento sensible del grado de quemado, contribuyendo a elevar la eficacia en el hogar de combustión.

- La combustión de *char* de biomasa junto con *char* de carbón no entraña ninguna mejora, es decir, no existe interacción en la combustión de los *chars*. Sin embargo, cuando la mezcla se realiza con las muestras originales, sin desvolatilizar, se observa una mejora en la ignición y combustión del carbón. Por tanto, los efectos sinérgicos observados en el grado de quemado se deben principalmente a la combustión de los volátiles de la biomasa.

- En los experimentos de oxicombustión en el reactor de flujo en arrastre, se produce una reducción homogénea de los NO debido a la presencia de mayores concentraciones de CO. La adición de biomasa potencia este efecto, disminuyendo las emisiones de NO en las mezclas de carbón y biomasa.

8. Referencias bibliográficas

Abraham, B. M., Asbury, J. G., Lynch, E. P., Teotia, A. P. S. "Coal-oxygen process provides CO_2 for enhanced recovery". *Oil Gas Journal*, 80, 68-70, 1982.

Álvarez, L. "Captura de CO_2 mediante oxicombustión. Aplicación de técnicas de fluidodinámica computacional". Tesis doctoral. Universidad de Oviedo, Octubre 2012.

Andersen, J., Rasmussen, C. L., Giselsson, T., Glarborg, P. "Global combustion mechanisms for use in CFD modeling under oxy-fuel conditions". *Energy & Fuels*, 23, 1379-1389, 2009.

Andersson, K., Johansson, R., Hjärtstam, S., Johnsson F, Leckner, B. "Radiation intensity of lignite-fired oxy- fuel flames". *Experimental Thermal and Fluid Science*, 33, 67-76, 2008.

Andersson, K., Johansson, R., Johnsson, F., Leckner, B. "Radiation intensity of propane-fired oxy-fuel flames: Implications for soot formation". *Energy & Fuels*, 22, 1535-1541, 2008.

Andersson, K., Johansson, R. Johnsson, F. "Thermal radiation in oxy-fuel flames". *International Journal of Greenhouse Gas Control*, 5S, S58-65, 2011.

Arias, B. "Comportamiento interactivo de mezclas de carbones en combustión. Utilización de técnicas de fluidodinámica computacional". Tesis doctoral. Universidad de Oviedo, Junio 2004.

Arias, B., Pevida, C., Fermoso, J., Plaza, M.G., Rubiera, F., Pis, J.J. "Influence of torrefaction on the grindability and reactivity of woody biomass". *Fuel Processing Technology,* 89, 169-175, 2008.

Arias, B., Pevida, C., Rubiera, F., Pis, J.J. "Effect of biomass blending on coal ignition and burnout during oxy-fuel combustion". *Fuel,* 87, 2753–2759, 2008.

Atal, A., Levendis, Y.A. "Comparison of the combustion behaviour of pulverized waste tyres and coal". *Fuel*, 74, 1570-1581, 1995.

Austin, P.J., Kauffman, C.W., Sichel, M. "Ignition and volatile combustion of cellulosic dust particles". *Combustion Science and Technology*, 112, 187-198, 1996.

Beisheima, T., Leichta, A., Dietera, H., Scheffknechta, G. "Influence of steam on sulfur capture with limestone under oxy-fuel fired conditions in batch BFB experiments" 3rd Oxyfuel Combustion Conference *OCC3*. Ponferrada. España. 9-13 septiembre 2013.

Bejarano, P. A., Levendis, Y. A. "Single-coal-particle combustion in O_2/N_2 and O_2/CO_2 environments". *Combustion and Flame*, 153, 270-287, 2008.

Bhatia, S.K., Perlmutter, D.D. "A random pore model for fluid-solid reactions: I. Isothermal, kinetic control". *AIChE Journal*, 26 (2), 379-386, 1980.

BP "Statistical Review of World Energy". Junio 2013.

Brix, J., Jensen, P. A., Jensen, A. D. "Coal devolatilization and char conversion under suspension fired conditions in O_2/N_2 and O_2/CO_2 atmospheres". *Fuel*, 89, 3373-3380, 2010.

Buhre, B.J.P., Elliott, L.K., Sheng, C.D., Gupta, R.P., Wall T.F. "Oxy-fuel combustion technology for coal-fired power generation" *Progress in Energy and Combustion Science,* 31, 283–307, 2005.

Carpenter, A.M., Skorupska, N.M. "Coal combustion-analysis and testing". IEACR/64, IEA Coal Research, Londres, 1993.

Cieplik, M., Houkema, M. "ECN practice-driven biomass cofiring R&D services". *IEA-CCC workshop "Co-firing biomass with coal",* Drax power Station, 26 Junio 2011.

CIUDEN. http://ciuden.es/index.php/es/tecnologias/tecnologias-cac/transporte, consultada en enero 2014.

Demirbas A. "Combustion characteristics of different biomass fuels". *Progress in Energy and Combustion Science*, 30, 219-230, 2004.

De Soete, G. G. "Overall reaction rates of NO and N_2 formation from fuel nitrogen". *Symposium (International) on Combustion*, 15, 1093-1102, 1975.

ELCOGAS. http://www.elcogas.es/es/tecnologia-gicc/tecnologia-diseno/captura-co2, consultada en enero 2014.

ENDESA. http://www.endesa.com/es/conoceendesa/lineasnegocio/principalesproyectos/CapturadeCO2, consultada en enero 2014.

Essenhigh, R.H., Misra, M.K., Shaw, D.W. "Ignition of coal particles: a review". *Combustion and Flame*, 77, 3–30, 1989.

Faúndez, J., Arenillas, A., Rubiera, F., García, X., Gordon A.L., Pis J.J. "Ignition behaviour of different rank coals in an entrained flow reactor". *Fuel*, 84, 2172-2177, 2005.

Faúndez, J., Arias, B., Rubiera, F., Arenillas, A., García, X., Gordon, A.L., Pis, J.J. "Ignition characteristics of coal blends in an entrained flow reactor". *Fuel,* 86, 2076-2080, 2007.

Fei, H., Hu, S., Xiang, J., Sun, L., Fu, P., Chen, G. "Study on coal chars combustion under O_2/CO_2 atmosphere with fractal random pore model". *Fuel*, 90, 441-448, 2011.

Feng, B., Bhatia, S.K. "Variation of the pore structure of coal chars during gasification". *Carbon*, 41, (3), 507-523, 2003.

Fermoso, J., Stevanov, C., Moghtaderi, B., Arias, B., Pevida, C., Plaza, M.G., Rubiera, F., Pis, J.J. "High-pressure gasification reactivity of biomass chars produced at different temperatures". *Journal of Analytical and Applied Pyrolysis*, 85 (1-2), 287-293, 2009.

Fleig, D., Normann, F., Andersson, K., Johnsson, F., Leckner, B. "The fate of sulphur during oxy-fuel combustion of lignite". *Energy Procedia*, 1, 383-390, 2009.

Fryda, L. , Sobrino, C., Cieplik, M. , van de Kamp, W.L. "Study on ash deposition under oxyfuel combustion of coal/biomass blends" *Fuel*, 89, 1889–1902, 2010.

Glarborg, P., Bentzen, L. B. "Chemical effects of a high CO_2 concentration in oxy-fuel combustion of methane". *Energy & Fuels*, 22, 291-298, 2008.

Gharebaghi, M., Hughes, K. J., Porter, R. T. J., Pourkashanian, M., Williams, A. "Mercury transformation in air-coal and oxy-coal combustion: a modelling approach". *Proceedings of the Combustion Institute,* 33, 1779-1786, 2011.

Giménez-López, J., Martínez, M., Millera, A., Bilbao, R., Alzueta, M. U. "SO_2 effects on CO oxidation in a CO_2 atmosphere, characteristic of oxy-fuel conditions", *Combustion and Flame*, 158, 48-56, 2011.

González, A.S., Plaza, M.G., Rubiera, F., Pevida, C. "Sustainable biomass-based carbon adsorbents for post-combustion CO_2 capture". *Chemical Engineering Journal,* 230, 456-465, 2013.

Hamor, R.J., Smith, I.W., Tyler, R.J. "Kinetics of combustion of a pulverized brown coal char between 630 and 2200 K". *Combustion and Flame*, 21, (2), 153-162, 1973.

Hecht, E. S., Shaddix, C. R., Molina, A., Haynes, B. S. "Effect of CO_2 gasification reaction on oxy-combustion of pulverized coal char". *Proceedings of the Combustion Institute*, 33, 1699-1706, 2011.

Hjärtstam, S., Johnsson, F., Andersson, K., Leckner, B. "Combustion characteristics of lignite-fired oxy-fuel flames". *Fuel*, 88, 2216-2224, 2009.

Horn, F. L., Steinberg, M. "Control of carbon dioxide emissions from a power plant (and use in enhanced oil recovery)". *Fuel*, 61, 415-422, 1982.

Hurtado, A. "Almacenamiento geológico de CO_2: Metodología de estimación de capacidades". *CONAMA*. Madrid, 2008.

IDAE. "Biomasa: Producción eléctrica y cogeneración". 2007.

IFN3. "Tercer ciclo del Inventario Forestal Nacional", MAGRAMA, 2007.

IPCC. "IPCC special report on carbon dioxide capture and storage", 2005.

IPCC "Resumen para Responsables de Políticas. En, Cambio Climático 2007: Impactos y Vulnerabilidad. Contribución del Grupo de Trabajo II al Cuarto Informe de Evaluación del IPCC, M.L. Parry, O.F. Canziani, J.P. Palutikof, P.J. van der Linden, C.E. Hanson, Eds., Cambridge University Press, Cambridge, Reino Unido, 2007.

IPCC. "Climate Change 2013. The Physical Science Basis Working Group I Contribution to the Fifth Assessment Report of the Intergovernmental Panel on Climate Change Summary for Policymakers. Edited by Thomas F. 2013.

Jurado, N., Darabkhani, H., Anthony, E.J., Oakey, J. "Co-firing performance of a retrofitted oxy-combustor burning coal/biomass blends: Experimental and simulation study". 3rd Oxyfuel Combustion Conference *OCC3*. Ponferrada. España. 9-13 septiembre 2013.

Kazanc, F., Khatami, R., Manoel Crnkovic, P., Levendis, Y.A. "Emissions of NO_x and SO_2 from coals of various ranks, bagasse, and coal-bagasse blends burning in O_2/N_2 and O_2/CO_2 environments". *Energy & Fuels*, 25, 2850-2861, 2011.

Kevin, E., John, T., Kiehl, J. "Earth's global energy budget" *Bulletin of the American Meteorological Society*, 2008.

Khare, S. P., Wall, T. F., Farida, A. Z., Liu, Y., Moghtaderi, B., Gupta, R. P. "Factors influencing the ignition of flames from air-fired swirl pf burners retrofitted to oxy-fuel". *Fuel*, 87, 1042-1049, 2008.

Khatami, R., Levendis, Y.A. "On the deduction of single coal particle combustion temperature from three-color optical pyrometry". *Combustion and Flame*, 158, 1822-1836, 2011.

Khatami, R., Stivers, C., Joshi, K., Levendis, Y. A., Sarofim, A. F. "Combustion behavior of single particles from three different coal ranks and from sugar cane bagasse in O_2/N_2 and O_2/CO_2 atmospheres". *Combustion and Flame*, 159, 1253-1271, 2012.

Levenspiel, O. "Ingeniería de las reacciones químicas". Barcelona, Ed. Reverté, 1979.

Levendis, Y, A., Kelvin Rafael E, Hoyt CH. "Development of multicolor pyrometers to monitor the transient response of burning carbonaceous particles". *Review of Scientific Instruments*, 63, 3608, 1992.

Levendis, Y.A., Joshi K., Khatami R., Sarofim A.F. “Combustion behavior in air of single particles from three different coal ranks and from sugarcane bagasse”. *Combustion and Flame*, 158, 452, 2011.

Li, X., Rathman, R. K., Yu, J., Wang, Q., Wall, T., Lin, B. “Pyrolysis and combustion characteristics of an Indonesian low-rank coal under O_2/N_2 and O_2/CO_2 conditions”. *Energy & Fuels*, 24, 160-164, 2010.

Liu, Y., Geier M., Molina A., Shaddix C.R. “Pulverized coal stream ignition delay under conventional and oxy-fuel combustion conditions”. *International Journal of Greenhouse Gas Control,* S5, S36-S46, 2011.

Mendiara, T., Glarborg, P. “Reburn chemistry in oxy-fuel combustion of methane”. *Energy & Fuels*, 23, 3565-3572, 2009.

Miura, K., Hashimoto, K., Silveston, P.L. “Factors affecting the reactivity of coal chars during gasification, and indices representing reactivity”. *Fuel*, 68, 1461-1475, 1989.

Molina, A., Shaddix, C. R. “Ignition and devolatilization of pulverized bituminous coal particles during oxygen/carbon dioxide coal combustion”. *Proceedings of the Combustion Institute*, 31, 1905-1912, 2007.

Naredi, P., Pisupati, S. “Effect of CO_2 during coal pyrolysis and char burnout in oxy-coal combustion”. *Energy & Fuels*, 25, (6), 2452-2459, 2011.

Ndibe, C., Spörl, R., Maier, J., Scheffknecht, G. “Experimental study of NO and NO_2 formation in a pf oxy-fuel firing system”. *Fuel*, 107, 749-756, 2013.

Normann, F., Andersson, K., Leckner, B., Johnsson, F. “Emission control of nitrogen oxides in the oxy-fuel process”. *Progress in Energy and Combustion Science*, 35, 385-397, 2009.

Ochoa, J., Cassanello, M.C., Bonelli, P.R., Cukierman, A.L. “CO_2 gasification of Argentinean coal chars: a kinetic characterization”. *Fuel Processing Technology*, 74, 161-176, 2001.

ONU. “Nuestro futuro común”. Asamblea de las Naciones Unidas. Marzo 1987.

Okazaki, K., Ando, T. “NO_x reduction mechanism in coal combustion with recycled CO_2”. *Energy*, 22, 207-215, 1997.

Payne, R., Chen, S. L., Wolsky, A. M., Richter, W. F. “CO_2 recovery via coal combustion in mixtures of oxygen and recycled flue gas”. *Combustion Science and Technology*, 67, 1-16, 1989.

PER. “Plan de energías renovables 2005-2010”. Ministerio de Industria, Turismo y Comercio. Gobierno de España. Agosto 2005.

PER. “Plan de energías renovables 2011-2020”. Ministerio de Industria, Turismo y Comercio. Gobierno de España. Noviembre 2011.

Perrin, N. “Oxycombustion for coal power plants: advantages, solutions and projects”. *Clean Coal Technologies CCT*. Tesalónica. Grecia, 6-9 mayo 2013.

Pis, J.J. “El carbón como fuente de energía: procesos de combustión y gasificación”. Curso: Tendencias actuales en la utilización y conversión del carbón. INCAR-CSIC. Oviedo, 14-18 Mayo 2012.

Prado, A.J. “Almacenamiento geológico de CO_2: Selección de formaciones favorables”. *CONAMA*. Madrid, 2008.

PTECO_2. “Transporte de CO_2: estado del arte, alternativas y retos”. Asociación de la Plataforma Tecnológica Española del CO_2. Abril 2013.

PTECO_2. “Usos del CO_2: un camino hacia la sostenibilidad”. Asociación de la Plataforma Tecnológica Española del CO_2. Abril 2013.

PTECO_2. “Almacenamiento de CO_2: tecnologías, oportunidades y expectativas”. Asociación de la Plataforma Tecnológica Española del CO_2. Enero 2012.

Rathnam, R. K, Elliot, L. K., Wall, T. F., Liu, Y., Moghtaderi, B. “Nitrogen oxides behavior under oxy-combustion conditions”. *Fuel Procesing Technology*, 90, 797-802, 2009.

REE. “Avance del informe del sistema eléctrico español”. Diciembre 2013.

Rubiera, F., Fuertes, A.B., Pis, J.J., Artos, V., Marbán, G. “Changes in textural properties of limestone and dolomite during calcination”. Termochimica Acta, 179, 125-134, 1991.

Ruiz, C. “Almacenamiento geológico de CO_2: Criterios de selección de emplazamientos”. *CONAMA*. Madrid 2008.

Santos, S. “Challenges to demonstration. What is the current status to the development of oxyfuel combustion technology”. IEA Greenhouse Gas R&D Programme 2nd Flexiburn Workshop. 6 de Febrero 2013.

Sebastián, F., Royo, J., Gómez, M. "Cofiring versus biomass-fired power plants: GHG (Greenhouse Gases) emissions savings comparison by means of LCA (Life Cycle Assessment) methodology". *Energy,* 36, (4), 2029-2037, 2011.

Seepana, S., Jayanti, S. “Steam-moderated oxy-fuel combustion” *Energy Conversion and Management,* 51, 1981–1988, 2010.

Shaddix, C. R., Molina, A. “Particle imaging of ignition and devolatilization of pulverized coal during oxy-fuel combustion”. *Proceedings of the Combustion Institute*, 32, 2091-2098, 2011.

Sheng, C., Lu, Y., Gao, X., Yao, H. “Fine ash formation during pulverized coal combustion: A comparison of O_2/CO_2 combustion versus air combustion”. *Energy & Fuels*, 21, 435-440, 2007.

Sima-Ella, E., Yuan, G., Mays, T. “A simple kinetic analysis to determine the intrinsic reactivity of coal chars”. Fuel, 84, 1920-1925, 2005.

Solà, R., Oltra, C., Di Masso, M., Sala, R. “Aceptación social de la captura y almacenamiento de CO_2 (CAC)”. CIEMAT-Centro de Investigación Sociotécnica (Barcelona). *CONAMA*. Madrid, 2008.

Stanger, R., Wall, T. “Sulphur impacts during pulverised coal combustion in oxy-fuel technology for carbon capture and storage”. *Progress in Energy and Combustion Science*, 37, 69-88, 2011.

Stam, A., Ploumen, P., Brem, G. “Ash related aspects of oxy-combustion of coal and biomass: A thermodinamic approach” The 34th international technical conference on coal utilization and fuel systems, Clearwater, Florida, USA. 2009.

Statoil. http://www.statoil.com/AnnualReport2010/en/Pages/frontpage.aspx, Marzo 2014.

Stein-Brzozowska, G. “Deposits and high temperature corrosion during oxyfuel combustion”. TCCS-7. Trondheim. 4-6 Junio, 2013.

Strömberg, L., Lindgren, G., Jacoby, J., Giering, R., Anheden, M., Burchhardt, U., Altmann, H., Kluger, F., Stamatelopoulos, G.-N. “Update on Vattenfall’s 30 MWth oxyfuel pilot plant in Schwarze Pumpe”. *Energy Procedia*, 1, 581-589, 2009.

Smart, J.P., Pate, R., Riley, G.S. “Oxy-fuel combustion of coal and biomass, the effect on radiative and convective heat transfer and burnout”. *Combustion and Flame*, 157, 2230-2240, 2010.

Smart, J. P., Riley, G. S. “On the effects of firing semi-anthracite and bituminous coal under oxy-fuel firing conditions”. *Fuel*, 90, 2812-2816, 2011.

Smith, I.W. “The combustion rates of coal chars: A review”. *Symposium (International) on Combustion*, 19, 1045-1065, 1982.

Suriyawong, A., Gamble, M., Lee, M. H., Axelbaum, R., Biswas, P. “Submicrometer particle formation and mercury speciation under O_2–CO_2 coal combustion”. *Energy & Fuels*, 20, 2357-2353, 2006.

Taniguchi, M., Shibata, T., Kobayashi, H. “Prediction of lean flammability limit and flame propagation velocity for oxy-fuel fired pulverized coal combustion”. *Proceedings of the Combustion Institute*, 33, (2), 3391-3398, 2011a.

Taniguchi, M., Yamamoto, K., Okazaki, T., Rehfeldt, S., Kuhr, C. “Application of lean flammability limit study and large eddy simulation to burner development for an oxy-fuel combustion system”. *International Journal of Greenhouse Gas Control*, 5S, (1), S111-S119, 2011b.

Termuehlen, H., Emsperger, W. “Clean and efficient coal-fired power plants”. ISBN 0-7918-0194-2, American Society of Mechanical Engineers, Nueva York, 2003.

Timothy, A. “Reactivity of Australian coal-derived chars to carbon dioxide”. *Fuel*, 61, 2, 145-149, 1982.

Toftegaard, M.B., Brix, J., Jensen, P.A., Glarborg, P., Jensen, A.D. “Oxy-fuel combustion of solid fuels”. *Progress in Energy and Combustion Science*, 36 (5), 581-625, 2010.

Tooper J. Closing session. *3rd Oxyfuel Combustion Conference OCC3*. Ponferrada. España. 9-13 septiembre 2013

Tsai, C.-Y., Scaroni, A.W. “Pyrolysis during the initial stages of pulverized-coal combustion”. *Symposium (International) on Combustion*, 20, (1), 1455-1462, 1985.

UE. “Sobre el futuro de la captura y almacenamiento de carbono en Europa” Comunicación de la Comisión Europea (COM(2013)0180), Bruselas. 27 de marzo 2013.

UE. “A policy framework for climate and energy in the period from 2020 to 2030”. Comunicación del Parlamento Europeo. COM2014/15 Bruselas, 22 de enero 2014.

UNESA. “Memoria 2012”. Asociación Española de la Industria Eléctrica. 2012.

Várhegyi, G., E., Till, F. “Comparison of temperature-programmed char combustion in CO_2-O_2 and Ar-O_2 mixtures at elevated pressure”. *Energy & Fuels*, 13, 539-540, 1999.

Wall, T.F., Liu, Y., Spero, C., Elliott, L., Khare, S., Rathnam, R., Zeenathal, F., Moghtaderi, B., Buhre, B., Sheng., C., Gupta, R., Yamada, T., Makino, K., Yu, J. “An overview on oxyfuel coal combustion-State of the art research and technology development”. *Chemical Engineering Research and Design*, 87, (8), 1003-1016, 2009a.

Wall, T.F “Coal based oxy-combustion for carbon capture and storage: status, prospects, research needs and roadmap to commercialisation.” Purdue University Energy Center. 28 Mayo, 2009b.

Wall, T.F., Stanger, R., Santos, S. “Demonstrations of coal-fired oxy-fuel technology for carbon capture and storage and issues with commercial deployment”. *International Journal of Greenhouse Gas Control*, 5S, (1), S5-S15, 2011.

Walker, P.L.Jr., Rusinko, F., Austin, L.G. “Advances in catalysis”, Vol. 11, Ed. Eley, D.D., Serwood, P.W., Weisz, P.B., Academic Press, New York, 1959.

WEC. “Survey of energy resources 2010” World Energy Council, ISBN: 978-0-946121-021, London, United Kingdom. 2010.

Williams, A., Pourkashanian M, Jones J.M. “Combustion of pulverised coal and biomass”. *Progress in Energy and Combustion Science*, 27, 587, 2001.

Wornat, M.J., Hurt, R.H., Davis, K.A., Yang, N.Y.C. “Single-particle combustion of two biomass chars”. *Symposium (International) on Combustion*, 26, 3075, 1996.

ZEP. “Matrix of Technologies”. EU Zero Emissions Platform, http://www.zeroemissionsplatform.eu. Consultada en Marzo 2014.

ZEP. “Recommendations for Research to Support the Deployment of CCS in Europe Beyond 2020”. EU Zero Emissions Platform, http://www.zeroemissionsplatform.eu. Consultada en Marzo 2014.

Zhang, L., Binner, E., Li, C.H. “In situ diagnostics of Victorian brown coal combustion in O_2/N_2 and O_2/CO_2 mixtures in drop tube furnace”. *Fuel*, 89, 2703-2712, 2010.

Zolin, A., Jensen, A., Storm Pedersen, L., Dam-Johansen, K. “A comparison of coal char reactivity determined from thermogravimetric and laminar flow reactor experiments“. *Energy & Fuels*, 12, (2), 268-276, 1998.

Anexo I - Informe de factor de impacto de las publicaciones

Tal como señala el reglamento de doctorado se exponen a continuación el factor de impacto, según "Journal Citación Report" del año 2012, de las revistas en las que se han publicado los trabajos presentados en esta tesis:

I Single particle ignition and combustion of anthracite, semi-anthracite and bituminous coals in air and simulated oxy-fuel conditions. Combustion and Flame.
J. Riaza, R. Khatami, Y.A. Levendis, L. Álvarez, M.V. Gil, C. Pevida, F. Rubiera, J.J. Pis. Combustion and Flame. 161 (2014) 1096–1108. DOI:0.1016/j.combustflame.2013.10.004

Factor de impacto **Combustion and Flame**: **3,599**

Posición en el área según índice de impacto:
Thermodynamics 3 de 55
Energy and fuels 15 de 81
Engineering, multidiscipline 1 de 90
Engineering, chemical 8 de 133

II Combustion of Single Biomass Particles in Air and in Oxy-Fuel Conditions.
J. Riaza, R. Khatami, Y. A. Levendis, L. Álvarez, M.V. Gil, C. Pevida, F. Rubiera, J.J. Pis Biomass and Bioenergy. doi: 10 10.1016/j.biombioe.2014.03.018.1

Factor de impacto **Biomass and Bioenergy**: **2,975**

Posición en el área según índice de impacto:
Energy and fuels 20 de 81
Biotechnology and applied microbiology 48 de 160
Agricultural Engineering, 4 de 12

III Kinetic models for the oxy-fuel combustion of coal and coal/biomass blend chars obtained in N_2 and CO_2 atmospheres
M.V. Gil, J. Riaza, L. Álvarez, C. Pevida, J.J. Pis, F. Rubiera. Energy 2012. 48 (1) pp. 510–518. doi:10.1016/j.energy.2012.10.033

Factor de impacto **Energy**: **3,651**

Posición en el área según índice de impacto:
Thermodynamics 2 de 55
Energy and fuels 14 de 81

IV Oxy-fuel combustion kinetics and morphology of coal chars obtained in N_2 and CO_2 atmospheres in an entrained flow reactor.
M.V. Gil, J. Riaza, L. Álvarez, C. Pevida, J.J. Pis, F. Rubiera. Applied Energy 2012. 91 (1) pp. 67 – 74. doi:10.1016/j.apenergy.2011.09.017

Factor de impacto **Applied Energy**: **4,781**

Posición en el área según índice de impacto:
Energy and fuels 6 de 81
Engineering, chemical 6 de 133

V Effect of oxy-fuel combustion with steam addition on coal ignition and burnout in an entrained flow reactor,
J. Riaza, L. Álvarez, M.V. Gil, C. Pevida, J.J. Pis, F. Rubiera, Energy 2011. 36 (8) pp. 5314 – 5319. doi:10.1016/j.energy.2011.06.039

Factor de impacto **Energy**: **3,651**

Posición en el área según índice de impacto:
Thermodynamics 2 de 55
Energy and fuels 14 de 81

VI NO Emissions in oxy-coal combustion with addition of steam in an entrained flow reactor.
L. Álvarez, J. Riaza, M.V. Gil, C. Pevida, J.J. Pis, F. Rubiera. Greenhouse Gases: Science and Technology 2011. 1 (2) pp. 180-190. doi:10.1002/ghg.016

Factor de impacto **Greenhouse Gases: Science and Technology**: **2,679**

Posición en el área según índice de impacto:
Energy and fuels 26 de 81
Engineering, environmental 12 de 42
Environmental sciences 57 de 210

VII A study of oxy-coal combustion with steam addition and biomass blending by thermogravimetric analysis.
M.V. Gil, J. Riaza, L. Álvarez, C. Pevida, J.J. Pis, F. Rubiera. Journal of Thermal Analysis and Calorimetry 2012. 109 (1) pp. 49 – 55. doi:10.1007/s10973-011-1342-y

Factor de impacto **Journal of Thermal Analysis and Calorimetry**: **1,982**

Posición en el área según índice de impacto:
Chemistry, analytical 37 de 75
Chemistry, physical 75 de 80

VIII Ignition behaviour of coal and biomass blends under oxyfiring conditions with steam additions.
J. Riaza, L. Álvarez, M.V. Gil, R. Khatami, Y.A. Levendis, J.J. Pis, C. Pevida, F. Rubiera. Greenhouse Gases: Science and Technology 2013. 3 (5), pp. 397-414. doi:10.1002/ghg.1368

Factor de impacto **Greenhouse Gases: Science and Technology: 2,679**

Posición en el área según índice de impacto:
Energy and fuels 26 de 81
Engineering, environmental 12 de 42
Environmental sciences 57 de 210

IX Oxy-fuel combustion of coal and biomass blends.
J. Riaza, M.V. Gil, L. Álvarez, C. Pevida, J.J. Pis, F. Rubiera. Energy 2012. 41 (1) pp. 429 – 435. doi: 10.1016/j.energy.2012.02.057

Factor de impacto **Energy**: **3,651**

Posición en el área según índice de impacto:
Thermodynamics 2 de 55
Energy and fuels 14 de 81

Anexo II - Producción Científica no incluida

Comunicaciones a congresos realizados a partir del trabajo de esta tesis doctoral:

- L. Álvarez, J. Riaza, F. Rubiera, C. Pevida, J.J. Pis. "*Co-combustión de mezclas de carbón y biomasa en condiciones de oxicombustión*". **X Reunión del Grupo Español del Carbón**. Oral. 9-12 Mayo 2010. Gerona, España.

- J. Riaza, L. Álvarez, F. Rubiera, J.J. Pis, C. Pevida. *"Co-combustión de mezclas de carbón y biomasa en un reactor de flujo en arrastre*". **X Reunión del Grupo Español del Carbón**. Póster. 9-12 Mayo 2010 Gerona, España.

- L. Alvarez, J. Riaza, C. Pevida, F. Rubiera, J.J. Pis. "*Co-combustion of coal and biomass blends under different oxy-fuel atmospheres.*" **8th European Conference on Coal Research and its Applications.** Oral. 6-8 Septiembre 2010. Leeds, UK.

- J. Riaza, L. Álvarez, M.V. Gil, C. Pevida, F. Rubiera, J.J. Pis. "*Evaluación de la combustibilidad de carbones de distinto rango en atmósferas de oxicombustión*". **XI Reunión del Grupo Español del Carbón.** Póster. 2011. Badajoz, España.

- J. Riaza, L. Álvarez, M.V. Gil, C. Pevida, F. Rubiera, J.J. Pis. "*Co-combustion of coal and biomass blends in an entrained flow reactor under oxy-fuel atmospheres*". **International Conference on Coal Science & Technology**, ICCS&T2011. Póster. 9-13 Octubre 2011. Oviedo. España.

- J. Riaza *"Captura de CO_2 en centrales termoeléctricas de carbón y biomasa*". **I Jornadas de doctorado Universidad de Oviedo**. Póster. 15-16 Diciembre 2011. Oviedo. España.

- J. Riaza, L. Álvarez, M.V. Gil, C. Pevida, F. Rubiera, J.J. Pis. "*Oxy-fuel ignition and combustion of coal and biomass blends in an entrained flow reactor*". **ANQUE'S ICCE.** 24-27 Junio 2012. Póster. Sevilla. España.

- J. Riaza, L. Álvarez, M.V. Gil, C. Pevida, F. Rubiera, J.J. Pis. *"Ignition of coal and biomass blends under oxy-fuel combustion conditions*". **9th European Conference on Coal Research and its Applications**. Póster. 10-12 Septiembre 2012. Nottingham, Reino Unido.

- J. Riaza, L. Álvarez, M.V. Gil, C. Pevida, J.J. Pis, F. Rubiera "*Ignition and NO emissions of coal and biomass blends under different oxy-fuel atmospheres*". **International conference on Greenhouse Gas Control Technologies GHGT-11**. Póster. 18-22 Noviembre 2012, Kyoto International Conference Center, Japón.

- J. Riaza *"Combustión de mezclas de carbón y biomasa".* **II Jornadas de doctorado Universidad de Oviedo**. Póster. 29-30 Noviembre 2012. Oviedo. España.

- J. Riaza, L. Álvarez, M.V. Gil, C. Pevida, J.J. Pis, F. Rubiera. *"Coal and biomass blends oxy-fuel combustion in an entrained flow reactor"*. **Clean Coal Technologies CCT 2013.** Oral. 12-16 May 2013, Tessaloniki, Grecia.
- J. Riaza, L. Álvarez, M.V. Gil, C. Pevida, J.J. Pis, F. Rubiera **"**O*xicombustión de mezclas de carbón y biomasa en reactor de lecho en arrastre".* **XII Reunión del Grupo Español del Carbón.** Keynote, 20-23 Octubre 2013, Madrid, España.
- J. Riaza, L. Álvarez, M.V. Gil, C. Pevida, J.J. Pis, F. Rubiera *"Effect of oxy-fuel combustion with steam and biomass addition on coal burnout in an entrained flow reactor".* **3rd Oxyfuel Combustion Conference OCC3.** Oral. 6-9 Septiembre 2013, Ponferrada, España.
- J. Riaza "*Captura de CO_2 en centrales termoeléctricas de carbón y biomasa"* **III Jornadas de doctorado Universidad de Oviedo**. Póster. 19-20 Diciembre 2013. Oviedo. España.

Otras comunicaciones a congresos en las que ha participado el autor de esta tesis doctoral:

- J. Riaza, L. Álvarez, M.V. Gil, C. Pevida, J.J. Pis, F. Rubiera "*Co-combustion de carbón y biomasa en planta piloto de lecho fluidizado"***. XII Reunión del Grupo Español del Carbón.** Póster. 20-23 Octubre 2013, Madrid, España.
- L. Álvarez, M. Gharebaghi, M. Pourkashanian, A. Williams, J. Riaza, C. Pevida, J.J. Pis, F. Rubiera. "*Modelización CFD de la oxicombustión de carbón en un reactor de flujo en arrastre***". XI Reunión del Grupo Español del Carbón**. Oral. 2011. Badajoz, España.
- L. Álvarez, M. Gharebaghi, A. Williams, M. Pourkashanian, J. Riaza, C. Pevida, J.J. Pis, F. Rubiera. "*CFD modelling of oxy-coal combustion in an entrained flow reactor*". **Fifth International Conference on Clean Coal Technologies,** CCT2011. Oral. 8-12 Mayo 2011. Zaragoza. España.
- L. Álvarez, M. Gharebaghi, A. Williams, M. Pourkashanian, J. Riaza, C. Pevida, J.J. Pis, F. Rubiera. "*Experimental and numerical investigations of oxy-coal combustion in an entrained flow reactor*". **International Conference on Coal Science & Technology**, ICCS&T2011. Oral. 9-13 Octubre 2011. Oviedo. España.
- L. Álvarez, M. Gharebaghi, J.M. Jones, A. Williams, M. Pourkashanian, J. Riaza, C. Pevida, J.J. Pis, F. Rubiera. "*Prediction of volatile and NO precursosr release in the CFD modelling of oxy-coal combustion*". **9th European Conference on Coal Research and its Applications**. Oral. 10-12 Septiembre 2012. Nottingham, Reino Unido.

Otras publicaciones en las que ha participado el autor de esta tesis doctoral:

- L. Álvarez, M. Gharebaghi, M. Pourkashanian, A. Williams, J. Riaza, C. Pevida, J.J. Pis, F. Rubiera. *"CFD Modelling of oxy-coal combustion in an entrained flow reactor*". **Fuel Processing Technology** 2011. 92 (8) pp. 1489 –1497. doi:10.1016/j.fuproc.2011.03.010
- L. Álvarez, M. Gharebaghi, J.M. Jones, M. Pourkashanian, A. Williams, J. Riaza, C. Pevida, J.J. Pis, F. Rubiera. *"Numerical investigation of NO emissions from an entrained flow reactor under oxy-coal conditions".* **Fuel Processing Technology** 2012. 93 (1) pp. 53 – 64. doi:10.1016/j.fuproc.2011.09.011
- L. Álvarez, C. Yin, J. Riaza, C. Pevida, J.J. Pis, F. Rubiera "*Oxy-coal combustion in an entrained flow reactor: Application of specific char and volatile combustion and radiation models for oxy-firing conditions*" **Energy** 2013. 62, pp. 255-268. doi:10.1016/j.energy.2013.08.063
- L. Álvarez, M. Gharebaghi, J.M. Jones, M. Pourkashanian, A. Williams, J. Riaza, C. Pevida, F. Rubiera "*CFD modeling of oxy-coal combustion: Prediction of burnout, volatile and NO precursors release*". **Applied Energy** 2013. 104, pp. 653-665. doi:10.1016/j.apenergy.2012.11.058
- J. Riaza, L. Álvarez, M.V. Gil, C. Pevida, J.J. Pis, F. Rubiera "*Ignition and NO emissions of coal and biomass blends under different oxy-fuel atmospheres".* **Energy Procedia** 2013. 37, 1405-1412, doi:10.1016/j.egypro.2013.06.016
- J. Riaza, L. Álvarez, M.V. Gil, C. Pevida, F. Rubiera "Fundamentals of oxy-fuel carbón capture technology for pulverized fuel boilers. Combustion: types of reactions, fundamental processes and advanced technologies". Book chapter. **Nova Science Publishers**, Inc., 2014 ISBN 978-1-62948-969-8
- L. Álvarez, C. Yin, J. Riaza, C. Pevida, J.J. Pis, F. Rubiera "*Biomass co-firing under oxy-fuel conditions: A computational fluid dynamics modelling study and experimental validation*". **Fuel Processing Technology** 2014. 120, pp. 22 – 33. doi:10.1016/j.fuproc.2013.12.005

PrEM

Energy Processes and
Emission Reduction Group

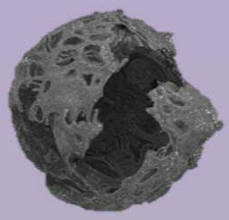

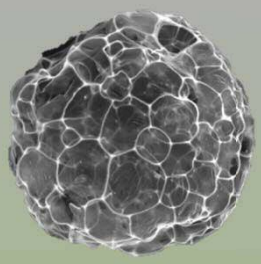

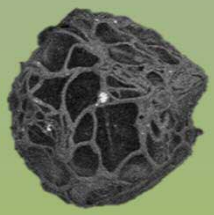

Instituto Nacional del Carbón
INCAR-CSIC
Francisco Pintado Fe, 26
33011, Oviedo
www.incar.csic.es